Exploring the Partonic Structure of the Nucleon on the Light-Cone

dissertation submitted by

Manuel Pincetti

to obtain the degree of

Dottore di Ricerca in Fisica

Supervisors: Prof. Sigfrido Boffi

Dr. Barbara Pasquini

Referee: Prof. Lech Szymanowski

To my sister Giulia

"The average Ph.D. thesis is nothing but a transference of bones from one graveyard to another."
J. Frank Dobie (1888 - 1964),
A Texan in England, 1945.

Contents

Chapter 1

Introduction

1.1 Strong Interactions

To date the so-called Standard Model (SM) represents a consistent, renormalizable and calculable (within the actual limits of computational power) theory of all known phenomena in particle physics. It apparently describes three of the four known forces; indeed it accounts for the electromagnetic, weak and strong interactions which characterize all microscopic processes. Anyway the SM is certainly not the final theory of particle physics. It was created by crudely splicing the electro-weak theory and the present theory of strong interactions, Quantum Chromo-Dynamics (QCD), and for this reason the theory is rather unwieldy and inelegant.

However, it seems to be able to explain an enormous body of experimental data, ranging from hadronic sum rules to neutrino scattering experiments. In fact, there is no piece of experimental data that violates the SM.

On the other hand there are many open questions to be answered. Among the open questions one of the most challenging and still far to be solved is related to the strong force and, in particular, to the impossibility of applying perturbation theory at small energies because of the high value of the strong coupling constant. The high value of the strong coupling constant implies that results obtained through a perturbative expansion, which is the main theoretical tools in weakly interacting theories such as the electro-weak one, are much less reliable, because higher order diagrams can give corrections even greater that the tree level first order result, so the development of a coherent Quantum Field Theory (QFT) for the strong interactions proceeded slowly. Indeed, although the hadron structure is believed to be described by QCD, the actual solution of the problem is notoriously difficult to achieve. Up to now the only systematic theoretical approach that has been very successful is based on solving numerically QCD on a space-time lattice.

The birth of strong interactions dates back to the beginning of the last century when they were assumed to account for the formation of the atomic nuclei.

They were called strong because the forces interplaying among protons must overcome the Coulomb electromagnetic repulsion to generate nuclear bindings. In the 1940s, the first seminal breakthrough in the strong interactions was the realization that the force binding the nucleus together could be mediated by the exchange of π mesons [1]. The theoretical predictions of Yukawa were then confirmed by experimentalists that found the π meson in cosmic ray experiments, therefore the pion was deduced to be the carrier of the nuclear force that binds the nucleus together. However, this discovery was tempered by the fact that the pion-nucleon coupling constant was much greater than one. So, although the Yukawa meson theory as a quantum field theory was known to be renormalizable, perturbation theory was unrealiable when applied to that. Non-perturbative effects, which were exceedingly difficult to calculate, become dominant.

Furthermore, the experimental situation became confusing when many resonances began to be discovered in particle accelerators. This observation put once more forward the necessity of finding a unified theoretical framework; nevertheless, none of the proposed schemes was able to refer explicitly to the features of the interacting particles, focusing rather on general properties of the scattering amplitude. For instance Goldberger and his colleagues assumed the *scattering* matrix S was an analytic function that satisfied certain dispersion relations [2]. In lack of a dynamical picture for this new force, static models, based on symmetry principles, filled the void. The concept of symmetry has a precise mathematical content, representing the invariance of physical laws under a certain group of transformations; it is also intimately connected to the concept of conservation law. Already in the 30's, Heisenberg exploited the unitary symmetry SU(2) (strong isospin) to explain the charge independence of nuclear forces (equal $p-p$, $p-n$ and $n-n$ interactions, if in the same type of state), and this symmetry was explicitly broken only by (charge dependent) electromagnetic interactions; the discovery of the "strange" particles suggested to extend the symmetry group to (flavour) SU(3): it was the birth of the Constituent Quark Model (CQM). Gell-Mann, Ne'eman and Zweig [3] building on earlier works of Sakata and others [4], tried to explain the hadron spectrum with the symmetry group SU(3). Using a composite combination of the "up", "down" and "strange" quarks (triplet) as fundamental representation of the Lie group one could, in fact, explain all the hadrons discovered at that time. The picture was: hypotetic spin 1/2 fermions with fractional charge which combines to form hadrons. Three quarks form a baryon and a quark-antiquark pair forms a meson. The quark model could predict with relative ease the masses and properties of particles that were not yet discovered and for this reason a simple picture of the strong interactions was beginning to emerge. But this picture even if predictive was still crude and approximate.

The existence of particular combinations (such as the $\Delta^{++} = \{uuu\}$, with spin 3/2, which is a symmetric state both in its flavour and space-spin part) and the need to preserve the Fermi-Dirac statistics (forcing totally antisym-

metric states) induced the introduction of a further degree of freedom [5], later called "colour" (with three possibilities: red, green and blue) [6], whose interactions are described by the same SU(3) group as flavour, but with the constraint to form colourless hadrons (coloured free particles were never observed in nature). This refined CQM model allowed the construction of equal spin-parity hadronic multiplets and made many interesting predictions on hadrons properties (mass, spin,...) possible; it also predicted the existence of new particles, such as the hyperon Ω^-, later discovered in experiments. Nevertheless, even this representation was still far from being conclusive: quarks had no experimental evidences, no information on the force among quarks was provided (so the model couldn't exclude exotic combinations of quarks) and moreover the SU(3) flavour symmetry probably was not exact, since the mass degeneration of the multiplets was only approximate. Moreover, studying only the "extrinsic" properties of hadrons was certainly not enough to unveil their structure in details. With the purpose to unmask the inner structure of nucleons in the late 60s at Stanford linear Accelerator Collider (SLAC) experiments started what later have been called *deep inelastic scattering* (DIS) experiments. These kind of experiments, taking inspirations from the former experiments performed by Hofstader and collaborators that lead to the direct observation of the non point-like structure of the nucleon [7], consisted in a focused beam of particles scattered by the interaction with a target. The interaction proceeded via the exchange of a virtual photon with high energy and momentum. The way scattering took place yielded information on the structure of the target itself. The usefulness of employing an electromagnetic probe resided in the fact that it doesn't interact strongly with the nucleon, thus having a mean free path and then a sensitivity to the details of the internal nucleon structure much larger than those of a strong interacting particle. Moreover, the nucleon is probed with a spatial resolution directly connected, through the uncertainty principle, with the transferred momentum of the virtual exchanged photon (in a one photon approximation): if Q represents the scale of the process ($Q = \sqrt{(q^\mu)^2}$, with q^μ the virtual photon 4-momentum), the associated probing wavelength is given by $\lambda \sim \hbar/Q$, so that at high energies we could possibly 'see' small constituents inside the target nucleon. Hofstadter and collaborators employed electrons beams of about 100 MeV on nuclei, finding that was possible to describe the form of these through proper functions, the *form factors*, experimentally accessible; these could next be linked, through a Fourier transform, to the internal charge distribution of the probed nuclei, and they determined the deviation of the scattering cross section from the ideal theoretical situation of point-like targets:

$$\frac{d\sigma}{d\Omega} = \sigma_R |F(q)|^2; \qquad \text{with} \qquad F(q) = \int \mathrm{d}r e^{iq\cdot r}\rho(r), \tag{1.1}$$

where σ_R is the Rutherford cross section for the relativistic scattering of two point-like charged particles. The experimental information on form factors (F) then allows to draw some conclusions on the nuclear charge distribution

(ρ), or for example to estimate its mean radius. The same principle can be extended to lepton-hadron scattering, e.g. $e^- - N$. Describing the nucleon as a Dirac particle with non-trivial internal structure one arrives to the following expression for the inclusive cross section,

$$\frac{d\sigma}{d\Omega} = \sigma_M \frac{E'}{E}\left[\left(F_1^2(Q^2) + \tau F_2^2(Q^2)\right) + 2\tau\left(F_1(Q^2) + F_2(Q^2)\right)^2 \tan^2\frac{\theta_e}{2}\right]\delta\left(\nu - \frac{Q^2}{2M}\right), \tag{1.2}$$

where E and E' are the initial and final lepton energies, $\nu = E - E'$, θ_e is the lepton scattering angle in the target rest frame, $\tau = Q^2/4M^2$ is a kinematical factor, $\sigma_M = (4e^2/16\pi^2 Q^4)E'^2\cos\frac{\theta_e}{2}$ is the Mott cross section for Coulomb elastic scattering on a point-like particle (it is the relativistic counterpart of σ_R) and $F_{1/2}(Q^2)$ are the so-called Dirac and Pauli form factors which encode the additional information and whose Q^2-dependence means that a deviation from the pure point-like behaviour has set in. Friedmann, Kendall and Taylor at SLAC studied the same inclusive scattering of electrons on nucleons ($ep \to eX$) but in a particular regime (deep inelastic regime) drawing some important conclusions. In the proton rest frame, the transferred energy and momentum are $\nu = E - E'$ and $Q^2 = 4EE'\sin^2(\theta_e/2)$; defining the adimensional variable (Bjorken-x) $x_B = Q^2/2p\cdot q$, the deep inelastic regime is specified by the following conditions

$$\text{DIS} \quad \text{regime} \; = \left\{ \begin{array}{cc} \nu \to \infty \\ |q^2| \to \infty \\ x_B \quad \text{const.} \end{array} \right\}. \tag{1.3}$$

The relativistic invariant x_B represents a index of the inelasticity of the process and has support between $[0, 1]$. The elastic limit is reached when $x_B = 1$.

In a completely general way the cross section for the inelastic reaction can be expressed as

$$\frac{d^2\sigma}{d\Omega dE'} = \frac{\alpha^2}{q^4}\frac{E'}{E}L_{\mu\nu}W^{\mu\nu}, \tag{1.4}$$

where

$$L_{\mu\nu}(k,k') = \frac{1}{2}\text{Tr}(\gamma_\alpha k'^\alpha \gamma_\mu \gamma_\beta k^\beta \gamma_\nu) = 2\left(k'_\mu k_\nu + k_\mu k'_\nu - \frac{Q^2}{2}g_{\mu\nu}\right), \tag{1.5}$$

and

$$W_{\mu\nu}(q,p) = -\left(g_{\mu\nu} - \frac{q_\mu q_\nu}{q^2}\right)W_1(Q^2,\nu) + \left(p_\mu - q_\mu\frac{p\cdot q}{q^2}\right)\left(p_\nu - q_\nu\frac{p\cdot q}{q^2}\right)\frac{W_2(Q^2,\nu)}{M^2}, \tag{1.6}$$

are the leptonic and the hadronic tensor, respectively; and where we have indicated by means of p the nucleon 4-momentum and with k, k' the initial and final 4-momenta of the lepton. With the unpolarized leptons the formulae (1.5) and (1.6) represent the more general expression for the leptonic and hadronic tensor of the process, respecting conservation laws and invariance

under parity and time-reversal operations. W_1 and W_2 are unknown functions that describe the structure of the target. Contracting the two tensor Eq. (1.4) becomes

$$\frac{d^2\sigma}{d\Omega dE'} = \sigma_M \left[W_2 + 2W_1 \tan^2 \frac{\theta_e}{2} \right], \tag{1.7}$$

in which the two (structure) functions $W_{1,2}$ depend in general on the two indipendent variables Q^2 and ν.

The analysis of experimental results obtained by the groups lead by Friedman, Kendall and Taylor showed evidences of the so-called *scaling* phenomenon. This discovery was of great conceptual relevance. In DIS regime, i.e. at high energy and transferred momentum, keeping fixed x_B, the structure functions were no more dependent on Q^2 and ν independently, but rather exhibited a dependence on the adimensional Bjorken variable. This suggested a possible interpretation of the process as if the external probe was scattered through elastic collisions on elementary constituents of the target (in analogy with the Rutherford experiment with α particles), as we can understand from the definition of x_B and from the well-known elastic cross section on point-like Dirac target

$$\frac{d\sigma}{d\Omega} = \sigma_M \frac{E'}{E} \left[1 + 2\tau \tan^2 \frac{\theta_e}{2} \right] \delta \left(\nu - \frac{Q^2}{2M} \right). \tag{1.8}$$

Indeed, comparing Eq. (1.7) with Eq. (1.8) we can write down an explicit form of the Bjorken scaling as

$$\begin{aligned} 2MW_1(Q^2;\nu) &\rightarrow x_B \delta(1 - x_B) \equiv F_1(x_B), \\ \nu W_2(Q^2;\nu) &\rightarrow \delta(1 - x_B) \equiv F_2(x_B). \end{aligned} \tag{1.9}$$

This experimental breakthrough allowed to represent the lepton-hadron scattering as an incoherent sum of elastic scatterings on point-like particles inside the target. The observation of the DIS *scaling* was the first indirect dynamical evidence of the existence of elementary constituents in the nucleon, and is at the origin of the concept of '*parton*'.

The simplest explanation of scaling, already predicted by Bjorken using currents algebra and Regge asymptotics [8], came from Feynman's *parton* model [9], where the nucleon was assumed to consist of point-like constituents. The essence of the model can be summarized in this way. In a DIS process the hadronic target is represented as composed of a generic number n of partons, i.e. point-like virtual almost free particles, each one carrying a certain fraction x of the parent hadron 4-momentum. At high Q^2, the leptonic probe flies through the target in very short times, and the mean lifetime of the virtual states is further dilated though relativistic effects. Hence the nucleon in the process appears as 'freezed', and the partons are almost real (i.e. almost on shell). At high energies, moreover, the spatial resolution of the probe increases, so that the Born approximation (γ interacting with a parton only) does not seem a too crude hypothesis. Another fundamental hypothesis on which the

parton model is based is *factorization*. Supposing that initial partons correlations and final hadronization/ricombination processes are characterized by temporal scales much longer than those pertaining to the elementary scattering it is possible to factorize the hard electromagnetic interaction (calculable in perturbative QED) from the soft low energy processes describing the partonic structure of hadrons in the initial and final states. Under such an assumption the cross-section of the process can be written as a *convolution* of an elementary cross section $d\sigma^{el}$, describing the elastic interaction of the lepton with a parton of momentum xp (p the hadron 4-momentum) with proper distributions $q_f(x)$, thought of as probability densities of finding a parton with flavour f and carrying a momentum fraction x. The elementary cross-section $d\sigma^{el}$ is specific for the considered process, is theoretically calculable and does not depend on the target, while the parton distribution functions*, $q_f(x)$, describe the structure of the target, hence are *universal*, that means 'process independent', and can be extracted from the experimental data on different processes involving the same target. Thus the convolution describing the total cross-section reads

$$\frac{d^2\sigma}{d\Omega dE'}(P,q) = \sum_{a=f,\bar{f}} \int_0^1 dx \frac{d^2\sigma^{el}}{d\Omega dE'}(xp,q) q_a(x). \tag{1.10}$$

The elementary cross section can be derived postulating that partons are Dirac spin 1/2 particles of mass m. The hadronic tensor for a particle of 4-momentum p is

$$2mW^{el\mu\nu} = \frac{1}{2\pi} \int \frac{\mathrm{d}^3p'}{16\pi^3 2p'_0} (2\pi)^4 \delta^4(p+q-p') H^{el\mu\nu}, \tag{1.11}$$

$$H^{el\mu\nu} = e_f^2 2[p'^{\mu}p^{\nu} + p'^{\nu}p^{\mu} + g^{\mu\nu}(m^2 - p'\cdot p)], \tag{1.12}$$

while the leptonic tensor is given by Eq. (1.5). Finally the elementary cross-section reads

$$\frac{d^2\sigma^{el}}{d\Omega dE'} = \sigma_M \left[e_f^2 \frac{x}{\nu} + e_f^2 \frac{x_B}{M} \tan^2(\theta/2) \right] \delta(x - x_B), \tag{1.13}$$

The r.h.s of Eq. (1.10) in this regime can be written as:

$$\frac{d^2\sigma}{d\Omega dE'}(p,q) = \sigma_M \left[\frac{1}{\nu} F_2(x_B) + \frac{1}{M} F_1(x_B) \tan^2(\theta/2) \right]. \tag{1.14}$$

Substituting the two previous results in Eq. (1.10) we finally get the expression for the DIS structure functions in terms of partonic densities:

$$2x_B F_1(x_B) = F_2(x_B) = x_B \sum_{a=f,\bar{f}} e_a^2 q_a(x_B), \tag{1.15}$$

*The parton distribution function represent the probability of finding a parton with a fraction x of the longitudinal momentum of the parent nucleon. Two useful and widely adopted definitions are those of valence and sea quarks distributions: the first is given by $q_f^v(x) = q_f(x) - \bar{q}_f(x)$ and represents what remains after removing the virtual quark-antiquark pairs contributions coming from vacuum polarization, while the second just represents these very contributions, thus verifying $q_f(x) = q_f^v(x) + \bar{q}_f^{sea}(x)$.

where the first equality is called the Callan-Gross relation [10]. This has a great conceptual importance: decomposing the inelastic cross section on a spherical basis, we see that the Callan-Gross relation is equivalent to the request that in DIS regime the ratio $R = W_L/W_T$ between the response functions for longitudinal (W_L) and transverse (W_T) virtual photon polarizations goes to zero, since it is

$$F_2(x_B) = 2x_B F_1(x_B)\left(\frac{1+R}{1+2Mx/\nu}\right) \;\rightarrow\; 2x_B F_1(x_B), \;\text{ for }\; R \to 0, \nu \to \infty;$$

the $R \to 0$ DIS behaviour is indeed a well verified experimental fact, and the vanishing of the longitudinal response is a typical behaviour of a spin 1/2 particle (provided any parton transverse momentum in the infinite momentum frame can be neglected). Indeed, as the photon momentum is space-like we can Lorentz boost to a frame (Breit frame) with $E_\gamma = \nu = 0$, so that the photon carries no energy but only a longitudinal momentum Q; if the longitudinal proton momentum is $Q/2x_B$, only those quarks with momentum fraction $y = x_B$ can absorb the photon and conserve momentum, so that the interaction flips their longitudinal momentum from $-Q/2$ to $+Q/2$, so the structure functions are proportional to the density of partons with fraction x_B in the nucleon, weighted with the squared charge. Moreover, the helicity of a massless parton is conserved in vector or axial interactions, so the flipping of momentum requires that also the parton 1=2 spin is flipped; since the process is collinear (no orbital contribution), only transverse photons (helicity ± 1) can be absorbed, hence W_L must vanish in this case. If the partons were spin zero only longitudinal photons would instead contribute, so $W_T \to 0$.

The Feynman's Quark Parton Model (QPM) is surely a good model for the structure of the nucleon. Remarkably, such a simple picture explained many of the qualitative features of DIS experiments receiving many experimental confirmation during the years. However, it also presents serious unescapable limitations, evidenced for example by the so-called sum rules, integral relations that link parton distributions to known constants; of particular relevance is the momentum sum rule ($\sim$ means quark c neglected and $\theta_C \simeq 0$, no Cabibbo mixing)

$$\int_0^1 \mathrm{d}x \left[\frac{9}{2}\Big(F_2^{e^-p}(x) + F_2^{e^-n}(x)\Big) - \frac{3}{4}\Big(F_2^{\nu p}(x) + F_2^{\nu n}(x)\Big)\right] \sim \int_0^1 \mathrm{d}x x(u + \bar{u} + d + \bar{d} + s + \bar{s}) \doteq 1 - \epsilon, \tag{1.16}$$

with u, d and s the parton densities for the specified flavours (and the same for the antiquarks); experimental data pointed to a value of ϵ around 0.54-0.56, and that proves how only about a half of the nucleon momentum is indeed given by the quarks and antiquarks contributions, while the missing part is attributed to other neutral partons, without electro-weak interactions,

not included in the QPM and later identified with the gluons, i.e. the vector gauge bosons mediating strong interactions in QCD.

Furthermore, there was a compatibility problem concerning the relation between the CQM, which was able to reproduce many features of the low energy hadrons spectra, and the QPM, introduced as a dynamical model and based on the observation of DIS scaling at high energies: Feynman partons are spin 1/2 particles with fractional charge and flavour, as static quarks, but they have definitely smaller masses ($\simeq 0$) if compared with the about 300 MeV ($\simeq$ nucleon mass/3) postulated in CQM, and moreover constituent quarks appeared confined in hadrons while Feynman partons seemed to behave as quasi-free partons. For the identification of these two objects to hold, in order to have a bridge between these two pictures of the nucleon, the underlying exact QFT must show a strong dependence of its coupling constant from the involved energy scale Q^2. This and others fundamental features, such as the existence of the neutral gluons, are at the basis of Quantum Chromo-Dynamics (QCD), the QFT for the strong interactions, which among other successes and achievements manages in recovering the QPM as the first order approximation in a perturbative (only reliable at high energies) expansion in powers of the coupling constant α_s, while at the same time it predicts a colour confinement at low energies and momenta, thus justifying the basic hypothesis of the CQM. Indeed, using the theory of the *renormalization group*, it could be shown that the renormalized coupling constant varied with energy scale. At increasingly high energies, α_s becomes smaller and smaller, so that the quarks can be treated as if they were free point-like particles in the asymptotic domain. This effect was called *asymptotic freedom*. By means of a general analysis it is possible to see that non-Abelian gauge theories, like QCD, were the only field theories in which asymptotic freedom was exhibited.

1.2 Quantum Chromo-Dynamics

In the second half of the XX century, a guiding principle was defined to build renormalizable, namely predictive, QFTs: the gauge principle, that is the request of invariance of the Lagrangian density and hence of the related equation of motions under a certain group of local transformations, i.e. transformations depending on the space-time point of application. Historically, gauge invariance was first applied to electromagnetic interactions, requiring the Lagrangian of a free spinor field to be invariant under local phase transformations of $U(1)$: to realize this the introduction of an auxiliary vector gauge field, identified with the photon and interacting with the fermion, was necessary, producing the same result as the well known minimal substitution procedure and generating a conserved (electric) charge. The resulting QED was a perturbative theory, whose results were given as series in powers of the (small) coupling constant $\alpha_{e.m.}$, so that higher order contributions are nothing but small corrections to the first order (tree level) result and the theory has a strong predictive power,

though after a proper renormalization. The same principle can be extended to non-Abelian groups, i.e. groups with non-commutating Lie algebra generators, or to Yang-Mills gauge theories [11] (based on local SU(N)) with spontaneous symmetry breaking (SSB), where the ground state shares only part of the complete symmetries of the Lagrangian. In 1971, a dramatic discovery was made by t'Hooft [12]. Building on earlier pioneering works by Veltmann, Fadeev, Higgs and other, he showed that Yang-Mills gauge theory was renormalizable even when its symmetry group was "spontaneously broken". With this breakthrough, it became possible to write down renormalizable theories of weak interactions. An earlier gauge theory of Weinberg [29] and Salam [14] based on the symmetry group $\mathrm{SU}(2)_L \otimes \mathrm{U}(1)_Y$ was resurrected and gave rise to the electro-weak unification, where the SSB allowed for the generation of the fermions and gauge bosons masses by means of the Higgs-Kibble mechanism [15]. For strong interactions, the evidence of the three colours pointed at the SU(3) group as a good candidate, while the belief that gluons are massless suggested to consider an exact, i.e. not spontaneously broken, theory: the fundamental representation of the group is a colour triplet of fermion (quark) Dirac fields $\psi_f(x) = (\psi_R(x); \psi_G(x); \psi_B(x))^T$. ψ_f is the field operator for a quark of flavour f and mass m_f, in three possible colours (red, green e blue), and the most general colour local gauge transformation reads

$$\psi(x) \to e^{i\theta^a(x)t^a}\psi(x) \equiv U(x)\psi(x), \qquad [t^a, t^b] = if^{abc}t^c, \tag{1.17}$$

where $\theta^a(x)$ are eight real functions and we have explicitly indicated the non-commutative SU(3) Lie algebra of the generators of the unitary transformations that mix quarks with different colours. The request of gauge invariance naturally gives origin to the concept of covariant derivative, which forces the introduction of eight additional Lorentz vector (i.e. spin 1) fields, the gluons A^a_μ which mediate the strong force, and generate interaction terms between these gauge fields and the quark spinors, through the coupling g_s:

$$D_\mu \equiv \partial_\mu - ig_s A^a_\mu t^a. \tag{1.18}$$

Under colour SU(3) transformations the gauge fields have to change so that D_μ transforms exactly under the action of $U(x)$, in such a way to render the term $\bar{\psi}(x)i\gamma^\mu D_\mu \psi(x)$ a gauge invariant object:

$$A^a_\mu(x)t^a \longrightarrow U(x)\left(A^a_\mu(x)t^a + \frac{i}{g_s}\partial_\mu\right)U^\dagger(x), \tag{1.19}$$

and their dynamical content is described by the gauge invariant term

$$F^a_{\mu\nu}F^{a\mu\nu}, \qquad \text{with} \qquad F^a_{\mu\nu} = \partial_\mu A^a_\nu - \partial_\nu A^a_\mu + g_s f^{abc}A^b_\mu A^c_\nu. \tag{1.20}$$

We notice that the last term in the field tensor (absent in abelian theories, such as QED, where the structure functions f^{abc} vanish) is at the origin of possible gluons self-interactions; these gauge bosons are massless, because a

mass term like $A^a_\mu A^{a\mu}$ in the Lagrangian would break gauge invariance, and we are also excluding SSB. The Lagrangian density, invariant in form under the simultaneous action of the transformations in Eqs. (1.17) and (1.19), is given by the following expression

$$\mathcal{L}_{QCD} = \bar{\psi}(x)\Big(i\gamma^\mu D_\mu - m\Big)\psi(x) - \frac{1}{4}F^a_{\mu\nu}F^{a\mu\nu}, \tag{1.21}$$

and it generates all the Feynman rules to calculate various elementary processes. The crucial aspects of QCD, as a renormalizable non-abelian gauge QFT, is the acknowledgement, achieved in '73[†] by Gross and Wilczek [17], and independently by Politzer [18], that its coupling constant decreases with increasing Q^2, and this *asymptotic freedom* perfectly fits with the observations emerged in SLAC experiments on DIS processes, and furthermore it justifies the basic assumptions of the QPM. The running of a gauge theory coupling is one of the results of the renormalization process, necessary to obtain finite quantities for observables whose calculation involves ultraviolet (UV) divergences connected with virtual loop processes, intimately connected with the tree level ones. Usually, a regularization scheme is first applied to divergent diagrams, and then the theory is renormalized by a subtle redefinition of some of the theory parameters, through proper counterterms. The result is a finite theory, which however presents an additional dependence on a spurious reference mass scale μ_R, at which the counterterms are calculated. The invariance of physics under changes of the arbitrary scale μ_R produces the Callan [19]-Symanzik [20] renormalization group equations (RGE) for the general (renormalized) Green function G:

$$\mu_R \frac{\mathrm{d}}{\mathrm{d}\mu_R} G = 0 \qquad \Rightarrow \qquad \left[\mu_R \frac{\partial}{\partial \mu_R} + \beta(g_s)\frac{\partial}{\partial g_s} + \gamma(g_s)\right] G = 0, \tag{1.22}$$

where γ is the anomalous field dimension and the β function is given by

$$\frac{\mathrm{d}}{\mathrm{d}\log(q^2)}\alpha_s(q^2) = \beta(\alpha_s), \tag{1.23}$$

thus it determines the behaviour of the strong coupling constant α_s with varying Q^2 scale. The crucial difference between QED and QCD stands in the sign of β. For QED is $\beta > 0$, meaning that the coupling is small at low Q^2-high distances (because the virtual fermion loops screen the bare charge), while at increasing energies (i.e. at smaller distances) the better spatial resolution allows to see the bare non-renormalized charge and the coupling tends to diverge. For QCD, by contrast, it is $\beta < 0$: the gluon self-interactions bring

[†]For a nice and pleasant historical introduction to the discovery of asymptotic freedom read:
M. Shifman, *Historical curiosity: how asymptotic freedom of the Yang-Mills theory could have been discovered three times before Gross, Wilczek, and Politzer, but was not*, p. 126 ff in [16].

about another (dominant) effect, i.e. the spreading of colour charge through the anti-screening connected with virtual gluons loops, so that now the coupling constant α_s increases for decreasing Q^2. We just report the general solution of Eq. (1.22), that can be put in the form

$$G \equiv F(t, \alpha_s) = F(0, \alpha_s(t)) \exp \int_{\alpha_s(0)}^{\alpha_s(t)} \mathrm{d}\alpha' \frac{\gamma(\alpha')}{\beta(\alpha')}. \tag{1.24}$$

As far as *confinement* is concerned, QCD cannot prove it, because of the loss of reliability of the perturbative approach at low energies, but it does neither exclude it, and rather it seems to be a natural consequence of the raising of the interaction strength at low Q^2. Better approaches in this direction are lattice QCD simulations and chiral effective theories.

Disposing of a rigorous quantum field theory for strong interactions, though with predictive power limited to the region of high energies, allows one to enlarge the field of research and to improve the agreement between the parton model results and the available experimental data. There are indeed many evidences that would require the introduction of proper corrections to QPM to be adequately understood: the already remembered sum rules, the parton distributions shape for $x_B \to 0$ (where gluons and sea quarks contributions become dominant), the scaling violations of the DIS structure functions (see Fig. 1.1) are only some examples of this kind of problematic topics. Concerning scaling violations, it is clear from the analysis of the experimental data that even in the Bjorken region the structure functions do not show perfect scaling, but rather present a weak Q^2-dependence, and therefore so do the quark distribution functions, which should then be indicated as $q(x, Q^2)$. The experimental data show how this variation of the structure functions, or scaling violation, is essentially logarithmic. Its understanding requires to go beyond the naive parton model to QCD. Suppose we assume that the wavefunction of the target has no high-momentum components (i.e. $p_T^2 \ll Q^2$). Then any Q^2-dependence can only come from the lepton-quark scattering process. Scaling results if the quark is treated as a point-like particle, and the trivial Q^2-dependence of the Mott cross section is factored out; on the other hand, in an interacting field theory as QCD the lepton-quark scattering will necessarily involve the so-called radiative corrections. As a matter of fact, we have just recalled how the creation of a reliable and meaningful QFT requires a proper renormalization process, in order to cancel the UV divergences connected with the absence of physical cutoffs on the momenta of the virtual particles involved in quantum loops diagrams (e.g.: wavefunctions and vertex renormalization) and to obtain finite quantities to be compared with experimental data. However, besides this kind of radiative corrections and corresponding divergences, in QCD (exactly as in QED) one must face also other sources of singularities, connected with other types of radiative processes: for practical purposes, we cannot separate e.g. the diagram for the scattering of an e^- off a quark from the analog graph in which moreover the same quark emits a soft gluon, that is a gluon whose

energy is below the detection threshold of a realistic instrument (or maybe a collinear gluon with respect to the emitting quark, so that the two particles are difficult to distinguish and resolve). This collinear soft radiation produces infrared (IR) divergences in the cross section of the $e^- - q$ scattering process; they can be partially canceled, when all diagrams of equal order, including those involving virtual gluons exchange, are considered, while another part of them are reabsorbed in the parton distributions through an operative redefinition of these unknown functions, depending on the factorization scale μ_F at which a given process takes place. By consequence, the parton densities develop a logarithmic dependence on the appropriate cutoff scale, in this case Q^2, which represents a (although weak) scaling violations: for example, $u(x, Q^2)$ now represents the numerical density of up quarks with momentum fraction x in the proton, when this one is probed with a spatial resolution determined by Q^2. At low Q^2 the resolution is too poor to distinguish the internal structure of the hadron, so that in this regime we expect the structure functions to be dominated by valence quarks, thus having their leading contribution for $x \sim 1/3$ (in the proton). At high Q^2, in contrast, we gain a sufficient resolution to 'see' virtual $q\bar{q}$ sea pairs and gluon emission processes, so that for increasing Q^2 the hadron momentum is shared by an increasing number of partons, so the F_2 function peak moves towards smaller x, where sea quarks and gluons distributions dominate. The net result is a violation of pure scaling, since now F_2 does not depend only on x but also on Q^2. The very good agreement of this picture with the experimental data on DIS scaling violations is certainly one of the main successes of perturbative QCD.

The Q^2-evolution of parton distributions is calculable in perturbative QCD and is described by the well known Dokshitzer-Gribov-Lipatov-Altarelli-Parisi (DGLAP) equations [21], which are coupled equations for the distributions of a quark (flavour q) and of a gluon in a hadron:

$$\begin{aligned}
\frac{\partial}{\partial \ln Q^2} q(x,Q^2) &= \frac{\alpha_s}{2\pi} \int_x^1 \frac{\mathrm{d}y}{y} \left[P_{qq}\left(\frac{x}{y}\right) q(y,Q^2) + P_{qg}\left(\frac{x}{y}\right) g(y,Q^2) \right], \\
\frac{\partial}{\partial \ln Q^2} g(x,Q^2) &= \frac{\alpha_s}{2\pi} \int_x^1 \frac{\mathrm{d}y}{y} \Bigg[P_{gq}\left(\frac{x}{y}\right) \left[q(y,Q^2) + \bar{q}(y,Q^2) \right] \\
&\qquad + P_{gg}\left(\frac{x}{y}\right) g(y,Q^2) \Bigg]. \qquad (1.25)
\end{aligned}$$

The P functions, which are known in QCD up to the third perturbative order, are called Altarelli-Parisi vertices or splitting functions, and their physical meaning is clear: $P_{qq}(z)$ represents for instance the probability for a quark q with a certain momentum fraction y to emit a gluon, thus rescaling its momentum faction to $x = zy$, with $0 \leq z \leq 1$. They are intrinsic process independent properties of QCD. These functions are of particular importance concerning the problem of hard/soft factorization, since, once a factorization scale μ_F is fixed, they determine the parton densities evolution with varying Q^2 , i.e. their partonic content, separating the contributions at scales $Q^2 < \mu_F^2$ (possibly di-

vergent, reabsorbed in a redefinition of the parton distribution) from those at scales $Q^2 > \mu_F^2$ (non-divergent and computed as radiative/perturbative corrections to the hard vertex of the process), which are also called Wilson coefficients. DGLAP are first order integro-differential equations, so once the parton distributions at a certain initial scale Q_0^2 are given they allow to calculate the evolution of these ones at any other scale to which the perturbative expansion still keeps being applicable.

Let's now analyze in better detail the effect of radiative corrections in QCD, in order to give a formal dress to the previous intuitive considerations. Defining $t \equiv \ln(Q^2/\mu_R^2)$, a generic DIS structure function can be written, admitting a possible Q^2 dependence, as

$$F(x,t) = \int_x^1 \frac{\mathrm{d}y}{y} q_0(y) \sigma_{point}\left(\frac{x}{y}, \alpha_s(t)\right) + O\left(\frac{1}{Q^2}\right), \tag{1.26}$$

where the first integral, involving the 'bare' parton distribution q_0 and the elementary cross section for the scattering of the leptonic probe off a point-like quark σ_{point}, represents the perturbative part of F, since it implicitly contains the perturbative series defining the running coupling constant $\alpha_s(t)$ (in powers of $\ln(Q^2/\Lambda_{QCD}^2)$), while the nonperturbative part has been simply indicated through the $O(1/Q^2)$ term, and indeed it admits an expansion in powers of the inverse hard scale $1/Q^2$, a procedure formalized by the so-called Operator Product Expansion (OPE) and depending on the twist expansion parameter [22]. At tree level, one can see that, defining $z = x/y$, the elementary cross section has the form

$$\sigma_{point}(z, \alpha_s(t)) = \sigma_{point}(z) = e^2 \delta(z-1), \tag{1.27}$$

i.e. only quarks with momentum fraction $y = x$ (here x coincides with the kinematical Bjorken variable x_B) can absorb the virtual photon, so that the naive parton model result for the structure function, with perfect scaling (i.e. t-independence) is recovered ($\delta(x/y - 1) = y\delta(x - y)$):

$$F(x,t) = F(x) = e^2 q_0(x). \tag{1.28}$$

Including also possible radiative processes, that is diagrams in which the active quark emits a gluon before or after the interaction with the lepton, one can show that the elementary cross section gets modified in

$$\sigma_{point}(z, \alpha_s(t)) = e^2 \left[\delta(z-1) + \frac{\alpha_s(t)}{2\pi}\left(tP(z) + f(z)\right)\right], \tag{1.29}$$

where the P functions encodes the information about the $q-g$ splitting vertex and f includes all the terms that are finite for $z \to 1$ (soft gluon limit); it can be both $y = x$ (virtual or sub-threshold gluons) or $y > x$ (real gluons, carrying away a $(y-x)$ momentum fraction); by studying the explicit form of this cross section (i.e. of P), one can recognize that the involved infrared divergences (for

the gluon energy $E_g \approx 0 \Rightarrow z \approx 1$) are canceled in the sum of the Born tree level-virtual gluon emission interference term with the real sub-threshold gluon emission contribution (Bloch-Nordsieck theorem [23]). In the limit of vanishing quark mass there are also collinear divergences ($\Theta_{q-g} \approx 0$): those related to the emission of a gluon by the quark after the electromagnetic vertex with the virtual photon are indeed canceled in the inclusive sum over the final states which are degenerate in the limit $m \to 0$ (Kinoshita-Lee-Nauenberg (KLN) Theorem [25]); the final result is that the elementary cross section acquires a logarithmic dependence on the scale of the process, $\sigma_{point} \sim \ln(Q^2/m^2)$. Nevertheless, the KLN theorem is not active for those collinear divergences linked to the emission of a gluon by the quark *before* the interaction with the γ^*: the usual way to deal with such a problem is to perform a factorization of the collinear divergences of the initial quark through a redefinition of the 'bare' scale-independent parton density q_0:

$$q_0(y) \to q(y,t) \equiv q_0(y) + \Delta q(y,t), \quad \text{with} \quad \Delta q(y,t) \equiv \frac{\alpha_s(t)}{2\pi} t \int_y^1 \frac{\mathrm{d}y'}{y'} q_0(y') P\left(\frac{y}{y'}\right); \tag{1.30}$$

now $q(y,t)$ is intrinsically t-dependent and thus introduces scaling violations. The DIS structure function gets modified as follows (at order $\alpha_s(t)$):

$$F(x,t) = \int_x^1 \frac{\mathrm{d}y}{y} q(y,t) e^2 \left[\delta(z-1) + \frac{\alpha_s(t)}{2\pi} f(z)\right], \tag{1.31}$$

as a matter of fact (with $z = x/y$):

$$\begin{aligned}
& \int_x^1 \frac{\mathrm{d}y}{y} q(y,t) e^2 \left[\delta\left(\frac{x}{y} - 1\right) + \frac{\alpha_s(t)}{2\pi} f\left(\frac{x}{y}\right)\right] \\
= & \int_x^1 \frac{\mathrm{d}y}{y} \left[q_0(y) + \frac{\alpha_s}{2\pi} t \int_y^1 \frac{\mathrm{d}y'}{y'} q_0(y') P\left(\frac{y}{y'}\right)\right] e^2 \left[\delta\left(\frac{x}{y} - 1\right) + \frac{\alpha_s(t)}{2\pi} f\left(\frac{x}{y}\right)\right] \\
= & \int_x^1 \frac{\mathrm{d}y}{y} q_0(y) e^2 \left[\delta\left(\frac{x}{y} - 1\right) + \frac{\alpha_s(t)}{2\pi} f\left(\frac{x}{y}\right) + \frac{\alpha_s(t)}{2\pi} t P\left(\frac{x}{y}\right)\right] + o\left(\alpha_s(t)\right) \\
= & \int_x^1 \frac{\mathrm{d}y}{y} q_0(y) \sigma_{point}\left(\frac{x}{y}, \alpha_s(t)\right) + O(\alpha_s(t)) = F(x,t) + O\left(\alpha_s(t)\right),
\end{aligned} \tag{1.32}$$

where σ_{point} is that of Eq. (1.29) and we performed the integrals of the delta functions regardless of the fact that the integration domain is finite (this is an acceptable approximation). Eq. (1.31) directly implies that we can now write

$$F(x,t) = e^2 q(x,t) + O(\alpha_s(t)), \tag{1.33}$$

so that, comparing this last expression with the naive parton model one of Eq. (1.28), we conclude that at leading order (LO), i.e. to the lowest order in α_s, we exactly recover our previous parton model result, but now in terms of scale-dependent parton distribution functions (so that perfect scaling is hopeless lost). Furthermore, deriving $q(x,t)$ with respect to the t variable we can

find out the evolution equation of our new parton density with varying Q^2 scale:

$$\begin{aligned}\frac{\mathrm{d}}{\mathrm{d}t}q(x,t) &= \frac{d}{dt}\left(q_0(x)+\frac{\alpha_s(t)}{2\pi}t\int_x^1\frac{\mathrm{d}y}{y}q_0(y)P\left(\frac{x}{y}\right)\right)\\ &= \frac{\alpha_s(t)}{2\pi}\int_x^1\frac{\mathrm{d}y}{y}q_0(y)P\left(\frac{x}{y}\right)+O(\alpha_s^2(t))\\ &= \frac{\alpha_s(t)}{2\pi}\int_x^1\frac{\mathrm{d}y}{y}\left(q(y,t)-\Delta q(y,t)\right)P\left(\frac{x}{y}\right)+O(\alpha_s^2(t)),\end{aligned} \tag{1.34}$$

having used the fact that $\mathrm{d}\alpha_s(t)/\mathrm{d}t \equiv \beta(\alpha_s(t)) = -b\alpha_s^2(t)+\ldots$, and recalling that $\Delta q(y;t)$ is itself proportional to $\alpha_s(t)$, its contribution in the last expression can be embedded in the generic $O(\alpha_s^2(t))$ term, so the final result is

$$\frac{\mathrm{d}}{\mathrm{d}t}q(x,t) = \frac{\alpha_s(t)}{2\pi}\int_x^1\frac{\mathrm{d}y}{y}q(y,t)P\left(\frac{x}{y}\right)+O(\alpha_s^2(t)), \tag{1.35}$$

where P is the Altarelli-Parisi function describing the splitting of a quark in a quark plus a gluon. Considering also the gluon density $g(x,t)$, this latter result is immediately generalizable, thus recovering the DGLAP equations. The last equation is an integro-differential evolution equation of difficult solution, but it can be simplified noticing that it indeed becomes an ordinary differential equation for the Mellin moments of the parton densities,

$$q_n(t) \equiv \int_0^1 dx x^{n-1}q(x,t). \tag{1.36}$$

As a matter of fact, we can write (neglecting $O(\alpha_s^2(t))$ terms)

$$\frac{d}{dt}q_n(t) = \int_0^1 \mathrm{d}x x^{n-1}\frac{d}{dt}q(x,t) = \int_0^1 \mathrm{d}x x^{n-1}\frac{\alpha_s(t)}{2\pi}\int_x^1\frac{\mathrm{d}y}{y}q(y,t)P\left(\frac{x}{y}\right), \tag{1.37}$$

and at this point we should notice that $\int_0^1 \mathrm{d}x\int_x^1 \mathrm{d}y\cdots = \int_0^1 dy\int_0^y \mathrm{d}x\ldots$, so that introducing the new variable $z \equiv x/y$ ($x=y \Rightarrow z=1$) the previous expression becomes

$$\frac{\mathrm{d}}{\mathrm{d}t}q_n(t) = \frac{\alpha_s(t)}{2\pi}\left[\int_0^1 \mathrm{d}y y^{n-1}q(y,t)\right]\left[\int_0^1 \mathrm{d}z z^{n-1}P(z)\right] = \frac{\alpha_s(t)}{2\pi}P_n q_n(t); \tag{1.38}$$

by using $\mathrm{d}\alpha_s(t)/\mathrm{d}t \equiv \mathrm{d}\alpha'/\mathrm{d}t = \beta(\alpha') = -b\alpha'^2+\ldots$ we can solve the previous ordinary differential equation thus finding out the DGLAP solution in terms of Mellin moments of the parton density $q(x;t)$, that is, in the parton model (identified with QCD@LO), of the structure function $F(x,t) = e^2q(x,t)$:

$$q_n(t) = \left[\frac{\bar{\alpha}_s}{\alpha_s(t)}\right]^{\frac{P_n}{2\pi b}}q_n(0), \qquad \left(b = \frac{11n_c-2n_F}{12\pi}\right) \tag{1.39}$$

where $\bar{\alpha}_s$ denotes the coupling constant at the initial considered scale (and $P_n/2\pi b$ is often called *anomalous dimension*). The connection of these considerations with the renormalization group formalism is obtained by exploiting the Operator Product Expansion techniques [24]: through the analiticity properties of the forward virtual Compton scattering amplitude one can show that the Mellin moments of DIS structure functions are related to the single terms of the OPE expansion (which is a series in powers of the inverse hard scale, $1/Q$) for the product of the two involved e.m. current operators, $J_\mu(\xi)J_\nu(0)$, and exactly to the Fourier transforms of the corresponding Wilson coefficients (of order n, $c_n(Q^2)$, for the n-th Mellin moment) multiplied by the reduced matrix elements of the associated regular local operators $\hat{O}_n$ (Momentum Sum Rule):

$$\int_0^1 \mathrm{d}x x^{n-1} F(x, Q^2) \equiv M_n(Q^2) \propto c_n(Q^2) h_n; \tag{1.40}$$

with $\langle P|\hat{O}_n^{\mu_1 \cdots \mu_n}|P\rangle = h_n p^{\mu_1} \ldots p^{\mu_n}$. The Wilson coefficients $c_n(Q^2)$ are independent of the target, and one finds that their scale evolution, which can be calculated in pQCD, encodes the whole Q^2 variation of the DIS structure functions Mellin moments $M_n(Q^2)$; on the other hand, the hadronic matrix elements can be simulated on lattice: we thus can obtain information on the M_n moments, which are the experimentally accessible quantities. Moreover, since the matrix elements of currents products satisfy the RGE, being indeed Green's functions, the same holds true for the Mellin moments M_n, related to those matrix elements by the just remembered momentum sum rule of Eq. (1.40); therefore, from the general solution of the RGE (see Eq. (1.24)), for M_n we have

$$M_n(t, \alpha_s) = c_n(t = 0, \alpha_s(t)) \exp\left(\int_{\bar{\alpha}_s}^{\alpha_s(t)} \mathrm{d}\alpha' \frac{\gamma_n(\alpha')}{\beta(\alpha')} \right) h_n(\alpha_s), \tag{1.41}$$

at the lowest order, identifying M_n with q_n and with

$$\gamma_n(\alpha') = \frac{P_n}{2\pi}\alpha' + \ldots, \quad \beta(\alpha') = -b\alpha'^2 + \ldots, \quad h_n(\alpha_s) = 1, \tag{1.42}$$

we finally have

$$q_n(t) = q_n(0) \exp\left(\int_{\bar{\alpha}_s}^{\alpha_s(t)} \mathrm{d}\alpha' \frac{\gamma_n(\alpha')}{\beta(\alpha')} \right) = \left[\frac{\bar{\alpha}_s}{\alpha_s(t)} \right]^{\frac{P_n}{2\pi b}} q_n(0). \tag{1.43}$$

We thus see that solving the RGE for the Mellin moments of DIS structure functions we recovered the previously found result for $q_n(t)$, derived as a solution of the Mellin representation of DGLAP evolution equations. This concludes our research for a connection between RGE and DGLAP equations. In all the previous considerations we referred for simplicity to non-singlet (e.g. valence) structure functions, which do not involve gluons; the Q^2- evolution

of singlet structure functions (such as F_2) is indeed more complicated, since quarks and gluon field operators mix under QCD renormalization (hence the usual 2×2 matrix formalism), but the previous conclusions remain untouched. Finally, notice that, given an analytic continuation of a set of moments $M_n(Q^2)$, there is a standard method for reconstructing the corresponding structure function F (supposed non-singlet, for simplicity), i.e. the Inverse Mellin Transform (IMT):

$$xF(x,Q^2) = \frac{1}{2\pi i}\int_{c-i\infty}^{c+i\infty} \mathrm{d}n x^{1-n} M_n(Q^2), \tag{1.44}$$

where c is chosen so that the integral exists. Using the momentum sum rule of Eq. (1.40) to express the Mellin moments $M_n(Q^2)$ in terms of Wilson coefficient functions $c_n(Q^2)$ and local operators hadronic matrix elements, the IMT $xF(x,Q^2)$ turns out to be just the convolution of the IMT of $c_n(Q^2)$ (denoted as C) and the IMT of the reduced hadronic matrix element $\langle P|\hat{O}_n|P\rangle$ (denoted as F), i.e.

$$xF(x,Q^2) = \int_x^1 \frac{\mathrm{d}y}{y} C\left(\frac{x}{y}, Q^2, \mu^2\right)\left(yF(y,\mu^2)\right), \tag{1.45}$$

having reintroduced an explicit dependence on a renormalization scale μ^2 (which was implicit in c_n and $\hat{O}_n$). This is an extremely important result: in particular, the C coefficient function is totally independent of the structure of the target, so it contains no non-perturbative information and can be treated in perturbation theory; this property is what before we have called *factorization* [26]. Clearly, if we can evaluate the structure function of the target at any renormalization scale μ^2, then Eq. (1.44) allows us to calculate it at all higher values of Q^2. Moreover, higher order QCD corrections do not alter this fundamental result, but they just make C more complex and thus harder to compute (for this reason, μ^2 cannot be too low).

1.3 Light-Front Quantum Chromo-Dynamics

The description of relativistic bound states is a great challenge for QCD. The conventional formalism is the Bethe-Salpeter (BS) formalism in which an hadron is described by a covariant wavefunction (WF) that depends upon the momenta of its partonic constituents (quarks and antiquarks). Although formally correct, this formalism is of little use in the description of such systems because the coupling of different channels, or partonic configurations, is usually large in highly relativistic systems (enough energy for the creation of many particles). For this reason typically the physics of bound states depends on the interplay between a large number of channels. A meson for instance is a superposition of states involving a $q\bar{q}$ pair, a $q\bar{q}$ pair plus a gluon, two $q\bar{q}$ pairs and so on. In the BS framework this interplay among channels is implicit since the meson is described entirely by a $q\bar{q}$ WF

$$\Psi^{BS}(k_1,k_2) = \langle 0|T\left\{\Psi(k_1)\bar{\Psi}(k_2)\right\}|M\rangle. \tag{1.46}$$

Reference to all other partonic configurations is buried inside the potential and irreducible scattering amplitudes become largely intractable. Even in situations where a single channel dominates, the formalism is still quite complicated and non-intuitive. For instance the BS wavefunction has no simple probabilistic interpretation. Because of such complications the BS formalism has been largely abandoned.

Intuitively one would like to describe hadrons in terms of a series of WFs, one for each channel, just as one would in non-relativistic quantum mechanics by means of a "Fock-state" decomposition, e.g.

$$|\pi\rangle = \sum_{q\bar{q}} \Psi_{q\bar{q}/\pi}|q\bar{q}\rangle + \sum_{q\bar{q}g} \Psi_{q\bar{q}g/\pi}|q\bar{q}g\rangle + \cdots . \tag{1.47}$$

In principle and formally this can be done by quantizing QCD at particular time, say $t = 0 = x^0$, and using the so-called creation and annihilation operators to define the basis states. This approach presents a great difficulty: the zero-particle state is not an eigenstate of the Hamiltonian. Indeed interaction terms in the Hamiltonian give contributions that create particles from the zero-particle state. As a result not all of the bare quanta in an hadronic Fock state need to be associated with the hadron (connetted); some may be disconnected and possibly quite remote elements of the vacuum. This greatly complicates the interpretation of hadronic WFs. Another difficulty is related to the Lorentz covariance of the formalism. Since the quantization surface $x^0 = t = 0$ is not invariant under boosts, boosting a state inevitably involves the dynamical evolution of parts of the state. Thus boost operators tend to create all sorts of additional quanta.

Fortunately there is a convenient and intuitive formalism, originally due to Dirac [27], that avoids these problem. This is based on the "light-cone (LC) quantization" of QCD, where the theory is quantized at a particular value of the light cone time $\tau = (t + x^3)/\sqrt{2} = (x^0 + x^3)/\sqrt{2}$, rather than at a particular time t. In this formalism the WF describes the hadron's composition at particular τ, and the temporal evolution of the state is generated by the light-cone hamiltonian: $H_{LC} \equiv P^- \equiv (P^0 - P^3)/\sqrt{2}$, conjugate to τ.
Let's give a more detailed description of LC formalism.

Dirac showed that there are three independent parameterizations of the space and time that can not be mapped on each other by Lorentz transformations and discussed three forms of Hamiltonian dynamics. In the equal-time Hamiltonian formulation of field theory, quantization conditions in the form of commutator (or anticommutaor) of dynamical fields and their conjugate momenta are specified on the space-like hypersurface $x^0 = 0$ and the Hamiltonian generates the time-evolution of the system (Dirac called it *instant form* as the kinematical part of the Lorentz group leaves the instant invariant). In the *front form*, the quantization conditions are specified on a light-like hypersurface $x^+ = (x^0 + x^3)/\sqrt{2} = 0$ (called a light-front) and the light-front (LF) Hamiltonian generates the evolution for a new time (x^+). This formulation is known as the LF Hamiltonian field theory. Another form that Dirac

mentioned is the *point form* of Hamiltonian dynamics where the quantization hypersurface is given by the hyperboloid $x^\mu x_\mu = \kappa^2$ with $x^0 > 0$ and $\kappa^2 > 0$, and the Lorentz group leaves a point invariant. In principle the three forms of relativistic dynamics are completely equivalent and so there is no a well defined guideline to decide which parameterization one should use. However, the front form has the largest stability group, the subgroup of the Poincaré group that maps the quantization hypersurface onto itself and, moreover, high energy experiments (e.g., deep inelastic scattering) probe the hadrons near the light-cone. These considerations motivate people to use LF parametrization of space and time to explore the QCD observables. One may hope that for highly relativistic systems in which cases the world-line lies very close to the light-cone, physics will be more transparent and it will be relatively easy to extract them if one uses light-front field theory.
In the context of current algebra, Fubini and Furlan [28] introduced another notion of Lorentz frame known as *Infinite-Momentum Frame* (IMF) as a limit of a reference frame moving with almost the speed of light. Weinberg [29] using old-fashioned perturbation theory for scalar meson showed that vacuum structures become simplified in the infinite-momentum limit. Later, Susskind [30] established that although the Lorentz transformation required to arrive at IMF is evidently singular ($\gamma = 1/\sqrt{1 - v^2/c^2} \to \infty$ as $v \to c$), the singularity cancels in the calculation of physical objects (like Poincaré generators) and results in an effective coordinate change given by

$$x^\pm = (x^0 \pm x^3)/\sqrt{2}, \qquad \mathbf{x}_\perp = \{x^1, x^2\}, \tag{1.48}$$

the same as the light-front coordinate we defined before. Thus, one can see that what one obtains after going through singular limiting procedure in IMF is built in quite naturally in the light front field theory. In particular it can be shown that for the DIS the standard quantum field theory with boost to the IFM is equivalent to the quantization on the light-cone. That is why, light-front field theories are also sometimes referred as field theories in the infinite-momentum frame. For a review and exhaustive list of references on light-front field theories see Ref. [31].

The inner product between two four-vectors is defined on the light front as

$$x \cdot y = x^+ y^- + x^- y^+ - \mathbf{x}_\perp \cdot \mathbf{y}_\perp. \tag{1.49}$$

In analogy with the light-front space-time variables, the light-front four momenta are defined as

$$k^\pm = (k^0 \pm k^3)/\sqrt{2}, \qquad \mathbf{k}_\perp = \{k^1, k^2\},$$

where k^- being conjugate to x^+ is the light front energy and k^+ which is conjugate to x^- is the light-front longitudinal momentum. With the above definitions, the dispersion relation, i.e., the relation between light-front energy

k^- and the spatial components of momenta $(k^+, \mathbf{k}_\perp)$, for an on mass-shell particle of mass m, is given by,

$$k^- = \frac{\mathbf{k}_\perp^2 + m^2}{k^+}. \tag{1.50}$$

One of the remarkable features of this relativistic dispersion relation is that there is no square root involved in contrast to the relativistic equal-time dispersion relation $E = \sqrt{(\vec{\mathbf{k}})^2 + m^2}$. The numerator in Eq. (1.50) being always positive implies that the particles with positive light-front energy (k^-) always carry positive longitudinal momentum ($k^+ \geq 0$). As usual, the particles with negative k^- which must have negative k^+ are mapped to antiparticles with positive k^- and k^+. As a consequence, we always have $k^+ \geq 0$ for real particles. Thirdly, k^- becomes large for the large value of $\mathbf{k}_\perp$ as well as very small values of k^+. This makes light-front renormalization aspects very different from the usual one. Lastly, the dependence on the transverse momenta $\mathbf{k}_\perp$ is just like a non-relativistic dispersion relation.

The above dispersion relation has profound consequences in the vacuum structure of light-front field theory. The vacuum state is always an eigenstate of the longitudinal momentum $\hat{P}^+|0\rangle = 0$. The positivity condition of k^+ ($k^+ \geq 0$) implies that the vacuum $|0\rangle$ is either a no-particle state or, at most can have particles with longitudinal momenta exactly equal to zero. Now, if we consider a cut-off theory where longitudinal momentum is restricted to be $P^+ = \epsilon$, the vacuum state $|0\rangle$ becomes completely devoid of any particle and therefore, an eigenstate of the full interacting Hamiltonian with zero eigenvalue. Thus, the light-front vacuum becomes trivial. As we have already noticed this result has no similarity to what happens for the equal-time case where the vacuum has highly complicated structure. In equal-time case, vacuum can contain infinite number of particles moving with positive and negative momenta adding up to zero. Another aspect of the cutoff $P^+ = \epsilon$ is that it automatically puts a restriction on the number of constituent particles a state with finite P^+ can have. A composite state with total longitudinal momentum P^+ now can have at most P^+/ϵ constituents. This again simplifies the Fock space expansion for the hadronic bound states. Again, as small k^+ means high energy (large k^-), one can hope to have a few body description for the low lying hadron states and reconcile QCD with CQM which is beyond hope in equal-time formalism.

Anyway, the advantages of light-cone quantization do not come for free. The quantization surface $\tau = 0$ is not invariant under arbitrary rotations or even under parity inversion. As a consequence the operators that generate these transformations are as complicated as the light-cone Hamiltonian, making it difficult to specify, for instance, the spin of a particular hadronic state.

1.4 Nucleon State Representation and Light-Cone Wave Functions

The representation of the nucleon state is based on the definition of a set of basis for the quantum theory. To quantize QCD on LC one defines commutators for the independent fields at a particular LC time τ. These commutation relations lead immediately to the definition of the Fock state.

Starting from the Lagrangian density for QCD (1.21) in LC physical gauge $A^+ = 0$ and at a given LC time, say $\tau = 0$, the independent dynamical fields are $\psi_\pm \equiv \Lambda_\pm \psi$ and $A^i_\perp$ with conjugate fields $i\psi^\dagger_\pm$ and $\partial^+ A^i_\perp$, where $\Lambda^\pm \equiv \gamma^0\gamma^\pm/2$ are projection operators on "good" (Λ^+), or "bad" (Λ^-) components of the field ($\Lambda_+\Lambda_- = 0, \Lambda^2_\pm = \Lambda_\pm, \Lambda_+ + \Lambda_- = 1$) and $\partial^\pm = (\partial^0 \pm \partial^3)/\sqrt{2}$. The independent dynamical variables are the good component while the other fields in $\mathcal{L}$ can be expressed in terms of ψ_+ and $A^i_\perp$ using the equations of motion:

$$\begin{aligned}
\psi_- &\equiv \Lambda_-\psi = \frac{1}{i\partial^+}\left[i\mathbf{D}_\perp \cdot \gamma^0\gamma_\perp + \gamma^0 m\right]\psi_+ \\
A^+ &= 0, \\
A^- &= \frac{2}{i\partial^+} i\partial_\perp \cdot \mathbf{A}_\perp + \frac{2g_s}{(i\partial^+)^2}\left\{\left[i\partial^+ A^i_\perp, A^i_\perp\right] + 2\psi^\dagger_+ t^a \psi_+ t^a\right\}. \qquad (1.51)
\end{aligned}$$

To quantize, we expand the fields (neglecting flavour and colour indexes for sake of clarity) at $\tau = 0$ in terms of creation and annihilation operators ($\tilde{k} = (k^+, \mathbf{k}_\perp)$),

$$\begin{aligned}
\psi_+(x) &= \int \frac{\mathrm{d}k^+ \mathrm{d}^2\mathbf{k}_\perp}{16\pi^3 k^+}\Theta(k^+)\sum_\lambda \Big\{ b(\tilde{k},\lambda)u_+(\tilde{k},\lambda)e^{-ik\cdot x} \\
&\qquad + b(\tilde{k},\lambda)u_+(\tilde{k},\lambda)e^{ik\cdot x}\Big\}, \quad \tau = x^+ = 0 \\
A^i_+(x) &= \int \frac{\mathrm{d}k^+ \mathrm{d}^2\mathbf{k}_\perp}{16\pi^3 k^+}\Theta(k^+)\sum_\lambda \Big\{ a(\tilde{k},\lambda)\varepsilon^i_\perp(\lambda)e^{-i\mathbf{k}\cdot\mathbf{x}} + \text{ h.c.}\Big\}, \quad \tau = x^+ = 0,
\end{aligned} \qquad (1.52)$$

with commutation relations:

$$\begin{aligned}
\left\{b^{c'}_{q'}(\tilde{k}',\lambda'), b^{\dagger c}_q(\tilde{k},\lambda)\right\} &= \left\{d^{c'}_{q'}(\tilde{k}',\lambda'), d^{\dagger c}_q(\tilde{k},\lambda)\right\} \\
&= 16\pi^3 k^+ \delta(k'^+ - k^+)\delta^{(2)}(\mathbf{k'}_\perp - \mathbf{k}_\perp)\delta_{q'q}\delta_{\lambda'\lambda}\delta_{c'c}, \\
\left[a^{c'}(\tilde{k}',\lambda'), a^{\dagger c}(\tilde{k},\lambda)\right] &= 16\pi^3 k^+ \delta(k'^+ - k^+)\delta^{(2)}(\mathbf{k'}_\perp - \mathbf{k}_\perp)\delta_{\lambda'\lambda}\delta_{c'c}, \\
\left\{b^{c'}_{q'}(\tilde{k}',\lambda'), b^{c}_q(\tilde{k},\lambda)\right\} &= \left\{d^{c'}_{q'}(\tilde{k}',\lambda'), d^{c}_q(\tilde{k},\lambda)\right\} = \cdots = 0,
\end{aligned} \qquad (1.53)$$

where the symbols q and c represent respectively the flavour and the colour of the quark, while λ is the quark or gluon helicity. These definitions imply

canonical commutation relations for the fields with their conjugates ($\tau = x^+ = y^+ = 0, \tilde{x} = (x^-, \mathbf{x}_\perp)$):

$$\begin{aligned} \left\{\psi_+(\tilde{x}), \psi_+^\dagger(\tilde{y})\right\} &= \Lambda_+ \delta^3(\tilde{x} - \tilde{y}), \\ \left[A^i(\tilde{x}), \partial^+ A_\perp^j(\tilde{y})\right] &= i\delta^{ij}\delta^3(\tilde{x} - \tilde{y}). \end{aligned} \tag{1.54}$$

The creation and annihilation operators define the Fock state basis for the theory at $\tau = 0$, with vacuum $|0\rangle$ defined such that $b|0\rangle = d|0\rangle = a|0\rangle = 0$.

Using the creation operators we can define a set of basis for the quantum theory:

$$\begin{aligned} &|0\rangle \\ &|q\bar{q}; \tilde{k}_i, \lambda_i\rangle = b^\dagger(\tilde{k}_1, \lambda_1) d^\dagger(\tilde{k}_2, \lambda_2)|0\rangle \\ &|qqg; \tilde{k}_i, \lambda_i\rangle = b^\dagger(\tilde{k}_1, \lambda_1) d^\dagger(\tilde{k}_2, \lambda_2) a^\dagger(\tilde{k}_3, \lambda_3)|0\rangle \\ &|q\bar{q}q\bar{q}; \tilde{k}_i, \lambda_i\rangle = b^\dagger(\tilde{k}_1, \lambda_1) d^\dagger(\tilde{k}_2, \lambda_2) b^\dagger(\tilde{k}_3, \lambda_3) d^\dagger(\tilde{k}_4, \lambda_4)|0\rangle \\ &\vdots \end{aligned} \tag{1.55}$$

where $b^\dagger, d^\dagger$ and $a^\dagger$ create bare quarks, antiquarks and gluons having three momenta $\tilde{k}_i$ and helicities λ_i. Certainly these Fock-states are generally not eigenstates of the full LC Hamiltonian, H_{LC}. However, as already stated, the zero particle state is the only one with zero total P^+, since all quanta must have positive k^+, and thus this state cannot mix with the other states in the basis. From the (anti)commutation rules in Eq. (1.53) it is easy to derive the normalization of the single-parton (quark, antiquark or gluon) momentum eigenstates created by $b^\dagger, d^\dagger$ and $a^\dagger$,

$$\langle s'; \tilde{k}', \lambda', c'|s; \tilde{k}, \lambda, c\rangle = 16\pi^3 k^+ \delta(k'^+ - k^+)\delta^{(2)}(\mathbf{k'}_\perp - \mathbf{k}_\perp)\delta_{s's}\delta_{\lambda'\lambda}\delta_{c'c}, \tag{1.56}$$

for parton s, s' of any kind. A generic hadronic state characterized by the momentum P and helicity λ is written as

$$|H; P, \lambda\rangle = \sum_{N,\beta} \int \left[\frac{\mathrm{d}x}{\sqrt{x}}\right]_N \left[\mathrm{d}^2\mathbf{k}_\perp\right]_N \Psi^\lambda_{N,\beta}(r)|N, \beta; k_1, ..., k_N\rangle, \tag{1.57}$$

where $\Psi^\lambda_{N,\beta}(r)$, with r collective notation for the space and momentum dependence $(x_i, \mathbf{k}_{\perp i})$, is the momentum light-cone wave function (LCWF) of the N-parton Fock state $|N, \beta; k_1, ..., k_N\rangle$. The index β labels its partonic composition, and the helicity and colour of each parton; while the integration measures in the previous equation are defined by

$$\begin{aligned} \left[\frac{\mathrm{d}x}{\sqrt{x}}\right]_N &\equiv \prod_{i=1}^N \frac{\mathrm{d}x_i}{\sqrt{x_i}} \delta\left(1 - \sum_{i=1}^N x_i\right), \\ \left[\mathrm{d}^2\mathbf{k}_\perp\right]_N &\equiv \frac{1}{(16\pi^3)^{N-1}} \prod_{i=1}^N \mathrm{d}^2\mathbf{k}_{\perp i} \delta^{(2)}\left(\sum_{i=1}^N \mathbf{k}_{\perp i} - \mathbf{p}_\perp\right). \end{aligned} \tag{1.58}$$

The LCWF in Eq. (1.57) is the *probability amplitude* for finding partons with momenta $(x_i P^+, x_i \mathbf{P}_\perp + \mathbf{k}_{\perp i})$ in the hadron. An interesting feature of LCWFs is that, in general, they do not depend on the momentum of the hadron, but only on the momentum coordinates of the partons relative to the hadron momentum. In other words, the center of mass motion can be separated from the relative motion of the partons [32]. As a consequence the LCWFs depend on x_i which is the longitudinal momentum fraction carried by the i-th parton $(0 \leq x_i \leq 1)$, and on $\mathbf{k}_{\perp i}$ the momentum "transverse" to the direction of the nucleon. Both of these are frame independent quantities.

In a completely general way, a N-parton state is defined as

$$|N, \beta; k_1, ..., k_N\rangle = \frac{1}{\sqrt{c_{N,\beta}}} \prod_i b^\dagger_{q_i}(\tilde{k}_i, \lambda_i, c_i) \prod_j d^\dagger_{q_j}(\tilde{k}_j, \lambda_j, c_j) \prod_l a^\dagger(\tilde{k}_l, \lambda_l, c_l)|0\rangle. \tag{1.59}$$

Owing to the (anti)commutation relations in Eq. (1.53) the states $|N, \beta; k_1, ..., k_N\rangle$ are completely (anti)symmetric under exchange of the momenta k_i of gluons (quarks) with identical quantum numbers. The normalization constant $c_{N,\beta}$ in Eq. (1.59) contains a factor $n!$ for each subset of n partons whose quantum number are identical, so that one has

$$\begin{aligned} &\Psi^{*\lambda}_{N,\beta'}(r')\Psi^\lambda_{N,\beta}(r)\langle N', \beta'; k'_1, ..., k'_N|N, \beta; k_1, ..., k_N\rangle \\ &= |\Psi^\lambda_{N,\beta}(r)|^2 \delta_{N'N}\delta_{\beta'\beta} \prod_i^N 16\pi^3 k_i^+ \delta(k_i'^+ - k_i^+)\delta^{(2)}(\mathbf{k}'_{\perp i} - \mathbf{k}_{\perp i}). \end{aligned} \tag{1.60}$$

The Kronecker delta $\delta_{\beta'\beta}$ implies that one does not introduce different labels β for states whose assignment of discrete quantum numbers for the individual partons only differs by a permutation.
Lastly, the hadron states are normalized as

$$\langle H; P', \lambda'|H; P, \lambda\rangle = 16\pi^3 P^+ \delta(P'^+ - P^+)\delta^{(2)}(\mathbf{P'}_\perp - \mathbf{P}_\perp)\delta_{\lambda'\lambda}, \tag{1.61}$$

with

$$\sum_{N,\beta} \int [dx]_N \left[d^2\mathbf{k}_\perp\right]_N |\Psi^\lambda_{N,\beta}(r)|^2 = 1. \tag{1.62}$$

An important issue to stress here is the following. The parton states (1.59) do not refer to a specific hadron, rather they are characterized by a set β of flavour, helicity and colour quantum numbers. Their coupling to a colour singlet hadron with definite quantum numbers, e.g. isospin, is incorporated in the LCWFs $\Psi^\lambda_{N,\beta}(r)$. Many of them are zero, and several of the non-zero ones are related to each other. For instance, it is possible to show (see later) that the valence (three quarks) Fock state of the nucleon has only one independent LCWF for all configurations where the quark helicities sum up to give the helicity of the nucleon [33], namely when the total angular momentum of the nucleon is reproduced by the quarks spin only without orbital angular momentum contribution. For higher Fock states there are in general several independent LCWFs.

1.5 Light-Cone Wave Functions: general properties

One great advantage of the Fock state description of hadrons is that much intuition exists about the behavior of bound state WFs. Any hadron state, such as a proton $|p\rangle$, must be an eigenstate of H_{LC}. Consequently, working in a frame where $p^+ = 1$, $p_\perp = 0$ and $p^+p^- = p^- = M^2$, the state $|p\rangle$ satisfies an equation

$$\left(M^2 - H_{LC}\right)|p\rangle = 0. \tag{1.63}$$

Projecting this onto the various Fock states $\langle qqq|, \langle (3q)q\bar{q}|, \langle (3q)g|, ...$ results in an infinite number of coupled integral eigenvalue equations,

$$\begin{aligned}\left(M^2 - \sum_i \frac{\mathbf{k}_{\perp i}^2 + m_i^2}{x_i}\right)\begin{bmatrix} \Psi_{qqq/p} \\ \Psi_{(3q)q\bar{q}/p} \\ \vdots \end{bmatrix} \\ = \begin{bmatrix} \langle qqq|V|qqq\rangle & \langle qqq|V|(3q)q\bar{q}\rangle & \dots \\ \langle (3q)q\bar{q}|V|qqq\rangle & \langle (3q)q\bar{q}|V|(3q)q\bar{q}\rangle & \dots \\ \vdots & \vdots & \ddots \end{bmatrix}\begin{bmatrix} \Psi_{qqq/p} \\ \Psi_{(3q)\bar{q}/p} \\ \vdots \end{bmatrix},\end{aligned} \tag{1.64}$$

where V encods the interaction part of H_{LC}. V involves completely irreducible interactions coupling Fock states. Diagrammatically "irreducible" means that one has to compute diagrams with no internal propagators. These equations determine the hadronic spectrum and wave functions. Even in the case in which the potential is essentially trivial, the many channels required to describe an hadronic state make the Eq. (1.64) very difficult to solve. However, this may not be necessary.

There are several approaches which have been developed to solve LC bound state equation non-perturbatively. One is the discretized light-cone quantization, pioneered by Brodsky and Pauli [34], in which the fields are expanded into complete sets of functions with periodic boundary condititons. Another is transverse lattice QCD which was introduced by Bardeen and Pearson [35]. In this case, the advantage of lattice, e.g. gauge invariant regulator, and the advantage of LC formalism are combined. Beside those there is an approach due to Perry and collaborators [36] based on Tamm-Dancoff approach [37], in which the Fock space is truncated to include only the Fock states that have a small number of particles.

An important feature that is immediately evident from Eq. (1.64) is that all WFs have the general form

$$\Psi_N^\lambda(x_i, \mathbf{k}_{\perp i}, \lambda_i) = \frac{1}{M^2 - \sum_i \left(\mathbf{k}_{\perp i}^2 + m_i^2\right)/x_i}(V\Psi). \tag{1.65}$$

Consequently Ψ_N^λ tends to vanish when

$$\mathcal{E} \equiv M^2 - \sum_i \frac{\mathbf{k}_{\perp i}^2 + m_i^2}{x_i} \to -\infty. \tag{1.66}$$

This can be understood intuitively. In the Fock state expansion we think of the bare quanta as being on mass shell but off LC energy shell, i.e. each parton comprising a state with $\tilde{p} = (p^+, \mathbf{p}_\perp)$ has

$$k_i^- = \frac{(x_i \mathbf{p}_\perp + \mathbf{k}_{\perp i})^2 + m_i^2}{x_i p^+} \Rightarrow k_i^2 = m_i^2, \tag{1.67}$$

but the sum over all k_i^- does not give P^-. In fact the difference is just

$$p^- - \sum_i k_i^- = \frac{\mathbf{p}_\perp^2 + M^2}{p^+} - \left(\sum_i \frac{\mathbf{k}_{\perp i}^2 + m_i^2}{x_i p^+} + \frac{\mathbf{p}_\perp^2}{p^+} \right) = \frac{\mathcal{E}}{p^+}. \tag{1.68}$$

The parameter $\mathcal{E}$ is a boost-invariant measure of how far off energy shell a Fock state is. Thus Eq. (1.65) implies that a physical particle has little probability of being in a Fock state far off shell. In general $\mathcal{E}$ is large when $\mathbf{k}_{\perp i}^2$ is large or x_i is small, i.e. the WF should vanish as $\mathbf{k}_{\perp i}^2 \to \infty$ or $x_i \to 0$. Formally such constraints appear as boundary conditions on the WFs.

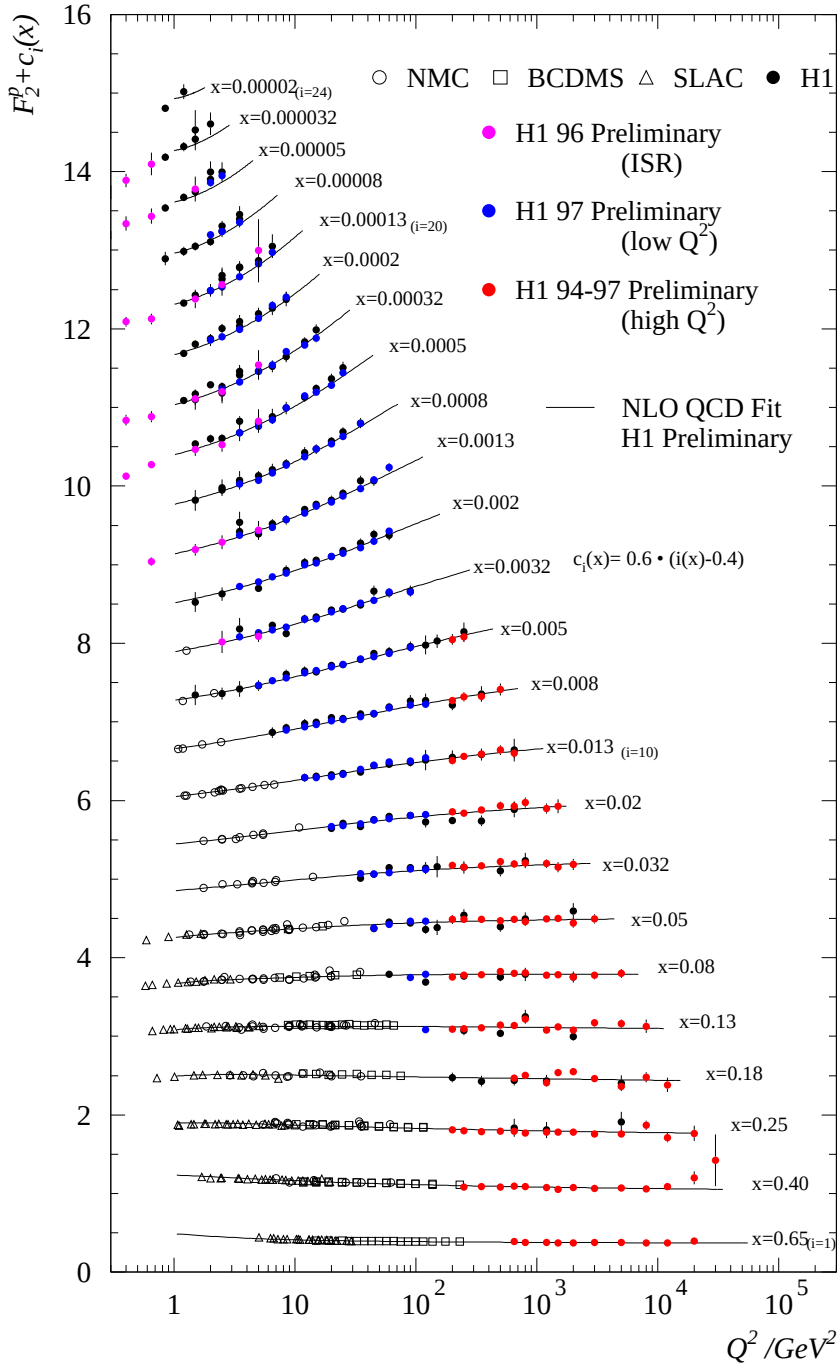

Figure 1.1: The figure shows the measurements of the H1 experiment at HERA of the proton structure function F_2^p. The momentum region includes sea quarks at momentum fractions $x = 10^{-5}$ up to the valence quark region. The virtuality Q^2 spans five orders of magnitude up to $Q^2 = 3{\times}10^4$ GeV^2. At these large Q^2 values the scattering process is sensitive to structures of size 10^{-3}fm.

Chapter 2

Light-Cone Wave Functions in the valence sector

2.1 Nucleon Distribution Amplitudes

We have seen the at leading twist all the information about the strong non-perturbative interactions at large distances is contained in wave functions describing the distribution in longitudinal momentum fractions, truncated from above by a characteristic virtuality of the order of the factorization scale. The factorization theorem and the renormalization group represent the ground for the convolution scheme of Brodsky and Lepage [47, 48] for describing the exclusive processes by means of LCWFs. In the convolution scheme the quantitative description of exclusive reactions, in which "intact" hadrons appear in the initial and final states, involves the detailed calculation of hadronic WFs. Indeed, the amplitude of the process becomes the product (convolution) of two (or more) factors, each depending only on the dynamics specific for that particular momentum: a process dependent hard-scattering amplitude and one (or more) universal (but factorization scheme dependent) *hadron distribution amplitude* (DA) that encapsulates the remaining soft contributions responsible for the bound-state dynamics through the LCWFs. A generic DA can formally be expressed in terms of LCWFs in this way,

$$\phi(x_i, \mu^2) \equiv \int_{\mathbf{k}_{\perp i}<\mu^2} \left[\mathrm{d}^2\mathbf{k}_\perp\right]_N \Psi_N(x_i, \mathbf{k}_{\perp i}). \tag{2.1}$$

The DAs are equally important and to a large extent complementary to conventional parton distributions which correspond to one-particle probability distribution for the parton momentum fraction in an *average* configuration. In a physical gauge (like the usual light-cone gauge, $A^+ = 0$, extensively used in literature) the DAs represent the probability amplitude for the hadron to consist of valence quarks* with fractional momenta x_i moving collinearly up to the

*There exists a large consensus that exclusive processes involving large momentum transfers are dominated by 'valence' components in hadron wave functions with the minimum

scale μ^2. The direct extraction directly from experiments is still a challenging task, but there are indications that it should become feasible. As a matter of fact, quantitative information for the pion distribution amplitude have already been provided by CLEO [50] and E791 [51] collaborations.

The notion of hadron distribution amplitudes in general refers to hadron-to-vacuum matrix elements of non-local operators built of quark and gluon fields at light-like separations. Referring to the nucleon and in particular to the proton we will deal with the matrix element

$$\langle 0|\epsilon^{ijk}u^{i'}_{\alpha}(z_1n)[z_1;z_0]_{i'i}u^{j'}_{\beta}(z_2n)[z_2;z_0]_{j'j}d^{k'}_{\gamma}(z_3n)[z_3;z_0]_{k'k}|P(p_1,s_1)\rangle, \qquad (2.2)$$

where $|P(p_1,s_1)\rangle$ denotes the proton state with momentum p_1, $p_1^2=M^2$ and helicity s_1. The symbols u,d are the quark field operators. The Greek letters α,β and γ stand for Dirac indexes, while the latin ones i,j and k for colour labels. n is a light-like null vector, $n^2=0$, the coefficients z_i are real numbers. The brackets $[z_i;z_0]$ represent the Wilson line, a path ordered gluonic exponential along the straight line connecting two arbitrary points z_in and z_0n,

$$[z_i;z_0]\equiv\mathcal{P}\exp\left[ig(z_i-z_0)\int_0^1 dt\, n_\mu A^\mu\Big(n[tz+(1-t)z]\Big)\right]. \qquad (2.3)$$

The Wilson lines have to be inserted to guarantee the gauge invariance for such a non local operator, but working in the LC gauge, they reduce to the identity. The most general spinorial and Lorentz decomposition of the matrix element (2.2) involves 24 invariant functions [52]:

$$\begin{aligned}
&\frac{4}{f_N}\langle 0|\,\varepsilon^{ijk}u^i_\alpha(z_1n)u^j_\beta(z_2n)d^k_\gamma(z_3n)\,|P(p_1,s_1)\rangle\\
&= \mathcal{S}_1MC_{\alpha\beta}\,(\gamma_5N)_\gamma+\mathcal{S}_2M^2C_{\alpha\beta}\,(\not n\gamma_5N)_\gamma\\
&\quad+\mathcal{P}_1M\,(\gamma_5C)_{\alpha\beta}\,N_\gamma+\mathcal{P}_2M^2\,(\gamma_5C)_{\alpha\beta}\,(\not nN)_\gamma\\
&\quad+\mathcal{V}_1\,(\not p_1C)_{\alpha\beta}\,(\gamma_5N)_\gamma+\mathcal{V}_2M\,(\not p_1C)_{\alpha\beta}\,(\not n\gamma_5N)_\gamma\\
&\quad+\mathcal{V}_3M\,(\gamma_\mu C)_{\alpha\beta}\,(\gamma^\mu\gamma_5N)_\gamma+\mathcal{V}_4M^2\,(\not nC)_{\alpha\beta}\,(\gamma_5N)_\gamma\\
&\quad+\mathcal{V}_5M^2\,(\gamma_\mu C)_{\alpha\beta}\,(i\sigma^{\mu\nu}n_\nu\gamma_5N)_\gamma+\mathcal{V}_6M^3\,(\not nC)_{\alpha\beta}\,(\not n\gamma_5N)_\gamma\\
&\quad+\mathcal{A}_1\,(\not p_1\gamma_5C)_{\alpha\beta}\,N_\gamma+\mathcal{A}_2M\,(\not p_1\gamma_5C)_{\alpha\beta}\,(\not nN)_\gamma\\
&\quad+\mathcal{A}_3M\,(\gamma_\mu\gamma_5C)_{\alpha\beta}\,(\gamma^\mu N)_\gamma+\mathcal{A}_4M^2\,(\not n\gamma_5C)_{\alpha\beta}\,N_\gamma\\
&\quad+\mathcal{A}_5M^2\,(\gamma_\mu\gamma_5C)_{\alpha\beta}\,(i\sigma^{\mu\nu}n_\nu N)_\gamma+\mathcal{A}_6M^3\,(\not n\gamma_5C)_{\alpha\beta}\,(\not nN)_\gamma\\
&\quad+\mathcal{T}_1\,(p_1^\nu i\sigma_{\mu\nu}C)_{\alpha\beta}\,(\gamma^\mu\gamma_5N)_\gamma+\mathcal{T}_2M\,(n^\mu p_1^\nu i\sigma_{\mu\nu}C)_{\alpha\beta}\,(\gamma_5N)_\gamma\\
&\quad+\mathcal{T}_3M\,(\sigma_{\mu\nu}C)_{\alpha\beta}\,(\sigma^{\mu\nu}\gamma_5N)_\gamma+\mathcal{T}_4M\,(p_1^\nu\sigma_{\mu\nu}C)_{\alpha\beta}\,(\sigma^{\mu\varrho}n_\varrho\gamma_5N)_\gamma\\
&\quad+\mathcal{T}_5M^2\,(n^\nu i\sigma_{\mu\nu}C)_{\alpha\beta}\,(\gamma^\mu\gamma_5N)_\gamma+\mathcal{T}_6M^2\,(n^\mu p_1^\nu i\sigma_{\mu\nu}C)_{\alpha\beta}\,(\not n\gamma_5N)_\gamma\\
&\quad+\mathcal{T}_7M^2\,(\sigma_{\mu\nu}C)_{\alpha\beta}\,(\sigma^{\mu\nu}\not n\gamma_5N)_\gamma+\mathcal{T}_8M^3\,(n^\nu\sigma_{\mu\nu}C)_{\alpha\beta}\,(\sigma^{\mu\varrho}n_\varrho\gamma_5N)_\gamma \qquad (2.4)
\end{aligned}$$

number of Fock constituents [47, 49].

where N_γ is the nucleon spinor, C the charge conjugation matrix, $\sigma_{\mu\nu} = \frac{i}{2}[\gamma_\mu, \gamma_\nu]$ and f_N is the value of the nucleon wave function at the origin, estimated through QCD sum rules to be of order 5.3×10^{-3} GeV^2 [53]. The factor 4 on the l.h.s. is introduced for later convenience. Each of the 24 functions $\mathcal{S}_i, \mathcal{P}_i, \mathcal{A}_i, \mathcal{V}_i, \mathcal{T}_i$ depends on the scalar product $p_1 \cdot n$.

The invariant functions in Eq. (2.4) do not have a definite twist yet. For the twist classification, it is convenient to go over to the infinite momentum frame. To this end we introduce the second light-like vector

$$p^\mu = p_1^\mu - \frac{1}{2} n^\mu \frac{M^2}{p \cdot n}, \qquad p^2 = 0, \tag{2.5}$$

so that $p_1 \to p$ if the nucleon mass can be neglected $M \to 0$. Assume for a moment that the nucleon moves in the positive $\mathbf{e_z}$ direction, then p^+ and n^- are the only non-vanishing components of p and n, respectively. The infinite momentum frame can be visualized as the limit $p^+ \sim Q \to \infty$ with fixed $p_1 \cdot n = p \cdot n \sim 1$ where Q is the large scale in the process. Expanding the matrix element in powers of $1/p^+$ introduces the power counting in Q. In this language twist counts the suppression in powers of p^+. Similarly, the nucleon spinor $N_\gamma(p_1, s_1)$ has to be decomposed in "large" and "small" components as

$$N_\gamma(p_1, s_1) = \frac{1}{2p \cdot n} \left(\not{p}\not{n} + \not{n}\not{p}\right) N_\gamma(p_1, s_1) = N_\gamma^+(p_1, s_1) + N_\gamma^-(p_1, s_1), \tag{2.6}$$

where we have introduced two projection operators

$$\Pi^+ = \frac{\not{p}\not{n}}{2p \cdot n} \quad , \quad \Pi^- = \frac{\not{n}\not{p}}{2p \cdot n} \tag{2.7}$$

that project onto the "plus" and "minus" components of the spinor. Note the useful relations

$$\not{p} N(P) = M N^+(P), \qquad \not{n} N(P) = \frac{2pn}{M} N^-(P) \tag{2.8}$$

that follow readily from the Dirac equation $\not{p}_1 N(P) = M N(P)$.

Using the explicit expressions for $N(P)$ it is easy to see that $\Pi^+ N = N^+ \sim \sqrt{p^+}$ while $\pi^- N = N^- \sim 1/\sqrt{p^+}$. To give an example of how such power counting works, decompose the Lorentz structure in front of $\mathcal{V}_1$ in Eq. (2.4) in terms of light-cone vectors

$$\begin{aligned} (\not{p}C)_{\alpha\beta} (\gamma_5 N)_\gamma &= (\not{p}C)_{\alpha\beta} \left(\gamma_5 N^+\right)_\gamma + (\not{p}C)_{\alpha\beta} \left(\gamma_5 N^-\right)_\gamma \\ &\quad + \frac{M^2}{2p \cdot n} (\not{n}C)_{\alpha\beta} \left(\gamma_5 N^+\right)_\gamma + \frac{M^2}{2p \cdot n} (\not{n}C)_{\alpha\beta} \left(\gamma_5 N^-\right)_\gamma \end{aligned} \tag{2.9}$$

The first structure on the r.h.s. is of order $(p^+)^{3/2}$, the second of order $(p^+)^{1/2}$, the third of order $(p^+)^{-1/2}$ and the fourth $(p^+)^{-3/2}$, respectively. These contributions are interpreted as twist-3, twist-4, twist-5 and twist-6, respectively,

and it follows that the invariant function $\mathcal{V}_1$ contributes to all twists starting from the leading one. Such an effect is familiar from deep inelastic scattering, where the twist-3 structure function $g_2(x,Q^2)$ receives the so-called Wandzura-Wilczek contribution related to the leading-twist structure function $g_1(x,Q^2)$ [55].

The twist classification based on counting of powers of $1/p^+$ is mathematically similar to the light-cone quantisation approach of [54]. In this language, one decomposes the quark fields contained in the matrix element Eq. (2.4) in 'plus' and 'minus' components $q = q^+ + q^-$ in the same manner as done above with the nucleon spinor Eq. (2.6). The leading twist amplitude is identified as the one containing three 'plus' quark fields while each 'minus' component introduces one additional unit of twist. Up to possible complications due to isospin, one expects, therefore, to find eight independent three-quark nucleon distribution amplitudes: One corresponding to the twist-3 operator $(u^+u^+d^+)$, three related to the possible twist-4 operators $(u^+u^+d^-),(u^+u^-d^+),(u^-u^+d^+)$, three more amplitudes of twist-5 of the type $(u^-u^-d^+),(u^-u^+d^-),(u^+u^-d^-)$ and one amplitude of twist-6 having the structure $(u^-u^-d^-)$.

Alternatively, distribution amplitudes of definite twist correspond to the decomposition of Eq. (2.4) in different light-cone components. After a simple algebra, we arrive at the following definition of light-cone nucleon distribution amplitudes:

$$
\begin{aligned}
&\frac{4}{f_N}\,\langle 0|\,\varepsilon^{ijk} u^i_\alpha(z_1 n) u^j_\beta(z_2 n) d^k_\gamma(z_3 n)\,|P\rangle = \\
&\quad = S_1 M C_{\alpha\beta}\left(\gamma_5 N^+\right)_\gamma + S_2 M C_{\alpha\beta}\left(\gamma_5 N^-\right)_\gamma \\
&\qquad + P_1 M\,(\gamma_5 C)_{\alpha\beta}\,N^+_\gamma + P_2 M\,(\gamma_5 C)_{\alpha\beta}\,N^-_\gamma \\
&\qquad + V_1\,(\not{p} C)_{\alpha\beta}\left(\gamma_5 N^+\right)_\gamma + V_2\,(\not{p} C)_{\alpha\beta}\left(\gamma_5 N^-\right)_\gamma \\
&\qquad + \frac{V_3}{2} M\,(\gamma_\perp C)_{\alpha\beta}\left(\gamma^\perp\gamma_5 N^+\right)_\gamma + \frac{V_4}{2} M\,(\gamma_\perp C)_{\alpha\beta}\left(\gamma^\perp\gamma_5 N^-\right)_\gamma \\
&\qquad + V_5 \frac{M^2}{2pz}\,(\not{n} C)_{\alpha\beta}\left(\gamma_5 N^+\right)_\gamma + \frac{M^2}{2pz} V_6\,(\not{n} C)_{\alpha\beta}\left(\gamma_5 N^-\right)_\gamma \\
&\qquad + A_1\,(\not{p}\gamma_5 C)_{\alpha\beta}\,N^+_\gamma + A_2\,(\not{p}\gamma_5 C)_{\alpha\beta}\,N^-_\gamma + \frac{A_3}{2} M\,(\gamma_\perp\gamma_5 C)_{\alpha\beta}\left(\gamma^\perp N^+\right)_\gamma \\
&\qquad + \frac{A_4}{2} M\,(\gamma_\perp\gamma_5 C)_{\alpha\beta}\left(\gamma^\perp N^-\right)_\gamma + A_5 \frac{M^2}{2pz}\,(\not{n}\gamma_5 C)_{\alpha\beta}\,N^+_\gamma + \frac{M^2}{2pz} A_6\,(\not{n}\gamma_5 C)_{\alpha\beta}\,N^-_\gamma \\
&\qquad + T_1\,(i\sigma_{\perp p} C)_{\alpha\beta}\left(\gamma^\perp\gamma_5 N^+\right)_\gamma + T_2\,(i\sigma_{\perp p} C)_{\alpha\beta}\left(\gamma^\perp\gamma_5 N^-\right)_\gamma \\
&\qquad + T_3 \frac{M}{pn}\,(i\sigma_{p n} C)_{\alpha\beta}\left(\gamma_5 N^+\right)_\gamma + T_4 \frac{M}{pn}\,(i\sigma_{n p} C)_{\alpha\beta}\left(\gamma_5 N^-\right)_\gamma \\
&\qquad + T_5 \frac{M^2}{2pz}\,(i\sigma_{\perp n} C)_{\alpha\beta}\left(\gamma^\perp\gamma_5 N^+\right)_\gamma + \frac{M^2}{2pn} T_6\,(i\sigma_{\perp n} C)_{\alpha\beta}\left(\gamma^\perp\gamma_5 N^-\right)_\gamma \\
&\qquad + M \frac{T_7}{2}\,(\sigma_{\perp\perp'} C)_{\alpha\beta}\left(\sigma^{\perp\perp'}\gamma_5 N^+\right)_\gamma + M \frac{T_8}{2}\,(\sigma_{\perp\perp'} C)_{\alpha\beta}\left(\sigma^{\perp\perp'}\gamma_5 N^-\right)_\gamma ,
\end{aligned}
\tag{2.10}
$$

	twist-3	twist-4	twist-5	twist-6
vector	V_1	V_2 , V_3	V_4 , V_5	V_6
pseudo-vector	A_1	A_2 , A_3	A_4 , A_5	A_6
tensor	T_1	T_2 , T_3 , T_7	T_4 , T_5 , T_8	T_6
scalar		S_1	S_2	
pseudo-scalar		P_1	P_2	

Table 2.1: Twist classification of the distribution amplitudes in Eq. (2.10).

where $\perp$ stands for the projection transverse to n, p, e.g. $\gamma_\perp \gamma^\perp = \gamma^\mu g^\perp_{\mu\nu} \gamma^\nu$ with $g^\perp_{\mu\nu} = g_{\mu\nu} - (p_\mu n_\nu + n_\mu p_\nu)/pn$, and $\sigma^{pn} = \sigma^{\mu\nu} p_\mu n_\nu$.

By power counting we identify three twist-3 distribution amplitudes V_1, A_1, T_1, nine twist-4 and twist-5, respectively, and three twist-6 distributions, see Table 2.1. Each distribution amplitude $F = V_i, A_i, T_i, S_i, P_i$ can be represented as

$$F(z_i p \cdot n) = \int \mathcal{D}x \, e^{-ipn \sum_i x_i z_i} F(x_i) \,, \tag{2.11}$$

where the functions $F(x_i)$ depend on the dimensionless variables x_i, $0 < x_i < 1, \sum_i x_i = 1$ which correspond to the longitudinal momentum fractions carried by the quarks inside the nucleon. The integration measure is defined as

$$\int \mathcal{D}x = \int_0^1 \mathrm{d}x_1 \mathrm{d}x_2 \mathrm{d}x_3 \, \delta(x_1 + x_2 + x_3 - 1) \,. \tag{2.12}$$

Comparision of the expansions in Eq. (2.4) and Eq. (2.10) then leads to the expressions for the invariant functions $\mathcal{V}_i, \mathcal{A}_i, \mathcal{T}_i, \mathcal{S}_i, \mathcal{P}_i$ in terms of the distribution amplitudes.

In our analysis we will focus on the three leading twist-three DAs, V_1, A_1, and T_1.

Because of the symmetry properties of the operator in Eq. (2.2) it is easy to see that the three invariant functions can be expressed in term of a single function Φ (see Appendix A). Indeed, labeling with 1, 2 or 3 the arguments of the DAs the following relations hold:

$$V_1(1,2,3) = V_1(2,1,3), \;\; A_1(1,2,3) = -A_1(2,1,3), \;\; T_1(1,2,3) = T_1(2,1,3). \tag{2.13}$$

As a result one has,

$$2T_1(1,2,3) = \Phi(1,3,2) + \Phi(2,3,1), \;\; \Phi(1,2,3) = V_1(1,2,3) - A_1(1,2,3). \tag{2.14}$$

2.1.1 Overlap Representation for the Nucleon Distribution Amplitudes

In this section we express the left-hand side of Eq. (2.10) by means of the LCWFs overlap representation [56]. The overlap representation is a general formalism, that has origin from the Drell-Yan formula [57] for the electromagnetic form factors and can be conveniently used for the description of different quantities entering inclusive and exclusive processes, e.g. PDFs and Generalized Parton Distributions (GPDs) [58].

As stated, in our analysis we will focus on the three leading twist 3 DAs, V_1, A_1, and T_1.

We first introduce the Fourier transform[†] of the matrix element (2.2)

$$\begin{aligned} M^{\uparrow/\downarrow}_{\alpha\beta,\gamma} &= 4\mathcal{F}\Big(\langle 0|\epsilon^{ijk}u^i_\alpha(z_1n)u^j_\beta(z_2n)d^k_\gamma(z_3n)|P\rangle\Big) \\ &= f_N\Big[V_1(\not{p}C)_{\alpha\beta}(\gamma^5N^+)_\gamma + A_1(\not{p}\gamma^5C)_{\alpha\beta}(N^+)_\gamma + T_1(i\sigma_{p\mu}C)_{\alpha\beta}(\gamma^\mu\gamma^5N^+)_\gamma\Big], \end{aligned} \tag{2.15}$$

where α, β and γ are Dirac indexes and $\uparrow$ / $\downarrow$ indicates the helicity value of the proton. Inverting Eq. (2.15) we can write the three DAs as follows (see Appendix B)

$$\begin{aligned} V_1 &= \frac{1}{f_N}\frac{1}{\sqrt[4]{2}}(p_1^+)^{-\frac{3}{2}}\Big(M^\uparrow_{12,1} + M^\uparrow_{21,1}\Big); \\ A_1 &= \frac{1}{f_N}\frac{1}{\sqrt[4]{2}}(p_1^+)^{-\frac{3}{2}}\Big(M^\uparrow_{21,1} - M^\uparrow_{12,1}\Big); \\ T_1 &= -\frac{1}{f_N}\frac{1}{\sqrt[4]{2}}(p_1^+)^{-\frac{3}{2}}M^\uparrow_{11,2}. \end{aligned} \tag{2.16}$$

Substituting in Eq. (2.15) the general Fourier expansion in momentum space of the free quark field of flavour q and colour c [47] from Eq. (1.52), and recalling that the auxiliary vector n has only the "minus" component different

[†]The symbol $\mathcal{F}$ represents the Fourier transform $(p\cdot n)^3\int\prod_j \frac{\mathrm{d}z_j}{(2\pi)^3}\exp[i\sum_k x_k z_k p\cdot n]$.

from zero, one finds

$$
\begin{aligned}
& 4\mathcal{F}\Big(\langle 0|\epsilon^{ijk}u^i_\alpha(z_1n)u^j_\beta(z_2n)d^k_\gamma(z_3n)|P(p_1,s_1)\rangle\Big) \\
= \;& 4(p\cdot n)^3\int_{-\infty}^{+\infty}\prod_j\frac{\mathrm{d}z_j}{(2\pi)^3}e^{ix_kz_k(p\cdot n)}\langle 0|\epsilon^{ijk}u^i_\alpha(z_1n)u^j_\beta(z_2n)d^k_\gamma(z_3n)|P(p_1,s_1)\rangle \\
= \;& \langle 0|\frac{\epsilon^{ijk}}{2}\int_{-\infty}^{+\infty}\prod_j\frac{\mathrm{d}z_j}{(2\pi)^3}e^{\frac{i}{2}x_kz_k}\int\frac{\mathrm{d}k_1^+\mathrm{d}^2\mathbf{k}_{1\perp}}{16\pi^3k_1^+}\int\frac{\mathrm{d}k_2^+\mathrm{d}^2\mathbf{k}_{2\perp}}{16\pi^3k_2^+}\int\frac{\mathrm{d}k_3^+\mathrm{d}^2\mathbf{k}_{3\perp}}{16\pi^3k_3^+} \\
& \times\sum_{\lambda_1,\lambda_2,\lambda_3}\Big\{b^i_1(\tilde{k}_1,\lambda_1)u_{+\alpha}(\tilde{k}_1,\lambda_1)\exp[-ik_1^+z_1n^-+i\mathbf{k}_{1\perp}\cdot\mathbf{n}_\perp] \\
& +d^{\dagger i}_1(\tilde{k}_1,\lambda_1)v_{+\alpha}(\tilde{k}_1,\lambda_1)\exp[ik_1^+z_1n^--i\mathbf{k}_{1\perp}\cdot\mathbf{n}_\perp]\Big\} \\
& \times\Big\{b^j_2(\tilde{k}_2,\lambda_2)u_{+\beta}(\tilde{k}_2,\lambda_2)\exp[-ik_2^+z_2n^-+i\mathbf{k}_{2\perp}\cdot\mathbf{n}_\perp] \\
& \;+d^{\dagger j}_2(\tilde{k}_2,\lambda_2)v_{+\beta}(\tilde{k}_2,\lambda_2)\exp[ik_2^+z_2n^--i\mathbf{k}_{2\perp}\cdot\mathbf{n}_\perp]\Big\} \\
& \times\Big\{b^k_3(\tilde{k}_3,\lambda_3)u_{+\gamma}(\tilde{k}_3,\lambda_3)\exp[-ik_3^+z_3n^-+i\mathbf{k}_{3\perp}\cdot\mathbf{n}_\perp] \\
& \;+d^{\dagger k}_3(\tilde{k}_3,\lambda_3)v_{+\gamma}(\tilde{k}_3,\lambda_3)\exp[ik_3^+z_3n^--i\mathbf{k}_{3\perp}\cdot\mathbf{n}_\perp]\Big\} \\
& \times\Theta(k_1^+)\Theta(k_2^+)\Theta(k_3^+)|P(p_1,s_1)\rangle \\
= \;& \langle 0|\frac{\epsilon^{ijk}}{2}\int_{-\infty}^{+\infty}\prod_j\frac{\mathrm{d}z_j}{(2\pi)^3}e^{\frac{i}{2}\Sigma_kx_kz_k}\int\frac{\mathrm{d}k_1^+\mathrm{d}^2\mathbf{k}_{1\perp}}{16\pi^3k_1^+}\int\frac{\mathrm{d}k_2^+\mathrm{d}^2\mathbf{k}_{2\perp}}{16\pi^3k_2^+}\int\frac{\mathrm{d}k_3^+\mathrm{d}^2\mathbf{k}_{3\perp}}{16\pi^3k_3^+} \\
& \times\sum_{\lambda_1,\lambda_2,\lambda_3}\Big\{b^i_1(\tilde{k}_1,\lambda_1)b^j_2(\tilde{k}_2,\lambda_2)b^k_3(\tilde{k}_3,\lambda_3)u_{+\alpha}(\tilde{k}_1,\lambda_1)u_{+\beta}(\tilde{k}_2,\lambda_2)u_{+\gamma}(\tilde{k}_3,\lambda_3) \\
& \times\exp[-i(k_1^+z_1n^-+k_2^+z_2n^-+k_3^+z_3n^-)] \\
& \;+b^i_1(\tilde{k}_1,\lambda_1)b^j_2(\tilde{k}_2,\lambda_2)d^{\dagger k}_3(\tilde{k}_3,\lambda_3)u_{+\alpha}(\tilde{k}_1,\lambda_1)u_{+\beta}(\tilde{k}_2,\lambda_2)v_{+\gamma}(\tilde{k}_3,\lambda_3) \\
& \times\exp[-i(k_1^+z_1n^-+k_2^+z_2n^--k_3^+z_3n^-)] \\
& \;+b^i_1(\tilde{k}_1,\lambda_1)d^{\dagger j}_2(\tilde{k}_2,\lambda_2)b^k_3(\tilde{k}_3,\lambda_3)u_{+\alpha}(\tilde{k}_1,\lambda_1)v_{+\beta}(\tilde{k}_2,\lambda_2)u_{+\gamma}(\tilde{k}_3,\lambda_3) \\
& \times\exp[-i(k_1^+z_1n^--k_2^+z_2n^-+k_3^+z_3n^-)] \\
& \;+d^{\dagger i}_1(\tilde{k}_1,\lambda_1)b^j_2(\tilde{k}_2,\lambda_2)b^k_3(\tilde{k}_3,\lambda_3)v_{+\alpha}(\tilde{k}_1,\lambda_1)u_{+\beta}(\tilde{k}_2,\lambda_2)u_{+\gamma}(\tilde{k}_3,\lambda_3) \\
& \times\exp[-i(-k_1^+z_1n^-+k_2^+z_2n^-+k_3^+z_3n^-)] \\
& \;+b^i_1(\tilde{k}_1,\lambda_1)d^{\dagger j}_2(\tilde{k}_2,\lambda_2)d^{\dagger k}_3(\tilde{k}_3,\lambda_3)u_{+\alpha}(\tilde{k}_1,\lambda_1)v_{+\beta}(\tilde{k}_2,\lambda_2)v_{+\gamma}(\tilde{k}_3,\lambda_3) \\
& \times\exp[-i(k_1^+z_1n^--k_2^+z_2n^--k_3^+z_3n^-)] \\
& \;+d^{\dagger i}_1(\tilde{k}_1,\lambda_1)b^j_2(\tilde{k}_2,\lambda_2)d^{\dagger k}_3(\tilde{k}_3,\lambda_3)v_{+\alpha}(\tilde{k}_1,\lambda_1)u_{+\beta}(\tilde{k}_2,\lambda_2)v_{+\gamma}(\tilde{k}_3,\lambda_3) \\
& \times\exp[-i(-k_1^+z_1n^-+k_2^+z_2n^--k_3^+z_3n^-)] \\
& \;+d^{\dagger i}_1(\tilde{k}_1,\lambda_1)d^{\dagger j}_2(\tilde{k}_2,\lambda_2)b^k_3(\tilde{k}_3,\lambda_3)v_{+\alpha}(\tilde{k}_1,\lambda_1)v_{+\beta}(\tilde{k}_2,\lambda_2)u_{+\gamma}(\tilde{k}_3,\lambda_3) \\
& \times\exp[-i(-k_1^+z_1n^--k_2^+z_2n^-+k_3^+z_3n^-)] \\
& \;+d^{\dagger i}_1(\tilde{k}_1,\lambda_1)d^{\dagger j}_2(\tilde{k}_2,\lambda_2)d^{\dagger k}_3(\tilde{k}_3,\lambda_3)v_{+\alpha}(\tilde{k}_1,\lambda_1)v_{+\beta}(\tilde{k}_2,\lambda_2)v_{+\gamma}(\tilde{k}_3,\lambda_3) \\
& \times\exp[i(k_1^+z_1n^-+k_2^+z_2n^-+k_3^+z_3n^-)]\Big\} \\
& \times\Theta(k_1^+)\Theta(k_2^+)\Theta(k_3^+)|P(p_1,s_1)\rangle\cdot
\end{aligned}
\tag{2.17}
$$

The last expression contains eight combinations of annihilators of good components of the quark and antiquark fields. Since we are going to perform a constituent quark model calculation in which the only degrees of freedom are represented by the three valence quarks (lower Fock state component, no antiquarks) we take into account only the combination with three annihilators of the good component of the quark fields, i.e. $b_1^i(\tilde{k}_1,\lambda_1)b_2^j(\tilde{k}_2,\lambda_2)b_3^k(\tilde{k}_3,\lambda_3)$. In such a way the previous equation becomes,

$$\begin{aligned}
&\langle 0|\frac{\epsilon^{ijk}}{2}\int_{-\infty}^{+\infty}\prod_j \frac{\mathrm{d}z_j}{(2\pi)^3}e^{\frac{i}{2}\Sigma_k x_k z_k}\int\frac{\mathrm{d}k_1^+\mathrm{d}^2\mathbf{k}_{1\perp}}{16\pi^3 k_1^+}\int\frac{\mathrm{d}k_2^+\mathrm{d}^2\mathbf{k}_{2\perp}}{16\pi^3 k_2^+}\int\frac{\mathrm{d}k_3^+\mathrm{d}^2\mathbf{k}_{3\perp}}{16\pi^3 k_3^+}\\
&\times\sum_{\lambda_1,\lambda_2,\lambda_3}\Big\{b_1^i(\tilde{k}_1,\lambda_1)b_2^j(\tilde{k}_2,\lambda_2)b_3^k(\tilde{k}_3,\lambda_3)u_{+\alpha}(\tilde{k}_1,\lambda_1)u_{+\beta}(\tilde{k}_2,\lambda_2)u_{+\gamma}(\tilde{k}_3,\lambda_3)\\
&\times\exp[-i(k_1^+z_1n^- + k_2^+z_2n^- + k_3^+z_3n^-)]\Theta(k_1^+)\Theta(k_2^+)\Theta(k_3^+)|P(p_1,s_1)\rangle,
\end{aligned}$$

and performing the integrations over the z_i variables, one finds the following expression:

$$\begin{aligned}
&\langle 0|4(p_1^+)^3\epsilon^{ijk}\int\frac{\mathrm{d}k_1^+\mathrm{d}^2\mathbf{k}_{1\perp}}{16\pi^3 k_1^+}\int\frac{\mathrm{d}k_2^+\mathrm{d}^2\mathbf{k}_{2\perp}}{16\pi^3 k_2^+}\int\frac{\mathrm{d}k_3^+\mathrm{d}^2\mathbf{k}_{3\perp}}{16\pi^3 k_3^+}\Theta(k_1^+)\Theta(k_2^+)\Theta(k_3^+)\\
&\times\sum_{\lambda_1,\lambda_2,\lambda_3}b_1^i(\tilde{k}_1,\lambda_1)b_2^j(\tilde{k}_2,\lambda_2)b_3^k(\tilde{k}_3,\lambda_3)u_{+\alpha}(\tilde{k}_1,\lambda_1)u_{+\beta}(\tilde{k}_2,\lambda_2)u_{+\gamma}(\tilde{k}_3,\lambda_3)\\
&\times\delta\Big(x_1p_1^+ - k_1^+\Big)\delta\Big(x_2p_1^+ - k_2^+\Big)\delta\Big(x_3p_1^+ - k_3^+\Big)|P(p_1,s_1)\rangle. \qquad (2.18)
\end{aligned}$$

To proceed in the calculation we have to substitute an expression for the proton state $|P(p_1,s_1)\rangle$. Specifing Eq. (1.57) to the case of a three-quark state, we get

$$\begin{aligned}
|P(p_1,s_1)\rangle \;=\; &\sum_{\lambda_i,\tau_i,c_i}\int\prod_{i=1'}^{3'}\frac{\mathrm{d}y_i}{\sqrt{y_i}}\int\frac{\prod_{i=1'}^{3'}\mathrm{d}\kappa_{i\perp}}{[2(2\pi)^3]^2}\delta\Big(1-\sum_{i=1'}^{3'}y_i\Big)\delta^{(2)}\Big(\sum_{i=1'}^{3'}\kappa_{i\perp}\Big)\\
&\times\tilde{\Psi}_\lambda^{N,[f]}(\{y_i,\kappa_{i\perp};\lambda_i,\tau_i,c_i\}_{i=1',\cdots,3'})\\
&\times\prod_{i=1'}^{3'}|y_ip_1^+,\kappa_{i\perp}+y_i\mathbf{p}_{1\perp},\lambda_i,\tau_i,c_i;q\rangle, \qquad (2.19)
\end{aligned}$$

with λ_i,τ_i and c_i spin, isospin and colour variables of the quarks, respectively. Since the final result is independent on the transverse components of the proton momentum, in the following we take $\mathbf{p}_{1\perp}=0$ for the sake of simplicity. With this prescription we can rewrite the partonic content of the proton as follows

$$\begin{aligned}
&\prod_{i=1'}^{3'}|y_ip_1^+,\kappa_{i\perp},\lambda_i,\tau_i,c_i;q\rangle =\\
&\frac{\epsilon^{lmn}}{\sqrt{3!}}\Big[b^{\dagger l}(y_{1'}p_1^+,\kappa_{1'\perp},\lambda_{1'},\tau_{1'})b^{\dagger m}(y_{2'}p_1^+,\kappa_{2'\perp},\lambda_{2'},\tau_{2'})b^{\dagger n}(y_{3'}p_1^+,\kappa_{3'\perp},\lambda_{3'},\tau_{3'})\Big]|0\rangle,
\end{aligned}$$

where l, m, n are colour indexes. Thus inserting the expression (2.19) for the proton ket in Eq. (2.18) we obtain

$$\begin{aligned}
&\langle 0|\frac{4(p_1^+)^3\epsilon^{ijk}}{\sqrt{3!}}\int\frac{\mathrm{d}k_1^+\mathrm{d}^2\mathbf{k}_{1\perp}}{16\pi^3k_1^+}\int\frac{\mathrm{d}k_2^+\mathrm{d}^2\mathbf{k}_{2\perp}}{16\pi^3k_2^+}\int\frac{\mathrm{d}k_3^+\mathrm{d}^2\mathbf{k}_{3\perp}}{16\pi^3k_3^+}\int\prod_{i=1'}^{3'}\frac{\mathrm{d}y_i}{\sqrt{y_i}}\frac{\mathrm{d}\kappa_{i\perp}}{[2(2\pi)^3]^2}\\
&\times\Theta(k_1^+)\Theta(k_2^+)\Theta(k_3^+)\delta\Big(1-\sum_{i=1'}^{3'}y_i\Big)\delta^{(2)}\Big(\sum_{i=1'}^{3'}\kappa_{i\perp}\Big)\sum_{\lambda_1,\lambda_2,\lambda_3}u_{+\alpha}(k_1^+,\lambda_1)\\
&\times u_{+\beta}(k_2^+,\lambda_2)u_{+\gamma}(k_3^+,\lambda_3)\sum_{\lambda_i,\tau_i,c_i}\tilde{\Psi}_\lambda^{N,[f]}(\{y_i,\kappa_{i\perp};\lambda_i,\tau_i,c_i\}_{i=1',\cdots,3'})\\
&\times b_1^i(\tilde{k}_1,\lambda_1)b_2^j(\tilde{k}_2,\lambda_2)b_3^k(\tilde{k}_3,\lambda_3)\delta\Big(x_1p_1^+-k_1^+\Big)\delta\Big(x_2p_1^+-k_2^+\Big)\delta\Big(x_3p_1^+-k_3^+\Big)\\
&\times\Big[b^{\dagger l}(y_{1'}p_1^+,\kappa_{1'\perp},\lambda_{1'},\tau_{1'})b^{\dagger m}(y_{2'}p_1^+,\kappa_{2'\perp},\lambda_{2'},\tau_{2'})b^{\dagger n}(y_{3'}p_1^+,\kappa_{3'\perp},\lambda_{3'},\tau_{3'})\Big]|0\rangle.
\end{aligned}\tag{2.20}$$

Using the commutation relations in Eqs. (1.53) after some algebra we find

$$\begin{aligned}
&\langle 0|\frac{4(p_1^+)^3}{\sqrt{3!}}\epsilon^{ijk}\int\frac{\mathrm{d}k_1^+\mathrm{d}^2\mathbf{k}_{1\perp}}{16\pi^3k_1^+}\int\frac{\mathrm{d}k_2^+\mathrm{d}^2\mathbf{k}_{2\perp}}{16\pi^3k_2^+}\int\frac{\mathrm{d}k_3^+\mathrm{d}^2\mathbf{k}_{3\perp}}{16\pi^3k_3^+}\int\prod_{i=1'}^{3'}\frac{\mathrm{d}y_i}{\sqrt{y_i}}\\
&\times\int\frac{\prod_{i=1'}^{3'}\mathrm{d}\kappa_{i\perp}}{[2(2\pi)^3]^2}\Theta(k_1^+)\Theta(k_2^+)\Theta(k_3^+)\delta\Big(1-\sum_{i=1'}^{3'}y_i\Big)\delta^{(2)}\Big(\sum_{i=1'}^{3'}\kappa_{i\perp}\Big)\\
&\times\sum_{\lambda_i,\tau_i,c_i}\tilde{\Psi}_\lambda^{N,[f]}(\{y_i,\kappa_{i\perp};\lambda_i,\tau_i,c_i\}_{i=1',\cdots,3'})\sum_{\lambda_1,\lambda_2,\lambda_3}u_{+\alpha}(k_1^+,\lambda_1)u_{+\beta}(k_2^+,\lambda_2)\\
&\times u_{+\gamma}(k_3^+,\lambda_3)\delta\Big(x_1p_1^+-k_1^+\Big)\delta\Big(x_2p_1^+-k_2^+\Big)\delta\Big(x_3p_1^+-k_3^+\Big)\\
&\times\Big[\{b_1^i,b_{3'}^{\dagger n}\}\{b_2^j,b_{2'}^{\dagger m}\}\{b_3^k,b_{1'}^{\dagger l}\}-\{b_1^i,b_{2'}^{\dagger m}\}\{b_2^j,b_{3'}^{\dagger n}\}\{b_3^k,b_{1'}^{\dagger l}\}\\
&\quad-\{b_1^i,b_{3'}^{\dagger n}\}\{b_2^j,b_{1'}^{\dagger l}\}\{b_3^k,b_{2'}^{\dagger m}\}+\{b_1^i,b_{1'}^{\dagger l}\}\{b_2^j,b_{3'}^{\dagger n}\}\{b_3^k,b_{2'}^{\dagger m}\}\\
&\quad+\{b_1^i,b_{2'}^{\dagger m}\}\{b_2^j,b_{1'}^{\dagger l}\}\{b_3^k,b_{3'}^{\dagger n}\}-\{b_1^i,b_{1'}^{\dagger l}\}\{b_2^j,b_{2'}^{\dagger m}\}\{b_3^k,b_{3'}^{\dagger n}\}\Big]|0\rangle,
\end{aligned}\tag{2.21}$$

in which for the sake of brevity we made use of the shorthand notation, $\{b_1^i,b_{1'}^{\dagger l}\}=\{b_1^i(\tilde{k}_1,\lambda_1),b_{1'}^{\dagger l}(y_{1'}p_1^+,\kappa_{1'\perp},\lambda_{1'},\tau_{1'})\}$ and analogous once. Then, re-

placing the anticommutators with their values (1.53) we get

$$
\begin{aligned}
&\frac{4(p_1^+)^3}{\sqrt{3!}}\epsilon^{ijk}\int\frac{\mathrm{d}k_1^+\mathrm{d}^2\mathbf{k}_{1\perp}}{16\pi^3k_1^+}\int\frac{\mathrm{d}k_2^+\mathrm{d}^2\mathbf{k}_{2\perp}}{16\pi^3k_2^+}\int\frac{\mathrm{d}k_3^+\mathrm{d}^2\mathbf{k}_{3\perp}}{16\pi^3k_3^+}\int\prod_{i=1'}^{3'}\frac{\mathrm{d}y_i}{\sqrt{y_i}}\\
&\times\int\frac{\prod_{i=1'}^{3'}\mathrm{d}\kappa_{i\perp}}{[2(2\pi)^3]^2}\Theta(k_1^+)\Theta(k_2^+)\Theta(k_3^+)\delta\Big(1-\sum_{i=1'}^{3'}y_i\Big)\delta^{(2)}\Big(\sum_{i=1'}^{3'}\kappa_{i\perp}\Big)\\
&\times\sum_{\lambda_i,\tau_i,c_i}\tilde{\Psi}_\lambda^{N,[f]}(\{y_i,\kappa_{i\perp};\lambda_i,\tau_i,c_i\}_{i=1',\cdots,3'})\sum_{\lambda_1,\lambda_2,\lambda_3}u_{+\alpha}(k_1^+,\lambda_1)u_{+\beta}(k_2^+,\lambda_2)\\
&\times u_{+\gamma}(k_3^+,\lambda_3)\delta\Big(x_1p_1^+-k_1^+\Big)\delta\Big(x_2p_1^+-k_2^+\Big)\delta\Big(x_3p_1^+-k_3^+\Big)y_{1'}y_{2'}y_{3'}(p_1^+)^3\\
&\times(16\pi^3)^3\Big\{\delta(y_{3'}p_1^+-k_1^+)\delta(y_{2'}p_1^+-k_2^+)\delta(y_{1'}p_1^+-k_3^+)\delta^{(2)}(\kappa_{3'\perp}-\mathbf{k}_{1\perp})\\
&\times\delta^{(2)}(\kappa_{2'\perp}-\mathbf{k}_{2\perp})\delta^{(2)}(\kappa_{1'\perp}-\mathbf{k}_{3\perp})\delta_{3'u}\delta_{\lambda_{3'}\lambda_1}\delta_{ni}\delta_{2'u}\delta_{\lambda_{2'}\lambda_2}\delta_{mj}\delta_{1'd}\delta_{\lambda_{1'}\lambda_3}\delta_{lk}\\
&-\delta(y_{2'}p_1^+-k_1^+)\delta(y_{3'}p_1^+-k_2^+)\delta(y_{1'}p_1^+-k_3^+)\delta^{(2)}(\kappa_{2'\perp}-\mathbf{k}_{1\perp})\\
&\times\delta^{(2)}(\kappa_{3'\perp}-\mathbf{k}_{2\perp})\delta^{(2)}(\kappa_{1'\perp}-\mathbf{k}_{3\perp})\delta_{2'u}\delta_{\lambda_{2'}\lambda_1}\delta_{mi}\delta_{3'u}\delta_{\lambda_{3'}\lambda_2}\delta_{nj}\delta_{1'd}\delta_{\lambda_{1'}\lambda_3}\delta_{lk}\\
&-\delta(y_{3'}p_1^+-k_1^+)\delta(y_{1'}p_1^+-k_2^+)\delta(y_{2'}p_1^+-k_3^+)\delta^{(2)}(\kappa_{3'\perp}-\mathbf{k}_{1\perp})\\
&\times\delta^{(2)}(\kappa_{1'\perp}-\mathbf{k}_{2\perp})\delta^{(2)}(\kappa_{2'\perp}-\mathbf{k}_{3\perp})\delta_{3'u}\delta_{\lambda_{3'}\lambda_1}\delta_{ni}\delta_{1'u}\delta_{\lambda_{1'}\lambda_2}\delta_{lj}\delta_{2'd}\delta_{\lambda_{2'}\lambda_3}\delta_{mk}\\
&+\delta(y_{1'}p_1^+-k_1^+)\delta(y_{3'}p_1^+-k_2^+)\delta(y_{2'}p_1^+-k_3^+)\delta^{(2)}(\kappa_{1'\perp}-\mathbf{k}_{1\perp})\\
&\times\delta^{(2)}(\kappa_{3'\perp}-\mathbf{k}_{2\perp})\delta^{(2)}(\kappa_{2'\perp}-\mathbf{k}_{3\perp})\delta_{1'u}\delta_{\lambda_{1'}\lambda_1}\delta_{li}\delta_{3'u}\delta_{\lambda_{3'}\lambda_2}\delta_{nj}\delta_{2'd}\delta_{\lambda_{2'}\lambda_3}\delta_{mk}\\
&+\delta(y_{2'}p_1^+-k_1^+)\delta(y_{1'}p_1^+-k_2^+)\delta(y_{3'}p_1^+-k_3^+)\delta^{(2)}(\kappa_{2'\perp}-\mathbf{k}_{1\perp})\\
&\times\delta^{(2)}(\kappa_{1'\perp}-\mathbf{k}_{2\perp})\delta^{(2)}(\kappa_{3'\perp}-\mathbf{k}_{3\perp})\delta_{2'u}\delta_{\lambda_{2'}\lambda_1}\delta_{mi}\delta_{1'u}\delta_{\lambda_{1'}\lambda_2}\delta_{lj}\delta_{3'd}\delta_{\lambda_{3'}\lambda_3}\delta_{nk}\\
&-\delta(y_{1'}p_1^+-k_1^+)\delta(y_{2'}p_1^+-k_2^+)\delta(y_{3'}p_1^+-k_3^+)\delta^{(2)}(\kappa_{1'\perp}-\mathbf{k}_{1\perp})\\
&\times\delta^{(2)}(\kappa_{2'\perp}-\mathbf{k}_{2\perp})\delta^{(2)}(\kappa_{3'\perp}-\mathbf{k}_{3\perp})\delta_{1'u}\delta_{\lambda_{1'}\lambda_1}\delta_{li}\delta_{2'u}\delta_{\lambda_{2'}\lambda_2}\delta_{mj}\delta_{3'd}\delta_{\lambda_{3'}\lambda_3}\delta_{nk}\Big\}.
\end{aligned}
$$

Now summing over the colour indexes the previous formula simplifies as follows

$$
\begin{aligned}
&-4(p_1^+)^3\int\frac{\mathrm{d}k_1^+\mathrm{d}^2\mathbf{k}_{1\perp}}{16\pi^3k_1^+}\int\frac{\mathrm{d}k_2^+\mathrm{d}^2\mathbf{k}_{2\perp}}{16\pi^3k_2^+}\int\frac{\mathrm{d}k_3^+\mathrm{d}^2\mathbf{k}_{3\perp}}{16\pi^3k_3^+}\int\prod_{i=1'}^{3'}\frac{\mathrm{d}y_i}{\sqrt{y_i}}\\
&\times\int\frac{\prod_{i=1'}^{3'}\mathrm{d}\kappa_{i\perp}}{[2(2\pi)^3]^2}\Theta(k_1^+)\Theta(k_2^+)\Theta(k_3^+)\delta\Big(1-\sum_{i=1'}^{3'}y_i\Big)\delta^{(2)}\Big(\sum_{i=1'}^{3'}\kappa_{i\perp}\Big)\\
&\times\sum_{\lambda_i,\tau_i}\tilde{\Psi}_\lambda^{N,[f]}(\{y_i,\kappa_{i\perp};\lambda_i,\tau_i\}_{i=1',\cdots,3'})\sum_{\lambda_1,\lambda_2,\lambda_3}u_{+\alpha}(k_1^+,\lambda_1)u_{+\beta}(k_2^+,\lambda_2)\\
&\times u_{+\gamma}(k_3^+,\lambda_3)\delta\Big(x_1p_1^+-k_1^+\Big)\delta\Big(x_2p_1^+-k_2^+\Big)\delta\Big(x_3p_1^+-k_3^+\Big)y_{1'}y_{2'}y_{3'}(p_1^+)^3
\end{aligned}
\tag{2.22}
$$

$$
\begin{aligned}
&\times(16\pi^3)^3\Big\{\delta(y_{3'}p_1^+-k_1^+)\delta(y_{2'}p_1^+-k_2^+)\delta(y_{1'}p_1^+-k_3^+)\delta^{(2)}(\kappa_{3'\perp}-\mathbf{k}_{1\perp})\\
&\times\delta^{(2)}(\kappa_{2'\perp}-\mathbf{k}_{2\perp})\delta^{(2)}(\kappa_{1'\perp}-\mathbf{k}_{3\perp})\delta_{3'u}\delta_{\lambda_{3'}\lambda_1}\delta_{2'u}\delta_{\lambda_{2'}\lambda_2}\delta_{1'd}\delta_{\lambda_{1'}\lambda_3}\\
&+\delta(y_{2'}p_1^+-k_1^+)\delta(y_{3'}p_1^+-k_2^+)\delta(y_{1'}p_1^+-k_3^+)\delta^{(2)}(\kappa_{2'\perp}-\mathbf{k}_{1\perp})\\
&\times\delta^{(2)}(\kappa_{3'\perp}-\mathbf{k}_{2\perp})\delta^{(2)}(\kappa_{1'\perp}-\mathbf{k}_{3\perp})\delta_{2'u}\delta_{\lambda_{2'}\lambda_1}\delta_{3'u}\delta_{\lambda_{3'}\lambda_2}\delta_{1'd}\delta_{\lambda_{1'}\lambda_3}\\
&+\delta(y_{3'}p_1^+-k_1^+)\delta(y_{1'}p_1^+-k_2^+)\delta(y_{2'}p_1^+-k_3^+)\delta^{(2)}(\kappa_{3'\perp}-\mathbf{k}_{1\perp})\\
&\times\delta^{(2)}(\kappa_{1'\perp}-\mathbf{k}_{2\perp})\delta^{(2)}(\kappa_{2'\perp}-\mathbf{k}_{3\perp})\delta_{3'u}\delta_{\lambda_{3'}\lambda_1}\delta_{1'u}\delta_{\lambda_{1'}\lambda_2}\delta_{2'd}\delta_{\lambda_{2'}\lambda_3}\\
&+\delta(y_{1'}p_1^+-k_1^+)\delta(y_{3'}p_1^+-k_2^+)\delta(y_{2'}p_1^+-k_3^+)\delta^{(2)}(\kappa_{1'\perp}-\mathbf{k}_{1\perp})\\
&\times\delta^{(2)}(\kappa_{3'\perp}-\mathbf{k}_{2\perp})\delta^{(2)}(\kappa_{2'\perp}-\mathbf{k}_{3\perp})\delta_{1'u}\delta_{\lambda_{1'}\lambda_1}\delta_{3'u}\delta_{\lambda_{3'}\lambda_2}\delta_{2'd}\delta_{\lambda_{2'}\lambda_3}\\
&+\delta(y_{2'}p_1^+-k_1^+)\delta(y_{1'}p_1^+-k_2^+)\delta(y_{3'}p_1^+-k_3^+)\delta^{(2)}(\kappa_{2'\perp}-\mathbf{k}_{1\perp})\\
&\times\delta^{(2)}(\kappa_{1'\perp}-\mathbf{k}_{2\perp})\delta^{(2)}(\kappa_{3'\perp}-\mathbf{k}_{3\perp})\delta_{2'u}\delta_{\lambda_{2'}\lambda_1}\delta_{1'u}\delta_{\lambda_{1'}\lambda_2}\delta_{3'd}\delta_{\lambda_{3'}\lambda_3}\\
&+\delta(y_{1'}p_1^+-k_1^+)\delta(y_{2'}p_1^+-k_2^+)\delta(y_{3'}p_1^+-k_3^+)\delta^{(2)}(\kappa_{1'\perp}-\mathbf{k}_{1\perp})\\
&\times\delta^{(2)}(\kappa_{2'\perp}-\mathbf{k}_{2\perp})\delta^{(2)}(\kappa_{3'\perp}-\mathbf{k}_{3\perp})\delta_{1'u}\delta_{\lambda_{1'}\lambda_1}\delta_{2'u}\delta_{\lambda_{2'}\lambda_2}\delta_{3'd}\delta_{\lambda_{3'}\lambda_3}\Big\}. \qquad (2.23)
\end{aligned}
$$

Looking at the expressions between braces it is easy to recognize that these six terms are equal. This consideration allows us to rewrite Eq. (2.23) in a more compact way

$$
\begin{aligned}
&-24(p_1^+)^3\int\frac{\mathrm{d}k_1^+\mathrm{d}^2\mathbf{k}_{1\perp}}{16\pi^3k_1^+}\int\frac{\mathrm{d}k_2^+\mathrm{d}^2\mathbf{k}_{2\perp}}{16\pi^3k_2^+}\int\frac{\mathrm{d}k_3^+\mathrm{d}^2\mathbf{k}_{3\perp}}{16\pi^3k_3^+}\int\prod_{i=1'}^{3'}\frac{\mathrm{d}y_i}{\sqrt{y_i}}\\
&\times\int\frac{\prod_{i=1'}^{3'}\mathrm{d}\kappa_{i\perp}}{[2(2\pi)^3]^2}\Theta(k_1^+)\Theta(k_2^+)\Theta(k_3^+)\delta\Big(1-\sum_{i=1'}^{3'}y_i\Big)\delta^{(2)}\Big(\sum_{i=1'}^{3'}\kappa_{i\perp}\Big)\\
&\times\sum_{\lambda_i,\tau_i}\tilde{\Psi}_\lambda^{N,[f]}(\{y_i,\kappa_{i\perp};\lambda_i,\tau_i\}_{i=1',\cdots,3'})\sum_{\lambda_{1,2,3}}u_{+\alpha}(k_1^+,\lambda_1)u_{+\beta}(k_2^+,\lambda_2)u_{+\gamma}(k_3^+,\lambda_3)\\
&\times\delta\Big(x_1p_1^+-k_1^+\Big)\delta\Big(x_2p_1^+-k_2^+\Big)\delta\Big(x_3p_1^+-k_3^+\Big)y_{1'}y_{2'}y_{3'}(p_1^+)^3\\
&\times(16\pi^3)^3\delta(y_{1'}p_1^+-k_1^+)\delta(y_{2'}p_1^+-k_2^+)\delta(y_{3'}p_1^+-k_3^+)\delta^{(2)}(\kappa_{1'\perp}-\mathbf{k}_{1\perp})\\
&\times\delta^{(2)}(\kappa_{2'\perp}-\mathbf{k}_{2\perp})\delta^{(2)}(\kappa_{3'\perp}-\mathbf{k}_{3\perp})\delta_{1'u}\delta_{\lambda_{1'}\lambda_1}\delta_{2'u}\delta_{\lambda_{2'}\lambda_2}\delta_{3'd}\delta_{\lambda_{3'}\lambda_3}.
\end{aligned}
$$

Integrating over the plus components of the quarks momenta $k_j^+,(j=1,...,3)$ one gets,

$$
\begin{aligned}
&-\frac{24}{x_1x_2x_3}\int\prod_{j=1}^{3}\mathrm{d}^2\mathbf{k}_{j\perp}\int\frac{\prod_{i=1'}^{3'}\mathrm{d}y_i}{\sqrt{y_i}}\int\frac{\prod_{i=1'}^{3'}\mathrm{d}\kappa_{i\perp}}{[2(2\pi)^3]^2}\delta\Big(1-\sum_{i=1'}^{3'}y_i\Big)\delta^{(2)}\Big(\sum_{i=1'}^{3'}\kappa_{i\perp}\Big)\\
&\times\sum_{\lambda_i,\tau_i}\tilde{\Psi}_\lambda^{N,[f]}(\{y_i,\kappa_{i\perp};\lambda_i,\tau_i\}_{i=1',\cdots,3'})\sum_{\lambda_1,\lambda_2,\lambda_3}u_{+\alpha}(x_1p_1^+,\lambda_1)u_{+\beta}(x_2p_1^+,\lambda_2)\\
&\times u_{+\gamma}(x_3p_1^+,\lambda_3)y_{1'}y_{2'}y_{3'}(p_1^+)^3\delta(y_{1'}p_1^+-x_1p_1^+)\delta(y_{2'}p_1^+-x_2p_1^+)\delta(y_{3'}p_1^+-x_3p_1^+)\\
&\times\delta^{(2)}(\kappa_{1'\perp}-\mathbf{k}_{1\perp})\delta^{(2)}(\kappa_{2'\perp}-\mathbf{k}_{2\perp})\delta^{(2)}(\kappa_{3'\perp}-\mathbf{k}_{3\perp})\delta_{1'u}\delta_{\lambda_{1'}\lambda_1}\delta_{2'u}\delta_{\lambda_{2'}\lambda_2}\delta_{3'd}\delta_{\lambda_{3'}\lambda_3}.
\end{aligned}
$$

Then integrating over $\mathrm{d}^2\mathbf{k}_{j\perp}$ and $\mathrm{d}y_i, (i = 1', ..., 3')$, and specifying the arguments of the LCWF we end up with the following expression

$$
\begin{aligned}
&-\frac{24}{\sqrt{x_1x_2x_3}}\int\frac{\prod_{i=1}^{3}\mathrm{d}\kappa_{i\perp}}{[2(2\pi)^3]^2}\delta^{(2)}\Big(\sum_{i=1}^{3}\kappa_{i\perp}\Big)\\
&\times\sum_{\lambda_1,\lambda_2,\lambda_3}u_{+\alpha}(x_1p_1^+,\lambda_1)u_{+\beta}(x_2p_1^+,\lambda_2)u_{+\gamma}(x_3p_1^+,\lambda_3)\\
&\times\tilde{\Psi}^{N,[f]}_{\lambda}(\{x_1,\kappa_{1\perp};\lambda_1,1/2\}\{x_2,\kappa_{2\perp};\lambda_2,1/2\}\{x_3,\kappa_{3\perp};\lambda_3,-1/2\}),
\end{aligned}
\tag{2.24}
$$

where for the sake of clarity we have replaced the (dummy) primed indexes $1', ..., 3'$ with the non primed ones. If instead of assume $\mathbf{p}_{1\perp} = 0$ we would have kept it in our calculations, the only difference we would find in the last formula would be that the Dirac delta on transverse momenta would read $\delta^{(2)}\Big(\sum_{i=1}^{3}\kappa_{i\perp} - \mathbf{p}_{1\perp}\Big)$.
The last formula represent the general model independent *overlap* representation for the matrix elements that enter in the definition of the DAs. The representation, apart from some kinematical factors, involves three spinors of the free quark fields and an integrated LCWF which encodes the low energy dynamics responsible for binding together the quarks to form a proton.

2.1.2 Matrix Elements for the Distribution Amplitudes

To have an expression for the nucleon DAs from Eq. (2.16) it is possible to see that the matrix elements one has to calculate are $M^{\uparrow}_{12,1}$, $M^{\uparrow}_{21,1}$ and $M^{\uparrow}_{11,2}$. Namely, specifying the result obtained in Eq. (2.24) for the three cases we get

$$
\begin{aligned}
M^{\uparrow}_{12,1} &= -\frac{24}{\sqrt{x_1x_2x_3}}\int\frac{\prod_{i=1}^{3}\mathrm{d}\kappa_{i\perp}}{[2(2\pi)^3]^2}\delta^{(2)}\Big(\sum_{i=1}^{3}\kappa_{i\perp}\Big)\\
&\quad\times u_{+1}(x_1p_1^+,1/2)u_{+2}(x_2p_1^+,-1/2)u_{+1}(x_3p_1^+,1/2)\\
&\quad\times\tilde{\Psi}^{N,[f]}_{1/2}(\{x_1,\kappa_{1\perp};1/2,1/2\}\{x_2,\kappa_{2\perp};-1/2,1/2\}\{x_3,\kappa_{3\perp};1/2,-1/2\})\\
&= -\frac{24}{\sqrt{2\sqrt{2}}}\Big(p_1^+\Big)^{\frac{3}{2}}\int\frac{\prod_{i=1}^{3}\mathrm{d}\kappa_{i\perp}}{[2(2\pi)^3]^2}\delta^{(2)}\Big(\sum_{i=1}^{3}\kappa_{i\perp}\Big)\\
&\quad\times\tilde{\Psi}^{N,[f]}_{1/2}(\{x_1,\kappa_{1\perp};1/2,1/2\}\{x_2,\kappa_{2\perp};-1/2,1/2\}\{x_3,\kappa_{3\perp};1/2,-1/2\});
\end{aligned}
\tag{2.25}
$$

$$
\begin{aligned}
M^{\uparrow}_{21,1} &= -\frac{24}{\sqrt{x_1x_2x_3}}\int\frac{\prod_{i=1}^{3}\mathrm{d}\kappa_{i\perp}}{[2(2\pi)^3]^2}\delta^{(2)}\Big(\sum_{i=1}^{3}\kappa_{i\perp}\Big)\\
&\times u_{+2}(x_1p_1^+,-1/2)u_{+1}(x_2p_1^+,1/2)u_{+1}(x_3p_1^+,1/2)\\
&\times\tilde{\Psi}^{N,[f]}_{1/2}(\{x_1,\kappa_{1\perp};-1/2,1/2\}\{x_2,\kappa_{2\perp};1/2,1/2\}\{x_3,\kappa_{3\perp};1/2,-1/2\})\\
&= -\frac{24}{\sqrt{2\sqrt{2}}}\Big(p_1^+\Big)^{\frac{3}{2}}\int\frac{\prod_{i=1}^{3}\mathrm{d}\kappa_{i\perp}}{[2(2\pi)^3]^2}\delta^{(2)}\Big(\sum_{i=1}^{3}\kappa_{i\perp}\Big)\\
&\times\tilde{\Psi}^{N,[f]}_{1/2}(\{x_1,\kappa_{1\perp};-1/2,1/2\}\{x_2,\kappa_{2\perp};1/2,1/2\}\{x_3,\kappa_{3\perp};1/2,-1/2\});
\end{aligned}
\tag{2.26}
$$

$$
\begin{aligned}
M^{\uparrow}_{11,2} &= -\frac{24}{\sqrt{x_1x_2x_3}}\int\frac{\prod_{i=1}^{3}\mathrm{d}\kappa_{i\perp}}{[2(2\pi)^3]^2}\delta^{(2)}\Big(\sum_{i=1}^{3}\kappa_{i\perp}\Big)\\
&\times u_{+1}(x_1p_1^+,1/2)u_{+1}(x_2p_1^+,1/2)u_{+2}(x_3p_1^+,-1/2)\\
&\times\tilde{\Psi}^{N,[f]}_{1/2}(\{x_1,\kappa_{1\perp};1/2,1/2\}\{x_2,\kappa_{2\perp};1/2,1/2\}\{x_3,\kappa_{3\perp};-1/2,-1/2\})\\
&= -\frac{24}{\sqrt{2\sqrt{2}}}\Big(p_1^+\Big)^{\frac{3}{2}}\int\frac{\prod_{i=1}^{3}\mathrm{d}\kappa_{i\perp}}{[2(2\pi)^3]^2}\delta^{(2)}\Big(\sum_{i=1}^{3}\kappa_{i\perp}\Big)\\
&\times\tilde{\Psi}^{N,[f]}_{1/2}(\{x_1,\kappa_{1\perp};1/2,1/2\}\{x_2,\kappa_{2\perp};1/2,1/2\}\{x_3,\kappa_{3\perp};-1/2,-1/2\}).
\end{aligned}
\tag{2.27}
$$

Then, inserting the expressions (C.14), (C.14) and (C.14) that we have derived in Appendix C for the LCWFs entering in the previous equations we obtain the final representation for the matrix elements $M^{\uparrow}_{12,1}, M^{\uparrow}_{21,1}$ and $M^{\uparrow}_{11,2}$,

$$
\begin{aligned}
M^{\uparrow}_{12,1} &= \frac{8}{\sqrt{2\sqrt{2}}}\Big(p_1^+\Big)^{\frac{3}{2}}\int\frac{\prod_{i=1}^{3}\mathrm{d}\kappa_{i\perp}}{[2(2\pi)^3]}\delta^{(2)}\Big(\sum_{i=1}^{3}\kappa_{i\perp}\Big)\Big[\frac{1}{M_0}\frac{\omega_1\omega_2\omega_3}{x_1x_2x_3}\Big]^{\frac{1}{2}}\psi(\kappa_1,\kappa_2,\kappa_3)\\
&\times\prod_i\frac{1}{\sqrt{N(x_i,\boldsymbol{k}_{\perp i})}}\Big\{\sqrt{2}\Big[a_1\kappa_2^R\kappa_3^L\Big]\\
&-(1/\sqrt{2})\Big[\kappa_1^L\kappa_2^Ra_3\Big]+(1/\sqrt{2})\Big[a_1a_2a_3\Big]\Big\};
\end{aligned}
\tag{2.28}
$$

$$
\begin{aligned}
M^{\uparrow}_{21,1} &= \frac{8}{\sqrt{2\sqrt{2}}}\Big(p_1^+\Big)^{\frac{3}{2}}\int\frac{\prod_{i=1}^{3}\mathrm{d}\kappa_{i\perp}}{[2(2\pi)^3]}\delta^{(2)}\Big(\sum_{i=1}^{3}\kappa_{i\perp}\Big)\Big[\frac{1}{M_0}\frac{\omega_1\omega_2\omega_3}{x_1x_2x_3}\Big]^{\frac{1}{2}}\psi(\kappa_1,\kappa_2,\kappa_3)\\
&\times\prod_i\frac{1}{\sqrt{N(x_i,\boldsymbol{k}_{\perp i})}}\Big\{\sqrt{2}\Big[\kappa_1^Ra_2\kappa_3^L)\Big]\\
&-(1/\sqrt{2})\Big[\kappa_1^R\kappa_2^La_3\Big]+(1/\sqrt{2})\Big[a_1a_2a_3\Big]\Big\};
\end{aligned}
\tag{2.29}
$$

$$
\begin{aligned}
M^{\uparrow}_{11,2} &= \frac{-8}{\sqrt{2\sqrt{2}}}\Big(p_1^+\Big)^{\frac{3}{2}}\int\frac{\prod_{i=1}^{3}\mathrm{d}\kappa_{i\perp}}{[2(2\pi)^3]}\delta^{(2)}\Big(\sum_{i=1}^{3}\kappa_{i\perp}\Big)\left[\frac{1}{M_0}\frac{\omega_1\omega_2\omega_3}{x_1x_2x_3}\right]^{\frac{1}{2}}\psi(\kappa_1,\kappa_2,\kappa_3)\\
&\times\prod_i\frac{1}{\sqrt{N(x_i,\boldsymbol{k}_{\perp i})}}\Big\{(1/\sqrt{2})\Big[\kappa_1^L a_2\kappa_3^R\Big)\Big]\\
&+(1/\sqrt{2})\Big[a_1\kappa_2^L\kappa_3^R\Big]+\sqrt{2}\Big[a_1a_2a_3\Big]\Big\};
\end{aligned}
\tag{2.30}
$$

where (as in Appendix C) we have introduced the shorthand notations, $a_i = (m + x_iM_0)$, $\kappa_i^{R/L} = \kappa_i^x \pm \kappa_i^y$ and $N(x_i, \boldsymbol{k}_{\perp i}) = [(m + x_iM_0)^2 + \boldsymbol{k}^2_{\perp,i}]$. Substituting in the Eqs. (2.16) the final results we have obtained for the three matrix elements we can give the general analytical representation for the DAs

$$
\begin{aligned}
V_1 &= \frac{1}{f_N}\frac{1}{\sqrt[4]{2}}(p_1^+)^{-\frac{3}{2}}\Big(M^{\uparrow}_{12,1}+M^{\uparrow}_{21,1}\Big)\\
&= \frac{8}{\sqrt{2}}\frac{1}{f_N}\left[\frac{1}{M_0}\frac{\omega_1\omega_2\omega_3}{x_1x_2x_3}\right]^{\frac{1}{2}}\int\frac{\prod_{i=1}^{3}\mathrm{d}^2\kappa_{i\perp}}{16\pi^3}\delta^{(2)}\Big(\sum_{i=1}^{3}\kappa_{i\perp}\Big)\psi(\kappa_1,\kappa_2,\kappa_3)\\
&\times\prod_i\frac{1}{\sqrt{N(x_i,\boldsymbol{k}_{\perp i})}}\Big\{\Big[a_1\kappa_2^R\kappa_3^L\Big]+\Big[a_1a_2a_3\Big]\\
&-\frac{1}{2}\Big[\kappa_1^L\kappa_2^R a_3\Big]-\frac{1}{2}\Big[\kappa_1^R\kappa_2^L a_3\Big]+\Big[\kappa_1^R a_2\kappa_3^L\Big]\Big\},
\end{aligned}
\tag{2.31}
$$

$$
\begin{aligned}
A_1 &= \frac{1}{f_N}\frac{1}{\sqrt[4]{2}}(p_1^+)^{-\frac{3}{2}}\Big(M^{\uparrow}_{21,1}-M^{\uparrow}_{12,1}\Big)\\
&= \frac{8}{\sqrt{2}}\frac{1}{f_N}\left[\frac{1}{M_0}\frac{\omega_1\omega_2\omega_3}{x_1x_2x_3}\right]^{\frac{1}{2}}\int\frac{\prod_{i=1}^{3}\mathrm{d}^2\kappa_{i\perp}}{16\pi^3}\delta^{(2)}\Big(\sum_{i=1}^{3}\kappa_{i\perp}\Big)\psi(\kappa_1,\kappa_2,\kappa_3)\\
&\times\prod_i\frac{1}{\sqrt{N(x_i',\boldsymbol{\kappa}_{\perp i})}}\Big\{\Big[\kappa_1^R a_2\kappa_3^L\Big]-\Big[a_1\kappa_2^R\kappa_3^L\Big]\\
&+\frac{1}{2}\Big[\kappa_1^L\kappa_2^R a_3\Big]-\frac{1}{2}\Big[\kappa_1^R\kappa_2^L a_3\Big]\Big\},
\end{aligned}
\tag{2.32}
$$

$$
\begin{aligned}
T_1 &= -\frac{1}{f_N}\frac{1}{\sqrt[4]{2}}(p_1^+)^{-\frac{3}{2}}M^{\uparrow}_{11,2}\\
&= \frac{8}{\sqrt{2}}\frac{1}{f_N}\left[\frac{1}{M_0}\frac{\omega_1\omega_2\omega_3}{x_1x_2x_3}\right]^{\frac{1}{2}}\int\frac{\prod_{i=1}^{3}\mathrm{d}^2\kappa_{i\perp}}{16\pi^3}\delta^{(2)}\Big(\sum_{i=1}^{3}\kappa_{i\perp}\Big)\psi(\kappa_1,\kappa_2,\kappa_3)\\
&\times\prod_i\frac{1}{\sqrt{N(x_i',\boldsymbol{\kappa}_{\perp i})}}\Big\{\Big[a_1a_2a_3\Big]+\frac{1}{2}\Big[a_1\kappa_2^L\kappa_3^R\Big]+\frac{1}{2}\Big[\kappa_1^L a_2\kappa_3^L\Big]\Big\}.
\end{aligned}
\tag{2.33}
$$

From the three expressions found for the leading-twist three DAs, Eqs. [(2.31)–(2.33)], one can easily see that the general symmetry properties for the DAs reported in Appendix A are satisfied.

2.1.3 Model Results

The analytical results of the previous section are independent on a specific model for the momentum part of the hadron WF. Namely, the assumption in the calculation is that the LCWFs describing the nucleon low energy structure can be factorized in a term describing the spin-isospin component and a term accounting for the momentum dependence, and where the spin-isospin part is SU(6) symmetric.

Since so far, as we have already stated, it is impossible to describe the momentum component of the WF governed by the low energy dynamics of strong interactions starting from first principles one has to rely on models. In particular, in this work we will focus our attention to relativistic Constituent Quark Models (CQMs). Such models are based on the hypotheses that the Fock state expansion is dominated by the valence quarks only and that the effective degrees of freedom of the theory are represented by the constituent quarks. In literature there are several relativistic CQMs, among the others we quote [60, 61, 62, 63]. The last two models have been extensively used (see later) by our group to give numerical predictions for parton distribution functions [64], generalized parton distribution functions [65], electro-magnetic form factors [66], spin densities [67] and other hadronic observables of great experimental interest [68].

The model of Ref. [62] is a relativized version of the hypercentral CQM of Ref. [69]. The hypercentral CQM is based on the mass operator $M = M_0 + V$, where M_0 is the free mass operator,

$$M_0 = \sum_{i=1}^{3} \sqrt{\vec{k}_{i\perp}^2 + m_i^2}, \tag{2.34}$$

with $\sum_{i=1}^{3} \vec{k}_{i\perp} = 0$ and m_i being the constituent quark masses. The interaction is taken of the form [69]

$$V = -\frac{\tau}{y} + \kappa_l y, \tag{2.35}$$

where $y = \sqrt{\vec{\rho}^2 + \vec{\lambda}^2}$ is the radius of the hypersphere in six dimensions and $\vec{\rho}$ and $\vec{\lambda}$ are the Jacobi coordinates,

$$\vec{\rho} = \frac{\vec{r}_1 - \vec{r}_2}{\sqrt{2}}, \qquad \vec{\lambda} = \frac{\vec{r}_1 + \vec{r}_2 - 2\vec{r}_3}{\sqrt{6}}. \tag{2.36}$$

The spin-isospin part of the WF is SU(6) symmetric and the model depends on three parameters, m_i, τ and κ_l, and is able to reproduce the basic features of the low-lying nucleon spectrum satisfactorily in spite of its simplicity.
On the other hand the model of reference [63] is a relativistic quark model in which the spin-isospin part is assumed to be SU(6) symmetric and the momentum part of the LCWF is described by means of a power-law behaviour of the kind

$$\psi(\{\kappa_{\perp i}\}) = \frac{N}{(M_0^2 + \beta^2)^\gamma}, \tag{2.37}$$

where M_0, as usual, is the free mass operator, whereas β and γ are the two (of the three with m_i) parameters of the model fitted to reproduce the magnetic moment of the proton and the axial coupling constant g_A. The best fit gives the values $m_i = 263$ MeV, $\beta = 607$ MeV and $\gamma = 3.5$.

An important feature of these LC CQMs is that the procedure of boosting the LCWFs obtained in the usual *instant form* of relativistic dynamics to the *front form* introduces terms with orbital angular momentum contributions different from zero [70]. Indeed, after the boost to the light-cone, even starting with the quarks in a S-wave configuration, one ends up with contributions from higher angular momentum waves (P and D) also.

In the following we report our model predictions for the Nucleon DAs obtained through the relativistic constituent quark model of Ref. [63].

Numerical Results for our model calculation

In this paragraph we show our numerical results for the nucleon Distribution Amplitudes obtained with the momentum part of the wavefunction (C.3) described with the model of reference [63]. In particular, in Fig. (2.1.3) and in Fig. (2.2) we plot, respectively, the DAs $\Phi(x_1, x_2, x_3) \doteq V_1(x_1, x_2, x_3) - A_1(x_1, x_2, x_3)$ and $V(x_1, x_2, x_3)$. While in Fig. (2.3) we report our result for the tensorial DA $T(x_1, x_2, x_3)$.

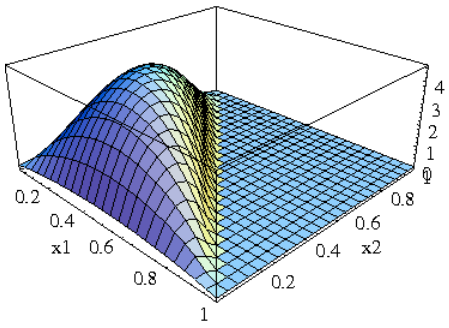

Figure 2.1: Distribution Amplitude $\Phi(x_1, x_2, x_3) \doteq V_1(x_1, x_2, x_3) - A_1(x_1, x_2, x_3)$ obtained within the relativistic constituent quark model of Ref. [63].

Results from other models or parameterizations

In the early eighties, after the pioneering works of Lepage and Brodsky [48], many applications of QCD were promoted to study exclusive processes, e.g. computing meson and nucleon form factors, as well as the first moment of the pion distribution amplitude (i.e. the f_π decay constant). In those years V.L. Chernyak, A.R. Zhitnitsky and I.R. Zhitnitsky attempted to reconstruct model distribution amplitudes from the few first moments for the pion [71],

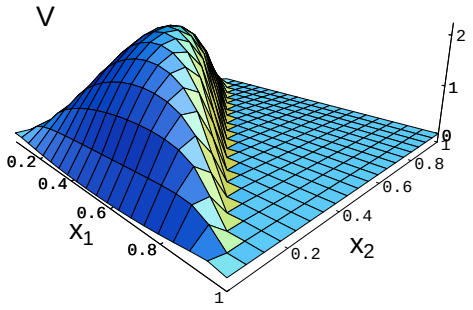

Figure 2.2: Distribution Amplitude $V(x_1, x_2, x_3)$.

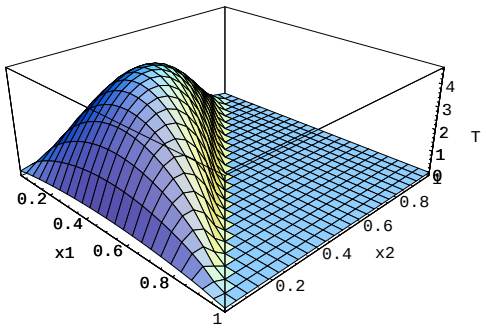

Figure 2.3: Distribution Amplitude $T(x_1, x_2, x_3)$.

the nucleon [72], and other hadrons [49]. The values of the moments were restricted in their approach by constraints extracted from QCD sum rules, and model distribution amplitudes as polynomials in the longitudinal momenta of the valence quarks were derived by means of moment inversion. An analysis for the nucleon on the basis of the first- and second-order moments, led the author to propose a nucleon DA which shows considerable asymmetry in the distribution of the longitudinal momentum of the valence quarks. Few years later an alternative distribution was suggested by Gari and Stefanis (GS) [73], constructed with the aim to yield helicity-conserving nucleon form factors which account for the possibility that the electron-neutron differential cross section is dominated by $G_{\rm E}^n$, while $G_{\rm M}^n$ is asymptotically small, or, equivalently that there is a sizeable neutron Pauli form factor overwhelming the Dirac one at all Q^2 values. The GS model gives very good agreement with the latest high-Q^2 SLAC data [74] on $G_{\rm M}^p$ (or F_1^p) and makes realistic predictions for the corresponding neutron form factor in the high-momentum region [75]. In contrast, as shown in Ref. [75], the CZ model overestimates both form factors almost by a factor of two in the region of 10-20 GeV^2, if realistic values of $\Lambda_{\rm QCD}$ around 200 MeV are used[‡]. But, on the theoretical side, a heavy price is paid: some

[‡]In the original CZ analysis, the value $\Lambda_{\rm QCD} = 100$ MeV was used. Such a low value is now de facto excluded by experiment.

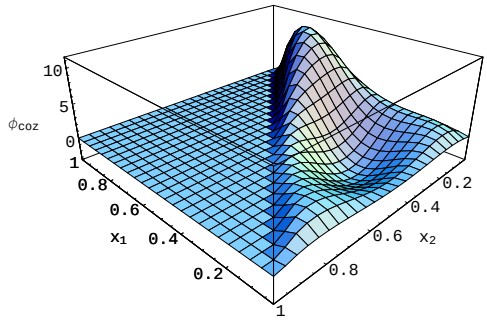

Figure 2.4: Distribution Amplitude Φ from the parametrization [76, 76].

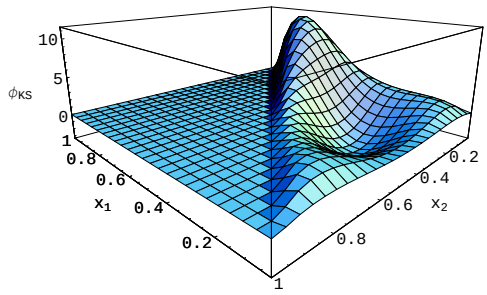

Figure 2.5: Distribution Amplitude Φ from [77].

moments of the GS model DA cannot match the requirements set by the CZ moment sum rules (MSRs) in the allowed saturation range [75]. Moreover, as it was shown later by Chernyak and coworkers [76], this model leads to a prediction for the ${}^3S_1 \to p\bar{p}$ decay width of charmonium which is several orders of magnitude smaller than the experimental value[§].

In 1987 the moment sum rules were re-evaluated by King and Sachrajda (KS) [77], spotting the gaps in the CZ analysis and shifting the range of the moment sum rule, albeit the gross features of the method were confirmed as well as the basic shape of the nucleon DA, Fig. (2.5).

A couple of years later, Chernyak, Ogloblin, and I. R. Zhitnitsky (COZ) [78] refined their previous sum rule for the second-order moments and extended their method to third-order moments. Their new MSRs comprise 18 terms with restricted margins of uncertainty relative to the previous CZ analysis and, in general, comply with the results of the KS computation, but contradict those obtained some years before on the lattice for the lowest two moments [79]. The same authors have also proposed a new model DA for the nucleon, see Fig. (2.4) – still restricted to polynomials of second degree in the longitudinal momentum – which satisfies all, but 6 of the new MSR, whereas the CZ amplitude and the

[§]Provided one uses again the favored value of the strong coupling constant $\alpha_s = 0.3$.

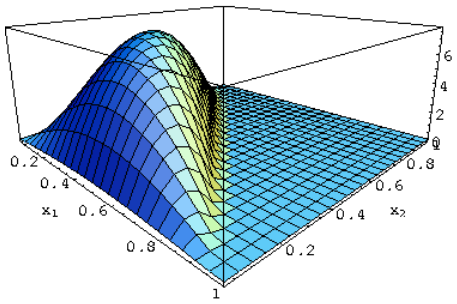

Figure 2.6: Distribution Amplitude Φ from [33].

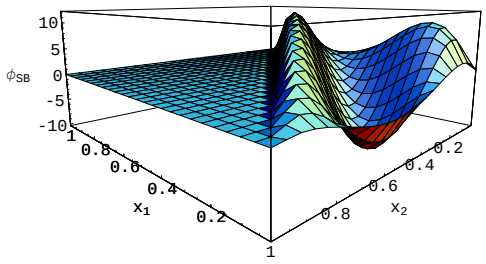

Figure 2.7: Distribution Amplitude Φ from [84].

GS one violate, respectively, 13 and 14 of them. The KS amplitude provides almost the same quality as that of COZ, with only 7 broken MSR. In the same year, Schäfer [80] presented a variety of model DAs for the nucleon, which incorporate polynomials of degree three in the longitudinal momentum, and found that such contributions play a token role, if properly incorporated.

The essence of these investigations is that DAs extracted from MSR are much broader than the usual asymptotic solution derived by Lepage and Brodsky (from the evolution equation, see later) and have a rich structure that is reflected in a quite asymmetric balance in the distribution of longitudinal momentum fractions among the valence quarks, accentuated by nodes.

In the same years a different and more physical approach has been pursued by Dziembowski [33], and subsequently refined by Dziembowski himself and Franklin [81], giving results pretty similar to those of the methods outlined before. Dziembowski describes the nucleon by means of a relativistic CQM based on the following assumptions: *i)* the nucleon states are dominated by the valence quark configuration with typical masses of about 330 MeV; *ii)* the valence component is a system described by a gaussian momentum-space WF

$$\psi(x_i, \mathbf{k}_{\perp i}) = A \exp\left[\frac{1}{6\alpha^2}\left(M^2 - \sum_{i=1}^{3}(\mathbf{k}_{\perp i}^2 + m_i^2)/x_i\right)\right], \qquad (2.38)$$

where α is the gaussian parameter determined by the value of the average quark transverse momentum, i.e. $\alpha^2 \approx \langle \mathbf{k}_\perp^2 \rangle$; and *iii)* the three-quark valence

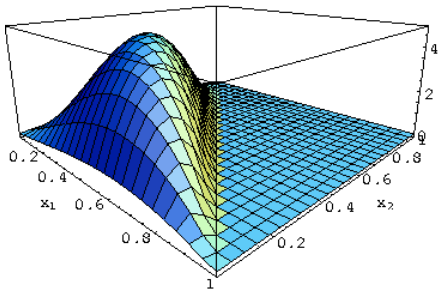

Figure 2.8: Distribution Amplitude Φ from [97].

system in the nucleon is an interacting particle state with the standard quark model spin-parity and isospin assignments determined with the Melosh unitary transformation linking the *instant form* to the *light-cone form*. Even though the momentum part of the WF is totally symmetric under the exchange of the individual momenta, the total WF including the spin-isospin components is asymmetric. As result the distribution in x_i of the DAs is not symmetric, see Fig. (2.6). However, for values of the quark masses $m \gtrsim \alpha$ the total WF gives a configuration in which the three quarks are treated at the same footing and that imitates the non-relativistic distribution amplitudes for which $x_i \approx 1/3$, i.e. each quark carries an equal fraction of the nucleon momentum.

In the work with Franklin [81], Dziembowski inspired by the model of De Rújula, Georgi and Glashow [82] introduces a stronger coupling between the spin-0 quark pair[¶]. With this asymmetric momentum WF, the mixed asymmetric spin-isospin combination is no longer equivalent to the mixed symmetric state. It can be observed that with this refined model the authors can give a better overall description of the CZ moments.

The next major step in the determination of nucleon DAs was done in the early nineties by Stefanis and Bergmann with the invention of the *heterotic conception*[‖] [83, 84, 85, 86]. Previously, the CZ model (or its descendants: KS and COZ models) on one hand and the GS model on the other hand were treated in the literature as competing alternatives – mutually excluding each other. In addition, either way, it was not possible to reconcile the theoretical MSR constraints with the experimental data because none of these models is able to give, simultaneously, a quantitatively satisfactory agreement with the form-factor and charmonium-decay data.

Perhaps understandably, in view of such distinctive models and predictions, the conventional view has been one of fragmentation. But the new idea, underlying the nucleon heterotic model, makes it possible to amalgamate the best

[¶]The motivation for emphasizing spin-zero clustering comes from QCD where the exchange of gluons provides attractive forces that are strongest in the spin-0 quark-quark state. The spin-0 spin-spin force is three times stronger than the spin-1 spin-spin force.

[‖]"Heterosis" in Greek means increased vigor due to cross-breeding.

features of COZ-type and GS-type DAs into a single mould, thus lifting the disparity between theory and experiment. The heterotic DA is a "hybrid" – sort of – and seems to have a foot in each of the previous models, Fig. (2.7). This duality is also reflected in its profile which, though distinctive in overall shape from both the COZ and the GS DAs, bears geometrical characteristics typical for both models.

The approach of Bergmann and Stefanis is the same of CZ and COZ works. Starting from the COZ nucleon DA in the parameter space of the coefficients of the inversion they systematically seek for solutions with ratios $|G_{\rm M}^n|/G_{\rm M}^p \leq 0.5$ that satisfy the QCD sum rules with a similar accuracy as the COZ nucleon DA. These solution appear as local minima with respect χ^2 criterion defined by the deviation from the sum rule. The heterotic solution is uniquely determined by the deviation by the inversion coefficients of that local minimum which corresponds to the smallest possible ratio, about 0.1. The nucleon DA derived in this way matches, up to the second order, the KS requirements better than the COZ one.

Similar ideas of heterosis were then applied by the same authors [87] to the DA of the $\Delta^+(1232)$ isobar, treating the MSR of Farrar et al. (FZOZ) [88] and those by Carlson and Poor (CP) [89] in combination. Again a heterotic DA was determined in between the CP and the FZOZ model DAs. Using the heterotic distribution amplitudes for the nucleon and the Δ, the transition form factor $G_{\rm M}^*$ was calculated [84, 87] within the standard convolution scheme and remarkable agreement with the available data was found. Even more, a recent reanalysis by Stuart et al. [90, 91], of the inclusive $e-p$ data in the $\Delta(1232)$ region by the SLAC experiment NE11, combined with low Q^2 data, high Q^2 data from the SLAC experiment E133, and missing mass squared data, finds results for the transition form factor systematically higher than the previous data analysis by Stoler [92] and confirms within the errors the "heterotic" predictions [93].

Despite the appearent good phenomenological results obtained through the MSR approach, in those years, a question rised about the reliability of the hadronic distribution amplitudes reconstructed from QCD sum rules. Many papers appeared in literature pointing out that the MSR are not stringent enough to fix the shape of the nucleon DA uniquely [73, 75, 95]. A similar analysis for the pion DA was given by Mikhailov and Radyushkin [94].

For this reason two others approaches have been studied [97, 96]. The first one due to Bolz and Kroll has the purpose of constructing the nucleon WF demanding that it provides an overlap contribution that completely controls the Dirac form factor at momentum transfer of about 10 GeV^2. Obviously this requirement does not fix the WF univocally. Indeed the authors used PDFs and $J/\Psi \to N\bar{N}$ decay reaction data as further constraints in their analysis. They describe the WF factorizing it in two parts: the first one coming from the solution of the QCD evolution equation accounting for the x_i dependence, while the second one describing the dependence on the transverse momenta

$\mathbf{k}_{\perp i}$ with a symmetric gaussian shape. In such a way they found a WF with few parameters (2 or 3) that can be fitted to the data (see Fig. (2.8)).

The second interesting approach [96] introduced in order to obtain a more reasonable model of the DAs which avoids the problems of unphysical oscillations (due to a failure in the fine-tuning of higher-order expansion coefficients) is the one followed by Eckardt, Hansper and Gari. They were guided by some criteria of simplicity that a physical distribution amplitude should fulfill in addition to QCD sum rules: functional simplicity (e.g. an exponential ansatz), minimum number of parameters, smooth, no oscillations, positive, substantially non-polynomial, and with no specific process (experiment) as input (process-independence). They called the model constructed in such a way "haplousterotic" (Ha^+) (from the greek word $\alpha\pi\lambda\omega\upsilon\sigma\tau\varepsilon\rho\omega\varsigma$ for "simpler"). Using the above criteria, the haplousterotic model amplitude was determined from the QCD sum-rule moments of COZ. The model has the

$$\Phi_N^{Ha+}(x) = N \exp\left[-\left(\frac{b_1^{(r)}}{r_1} + \frac{b_2^{(r)}}{r_2} + \frac{b_3^{(r)}}{r_3}\right)\right], \tag{2.39}$$

where N is a normalization factor, and the b_i are three parameters adjusted in order to change the position of the maximum according to the requirements of QCD sum rule moments, $r = (1/2, 1, 2, ...)$. Of course, for the purpose of investigation of the Q^2-evolution of the DA or its convergence properties, Φ_N^{Ha+} can be expanded into a series. It can be shown that it presents a nice convergence. But one can also notice that very high polynomial degrees are needed for the expansion to resemble the shape of the exact model. On the other hand, it is interesting to stress that the second degree approximation to Φ_N^{Ha+} looks very much like the early model of CZ [96].

2.1.4 Evolution and Moments of the Distribution Amplitudes

In our discussion in the previous sections we have often repeated and outlined that, with the present knowledge of strong interactions, it is impossible to calculate DAs and more generally all the other hadronic observables from first principles. This is because the low energy dynamics is governed by effects that, so far, cannot be described through the perturbative method, and for this reason they are often called non-perturbative effects. Nevertheless in this section we show how the perturbative QCD results obtained by Lepage and Brodsky in their seminal works [48] serve as a guideline to some of the models outlined in the previous section. The nucleon distribution amplitude (2.1) is the three-quark WF integrated over transverse momenta

$$\phi(x_i, \mu^2) \equiv \left(\ln \frac{\mu^2}{\Lambda^2_{\rm QCD}}\right)^{-\frac{3}{2}\frac{\gamma_f}{\beta}} \int_{\mathbf{k}_{\perp i}<\mu^2} \left[\mathrm{d}^2\mathbf{k}_\perp\right]_N \Psi_N(x_i, \mathbf{k}_{\perp i}), \tag{2.40}$$

where the logarithm in front of the integral is due to the WF renormalization for the UV divergences owing to gluon radiative corrections in the hard scattering amplitude (see Cap. 1), i.e. $Z_2 = \lim_{\mu^2\to\infty}\left(\ln\frac{\mu^2}{\Lambda^2}\right)^{-\frac{3}{2}\gamma_f\beta}$, $\beta \equiv (11-2n_f/3)/4$ is the Gell-Mann and Low function, with n_f number of flavours, and γ_f is the anomalous dimension associated with the quark self energy in the light-cone gauge,

$$\gamma_f = C_F\left(1+4\int_0^1 \mathrm{d}x\frac{x}{1-x}\right). \tag{2.41}$$

The physical content of Eq. (2.40) is that an external probe, for example, an off-shell photon, "sees" only the distribution of quarks over the longitudinal momenta inside the nucleon, while its transverse size requires wavelenghts $\sim \frac{1}{\mu}$, so that the distribution of quarks over the transverse plane is not resolved.

The gauge invariant DA $\phi(x_i,\mu^2)$ is intrinsically non-perturbative and universal**. The large momentum behaviour of these functions can be analyzed either using OPE techniques or, equivalently, by evolution equations analogous to DGLAP equations [21] in deep-inelastic scattering. Following the second approach, one takes derivatives with respect to Q^2 of Eq. (2.40) to arrive at evolution equations of the generic form [48]

$$\frac{\partial\,\phi(x_i,Q^2)}{\partial\ln Q^2} = \int_0^1 [dy]\,V\left(x_i,y_i,\alpha_{\rm s}(Q^2)\right)\phi(x_i,Q^2) \tag{2.42}$$

with distinct kernels $V\left(x_i,y_i,\alpha_{\rm s}(Q^2)\right)$ for each process at hand, which, to leading order in $\alpha_{\rm s}$, are computable from the single-gluon-exchange kernel.

To solve the evolution equation, ϕ has to be expressed as an orthogonal expansion in terms of appropriate functions which constitute an eigenfunction basis of the particular gluon-exchange kernel, i.e.,

$$\phi(x_i,Q^2) = \phi_{\rm as}(x_i)\sum_{n=0}^{\infty}B_n(\mu^2)\tilde{\phi}_n(x_i)\exp\left\{\int_{\mu^2}^{Q^2}\frac{d\bar{\mu}^2}{\bar{\mu}^2}\gamma_{\rm F}(g(\bar{\mu}^2))\right\}, \tag{2.43}$$

where $\phi_{\rm as}$ is the renormalization group asymptotic DA (see below) being proportional to the weight $w(x_i)$ of the particular orthogonal basis, and $\tilde{\phi}_n$ denotes the corresponding eigenfunctions. The coefficients B_n of this expansion are associated with matrix elements of composite lowest-twist operators with definite anomalous dimensions (after diagonalization of the evolution kernel) taken between the vacuum and the external hadron. They represent the non-perturbative input (integration constants of the renormalization group equation) in Eq. (2.43) and have to be determined at some initial scale of evolution μ^2 by non-perturbative techniques. The exponential factor in Eq. (2.43) takes care of momentum evolution according to the renormalization group and is

**Universal once it is used the same factorization scheme to cast the exclusive amplitudes for different processes in the convolution form.

governed by the quark anomalous dimension

$$\gamma_{\rm F} = \frac{\mu}{Z_2}\frac{\partial Z_2}{\partial \alpha_{\rm s}}\frac{\partial \alpha_{\rm s}}{\partial \mu}, \tag{2.44}$$

which in the axial gauge is [98]

$$\gamma_q = -\frac{\alpha_{\rm s}}{\pi} + O(\alpha_{\rm s}^2)\ . \tag{2.45}$$

The advantage of employing an eigenfunctions decomposition is that the evolution equation can be solved by diagonalization. Following Refs.[48, 99] the evolution equation for the nucleon DA is,

$$x_1x_2x_3\ \left[\frac{\partial}{\partial \xi}\tilde{\phi}(x_i,Q^2) + \frac{3}{2}\frac{C_{\rm F}}{\beta}\,\tilde{\phi}(x_i,Q^2)\right] = \frac{C_{\rm F}}{\beta}\int_0^1 [dy]\,V(x_i,y_i)\,\tilde{\phi}(y_i,Q^2)\ , \tag{2.46}$$

where $\phi = x_1x_2x_3\,\tilde{\phi}$, $C_{\rm F}$ is the Casimir operator for the fundamental representation of a group defined as $C_{\rm F} = (N^2-1)/2N$ with N the dimension of the symmetry group, e.g. $\mathrm{SU}(3)_c \Rightarrow C_{\rm F} = 4/3$. In the last equation, we have made use of the evolution "time" parameter

$$\xi \equiv \frac{\beta_0}{4\pi}\int_{\mu^2}^{Q^2}\frac{dk_\perp^2}{k_\perp^2}\,\alpha_{\rm s}(k_\perp^2) = \ln\frac{\alpha_{\rm s}(\mu^2)}{\alpha_{\rm s}(Q^2)} = \ln\frac{\ln Q^2/\Lambda^2_{\rm QCD}}{\ln \mu^2/\Lambda^2_{\rm QCD}}, \tag{2.47}$$

and of the relation

$$\frac{\partial}{\partial Q^2} = \frac{\partial \xi}{\partial Q^2}\frac{\partial}{\partial \xi} = \frac{\beta_0}{4\pi}\frac{\alpha_{\rm s}(Q^2)}{Q^2}\frac{\partial}{\partial \xi}. \tag{2.48}$$

Moreover the integrand $V(x_i,y_i)$ reads,

$$V(x_i,y_i) = 2x_1x_2x_3\sum_{j\neq i}\Theta(y_i-x_i)\,\delta(y_k-x_k)\,\frac{y_j}{x_j}\left[\frac{\delta_{h_i\bar{h}_j}}{x_i+x_j} + \frac{\Delta}{y_i-x_i}\right]\ . \tag{2.49}$$

Note that $V(x_i,y_i) = V(y_i,x_i)$ is the sum over single-gluon interactions between quark pairs $\{i,j\}$, and the subtraction prescription $\Delta\tilde{\phi}(y_i,Q^2) \equiv \tilde{\phi}(y_i,Q^2) - \tilde{\phi}(x_i,Q^2)$ ensures IR finiteness at $x_i = y_i$, i.e., $V(x_i,y_i)$ is not a function but a distribution. For antiparallel spins $\delta_{h_i\bar{h}_j} = 1$ and for parallel spins it equals 0. Note also that if no gluon is exchanged, each x_k in the initial and final wave function is the same because no longitudinal momentum is introduced by q^μ ($q^+ = 0$). The idea is to solve the evolution equation by employing factorization of the dependence on longitudinal momentum from that on the external (large) momentum scale Q^2 (cf. Eq. (2.43)). The latter is renormalization group controlled (Cap. 1) according to

$$\frac{\partial}{\partial \xi}\,\tilde{\phi}_n(x_i,Q^2) = -\gamma_n\,\tilde{\phi}_n(x_i,Q^2) \tag{2.50}$$

with solutions

$$\tilde{\phi}_n(x_i, Q^2) \simeq \tilde{\phi}_n(x_i) \left(\ln \frac{Q^2}{\Lambda^2_{\rm QCD}} \right)^{-\gamma_n} . \tag{2.51}$$

This allows us to write the full nucleon DA in the form

$$\phi(x_i, Q^2) = \phi_{\rm as}(x_i, Q^2) \sum_{n=0}^{\infty} B_n \, \tilde{\phi}_n(x_i) \left(\ln \frac{Q^2}{\Lambda^2_{\rm QCD}} \right)^{-\gamma_n} , \tag{2.52}$$

where $\phi_{\rm as} \equiv 120 x_1 x_2 x_3$ is the asymptotic solution, $\tilde{\phi}_n(x_i)$ are appropriate but not tabulated polynomials, and the expansion coefficients B_n encode the non-perturbative input of the bound-states dynamics at the factorization (renormalization) scale.

From the factorized form of $\tilde{\phi}_n(x_i, Q^2)$ in Eq. (2.51), it follows that the evolution equation for the x-dependence reduces to the characteristic equation

$$x_1 x_2 x_3 \left[\frac{3}{2} \frac{C_{\rm F}}{\beta} - \gamma_n \right] \tilde{\phi}(x_i) = \frac{C_{\rm B}}{\beta} \int_0^1 [dy] \, \frac{V(x_i, y_i)}{w(x_i)} \, \tilde{\phi}(y_i) , \tag{2.53}$$

where $w(x_i) = x_1 x_2 x_3 = x_1(1 - x_1 - x_3)x_3$ is the weight function of the orthogonal basis and $C_{\rm B} = (N_{\rm c} + 1)/2N_{\rm c} = 2/3$ the Casimir operator of the adjoint representation of $\mathrm{SU}(3)_{\rm c}$. To proceed, it is convenient to conceive of the kernel $V(x_i, y_i)$ as being an operator expanded over the polynomial basis [48] $|x_1^k \, x_3^l\rangle \equiv |k \, l\rangle$, (recall that because of momentum conservation, only two out of three x_i variables are linearly independent), i.e. to write

$$\hat{V} \equiv \int_0^1 [dy] \, V(x_i, y_i) \tag{2.54}$$

and convert Eq. (2.53) into the algebraic equation

$$\left[\frac{3}{2} \frac{C_{\rm F}}{\beta} - 2 \frac{C_B}{\beta} \, \frac{\hat{V}}{2w(x_i)} \right] \tilde{\phi}_n(x_i) = \gamma_n \, \tilde{\phi}_n(x_i) . \tag{2.55}$$

In this way, the action of the operator $\hat{V}$ can be completely determined by a matrix, namely:

$$\frac{\hat{V}|k \, l\rangle}{2w(x_i)} = \frac{1}{2} \sum_{i,j}^{i+j \leq M} U_{ij,kl} |i \, j\rangle . \tag{2.56}$$

The corresponding eigenvalues are then determined by the roots η_n of the characteristic polynomial that diagonalizes the matrix U [††]:

$$\hat{V} \, \tilde{\phi}_n(x_i) = -\eta_n \, w(x_i) \, \tilde{\phi}_n(x_i) , \tag{2.57}$$

[††]The explicit form of the matrix U was derived by Lepage and Brodsky [48] and can be found in Appendix A of Ref. [99]. Within the basis $|k \, l\rangle$, the matrix U can be diagonalized to provide eigenfunctions, which are polynomials of degree $M = k + l = 0, 1, 2, 3 \ldots$, with $M + 1$ eigenfunctions for each M. This was done in [48] by diagonalizing the $(M + 1) \times (M + 1)$ matrix $U_{ij,kl}$ with $i + j = k + l = M$ and results up to $M = 2$ were obtained.

so that the anomalous dimensions for order M are given by

$$\gamma_n(M) = \frac{1}{\beta}\left(\frac{3}{2}C_{\rm F} + 2\eta_n(M)C_{\rm B}\right) , \tag{2.58}$$

where the orthogonalization prescription

$$\int_0^1 [dx]\, w\,(x_i)\ \tilde{\phi}_m(x_i)\tilde{\phi}_n(x_i) = \frac{1}{N_m}\,\delta_{mn} \tag{2.59}$$

has been employed with N_m being appropriate normalization constants. This orthogonality condition is insufficient to determine the polynomial basis uniquely. This is because the orthogonality of polynomials depending on two (or more) variables via a generalization of the Hilbert-Schmidt method is not unique.

The non-perturbative input enters Eq. (2.52) through the coefficients $B_n(\mu^2)$ which represent non-perturbative matrix elements of appropriate three-quark operators interpolating between the proton and the vacuum. Their determination involves correlators of the form

$$\begin{aligned} I^{\,(n_1n_2n_3,m)}(q,z) &= i\int d^4x\, {\rm e}^{iq\cdot x}\langle 0|T\big(F_\gamma^{(n_1n_2n_3)}(0)\hat{J}_{\gamma'}^{(m)}(x)\big)|0\rangle(z\cdot\gamma)_{\gamma\gamma'} \\ &= (z\cdot q)^{\,n_1+n_2+n_3+m+3} I^{\,(n_1n_2n_3,m)}(q^2)\ , \end{aligned} \tag{2.60}$$

used by the authors of [72, 77, 76] as constraints for the determination of the moments of the DAs. In the previous equation, z is a light-like ($z^2 = 0$) auxiliary vector and the factor $(z\cdot\gamma)_{\gamma\gamma'}$ serves to project out the leading-twist structure of the correlator. The computation of the Wilson coefficients on the quark side of the correlator amounts to the perturbative evaluation of diagrams involving quark/gluon condensates [72]. It yields the theoretical side of the sum rule. The phenomenological side of the sum rule is obtained by saturating the correlator by the lowest-mass baryon states via dispersion relation. Reconciliation of the two sides of the sum rule with respect to the Borel parameter (which resembles momentum) determines the margin of permissible values for a particular moment. The three-quark operators in Eq. (2.60) are typified by the expression

$$O^{(n_1n_2n_3)} = (z\cdot P)^{-(n_1+n_2+n_3)}\prod_{i=1}^{3}\left(iz\cdot\frac{\partial}{\partial z_i}\right)^{n_i} O(z_i\cdot p)\big|_{z_i=0}. \tag{2.61}$$

Their matrix elements

$$\langle 0|O_\gamma^{(n_1n_2n_3)}(0)|P\rangle = f_{\rm N}(z\cdot P)^{\,n_1+n_2+n_3+1} N_\gamma\, O^{\,(n_1n_2n_3)} \tag{2.62}$$

are related to the moments

$$O^{(n_1n_2n_3)} = \int_0^1 [dx] x_1^{n_1}x_2^{n_2}x_3^{n_3}O(x_1,x_2,x_3), \tag{2.63}$$

where $O(x_i)$ stands for one of the amplitudes V_1, A_1, T_1, or linear combination of them. Because of the linear momentum conservation, $x_1 + x_2 + x_3 = 1$, not all the moments at a given order $M = n_1 + n_2 + n_3$ are linearly independent, namely

$$\phi_N^{(n_1,n_2,n_3)} = \phi_N^{(n_1+1,n_2,n_3)} + \phi_N^{(n_1,n_2+1,n_3)} + \phi_N^{(n_1,n_2,n_3+1)} \; . \tag{2.64}$$

For instance, at order $M = 3$ there are 20 moments out of which only 10 are strictly independent. Following [48] we consideration combinations formed by powers of the monomial $x_1 x_3$, i.e. the basis $|k\, l\rangle$. In term of this basis, the moment of ϕ_N read

$$\phi_N^{(n_1 n_2 n_3)} = \int_0^1 dx_1 \int_0^{1-x_1} dx_3 \left[\sum_{i=0}^{n_2} \sum_{j=0}^{i} (-1)^i \binom{n_2}{i} \binom{i}{j} x_1^{n_1+i-j} x_3^{n_3+j} \right] \phi_N(x_1, x_3), \tag{2.65}$$

and the strict moments are defined as

$$\phi_N^{(i0j)} = \int_0^1 [dx]\, x_1^i\, x_2^0\, x_3^j\, \phi_N(x_k, \mu^2). \tag{2.66}$$

Stefanis and Bergmann pointed out that it is possible to derive a closed-form expression of the expansion coefficients to any desired order of polynomial expansion:

$$\begin{aligned} \frac{B_n(Q^2)}{\sqrt{N_n}} &= \frac{\sqrt{N_n}}{120} \left[\frac{\ln(Q^2/\Lambda^2_{QCD})}{\ln(\mu^2/\Lambda^2_{QCD})} \right]^{-\gamma_n} \sum_{i,j=0}^{\infty} a_{ij}^n \; \phi_N^{(i0j)}(\mu^2) \\ &= B_n(\mu^2) \left[\frac{\ln(Q^2/\Lambda^2_{QCD})}{\ln(\mu^2/\Lambda^2_{QCD})} \right]^{-\gamma_n} . \end{aligned} \tag{2.67}$$

The projection coefficients a_{ij}^n and the normalization constant N_n up to order $M = 9$ have been calculated by Bergmann [99] in his Dissertation thesis with a polynomial basis orthogonal with respect to the weight $w(x_i) = x_1 x_2 x_3$ provided by the Appel polynomials [100]. Appell polynomials are special hypergeometric functions of the form

$$\mathcal{F}_{mn}^{(M)}(5, 2, 2; x_1, x_3) \equiv \mathcal{F}_{mn}(x_1, x_3) \; , \tag{2.68}$$

which constitute an orthogonal polynomial set on the triangle $T = T(x_1, x_3)$ with $x_1 > 0$, $x_3 > 0$, $x_1 + x_3 < 1$. They provide a suitable basis for solving the eigenvalue equations for the nucleon because within this basis $\hat{V}$ is block diagonal for different polynomial orders. Moreover, introducing a "symmetrized" basis of such polynomials according to

$$\begin{aligned} \tilde{\mathcal{F}}_{mn}(x_1, x_3) &= \frac{1}{2}[\mathcal{F}_{mn}(x_1, x_3) \pm \mathcal{F}_{nm}(x_1, x_3)] \\ &= \sum_{k,l=0}^{k+l \le m+n} Z_{kl}^{mn} |k\, l\rangle \end{aligned} \tag{2.69}$$

(where + refers to $m \geq n$ and − to $m < n$), $\hat{V}$ commutes with the permutation operator $P_{13} = [321]$ and thus becomes block diagonal within each sector of (definite) permutation-symmetry class of eigenfunctions for fixed order M. As a result, the kernel $\hat{V}$ can be analytically diagonalized up to order seven. This is related to the fact that the characteristic polynomial of matrices with rank four can be solved analytically. Beyond that order, its roots have to be determined numerically.

The utility of Eq. (2.67) is twofold. First the moments of DAs are not accurately determined. Thus, without the explicit relation between expansion coefficients and strict moments, one has to perform a simultaneous and self-consistent fit to the moment constraints, which becomes increasingly tedious as the moment-order grows. Second, we know that the orthogonalization procedure of polynomials with more than one variable is not unique. This means that in order to compare expansion coefficients B_n, obtained in different approaches, they ought to be normalized. The values of B_n without the knowledge of the normalization constant N_n are of no significance. However, having obtained Eq. (2.67) the knowledge of the normalization used in different approaches becomes superfluous. Modulo normalization, the coefficients B_n can be self-consistently computed on the basis of the universal strict moments. The link between B_n and the strict moments of ϕ_N is (B_0 is fixed to unity by the normalization of ϕ_N) [75]:

$$\begin{aligned}
B_1(\mu^2) &= \frac{1260}{120}\left[\Phi_N^{(100)} - \Phi_N^{(001)}\right]\Big|_{\mu^2} \\
B_2(\mu^2) &= \frac{420}{120}\left[\Phi_N^{(000)} - 3\Phi_N^{(010)}\right]\Big|_{\mu^2} \\
B_3(\mu^2) &= \frac{756}{120}\left[2\Phi_N^{(000)} - 7\Phi_N^{(100)} - 7\Phi_N^{(001)} + 8\Phi_N^{(200)} + 4\Phi_N^{(101)} + 8\Phi_N^{(002)}\right]\Big|_{\mu^2} \\
B_4(\mu^2) &= \frac{34020}{120}\left[\Phi_N^{(100)} - \Phi_N^{(001)} - \frac{4}{3}\Phi_N^{(200)} + \frac{4}{3}\Phi_N^{(002)}\right]\Big|_{\mu^2} \\
B_5(\mu^2) &= \frac{1944}{120}\left[2\Phi_N^{(000)} - 7\Phi_N^{(100)} - 7\Phi_N^{(001)} + \frac{14}{3}\Phi_N^{(200)} + 14\Phi_N^{(101)} + \frac{14}{3}\Phi_N^{(002)}\right]\Big|_{\mu^2}.
\end{aligned} \tag{2.70}$$

In the previous section, we outlined the results on the DAs obtained by different authors that employed the method of restricting the first moments of the DAs within intervals determined from QCD sum rules adapted to the LC [72, 77, 76]. As a matter of fact in such a way useful constraints can be obtained already with few moments. These are evaluated with the aid of correlators of the type (2.60) at some self-consistently determined normalization point $\mu_0 = \mu_F$ of order 1GeV at which a short-distance OPE can be safely performed. The constraints on the moments used to reconstruct model amplitudes for the nucleon, being the product of a fitting procedure, do not necessarily satisfy all sum-rule requirements. As mentioned before we stress that only the knowledge of Eq. (2.67) makes it possible to determine analytically a genuine

solution (if any exists) to the QCD sum rules. We know from previous consideration that the problem of determining an unknown distribution from a finite set of moments has no unique solution; this means that the expansion in terms of eigenfunctions is truncated after taking into account bilinear combinations of longitudinal momentum fractions and assuming that higher-order terms are of minor importance, if properly included. For instance, in Ref. [80] one can found a discussion on why the truncation at second order is justifiable. This is because the shape of the corresponding amplitude is a characteristic property of the entire series and the errors are of sub-leading importance.

In the following we report our results for the moments of the distribution amplitudes in comparison with other model calculations and lattice predictions. From the results it can be seen that our model predictions are in pretty good agreement both with the data fit of Bolz and Kroll [97] and very recent lattice simulations [101].

Table 2.2 shows the values obtained for the moments of the DA Φ up to third order ($l+m+n \leq 3$). The definition of the moments is as follows,

$$\phi^{(l,m,n)} = \int_0^1 [dx] x_1^l x_2^m x_3^n \Phi(x_1,x_2,x_3) \Big/ \int_0^1 [dx] \Phi(x_1,x_2,x_3), \tag{2.71}$$

with $[dx] = dx_1 dx_2 dx_3 \delta(1-x_1-x_2-x_3)$.

In Table 2.3 we report a comparison among our result for the moments of a DA defined as a linear combination of the moments of Φ and T, i.e. $\varphi^{(l,m,n)} = 1/3(\phi^{(l,m,n)} + 2T^{(l,n,m)})$ and the results from Lattice and other models calculations.

In the last Table 2.4 we show our predictions for evolved moments $\phi^{(l,m,n)}$ in comparison to our previous results at the hadronic scale and lattice predictions. To perform the evolution we used the algebraic expressions for the DAs in terms of the expansion coefficients B_n [75],

$$\begin{aligned} V_1(x_i) &= \phi_{\rm as}(x_i)\Big[(B_0+B_2-5B_3-5B_5) \\ &\quad +\frac{1}{2}(B_1-3B_2+11B_3+B_4+21B_5)(x_1+x_2) \\ &\quad -(B_1+B_4)x_3-(4B_3+14B_5)x_1x_2 \\ &\quad +\frac{1}{6}(12B_3-4B_4-28B_5)\left(x_1^2+x_2^2\right) \\ &\quad +\frac{1}{3}(24B_3+4B_4+14B_5)x_3^2\Big], \end{aligned} \tag{2.72}$$

$$\begin{aligned} A_1(x_i) &= \phi_{\rm as}(x_i)\Big[\frac{1}{2}(-B_1-3B_2+3B_3-B_4-7B_5)(x_1-x_2) \\ &\quad +\frac{1}{6}(-12B_3+4B_4+28B_5)\left(x_1^2-x_2^2\right)\Big], \end{aligned} \tag{2.73}$$

Table 2.2: Comparison of the strict moments $l+m+n \leq 3$ of the nucleon DA Φ between different model calculations or data fit: COZ Ref. [76], KS Ref. [77], SB Ref. [84], DF Ref. [81], BK fit Ref. [97], and Our; and the Lattice results of Ref. [101]

(l,m,n)	COZ	KS	SB	DF	BK	Our	LAT
0 0 0	1	1	1	1	1	1	1
1 0 0	$0.54-0.62$	$0.46-0.59$	0.572	0.582	0.381	0.346	0.394
0 1 0	$0.18-0.20$	$0.18-0.21$	0.184	0.213	0.309	0.331	0.302
0 0 1	$0.20-0.25$	$0.22-0.26$	0.244	0.207	0.309	0.323	0.304
2 0 0	$0.32-0.42$	$0.27-0.37$	0.338	0.367	0.179	0.152	0.18
0 2 0	$0.065-0.088$	$0.08-0.09$	0.066	0.085	0.125	0.142	0.132
0 0 2	$0.09-0.12$	$0.10-0.12$	0.170	0.083	0.125	0.137	0.138
1 1 0	$0.08-0.10$	$0.08-0.10$	0.139	0.108	0.101	0.099	0.113
1 0 1	$0.09-0.11$	$0.09-0.11$	0.096	0.106	0.101	0.096	0.112
0 1 1	$-0.03-0.03$	unreliable	0.018	-0.021	0.083	0.091	0.05
3 0 0	$0.21-0.25$		0.21	0.249	0.095	0.078	
0 3 0	$0.028-0.04$		0.039	0.041	0.059	0.071	
0 0 3	$0.048-0.056$		0.139	0.040	0.059	0.068	
2 1 0	$0.041-0.049$		0.079	0.060	0.042	0.038	
2 0 1	$0.044-0.055$		0.049	0.059	0.042	0.037	
1 2 0	$0.027-0.037$		0.050	0.040	0.036	0.037	
1 0 2	$0.037-0.0434$		0.037	0.039	0.036	0.035	
0 2 1	$-0.004-0.007$		-0.023	0.004	0.030	0.034	
0 1 2	$-0.005-0.008$		-0.007	0.005	0.030	0.033	

$$T_1(x_i) = \phi_{\rm as}(x_i)\Big[(B_0+B_2-5B_3-5B_5)+(-3B_2+7B_3+7B_5)\,x_3 + (4B_3+14B_5)\,x_1x_2+\left(8B_3+\frac{14}{3}B_5\right)\left(x_1^2+x_2^2\right)\Big]\,, \qquad (2.74)$$

where the appropriate coefficients evolved according Eq. (2.67) have to be inserted.

It can be pointed out that the evolution process does not affect so much our model predictions with respect to the hadronic scale.

2.2 Parton Distribution Functions

Others hadronic observables to which the LC CQM formalism of treating the low energy dynamics of strong interaction can be applied with success are the socalled parton distribution functions (PDFs) that we have already introduced in Cap. 1.

It is well-known that at the parton level the quark structure of the nucleon is described in terms of three quark distributions, namely the quark density $f_1(x)$, the helicity distribution $g_1(x)$ (also indicated $\Delta f(x)$), and the transversity distribution $h_1(x)$ (also indicated $\delta f(x)$). The first two distributions, and

Table 2.3: Moments of the DA $\varphi^{(l,m,n)}$ from four different model calculations: COZ Ref. [76], KS Ref. [77], DF Ref. [81] and Our; and from Lattice simulations [101].

(l,m,n)	COZ	KS	DF	LAT	Our
0 0 0	1	1	1	1	1
1 0 0	0.52	0.47	0.44	0.364	0.34
0 1 0	0.17	0.21	0.21	0.302	0.33
0 0 1	0.31	0.32	0.35	0.334	0.33
2 0 0	0.31	0.29	0.26	0.166	0.15
0 2 0	0.05	0.09	0.09	0.132	0.14
0 0 2	0.15	0.18	0.19	0.152	0.14
1 1 0	0.09	0.08	0.07	0.092	0.1
1 0 1	0.12	0.1	0.11	0.112	0.1
0 1 1	0.04	0.04	0.05	0.071	0.09

particularly $f_1(x)$, are now well established by experiments in the deep-inelastic scattering (DIS) regime and well understood theoretically as a function of the fraction x of the nucleon longitudinal momentum carried by the active quark [102]. Information on the last leading-twist distribution is missing on the experimental side because $h_1(x)$, being chiral-odd, decouples from inclusive DIS and therefore can not be measured in such a traditional source of information. Indeed, QCD conserves chirality (which concide with helicity in Infinite Momentum Frame), thus if a chiral-odd term appears in a strong interaction process another chiral odd term is needed to preserve chirality. Nevertheless some theoretical activity has been developed in calculating $h_1(x)$ and finding new experimental situations where it can be observed (for a recent review see Ref. [**?**]). Among the different proposals the polarized Drell-Yan (DY) dilepton production was recognized for a long time as the cleanest way to access the transversity distribution of quarks in hadrons [103, 104, 105, 106]. As a matter of fact, in pp and $p\bar{p}$ DY collisions with transversely polarized hadrons the leading order (LO) double transverse-spin asymmetry of lepton-pair production involves the product of two transversity distributions, thus giving direct access to them. However, such a measurement is not an easy task because of the technical problems of maintaining the beam polarization through the acceleration. The recently proposed experimental programs at RHIC [107] and at GSI [108] have raised renewed interest in theoretical predictions of the double transverse-spin asymmetry in proton-(anti)proton collisions with dilepton production [109, 110, 111].

Table 2.4: Comparison of the moments of the DA $\phi^{(l,m,n)}$: LAT, lattice simulations at $Q_0 = 2$ GeV; Our, present model calculation at the hadronic scale $Q_0 = 0.281$ GeV; Our Evol, present model calculation after evolution at $Q_0 = 2$ GeV.

(l,m,n)	LAT	Our	Our Evol
0 0 0	1	1	1
1 0 0	0.394	0.346	0.340
0 1 0	0.302	0.331	0.332
0 0 1	0.304	0.323	0.327
2 0 0	0.18	0.152	0.148
0 2 0	0.132	0.142	0.152
0 0 2	0.138	0.137	0.14
1 1 0	0.113	0.099	0.092
1 0 1	0.112	0.096	0.1
0 1 1	0.05	0.091	0.088

2.2.1 Light-cone Wave Functions representation of the Parton Distribution Functions

To give the overlap representation of the three leading twist PDFs we start from the general representation of the hadronic tensor for an inclusive DIS process, after assming LC dominance

$$2MW^{\mu\nu} \sim \frac{1}{2}\sum_f e_f^2 \int dk^- d\mathbf{k}_\perp \mathrm{Tr}\Big[\Phi(k,p,S)\gamma^\mu\gamma^+\gamma^\nu + \bar{\Phi}(k,p,S)\gamma^\nu\gamma^+\gamma^\mu\Big]\Big|_{k^+=xp^+}, \quad (2.75)$$

with

$$\begin{aligned}\Phi(k,p,S) &= \int \frac{d^4\xi}{(2\pi)^4} e^{-ik\cdot\xi}\langle p,s|\bar{\psi}(\xi)\psi(0)|p,s\rangle \\ &= \sum_{s_X}\int \frac{d\mathbf{p}_{X\perp}}{(2\pi)^3 2p_X^0}\langle p,s|\bar{\psi}_f(0)|p_X,s_X\rangle \\ &\quad \times\langle p_X,s_X|\psi_f(0)|p,s\rangle\delta^{(4)}(p-k-p_X), \end{aligned} \quad (2.76)$$

the quark-quark correlator, namely a bilocal operator of quark fields evaluated on an hadronic state of momentum p and helicity s, where the partons carry a LC momentum fraction $x = k^+/p^+$ and p_X is the momentum of the generic final state on which we sum over. $\bar{\Phi}(k,p,S)$, analogously, the correlator for the antiquark fields, which we do not take into account in the following.

From previous considerations we know that in LC kinematics the leading twist component are the, so-called, "good" components that can be isolated by means of the projector Λ^+. Applying the projector to the Eq. (2.76) it is possible to extract the PDFs. Indeed

$$\begin{aligned}
&\Lambda^+\left\{\int dk^- d\mathbf{k}_\perp \Phi(k,p,s)|_{k^+=xp^+}\right\}\gamma^+ \\
&= \Lambda^+\left\{\int \frac{d\xi^-}{2\pi} e^{ixp^+\xi^-}\langle p,s|\bar{\psi}_f(\xi^-)\psi_f(0)|p,s\rangle\Big|_{\xi^+=\xi_\perp=0}\right\}\gamma^+,
\end{aligned} \tag{2.77}$$

where $s=(0,\mathbf{s})$, $\mathbf{s}=(\lambda,\mathbf{s}_\perp)$. Through the trace operation

$$\Phi^{[\Gamma]}(x,s) = \int dk^- d\mathbf{k}_\perp \mathrm{Tr}\Big[\Phi(k,p,s)\Gamma\Big]\Big|_{k^+=xp^+}, \tag{2.78}$$

we get the formulation of the PDFs in terms of Fourier Transform of matrix elements of "good" component of bilocal operators

$$f_1(x) = \Phi^{[\gamma^+]} = \int \frac{d\xi^-}{2\pi} e^{ixp^+\xi^-}\langle p|\bar{\psi}_f(\xi^-)\gamma^+\psi_f(0)|p\rangle; \tag{2.79}$$

$$\lambda g_1(x) = \Phi^{[\gamma^+\gamma_5]} = \int \frac{d\xi^-}{2\pi} e^{ixp^+\xi^-}\langle p|\bar{\psi}_f(\xi^-)\gamma^+\gamma_5\psi_f(0)|p\rangle; \tag{2.80}$$

$$s^i_\perp h_1(x) = \Phi^{[i\sigma^{i+}\gamma_5]} = \int \frac{d\xi^-}{2\pi} e^{ixp^+\xi^-}\langle p|\bar{\psi}_f(\xi^-)i\sigma^{i+}\gamma_5\psi_f(0)|p\rangle. \tag{2.81}$$

Varying Γ on a Dirac matrices basis $(\mathbf{1},\gamma_5,\gamma_\mu,\gamma_5\gamma_\mu,\sigma_{\mu\nu})$ it is also possible to find the expression for the suppressed (non leading) PDFs. For instance at twist three they result

$$\begin{aligned}
\Phi^{[\mathbf{1}]}(x,s) &= \frac{M}{p^+}e(x), \\
\Phi^{[\gamma^i\gamma_5]}(x,s) &= \frac{M}{p^+}s^i_\perp g_T(x), \\
\Phi^{[i\sigma^{+-}\gamma_5]}(x,s) &= \frac{M}{p^+}\lambda h^L(x),
\end{aligned} \tag{2.82}$$

where the term $M/P^+ \sim M/Q$ is the suppressed contribution following the definition of effective twist.

Executing a calculation analogous to what done for the DAs we obtain [64, 65]

$$f_1^q(x) = \sum_{\lambda_i\tau_i}\sum_{j=1}^{3}\delta_{\tau_j\tau_q}\int [dx]_3[d\mathbf{k}_\perp]_3\,\delta(x-x_j)|\Psi_\lambda^{N,[f]}(\{x_i\},\{\mathbf{k}_{\perp,i}\};\{\lambda_i\},\{\tau_i\})|^2, \tag{2.83}$$

where the helicity λ of the nucleon can equivalently be taken positive or negative.

Analogously, the following simple expressions are obtained for the polarized quark distribution of flavor q [65]

$$g_1^q(x) = \sum_{\lambda_i \tau_i} \sum_{j=1}^{3} \delta_{\tau_j \tau_q} \, \mathrm{sign}\,(\lambda_j) \int [dx]_3 [d\mathbf{k}_\perp]_3 \, \delta(x - x_j) |\Psi_+^{N,[f]}(\{x_i\}, \{\mathbf{k}_{\perp,i}\}; \{\lambda_i\}, \{\tau_i\})|^2, \tag{2.84}$$

and for the quark transversity distributions $h_1^q(x)$ [65]:

$$h_1^q(x) = \sum_{\lambda_i^t \tau_i} \sum_{j=1}^{3} \delta_{\tau_j \tau_q} \, \mathrm{sign}\,(\lambda_j^t) \int [dx]_3 [d\mathbf{k}_\perp]_3 \, \delta(x - x_j) |\Psi_\uparrow^{N,[f]}(\{x_i\}, \{\mathbf{k}_{\perp,i}\}; \{\lambda_i^t\}, \{\tau_i\})|^2, \tag{2.85}$$

where λ_i^t is the transverse-spin component of the quark and, as usual, the trasversity basis for the nucleon spin states is obtained from the helicity basis as follows:

$$|p, \uparrow\rangle = \frac{1}{\sqrt{2}}(|p, +\rangle + |p, -\rangle), \qquad |p, \downarrow\rangle = \frac{1}{\sqrt{2}}(|p, +\rangle - |p, -\rangle). \tag{2.86}$$

Expressions (2.83), (2.84) and (2.85) exhibit the well known probabilistic content of parton distributions. Eq. (2.83) gives the probability of finding a quark with a fraction x of the longitudinal momentum of the parent nucleon, irrespective of its spin orientation. The helicity distribution $g_1^q(x)$ in Eq. (2.84) is the number density of quarks with helicity + minus the number density of quarks with helicity −, assuming the parent nucleon to have helicity +. The transversity distribution $h_1^q(x)$ in Eq. (2.85) is the number density of quarks with transverse polarization ↑ minus the number density of quarks with transverse polarization ↓, assuming the parent nucleon to have transverse polarization ↑.

In the framework of the LC CQM outlined for the DAs calculations we separate the spin-isospin component from the space part of the proton wave function assuming SU(6) symmetry (Appendix C). Thus we find

$$f_1^q(x) = \left(2\delta_{\tau_q 1/2} + \delta_{\tau_q -1/2}\right) \int [dx]_3 [d\mathbf{k}_\perp]_3 \, \delta(x - x_3) |\psi(\{x_i\}, \{\mathbf{k}_{\perp,i}\})|^2, \tag{2.87}$$

$$g_1^q(x) = \left(\frac{4}{3}\delta_{\tau_q 1/2} - \frac{1}{3}\delta_{\tau_q -1/2}\right) \int [dx]_3 [d\mathbf{k}_\perp]_3 \, \delta(x - x_3) |\psi(\{x_i\}, \{\mathbf{k}_{\perp,i}\})|^2 \mathcal{M}, \tag{2.88}$$

$$h_1^q(x) = \left(\frac{4}{3}\delta_{\tau_q 1/2} - \frac{1}{3}\delta_{\tau_q -1/2}\right) \int [dx]_3 [d\mathbf{k}_\perp]_3 \, \delta(x - x_3) |\psi(\{x_i\}, \{\mathbf{k}_{\perp,i}\})|^2 \mathcal{M}_T, \tag{2.89}$$

where [65, 112]

$$\mathcal{M} = \frac{(m + x_3 M_0)^2 - \vec{k}_{\perp,3}^2}{(m + x_3 M_0)^2 + \mathbf{k}_{\perp,3}^2}, \tag{2.90}$$

$$\mathcal{M}_T = \frac{(m + x_3 M_0)^2}{(m + x_3 M_0)^2 + \mathbf{k}_{\perp,3}^2}, \tag{2.91}$$

and the expectation values on the normalized nucleon momentum wavefunction of the contribution coming from Melosh rotations satisfy

$$2\langle \mathcal{M}_T \rangle = \langle \mathcal{M} \rangle + 1. \tag{2.92}$$

Therefore the following relations hold

$$h_1^u(x) = \frac{1}{2} g_1^u(x) + \frac{1}{3} f_1^u(x), \qquad h_1^d(x) = \frac{1}{2} g_1^d(x) - \frac{1}{6} f_1^d(x), \tag{2.93}$$

which are compatible with the Soffer inequality [113]:

$$|h_1^q(x)| \leq \frac{1}{2}[f_1^q(x) + g_1^q(x)]. \tag{2.94}$$

In the nonrelativistic limit, corresponding to $\mathbf{k}_\perp = 0$, i.e. $\mathcal{M}_T = \mathcal{M} = 1$, one obtains $h_1^u = g_1^u = \frac{2}{3} f_1^u$ and $h_1^d = g_1^d = -\frac{1}{3} f_1^d$ as expected from general principles [106].

Numerical Results for the Parton Distribution Functions in the LC CQM

As an application of the general formalism reviewed in the previous section we consider the valence-quark contribution to the parton distributions starting from an instant-form SU(6) symmetric wave function of the proton, Eqs. (C.3) and (C.4), derived in the relativistic quark model of Ref. [63]. In particular, we use the Lorentzian shape wavefunction of Ref. [63] with parameters fitted to the magnetic moments of the proton and the neutron and the axial-vector coupling constant g_A and giving also a good agreement with the experimental nucleon electro-weak form factors in a large Q^2 range.

The distributions in Eqs. (2.87), (2.88) and (2.89) are defined at the hadronic scale Q_0^2 of the model. In order to make predictions for experiments, a complete knowledge of the evolution up to NLO is indispensable. According to Ref. [114] we assume that twist-two matrix elements calculated at some low scale in a quark model can be used in conjunction with QCD perturbation theory. Starting from a scale where the long-range (confining) part of the interaction is dominant, we generate the perturbative contribution by evolution at higher scale. In the case of transversity the DGLAP Q^2 evolution equation [21] is simple. In fact, being chirally odd, the quark transversity distributions do not mix with the gluon distribution and therefore the evolution is of the non-singlet type. The LO anomalous dimensions were first calculated in Ref. [115]

but promptly forgotten. They were recalculated by Artru and Mekhfi [116]. The one-loop coefficient functions for Drell-Yan processes are known in different renormalization schemes [123, 124, 125]. The NLO (two-loop) anomalous dimensions were also calculated in the Feynman gauge in Refs. [126, 127] and in the light-cone gauge [128]. The two-loop splitting functions for the evolution of the transversity distribution were calculated in Ref. [128]. The LO DGLAP Q^2 evolution equation for the transversity distribution $h_1(x)$ was derived in Ref. [116] and its numerical analysis is discussed in Refs. [129, 130].

A numerical solution of the DGLAP equation for the transversity distribution $h_1(x)$ was given at LO and NLO in Refs. [131, 132]. In Ref. [131] the DGLAP integrodifferential equation is solved in the variable Q^2 with the Euler method replacing the Simpson method previously used in the cases of unpolarized [133] and longitudinally polarized [134] structure functions.

In the present analysis the FORTRAN code of Ref. [131] has been applied within the $\overline{MS}$ renormalization scheme and the input distributions calculated at the hadronic scale according to the LC CQM were evolved up to NLO. The model scale $Q_0^2 = 0.079$ GeV^2 was determined by matching the value of the momentum fraction carried by the valence quarks, as computed in the model, with that obtained by evolving backward the value experimentally determined at large Q^2. The strong coupling $\alpha_s(Q^2)$ entering the code at NLO is computed by solving the NLO transcendental equation numerically,

$$\ln \frac{Q^2}{\Lambda^2_{\rm NLO}} - \frac{4\,\pi}{\beta_0\,\alpha_s} + \frac{\beta_1}{\beta_0^2}\,\ln\left[\frac{4\,\pi}{\beta_0\,\alpha_s} + \frac{\beta_1}{\beta_0^2}\right] = 0\,, \tag{2.95}$$

as obtained from the renormalization group analysis [135]. It differs from the more familiar expression used in Ref. [131],

$$\frac{\alpha_s(Q^2)}{4\pi} = \frac{1}{\beta_0 \ln(Q^2/\Lambda^2_{\rm NLO})}\left(1 - \frac{\beta_1}{\beta_0^2}\,\frac{\ln\ln(Q^2/\Lambda^2_{\rm NLO})}{\ln(Q^2/\Lambda^2_{\rm NLO})}\right), \tag{2.96}$$

valid only in the limit $Q^2 \gg \Lambda^2_{\rm NLO}$, where $\Lambda_{\rm NLO}$ is the so-called QCD scale parameter.

Together with the input distributions at the hadronic scale the non-singlet (valence) contribution of the three parton distributions is shown in Figs. 2.9 to 2.11 at LO and NLO at different scales of Q^2. In the case of the unpolarized and polarized distributions, Figs. 2.9 and 2.10 respectively, the result of evolution of the total distributions is also presented. Quite generally, the Q^2 dependence of the evolution is weak within a given order, while small effects are introduced when going from LO to NLO, as exemplified by the dot-dashed curves at $Q^2 = 5$ GeV^2 in Figs. 2.9 to 2.11. Thus, convergence of the perturbative expansion is very fast and one can safely limit himself to LO.

The size of the d-quark distributions is always smaller than that of the u-quark distribution, particularly in the case of transversity, confirming results obtained with other models (see, e.g., [109]).

Taking into account that the model at the hadronic scale only considers valence quarks and the sea is only generated perturbatively, the overall behavior of $f_1(x)$ is in reasonable agreement with available parameterizations [136]. One may notice the faster fall-off of the tail of $f_1^u(x)$ at large x in our model with respect to the parametrization [136]. As for $g_1(x)$, the missing sea and gluon contributions are crucial to compare our model results with the available parameterizations [137]. However, comparison of $h_1(x)$ and $g_1(x)$ is legitimate because $h_1(x)$ is determined by valence contributions, as it is $g_1(x)$ in our model. As can be see in Figs. 2.10 and 2.11 they are rather different not only after evolution, but especially at the hadronic scale of the model. This contrasts with the popular guess $h_1(x) \approx g_1(x)$ motivated on the basis of the non-relativistic quark model.

In any case the Soffer inequality (2.94) at each order is always satisfied by the three quark distributions calculated with the LCWFs of the CQM (see Fig. 2.12). In contrast, saturation of the Soffer bound, i.e. assuming

$$|h_1^q(x)| = \frac{1}{2}\left[f_1^q(x) + g_1^q(x)\right], \tag{2.97}$$

is neither reached at the hadronic scale of the model nor is it a conserved property during evolution. In fact, starting at the hadronic scale with the transversity distribution given by Eq. (2.97), the result of LO and NLO evolution diverges from that obtained when calculating the transversity according to Eq. (2.97) after separate evolution of f_1 and g_1. Since the two sides of Eq. (2.97) give different results under evolution, in model calculations the choice of the initial hadronic scale is crucial. This fact should put some caution about the possibility of making predictions with the transversity distribution guessed from f_1 and g_1 as, e.g., in the case of the double transverse-spin asymmetry in DY processes (see Refs. [110, 111] and Fig. 2.18 below).

A similar situation occurs when the transversity distribution is derived from f_1 and g_1 according to the relations (2.93), with the difference that these relations are exact at the hadronic scale when only valence quarks are involved.

To conclude this subsection we point out that recently Anselmino and collaborators [117] performed the first phenomenological analysis of available data for the transversity distributions for up and down quarks showing that they have opposite sign and a smaller size than their positivity bounds, see Fig. (2.13). In [117] the authors analyzed the experimental data on semi-inclusive DIS coming from Hermes (DESY) and Compass (CERN) collaborations combined togheter with the data on fragmentation functions (FFs) coming from Belle (KEK). In this way they were able to extract for the first time in literature a parametrization for $h_1^{u/d}(x)$, even if with some crude assumptions, e.g. the mix of PDFs and FFs at different energy scale and/or the factorization among the x and $\mathbf{k}_\perp$ dependencies.

Our model predictions obtained using the model of Ref. [62] are in really good agreement with the phenomenological analysis of Ref. [117] how it can be seen from Fig. (2.14), where different model calculations are compared with

the parametrization, and from Fig. (2.15) where we show the comparison of our calculations with the brand-new refined analysis of Anselmino and collaborators [122].

Double-Transverse Spin Asymetry, A_{TT}

As we have stated before the most direct experimental way to access the poorly known transversity distribution is the Drell-Yan lepton pair production. Indeed, in such an experiment one can measure the double transverse-spin asymmetry A_{TT} defined as,

$$A_{TT} = \frac{d\sigma^{\uparrow\uparrow} - d\sigma^{\uparrow\downarrow}}{d\sigma^{\uparrow\uparrow} + d\sigma^{\uparrow\downarrow}}, \tag{2.98}$$

which (see Eq. (2.99)) involves the product of two transversity distributions. In the definition the arrows denote the transverse directions along which the two colliding hadrons are polarized,

At LO, i.e. considering only the quark-antiquark annihilation graph, the double transverse-spin asymmetry for the process $p^{\uparrow}p^{\uparrow} \to \ell^+\ell^- X$ mediated by a virtual photon is given by

$$A_{TT}^{pp} = a_{TT} \frac{\sum_q e_q^2 \left[h_1^q(x_1, Q^2) h_1^{\bar{q}}(x_2, Q^2) + (1 \leftrightarrow 2)\right]}{\sum_q e_q^2 \left[f_1^q(x_1, Q^2) f_1^{\bar{q}}(x_2, Q^2) + (1 \leftrightarrow 2)\right]}, \tag{2.99}$$

where e_q is the quark charge, Q^2 the invariant mass square of the lepton pair (dimuon), and $x_1 x_2 = Q^2/s$ where s is the Mandelstam variable. The quantity a_{TT} is the spin asymmetry of the QED elementary process $q\bar{q} \to \ell^+\ell^-$, i.e.

$$a_{TT}(\theta, \phi) = \frac{\sin^2\theta}{1 + \cos^2\theta} \cos(2\phi), \tag{2.100}$$

with θ being the production angle in the rest frame of the lepton pair and ϕ the angle between the dilepton direction and the plane defined by the collision and polarization axes.

After the first simple encouraging estimates [105], some phenomenological studies of DY dimuon production at RHIC have been presented [123, 124, 140, 141, 130, 142, 139] indicating that accessing transversity is very difficult under the kinematic conditions of the proposed experiments with pp collisions [107]. The main reason is that A_{TT}^{pp} in Eq. (2.99) involves the product of quark and antiquark transversity distributions. The latter are small in a proton, even if they were as large as to saturate the Soffer inequality; moreover, the QCD evolution of transversity is such that, in the kinematical regions of RHIC data, $h_1(x, Q^2)$ is much smaller than the corresponding values of $g_1(x, Q^2)$ and $f_1(x, Q^2)$. This makes the measurable A_{TT}^{pp} at RHIC very small, no more than a few percents [130, 142, 139].

A more favorable situation is expected by using an antiproton beam instead of a proton beam [108, 109, 110, 111, 64, 143]. In $p\bar{p}$ DY the LO asymmetry $A_{TT}^{p\bar{p}}$ is proportional to a product of quark transversity distributions from the proton and antiquark distributions from the antiproton which are connected by charge conjugation, e.g.

$$h_1^{u/p}(x) = h_1^{\bar{u}/\bar{p}}(x). \tag{2.101}$$

Therefore one obtains

$$A_{TT}^{p\bar{p}} = a_{TT} \frac{\sum_q e_q^2 \left[h_1^q(x_1, Q^2) h_1^q(x_2, Q^2) + h_1^{\bar{q}}(x_1, Q^2) h_1^{\bar{q}}(x_2, Q^2) \right]}{\sum_q e_q^2 \left[f_1^q(x_1, Q^2) f_1^q(x_2, Q^2) + f_1^{\bar{q}}(x_1, Q^2) f_1^{\bar{q}}(x_2, Q^2)) \right]}, \tag{2.102}$$

so that in this case the asymmetry is only due to valence quark distributions.

Quantitative estimates of $A_{TT}^{p\bar{p}}$ for the kinematics of the proposed $\mathcal{PAX}$ experiment at GSI [108] were presented in Refs. [109, 110, 111]. On the basis of predictions from the chiral quark-soliton model [109], the LO DY asymmetries turn out to be large, of the order of 50%, increasing with Q^2 and almost entirely due to u-quarks. In contrast, they are in the range 20–40% in a phenomenological analysis [110, 111] where $A_{TT}^{p\bar{p}}$ is appropriately evolved at NLO starting from two extreme possibilities at some typical low scale $\mu_0 \leq 1$ GeV. One assumption was $h_1(x) = g_1(x)$, as in the nonrelativistic case. The second ansatz for the transversity was the saturation of Soffer's inequality according to Eq. (2.97). The two possibilities have been considered to give a lower and upper bound for the transversity and, consequently, for the $A_{TT}^{p\bar{p}}$ asymmetry.

NLO effects hardly modify the asymmetry since the K factors of the transversely polarized and unpolarized cross sections are similar to each other and therefore almost cancel out in the ratio [144]. In addition, NLO effects are rather small on the quark distributions obtained as can be observed in Figs. 2.9–2.11. Therefore, we limit our analysis of the double-spin asymmetry to LO.

Using the unpolarized quark and transversity distributions derived in our LC CQM, results for $s = 45$ GeV^2 and different values of Q^2 are plotted in Fig. 2.16 in terms of the rapidity

$$y = \frac{1}{2} \ln \frac{x_1}{x_2}. \tag{2.103}$$

An asymmetry of about 30% (comparable with Refs. [110, 111]) is obtained, with a Q^2 dependence in agreement with Ref. [109].

This result confirms the possibility of measuring the double transverse-spin asymmetry under conditions that will be probed by the proposed $\mathcal{PAX}$ experiment. In such conditions, assuming the LO expression (2.102) for the observed asymmetry one could gain direct information on the transversity distribution

following previous analysis [109, 110, 111], where the quark densities $f_1^{q,\bar{q}}(x, Q^2)$ are taken from the GRV98 parametrizations [136]. The resulting transversity distributions could be compared with model predictions.

According to this strategy, with our model the antiquark distributions $h_1^{\bar{q}}(x, Q^2)$ are identically vanishing and $h_1^q(x, Q^2)$ contains only valence quark contributions. Assuming a negligible sea-quark contribution the corresponding asymmetry would thus give direct access to $h_1^q(x, Q^2)$ and would look like that shown in Fig. 2.17. The results indicate a strong Q^2 dependence suggesting moderate values of Q^2, e.g. $Q^2 = 5$ to 10 GeV^2, in order to have an appreciable asymmetry of about 10–20% at the proposed $\mathcal{PAX}$ experiment at GSI [108]. It is remarkable that, contrary to the result of Ref. [109], in our model Q^2 evolution produces a decreasing LO asymmetry with increasing Q^2 as a consequence of the opposite Q^2 dependence of the theoretical h_1 and the phenomenological f_1. In fact, in the range of x-values explored by the chosen kinematic conditions ($x \geq 0.3$) h_1 with its valence quark contribution has a larger fall-off with Q^2 than the GRV98 f_1 as shown in Fig. 2.9. Furthermore, one may notice that with this LC CQM a much lower asymmetry is predicted than with the chiral quark-soliton model [109] and even lower than the phenomenological analysis of Refs. [110, 111].

In general, one can anticipate upper and lower limits for the theoretical asymmetry depending on the upper and lower bounds that the transversity has to satisfy. The saturated Soffer bound (2.97), i.e. $h_1 = \frac{1}{2}(g_1 + f_1)$, represents the upper bound of h_1 at any scale. The lower bound is given by the nonrelativistic approximation $h_1 = g_1$. At the hadronic scale the transversity calculated with any LCWFs including valence quarks only should have intermediate values satisfying the conditions in Eq. (2.93). Under evolution Eq. (2.93) does no longer hold, but still the evolved transversity has to lie in between the correspondingly evolved upper and lower bounds. Assuming the LCWFs of our model, the same asymmetry shown in Fig. 2.17 at $Q^2 = 5$ GeV^2 is compared in Fig. 2.18 with the asymmetry calculated when the transversity is evolved starting from an input at the hadronic scale either given by the saturated Soffer bound $h_1 = \frac{1}{2}(g_1 + f_1)$ (dashed curve) or assuming the nonrelativistic approximation $h_1 = g_1$ (dotted curve), with f_1 and g_1 calculated in this LC CQM model. The difference between the dotted and solid curves gives an estimate of the relativistic effects in the calculation of h_1. On the other side, the model calculation with an input h_1 satisfying Eq. (2.93) leads to an asymmetry much lower than in the case of the saturated Soffer bound.

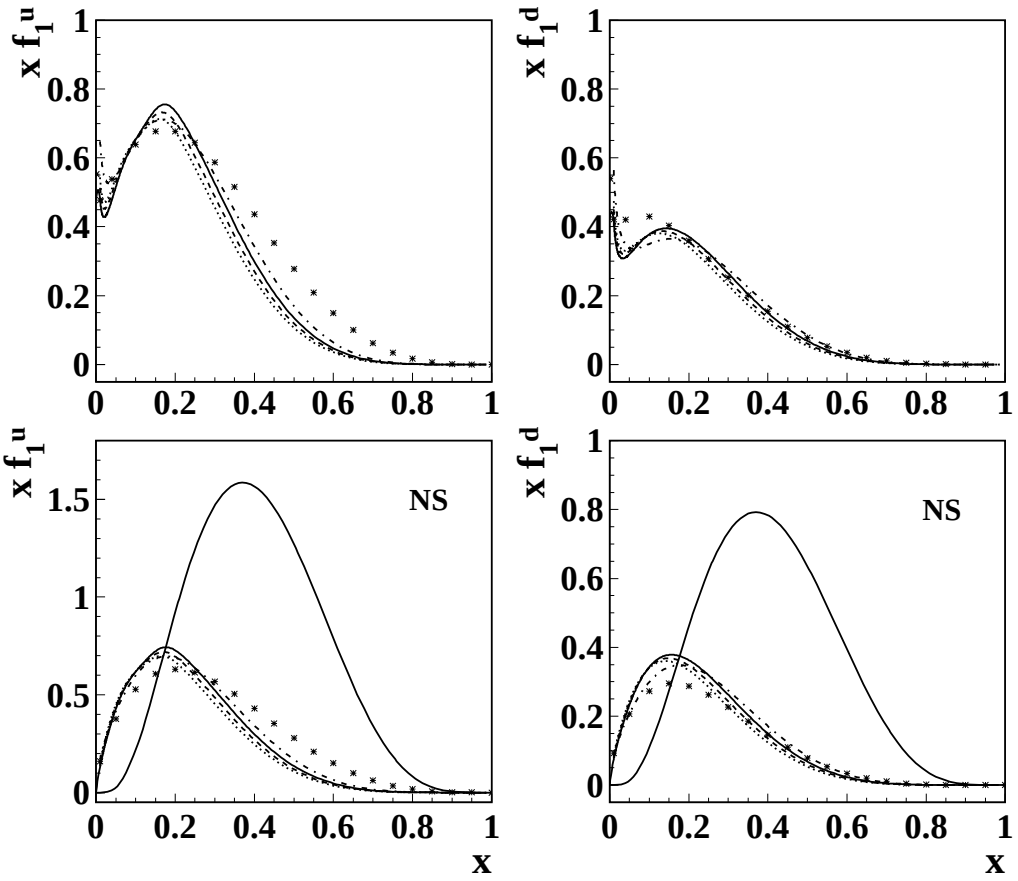

Figure 2.9: Evolution of the parton distribution for the u (left panel) and d (right panel) quark. In the lower panels starting from the hadronic scale $Q_0^2 = 0.079$ GeV^2 (upper curve), LO non-singlet distributions are shown at different scales ($Q^2 = 5$ GeV^2, solid lines; $Q^2 = 9$ GeV^2, dashed lines; $Q^2 = 16$ GeV^2, dotted lines) together with NLO distributions at $Q^2 = 5$ GeV^2 (dot-dashed lines). LO and NLO total distributions are shown in the upper panels with the same line convention. The parametrization of Ref. [136] NLO evolved at 5 GeV^2 is also shown by small stars.

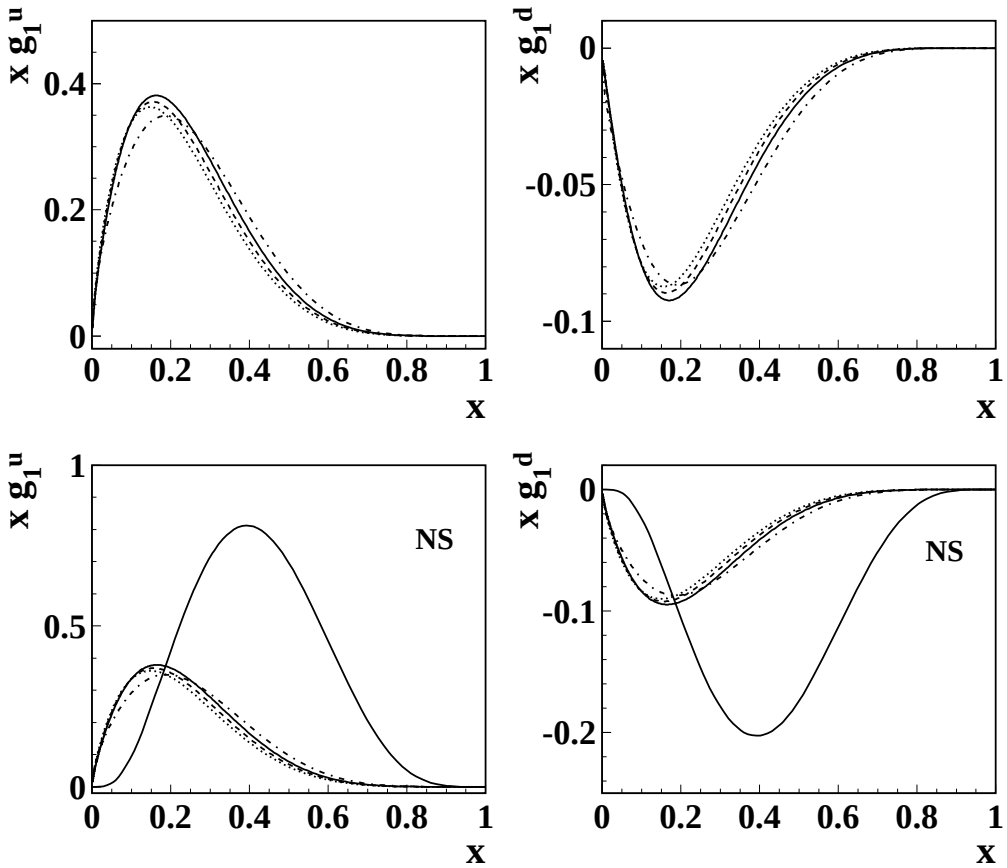

Figure 2.10: The same as in Fig. 2.9, but for the helicity distribution.

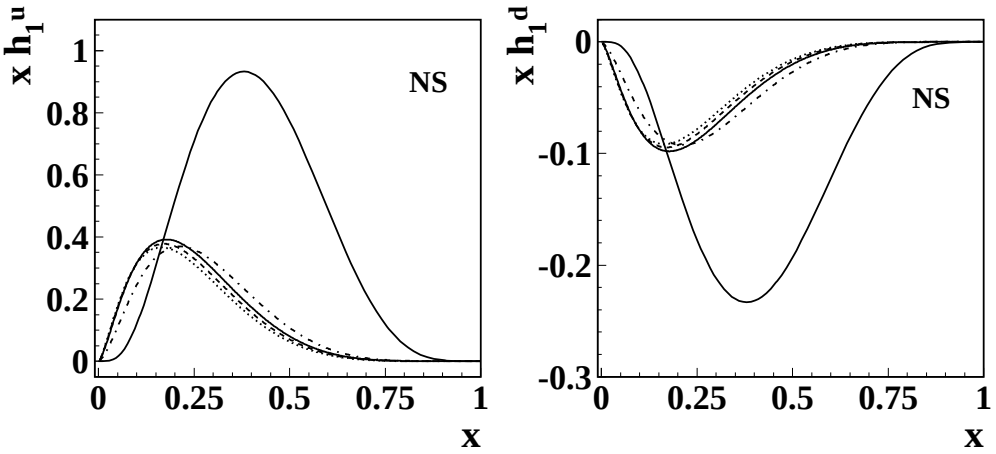

Figure 2.11: Evolution of the transversity distribution for the u (left panel) and d (right panel) quark. Starting from the hadronic scale $Q_0^2 = 0.079$ GeV^2 (upper curve), LO non-singlet distributions are shown at different scales ($Q^2 =$ 5 GeV^2, solid lines; $Q^2 = 9$ GeV^2, dashed lines; $Q^2 = 16$ GeV^2, dotted lines) together with NLO distributions at $Q^2 = 5$ GeV^2 (dot-dashed lines).

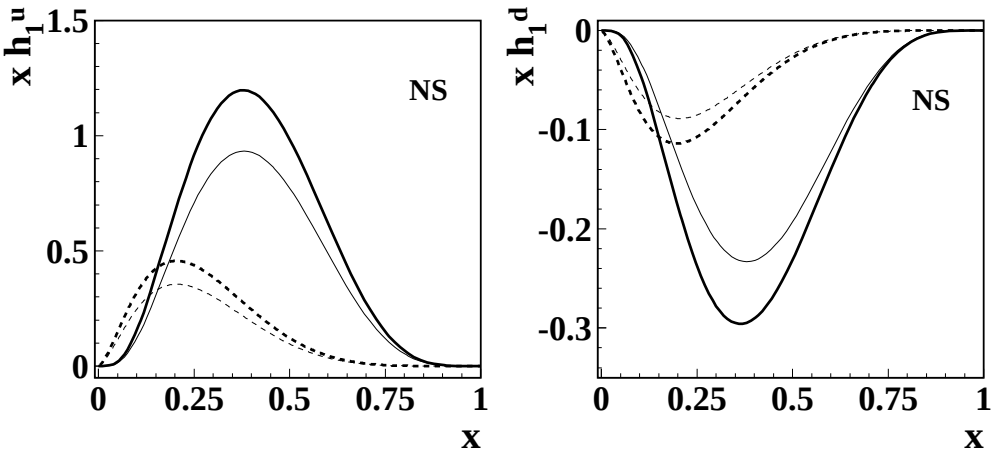

Figure 2.12: The transversity distribution obtained with the LCWFs of the present model (thin lines) compared with the Soffer bound, Eq. (2.97), (thick lines) for the u (left panel) and d (right panel) quark . Solid lines for the results at the hadronic scale $Q_0^2 = 0.079$ GeV^2, the dashed lines obtained by NLO evolution at $Q^2 = 9$ GeV^2, respectively.

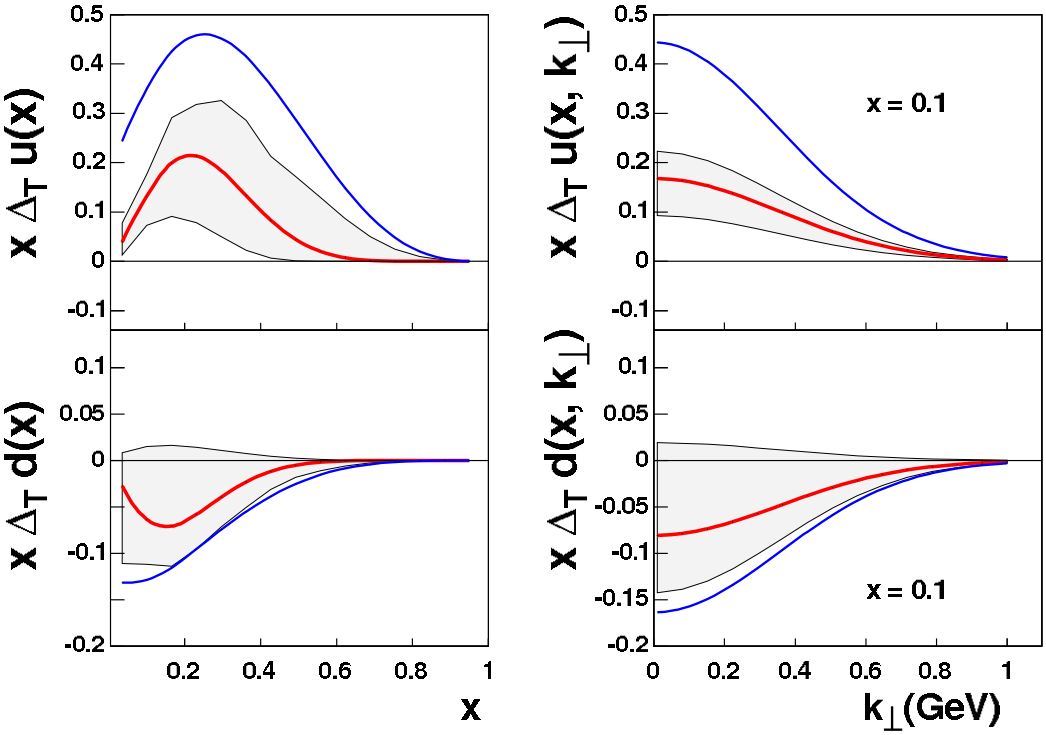

Figure 2.13: The transversity distribution functions for u and d quarks as determined through the global best fit of Ref. [117]. In the left panels, $xh_1^u(x) = x\Delta_T u(x)$ (upper plot) and $xh_1^d(x) = x\Delta_T d(x)$ (lower plot), are shown as functions of x at $Q^2 = 2.4$ GeV^2. The Soffer bound is also shown for comparison (bold blue line). In the right panels the unintegrated transversity distributions are presented, $x\Delta_T u(x, \mathbf{k}_\perp)$ (upper plot) and $x\Delta_T d(x, \mathbf{k}_\perp)$ (lower plot), as functions of $\mathbf{k}_\perp$ at a fixed value of $x = 0.1$. The shaded area in the plot quantifies the uncertainties in the determination of the free parameters.

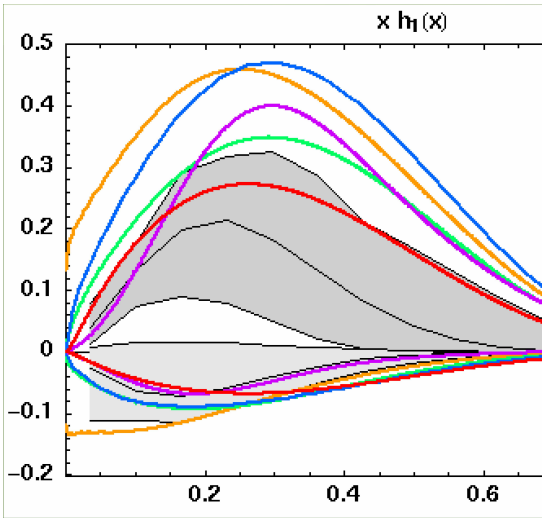

Figure 2.14: The transversity distribution functions for u and d quarks from different model calculations in comparison with the data fit of Ref. [117]. Shaded area [117], red curve: our model calculation obtained with the relativistic hypercentral quark model of Ref. [62], green curve [118], violet curve [119], blue curve [120] and orange curve [121].

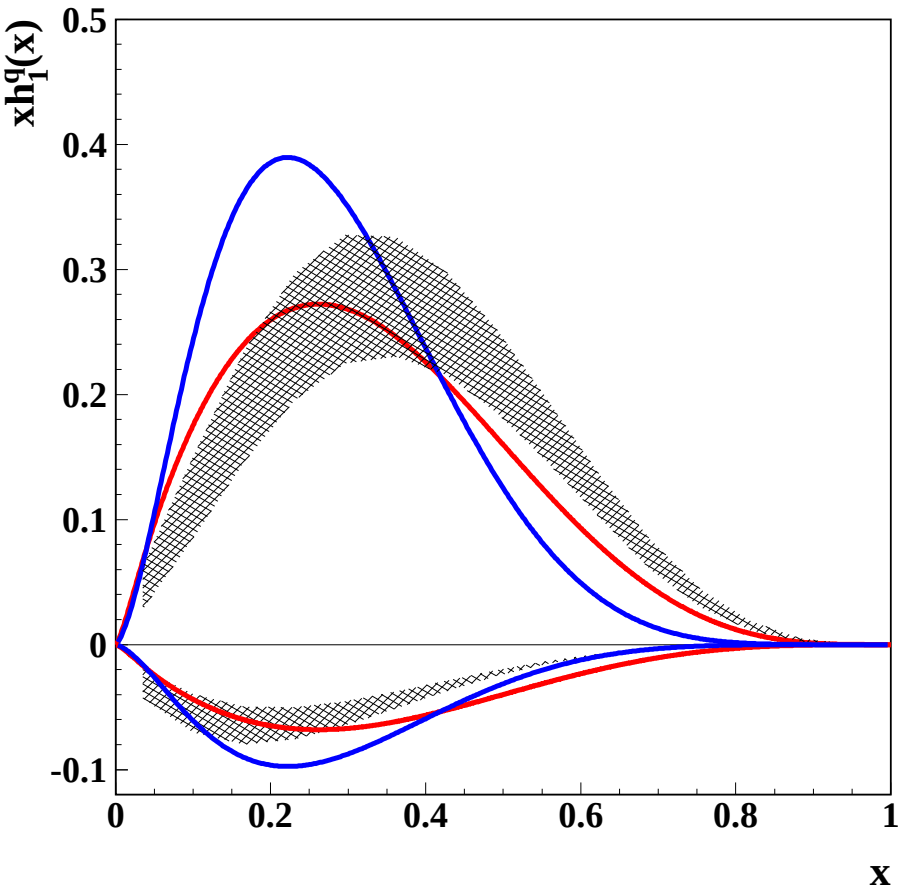

Figure 2.15: Comparison of the transversity distribution functions for u and d quarks between our model calculations and the global best fit of Ref. [122], with shaded area [117] representing the uncertainties in the free parameters. Red curve: our model calculation obtained with the relativistic hypercentral quark model of Ref. [62]; blue curve: our model calculation with the momentum part of the WF described by the model of Ref. [63].

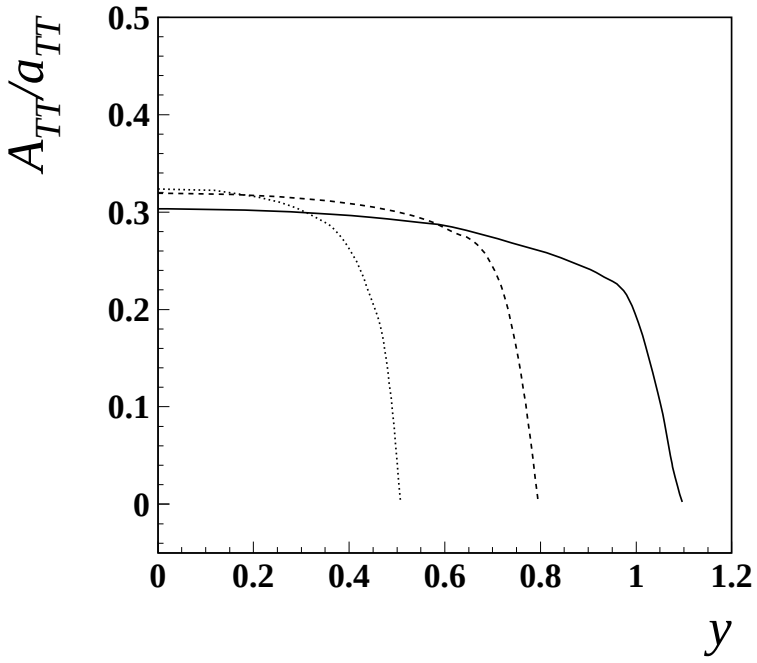

Figure 2.16: The double transverse-spin asymmetry $A_{TT}^{p\bar{p}}/a_{TT}$ calculated with the parton distributions of the present model as a function of the rapidity y at different scales: $Q^2 = 5$ GeV^2, solid line; $Q^2 = 9$ GeV^2, dashed line; $Q^2 = 16$ GeV^2, dotted line.

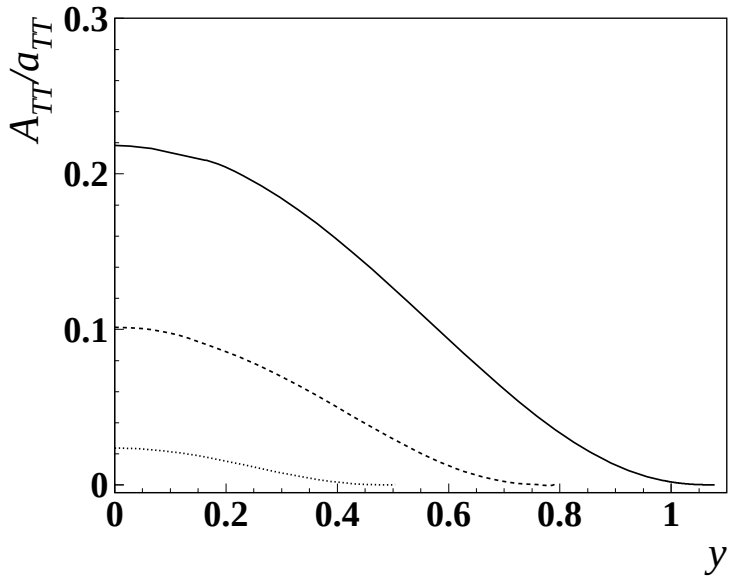

Figure 2.17: The same as in Fig. 2.16 but assuming the GRV98 [136] quark density.

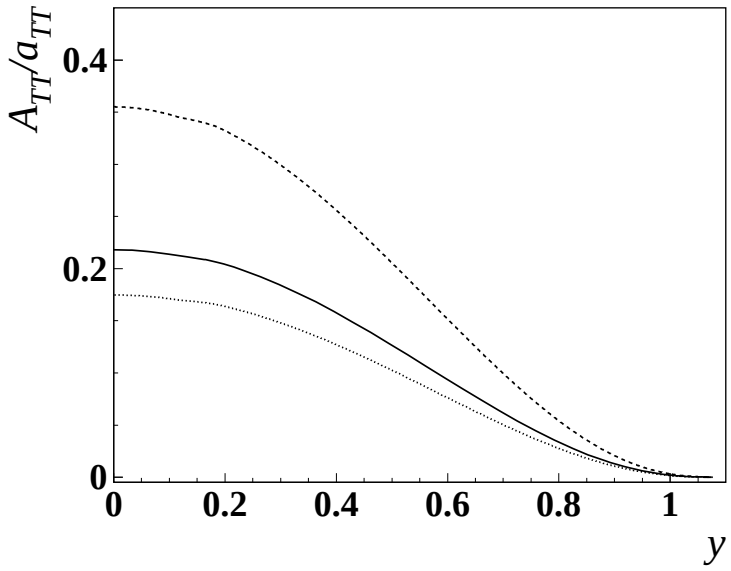

Figure 2.18: The double transverse-spin asymmetry $A_{TT}^{p\bar{p}}/a_{TT}$ as a function of the rapidity y at $Q^2 = 5$ GeV^2 and $s = 45$ GeV^2. Solid curve: calculation with h_1 obtained with the LCWFs of our LC CQM. Dashed curve: calculation with an input $h_1 = \frac{1}{2}(g_1 + f_1)$. Dotted curve: calculation with an input $h_1 = g_1$.

Chapter 3

Light-Cone Wave Functions and Meson-Cloud Model

3.1 Meson Cloud Model

With the advent of high precision data on DIS, understanding of the non-perturbative flavour and spin structure of the nucleon is becoming one of the pressing issues where the interests of particle and nuclear physics converge. At large Q^2 the perturbative QCD evolution is flavour independent and, to LO in $\log Q^2$, generates equal number of $\bar{u}$ and $\bar{d}$ sea quarks. For this reason, the deviation of the Gottfried Sum Rule from its classical value [145]

$$S_G = \int_0^1 [F_2^p(x) - F_2^n(x)] \frac{dx}{x} = \frac{1}{3} \tag{3.1}$$

observed by the New Muon Collaboration (NMC) at CERN [146, 147] has created a large interest on the possible sources of the violation. In the NMC experiment the neutron structure function which enters the sum rule is deduced from deep inelastic scattering off deuterium. It could be biased by nuclear two-body effects which were ignored in the NMC analysis. While shadowing effects [148, 149, 150, 151] cause the real value of the Gottfried Sum Rule to be even smaller than the value given by NMC, the anti-shadowing effect, due to the presence of virtual mesons which bound the deuteron, tends to restore the classical value [152, 151]. This can be understood as consequence of an internal asymmetry $\bar{d} > \bar{u}$ of the quarks in the proton (the opposite asymmetry is expected for the neutron if the proton-neutron charge symmetry holds). The asymmetry has then been confirmed by the NA51 collaboration group at CERN [153], by the E866 [154] collaboration at Fermilab and by the Hermes collaboration at HERA [155].

Non-perturbative effects must play an important role here. The effect of the asymmetry has been predicted by Thomas in a pioneering paper in 1983 [156] in the framework of the so-called Cloudy Bag Model and then, after the data

advent, other model calculations [157, 158], in which the physical nucleon contains an admixture of the πN and $\pi\Delta$ components in the Fock expansion, predicted effect of the asymmetry in agreement with that one deduced from the NA51 experiment.

The Gottfried Sum Rule [145] (GSR) addresses the value of the integral over x of the difference of the $F_2(x)$ structure function of the proton (p) and neutron (n). It is written* as

$$\int_0^1 [F_2^p(x) - F_2^n(x)] \ \frac{\mathrm{d}x}{x} = \int_0^1 \frac{4}{9}\left[u_p^v(x) - u_n^v(x)\right] + \frac{1}{9}\left[d_p^v(x) - d_n^v(x)\right] + 2\left\{\frac{4}{9}\left[\overline{u}_p(x) - \overline{u}_n(x)\right] - \frac{1}{9}\left[\overline{d}_p(x) - \overline{d}_n(x)\right]\right\}\mathrm{d}x, \tag{3.2}$$

where $u_p^v(x) \equiv u_p(x) - \overline{u}_p(x)$, etc. Baryon number conservation reduces the expression further to

$$S_G = \frac{1}{3} + \int_0^1 \frac{8}{9}\left[\overline{u}_p(x) - \overline{u}_n(x)\right] - \frac{2}{9}\left[\overline{d}_p(x) - \overline{d}_n(x)\right]\mathrm{d}x. \tag{3.3}$$

As seen from Eq. (3.3) the valence quarks do not influence the GSR violation although they are of crucial importance for the GSR integrand. Assuming further charge symmetry for the nucleon sea , i.e., $\overline{u}_p(x) = \overline{d}_n(x)$, etc. and making the standard assumption (SU(2) flavour symmetry of the sea) that $\overline{u}_p(x) = \overline{d}_p(x)$, one finds the classical value of 1/3. The NMC experiment [146] of the relevant structure functions, over the interval $0.004 \leq x \leq 0.8$, yielded when extrapolated to $0 \leq x \leq 1$,

$$\int_0^1 [F_2^p(x) - F_2^n(n)] \ \frac{\mathrm{d}x}{x} = 0.24 \pm 0.016\ , \tag{3.4}$$

at $Q^2 = 5$ GeV^2. It should be noted that QCD corrections do not play any role here. While the leading order corrections to the GSR cancel, the higher order corrections are negligibly small.

In the most general case not only the so-called $\mathrm{SU}(2)_Q$ [159] charge-symmetry is violated but also the isospin symmetry between proton and neutron $\mathrm{SU}(2)_I$. It has been argued in Ref. [160] that both the effects of asymmetric SU(2) sea and the proton-neutron isospin symmetry breaking will be very difficult to disentangle as they may, in general, lead to very much the same behaviour both in deep inelastic scattering and Drell-Yan processes. Anyway, a careful analysis [159] based on the σ-term suggests rather that the charge asymmetry should be greater than the isospin one.

*The structure functions $F_2(x)$ and the quark distribution functions $q(x)$ are, of course, functions of Q^2. However, the Q^2 dependence is suppressed to keep the expressions from being too cumbersome.

Since the standard DGLAP [21] evolution equations generate equal number of $\overline{u}u$ and $\overline{d}d$ pairs, one does not expect strong scale dependence of the GSR. The two-loop evolution gives a rather negligible effect [161]. The Pauli exclusion principle leads to some interference phenomena which produces only a small asymmetry [161].

The answer likely lies with more complicated non-perturbative physics. The presence of the pion-cloud in the nucleon gives a natural explanation of the excess of $\overline{d}$ over $\overline{u}$. It has been extensively analyzed in a series of papers [162, 163, 164, 165, 166, 167, 168] with the result for the GSR being dependent on the details of the model, especially on vertex form factors. Restricting the form factors by fitting to the cross sections for high-energy production of neutrons and Δ^{++} yields the GSR [167, 157] in rough agreement with that obtained by NMC [146, 147].

At present one has to rely on phenomenological models consistent with our knowledge in other branches of hadronic physics. The meson-cloud model (MCM) seems to satisfy this criterion.

The explanation of the $\bar{d} - \bar{u}$ asymmetry has probably been the first great success of the meson-cloud model, namely of those model where the nucleon is described as a bare nucleon surrounded by a mesonic cloud.

Nevertheless, this is not the only great achievements of such a kind of models. Indeed, for instance even in the late 80's another intriguing result, involving the spin structure of the proton, was found by the EMC collaboration and MCM contributed to its explanation. Their measured value of the Ellis-Jaffe Sum Rule [173] caused great excitement. After a smooth Regge extrapolation of the data they found

$$S^p_{EJ} = \int_0^1 g^p_1(x)\mathrm{d}x = 0.126 \pm 0.010(stat) \pm 0.015(syst). \tag{3.5}$$

This value is more then two standard deviations away from the original Ellis-Jaffe prediction ($S^p_{EJ} = 0.19$) [174] based on the assumption of vanishing polarized strange sea. Newer experiments of the SMC [175] and SLAC [176] collaborations give a somewhat larger value for S^p_{EJ}. The polarized deep inelastic scattering experiments at CERN have shown that, when supplemented with some information from semileptonic decays, only a small fraction of the proton spin is carried by valence quarks. These result gave rise to what later has been called "spin crisis", because the integral of the longitudinally polarized distribution function, g^p_1, is directly related to the nucleon spin; and a such a small value was completely unexpected. Indeed, it means that just about the 15% of the nucleon spin is carried by quarks. Few years later this breakthrough, simple estimates within the one-pion-exchange seemed to indicate that the meson-cloud effects could contribute to solve the crisis. More recently, the authors of Ref. [177] guessed that the proton spin problem could be solved (at least partially) by the orbital angular momentum carried by the $q\bar{q}$ pairs of the meson-cloud surrounding the bare proton. Others example of

the importance of the MCM in the description of phenomenology come from electro-magnetic form factors [178, 179, 180, 66] and charge densities [181]. The neutron electric charge form factor $G_{\rm E}^n(Q^2)$ presents a pronounced bump structure (and a dip in the other nucleon form factors) around $Q^2 = 0.2 - 0.3$ GeV^2 [178], which can be interpreted as a signature of a very long-range contribution of the pion-cloud extending out of 2 fm. The analysis of Ref. [181] showed that, as expected, the neutron charge density extracted from data has a positive core surrounded by a negative surface charge, peaking at just below 1 fm, which can be attributed to a negative pion-cloud.

For the sake of completeness, it must be said, however, that from dispersion relations analysis [182] the pion-cloud should peak much more inside the nucleon, at ~ 0.3 fm., and the desired bump-dip structure of Ref. [178] can only be achieved at the cost of low-mass poles close to the ω mass in the iso-scalar channel and to the three-pion threshold in the iso-vector channel [183]. In addition, while confirming the long range positively (negatively) charged component of the proton (neutron) charge density, a recent model-independent analysis [184] and a meson-cloud model calculation ([66]a) of the IMF charge density of partons in the transverse plane suggested that the neutron parton charge density is negative at the center.
All the results reported above suggested that a description of the proton, and more generally, of the nucleon in terms of its valence quarks component only, even if in many cases satisfactory and predictive, can not surely be considered exhaustive.
In the next section following Ref. [185] we extend the LCWF formalism to include the Fock state component involving five partons, i.e. a cluster of three quarks a $q\bar{q}$ pair; and then we apply this formalism to the calculation of the so-called nucleon to pion Transition Distribution Amplitudes recently introduced in literature.

3.2 Light-Cone Wave Function in the Meson Cloud Model

The problem of considering the meson-cloud surrounding a system of three valence quarks has been addressed already in the past in a variety of papers (see, e.g., [186, 187, 188, 189, 190, 191, 192, 193, 194] and references therein). Along the lines originally proposed in Refs. [195, 196, 197] and developed in [187], here a baryon-meson Fock-state expansion is used to construct the state $|\tilde{N}\rangle$ of the physical nucleon. In the one-meson approximation the state $|\tilde{N}\rangle$ is pictured as being part of the time a bare nucleon, $|N\rangle$, and part of the time a baryon-meson system, $|BM\rangle$. The bare nucleon is formed by three valence quarks identified as constituent quarks according to the ideas discussed in [200]. The model was originally revisited in Ref. [185] to study generalized parton distributions where the meson-cloud gives an essential contribution in the so-called

ERBL region.

The state, with four-momentum $p_N^\mu = (p_N^-, p_N^+, \mathbf{p}_{N\perp}) \equiv (p_N^-, \tilde{p}_N)$ and helicity λ, is an eigenstate of the light-cone Hamiltonian

$$H_{LC} = \sum_{B,M} \left[H_0^B(q) + H_0^M(q) + H_I(N, BM) \right], \tag{3.6}$$

i.e.

$$H_{LC}|\tilde{p}_N, \lambda; \tilde{N}\rangle = \frac{\mathbf{p}_{N\perp}^2 + M_N^2}{p_N^+}|\tilde{p}_N, \lambda; \tilde{N}\rangle. \tag{3.7}$$

Here $H_0^B(q)$ stands for the effective-QCD Hamiltonian which governs the constituent-quark dynamics, and leads to the confinement of three quarks in a baryon state; analogously, $H_0^M(q)$ describes the quark interaction in a meson state. Thus we assume that the three- and two-quark states with the quantum numbers of a baryon and a meson are the eigenstates of $H_0^B(q)$ and $H_0^M(q)$, e.g.

$$H_0^B|\tilde{p}_B, \lambda; B\rangle = \frac{\mathbf{p}_{B\perp}^2 + M_B^2}{p_B^+}|\tilde{p}_B, \lambda; B\rangle, \tag{3.8}$$

$$H_0^M|\tilde{p}_M, \lambda; M\rangle = \frac{\mathbf{p}_{M\perp}^2 + M_M^2}{p_M^+}|\tilde{p}_M, \lambda; M\rangle. \tag{3.9}$$

In Eq. (3.6), $H_I(N, BM)$ is the nucleon-baryon-meson interaction, and the sum is over all the possible baryon and meson configurations in which the nucleon can virtually fluctuate. Using perturbation theory, we can expand the nucleon wavefunction in terms of the eigenstates of the bare Hamiltonian $H_0 \equiv H_0^B(q) + H_0^M(q)$, i.e.

$$\begin{aligned} |\tilde{p}_N, \lambda; \tilde{N}\rangle &= \sqrt{Z}\left(|\tilde{p}_N, \lambda; N\rangle + \sum_{n_1}{}' \frac{|n_1\rangle\langle n_1|H_I|\tilde{p}_N, \lambda; N\rangle}{E_N - E_{n_1} + i\epsilon} \right. \\ &\left. + \sum_{n_1,n_2}{}' \frac{|n_2\rangle\langle n_2|H_I|n_1\rangle\langle n_1|H_I|\tilde{p}_N, \lambda; N\rangle}{(E_N - E_{n_2} + i\epsilon)(E_N - E_{n_1} + i\epsilon)} + \cdots \right), \end{aligned} \tag{3.10}$$

where $\sum'$ indicates the summation over BM intermediate states, and Z is the wavefunction renormalization constant. In the one-meson approximation, we truncate the series expansion of Eq. (3.10) to the first order in H_I, and as a result we obtain

$$\begin{aligned} |\tilde{p}_N, \lambda; \tilde{N}\rangle &= \sqrt{Z}|\tilde{p}_N, \lambda; N\rangle + \sum_{B,M} |\tilde{p}_N, \lambda; N(BM)\rangle \\ &= \sqrt{Z}|\tilde{p}_N, \lambda; N\rangle + \sum_{B,M} \int \frac{\mathrm{d}p_B^+ \mathrm{d}^2\mathbf{p}_{B\perp}}{2(2\pi)^3 p_B^+} \int \frac{\mathrm{d}p_M^+ \mathrm{d}^2\mathbf{p}_{M\perp}}{2(2\pi)^3 p_M^+} \\ &\quad \times \sum_{\lambda',\lambda''} \frac{\langle B(\tilde{p}_B, \lambda')M(\tilde{p}_M, \lambda'')|H_I|N(\tilde{p}_N, \lambda)\rangle}{E_N - E_B - E_M} |\tilde{p}_B, \lambda'; B\rangle\, |\tilde{p}_M, \lambda''; M\rangle. \end{aligned} \tag{3.11}$$

In Eq. (3.11), the normalization factor $\sqrt{Z}$ only affects the bare core $|N\rangle$, and not the meson-baryon component. As discussed in details in Refs. [198, 199], this prescription is consistent with assuming that the nucleon-baryon-meson coupling constant in H_I is taken equal to the renormalized value g_{NBM}, related to lowest order to the bare coupling g^0_{NBM} via $g_{NBM} = \sqrt{Z} g^0_{NBM}$.

Finally, the hadron states in Eq. (3.11) are normalized as

$$\langle p'^+, \mathbf{p}'_\perp, \lambda'; H | p^+, \mathbf{p}_\perp \lambda; H \rangle = 2(2\pi)^3 p^+ \delta(p'^+ - p^+) \delta^{(2)}(\mathbf{p}'_\perp - \mathbf{p}_\perp) \delta_{\lambda\lambda'}. \quad (3.12)$$

The nucleon wavefunction

In this subsection starting from Eq. (3.11) we report the derivation of the explicit general expression of the nucleon wavefunction on the basis of bare-nucleon and baryon-meson Fock states.

We first evaluate the energy denominator in Eq. (3.11) using the following expression for the energy of the particles in terms of light-front variables

$$E = \frac{1}{\sqrt{2}} \left(p^+ + \frac{\mathbf{p}_\perp^2 + M^2}{p^+} \right). \quad (3.13)$$

If we write the momenta of the baryon, $\tilde{p}_B$, and the meson, $\tilde{p}_M$, in terms of the intrinsic (nucleon rest-frame) variables, i.e.

$$\begin{array}{ll} p_B^+ = y p_N^+, & p_M^+ = (1-y) p_N^+, \\ \mathbf{p}_{B\perp} = \mathbf{k}_\perp + y\, \mathbf{p}_{N\perp}, & \mathbf{p}_{M\perp} = -\mathbf{k}_\perp + (1-y)\, \mathbf{p}_{N\perp}, \end{array} \quad (3.14)$$

we have

$$\begin{aligned} (E_N - E_B - E_M) &= \frac{1}{\sqrt{2} p_N^+} \left(M_N^2 - \frac{M_B^2 + \mathbf{k}_\perp^2}{y} - \frac{M_M^2 + \mathbf{k}_\perp^2}{1-y} \right) \\ &\equiv \frac{1}{\sqrt{2} p_N^+} \left(M_N^2 - M_{BM}^2(y, \mathbf{k}_\perp) \right), \end{aligned} \quad (3.15)$$

where

$$M_{BM}^2(y, \mathbf{k}_\perp) \equiv \frac{M_B^2 + \mathbf{k}_\perp^2}{y} + \frac{M_M^2 + \mathbf{k}_\perp^2}{1-y}, \quad (3.16)$$

is the invariant mass of the baryon-meson fluctuation.

Furthermore, the transition amplitude $\langle B(\tilde{p}_B, \lambda') M(\tilde{p}_M, \lambda'') | H_I | N(\tilde{p}_N, \lambda) \rangle$ in Eq. (3.11) can be rewritten as

$$\begin{aligned} &\langle B(\tilde{p}_B, \lambda') M(\tilde{p}_M, \lambda'') | H_I | N(\tilde{p}_N, \lambda) \rangle = \\ &= (2\pi)^3 \delta(p_B^+ + p_M^+ - p_N^+)\, \delta^{(2)}(\mathbf{p}_{B\perp} + \mathbf{p}_{M\perp} - \mathbf{p}_{N\perp}) V^\lambda_{\lambda',\lambda''}(N, BM), \end{aligned} \quad (3.17)$$

where the vertex function $V^\lambda_{\lambda',\lambda''}(N, BM)$ has the following general expression

$$V^\lambda_{\lambda',\lambda''}(N, BM) = \bar{u}_{N\alpha}(\tilde{p}_N, \lambda) v^{\alpha\beta\gamma} \chi_\beta(\tilde{p}_M, \lambda'') \psi_\gamma(\tilde{p}_B, \lambda'). \quad (3.18)$$

Here u_N is the nucleon spinor, χ and ψ are the field operators of the intermediate meson and baryon, respectively, and α, β, γ are bi-spinor and/or vector indices depending on the representation used for particles of given type.

Using the results of Eqs. (3.15) and (3.17), we find

$$\begin{aligned}|\tilde{p}_N,\lambda;\tilde{N}\rangle \quad &= \sqrt{Z}|\tilde{p}_N,\lambda;N\rangle + \sum_{B,M}\int\frac{\mathrm{d}y\mathrm{d}^2\mathbf{k}_\perp}{2(2\pi)^3}\frac{1}{\sqrt{y(1-y)}}\sum_{\lambda',\lambda''}\phi^{\lambda\,(N,BM)}_{\lambda'\lambda''}(y,\mathbf{k}_\perp)\\ &\times|yp_N^+,\mathbf{k}_\perp+y\mathbf{p}_{N\perp},\lambda';B\rangle\,|(1-y)p_N^+,-\mathbf{k}_\perp+(1-y)\mathbf{p}_{N\perp},\lambda'';M\rangle,\end{aligned} \tag{3.19}$$

where we introduced the function $\phi^{\lambda\,(N,BM)}_{\lambda'\lambda''}(y,\mathbf{k}_\perp)$ to define the probability amplitude for a nucleon with helicity λ to fluctuate into a virtual BM system with the baryon having helicity λ', longitudinal momentum fraction y and transverse momentum $\mathbf{k}_\perp$, and the meson having helicity λ'', longitudinal momentum fraction $1-y$ and transverse momentum $-\mathbf{k}_\perp$, i.e.

$$\phi^{\lambda\,(N,BM)}_{\lambda'\lambda''}(y,\mathbf{k}_\perp) = \frac{1}{\sqrt{y(1-y)}}\frac{V^\lambda_{\lambda',\lambda''}(N,BM)}{M_N^2-M_{BM}^2(y,\mathbf{k}_\perp)}. \tag{3.20}$$

We note that Eq. (3.19) is equivalent to the expression of the nucleon wavefunction obtained in the framework of "old-fashioned" time-ordered perturbation theory in the IMF (see Ref. [201]).

By imposing the normalization of the nucleon state as in Eq. (3.12), from Eq. (3.19) we obtain the following condition on the normalization factor Z

$$1 = Z + P_{BM/N}, \tag{3.21}$$

with

$$P_{BM/N} = \sum_{B,M}\int\frac{\mathrm{d}y\mathrm{d}^2\mathbf{k}_\perp}{2(2\pi)^3}\frac{1}{y(1-y)}\sum_{\lambda',\lambda''}\frac{|V^{1/2}_{\lambda',\lambda''}(N,BM)|^2}{[M_N^2-M_{BM}^2(y,\mathbf{k}_\perp)]^2}. \tag{3.22}$$

Here $P_{BM/N}$ is the probability of fluctuation of the nucleon in a baryon-meson state, and, accordingly, Z gives the probability to find the bare nucleon in the physical nucleon.

Partonic content of the nucleon wavefunction

We consider the component of the meson-baryon Fock state in Eq. (3.19).

The light-front state of the baryon is given by

$$\begin{aligned}|\tilde{p}_B,\lambda';\,B\rangle \;&=\; \sum_{\tau_i,\lambda_i}\int\left[\frac{\mathrm{d}x}{\sqrt{x}}\right]_3[\mathrm{d}^2\mathbf{k}_\perp]_3\Psi^{B,[f]}_{\lambda'}(\{x_i,\mathbf{k}_{\perp i};\lambda_i,\tau_i\}_{i=1,2,3})\\ &\times\prod_{i=1}^{3}\left|x_ip_B^+,\,\mathbf{p}_{i\perp},\lambda_i,\tau_i;q\right\rangle,\end{aligned} \tag{3.23}$$

where now the intrinsic variables of the quarks x_i and k_i^+ refer to the baryon rest frame, i.e. $x_i = p_i^+/p_B^+$ and $\mathbf{p}_{i\perp} = \mathbf{k}_{i\perp} + x_i \mathbf{p}_{B\perp}$ $(i = 1, 2, 3)$.

An analogous expression holds for the light-front state of the meson, i.e.

$$\begin{aligned} |\tilde{p}_M, \lambda''; M\rangle &= \sum_{\tau_i, \lambda_i} \int \frac{\mathrm{d}x_4 \mathrm{d}x_5}{\sqrt{x_4 x_5}} \frac{\mathrm{d}\mathbf{k}_{4\perp} \mathrm{d}\mathbf{k}_{5\perp}}{16\pi^3} \, \delta(1 - x_4 - x_5) \, \delta^{(2)}(\mathbf{k}_{4\perp} + \mathbf{k}_{5\perp}) \\ &\quad \times \Psi^{M,[f]}_{\lambda''}(\{x_i, \mathbf{k}_{\perp i}; \lambda_i, \tau_i\}_{i=4,5}) \prod_{i=4}^{5} \left| x_i p_M^+, \, \mathbf{p}_{i\perp}, \lambda_i, \tau_i; q \right\rangle , \end{aligned} \tag{3.24}$$

with $x_i = p_i^+/p_M^+$, $\mathbf{p}_{i\perp} = x_i \mathbf{p}_{M\perp} + \mathbf{k}_{i\perp}$ $(i = 4, 5)$.

When we insert the expressions of the baryon and meson states in Eq. (3.19), it is convenient to rewrite the kinematical variables of the partons as follows.

For $i = 1, 2, 3$:

$$\begin{aligned} x_i &= \frac{p_i^+}{p_B^+} = \frac{p_i^+}{p_N^+} \frac{p_N^+}{p_B^+} = \frac{\xi_i}{y}, \\ \mathbf{p}_{i\perp} &= x_i \mathbf{p}_{B\perp} + \mathbf{k}_{i\perp} = x_i \left(\mathbf{k}_\perp + y \, \mathbf{p}_{N\perp} \right) + \mathbf{k}_{i\perp} \\ &= \xi_i \mathbf{p}_{N\perp} + \mathbf{k}_{i\perp} + x_i \, \mathbf{k}_\perp \equiv \xi_i \mathbf{p}_{N\perp} + \mathbf{k}'_{i\perp}, \end{aligned}$$

where $\xi_i = p_i^+/p_N^+$ is the fraction of the longitudinal momentum of the nucleon carried by the quarks in the baryon, and $\mathbf{k}'_{i\perp}$ is the intrinsic transverse momentum of the quarks with respect to the nucleon rest frame.

For $i = 4, 5$:

$$\begin{aligned} x_i &= \frac{p_i^+}{p_M^+} = \frac{p_i^+}{p_N^+} \frac{p_N^+}{p_M^+} = \frac{\xi_i}{1 - y}, \\ \mathbf{p}_{i\perp} &= x_i \mathbf{p}_{M\perp} + \mathbf{k}_{i\perp} = x_i \left(-\mathbf{k}_\perp + (1 - y) \, \mathbf{p}_{N\perp} \right) + \mathbf{k}_{i\perp} \\ &= \xi_i \mathbf{p}_{N\perp} + \mathbf{k}_{i\perp} - x_i \, \mathbf{k}_\perp \equiv \xi_i \mathbf{p}_{N\perp} + \mathbf{k}'_{i\perp}, \end{aligned}$$

with $\xi_i = p_i^+/p_N^+$ and $\mathbf{k}'_{i\perp}$ the intrinsic variables of the quarks in the meson with respect to the nucleon rest frame. Accordingly we transform the variables of integration as follows.

For $i = 1, 2, 3$:

$$\begin{aligned} x_i &\rightarrow \xi_i = y \, x_i, \\ \mathbf{k}_{i\perp} &\rightarrow \mathbf{k}'_{i\perp} = \mathbf{k}_{i\perp} + x_i \, \mathbf{k}_\perp. \end{aligned}$$

For $i = 4, 5$:

$$\begin{aligned} x_i &\rightarrow \xi_i = (1 - y) \, x_i, \\ \mathbf{k}_{i\perp} &\rightarrow \mathbf{k}'_{i\perp} = \mathbf{k}_{i\perp} - x_i \, \mathbf{k}_\perp. \end{aligned}$$

The meson-baryon component of the nucleon wavefunction in Eq. (3.19) can then be written as

$$
\begin{aligned}
|\tilde{p}_N,\lambda;N(BM)\rangle \;=\; & \int \mathrm{d}y\,\mathrm{d}^2\mathbf{k}_\perp \int_0^y \prod_{i=1}^{3}\frac{\mathrm{d}\xi_i}{\sqrt{\xi_i}} \int_0^{1-y}\prod_{i=4}^{5}\frac{\mathrm{d}\xi_i}{\sqrt{\xi_i}} \int \frac{\prod_{i=1}^{5}\mathrm{d}\mathbf{k}'_{i\perp}}{[2(2\pi)^3]^4} \\
& \times \delta\left(y-\sum_{i=1}^{3}\xi_i\right)\delta^{(2)}\left(\mathbf{k}_\perp-\sum_{i=1}^{3}\mathbf{k}'_{i\perp}\right) \\
& \times \delta\left(1-\sum_{i=1}^{5}\xi_i\right)\delta^{(2)}\left(\sum_{i=1}^{5}\mathbf{k}'_{i\perp}\right) \\
& \times \sum_{\lambda',\lambda''}\sum_{\lambda_i,\tau_i}\frac{V^{\lambda}_{\lambda',\lambda''}(N,BM)}{M_N^2-M_{BM}^2(y,\mathbf{k}_\perp)}\tilde{\Psi}^{B,[f]}_{\lambda'}(\{\xi_i,\mathbf{k}'_{i\perp};\lambda_i,\tau_i\}_{i=1,2,3}) \\
& \times \tilde{\Psi}^{M,[f]}_{\lambda''}(\{\xi_i,\mathbf{k}'_{i\perp};\lambda_i,\tau_i\}_{i=4,5})\prod_{i=1}^{5}|\xi_i p_N^+,\,\mathbf{k}'_{i\perp}+\xi_i\mathbf{p}_{N\perp},\,\lambda_i,\,\tau_i;q\rangle,
\end{aligned}
\tag{3.25}
$$

where the wavefunctions $\tilde{\Psi}^{B,[f]}_{\lambda'}$ and $\tilde{\Psi}^{M,[f]}_{\lambda''}$ incorporate the Jacobian $\mathcal{J}$ of the transformation $x_i \to \xi_i$, i.e.

$$
\begin{aligned}
\tilde{\Psi}^{B,[f]}_{\lambda'}(\{\xi_i,\mathbf{k}'_{i\perp};\lambda_i,\tau_i\}_{i=1,2,3}) &= \sqrt{\mathcal{J}(\xi_1,\xi_2,\xi_3)}\tilde{\Psi}^{B,[f]}_{\lambda'}(\{x_i,\mathbf{k}_{i\perp};\lambda_i,\tau_i\}_{i=1,2,3}) \\
&= \frac{1}{y^{3/2}}\tilde{\Psi}^{B,[f]}_{\lambda'}(\{x_i,\mathbf{k}_{i\perp};\lambda_i,\tau_i\}_{i=1,2,3}),
\end{aligned}
\tag{3.26}
$$

$$
\begin{aligned}
\tilde{\Psi}^{M,[f]}_{\lambda''}(\{\xi_i,\mathbf{k}'_{i\perp};\lambda_i,\tau_i\}_{i=4,5}) &= \sqrt{\mathcal{J}(\xi_4,\xi_5)}\tilde{\Psi}^{M,[f]}_{\lambda''}(\{x_i,\mathbf{k}_{i\perp};\lambda_i,\tau_i\}_{i=4,5}) \\
&= \frac{1}{(1-y)}\tilde{\Psi}^{M,[f]}(\{x_i,\mathbf{k}_{i\perp};\lambda_i,\tau_i\}_{i=4,5}).
\end{aligned}
\tag{3.27}
$$

Finally, by introducing the following definition

$$
\begin{aligned}
\tilde{\Psi}^{5q,[f]}_{\lambda}(y,\mathbf{k}_\perp;\,\{\xi_i,\mathbf{k}'_{i\perp};\lambda_i,\tau_i\}_{i=1,\ldots,5}) \equiv & \sum_{\lambda',\lambda''}\frac{V^{\lambda}_{\lambda',\lambda''}(N,BM)}{M_N^2-M_{BM}^2(y,\mathbf{k}_\perp)} \\
& \times \tilde{\Psi}^{B,[f]}_{\lambda'}(\{\xi_i,\mathbf{k}'_{i\perp},\lambda_i,\tau_i\}_{i=1,2,3})\tilde{\Psi}^{M,[f]}_{\lambda''}(\{\xi_i,\mathbf{k}'_{i\perp},\lambda_i,\tau_i\}_{i=4,5}),
\end{aligned}
\tag{3.28}
$$

Eq. (3.25) can be simplified to the following expression:

$$
\begin{aligned}
|\tilde{p}_N, \lambda; N(BM)\rangle \;=\; & \int \mathrm{d}y\, \mathrm{d}^2\mathbf{k}_\perp \int_0^y \prod_{i=1}^{3} \frac{\mathrm{d}\xi_i}{\sqrt{\xi_i}} \int_0^{1-y} \prod_{i=4}^{5} \frac{\mathrm{d}\xi_i}{\sqrt{\xi_i}} \int 5\, \frac{\prod_{i=1}^{\mathrm{d}} \mathbf{k}'_{i\perp}}{[2(2\pi)^3]^4} \\
& \times \delta\left(y - \sum_{i=1}^{3} \xi_i\right) \delta^{(2)}\left(\mathbf{k}_\perp - \sum_{i=1}^{3} \mathbf{k}'_{i\perp}\right) \\
& \times \delta\left(1 - \sum_{i=1}^{5} \xi_i\right) \delta^{(2)}\left(\sum_{i=1}^{5} \mathbf{k}'_{i\perp}\right) \\
& \times \sum_{\lambda_i, \tau_i} \tilde{\Psi}_\lambda^{5q,\,[f]}(y, \mathbf{k}_\perp;\, \{\xi_i, \mathbf{k}'_{i\perp}; \lambda_i, \tau_i\}_{i=1,\ldots,5}) \\
& \times \prod_{i=1}^{5} |\xi_i p_N^+,\, \mathbf{k}'_{i\perp} + \xi_i \mathbf{p}_{N\perp},\, \lambda_i,\, \tau_i; q\rangle, \qquad (3.29)
\end{aligned}
$$

where $\tilde{\Psi}_\lambda^{5q,\,[f]}$ can be interpreted as the probability amplitude for finding in the nucleon a configuration of five partons composed by two clusters of three and two quarks, with total momentum $(yp_N^+, \mathbf{p}_{B\perp})$ and $((1-y)p_N^+, \mathbf{p}_{M\perp})$, respectively.

3.3 Transition Distribution Amplitudes

In this section we apply the MCM in LCWF formalism to the study of the nucleon to pion Transition Distribution Amplitudes.

It is well-known that in the last ten years through the factorization theorems [202] it has been possible to give a reliable theoretical treatment of hard exclusive processes that have been a challenge for QCD for long time. A huge class of exclusive processes, involving some hard scale Q^2, can now be treated on a firm perturbative QCD basis thanks to the advent of the Generalized Parton Distributions (GPDs) and Amplitudes (GDAs) [58, 203], in which one can absorb all the non-perturbative soft physics[†]. Nevertheless, in spite of their universality and flexibility the GPDs and GDAs do not exhaust the range of all possible ingredients entering exclusive hadronic processes, indeed there are some important processes to which they cannot be applied. Some formidable examples of this lack are represented by the $p\bar{p}$ annihilation, e.g. $p\bar{p} \to \gamma\gamma$, the meson production channel $p\bar{p} \to \gamma\pi^0$ that will be intensively studied at GSI-HESR antiproton program by the planned FAIR project [205], and by the meson photo-production process, $p\gamma \to \pi^0 p$, with forthcoming data from JLAB.

[†]For a detailed discussion on the different regimes of factorization for the GDAs and the TDAs cases see [204].

With the purpose of describing this peculiar kind of events, where, between the initial and the final state, takes place a transition from a baryon to a meson, we should introduce a new type of objects, the Transition Distribution Amplitudes (TDAs). The TDAs are a new class of non-perturbative quantities that extends the concept of GPDs. These observables, initially called Skewed Distribution Amplitudes (SDAs), have been introduced for the first time in [206], where the authors just guessed that these new mathematical objects had to be taken into account in the study of the hard exclusive electroproduction of a meson. Only recently Pire and collaborators have shown in a series of articles [207] that these new observables represent the ideal framework through which it is possible to describe the backward pion electro-production, e.g., $ep \to e'p'\pi_0$, as well as the meson production via a nucleon-antinucleon Drell-Yan process, e.g., $N\bar{N} \to \gamma^*\pi$, in the forward kinematics.
As can be deduced from Fig. (3.1) the nucleon to pion TDAs describe exactly how a baryon can turn into a meson, namely the "transition" from a baryonic to a mesonic state.

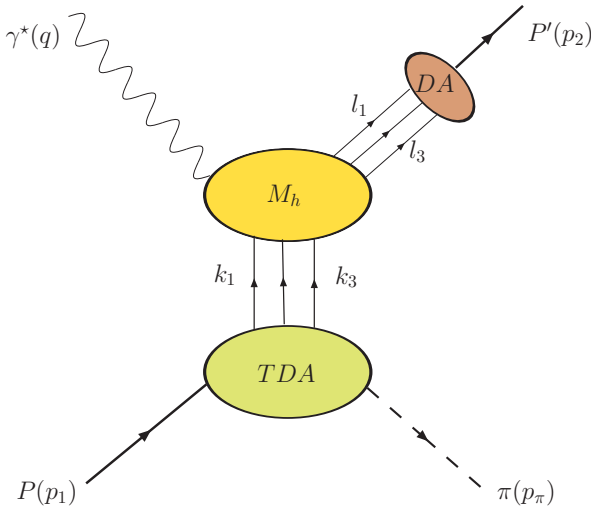

Figure 3.1: Sketch of the process $\gamma^\star p \to p'\pi_0$, that involves the TDAs.

Besides the nucleon to pion TDAs, other TDAs can be defined. Given that the initial and final state are different hadronic states, if those new hadronic objects are defined through a quark-antiquark operator (meson to meson or meson to photon transition), we call them *mesonic* transition distribution amplitudes (mTDAs), if they are defined through a three quark operator (baryon to meson or baryon to photon transition), we call them *baryonic* transition dis-

tribution amplitudes (bTDAs). Both appear in the description of hard exclusive processes, where a highly off-shell photon provides a hard scale permitting, on the one hand, to treat perturbatively the interaction between the photon and the quarks off the target, on the other hand to advocate the factorisation of the amplitude as a convolution of a hard amplitude M_h with the *universal* TDAs describing the non-perturbative transition between two hadronic states and DAs describing the formation of another hadron. Three examples are: the process $\gamma^\star\gamma \to A\pi$ at small t, with A a meson, where there appear the mesonic $\gamma \to \pi$ TDAs; the backward electro-production of a pion; and the third is a crossed process $\bar{p}p \to \gamma^\star\pi^0$. In those two last processes, there appear the baryonic $p \to \pi^0$ TDAs that we will study in detail within the MCM of Ref. [185].

The mTDAs possess an interpretation at the amplitude level and provide with information on how a meson and a photon look "alike". Rather, the bTDAs provide information on how one can find a meson or a photon inside a baryon. For this reason the study of bTDAs represents a crucial test for the meson-cloud contribution to the structure of the nucleon

3.3.1 Mesonic Transition Distribution Amplitudes

The mTDAs are defined starting from the correlator[‡]

$$\int \frac{dz^-}{2\pi} e^{ixP^+z^-} \langle \pi(p_\pi)|\bar{\psi}(-z/2)\Gamma\psi(z/2)|\gamma(p_\gamma,\varepsilon)\rangle_{|_{z^+=z_\perp=0}} \tag{3.30}$$

where Γ is one of the Dirac structure: γ^μ,$\gamma^\mu\gamma^5$ or $\sigma^{\mu\nu}$, and ε is the photon polarization vector. Depending which structure one takes into account it is possible to obtain four different mTDAs. Indeed,

$$\gamma^\mu \to \frac{1}{f_\pi}\varepsilon^{\mu\varepsilon P\Delta_\perp} V^\pi(x,\xi,\Delta^2); \quad \text{Vectorial} \tag{3.31}$$

$$\Gamma: \quad \gamma^\mu\gamma_5 \to \frac{1}{f_\pi}(\varepsilon\cdot\Delta)P^\mu A^\pi(x,\xi,\Delta^2); \quad \text{Axial} \tag{3.32}$$

$$\sigma^{\mu\nu} \to \varepsilon^{\mu\nu\rho\sigma}P_\sigma\Big[\varepsilon_\rho T_1^\pi(x,\xi,\Delta^2) \tag{3.33}$$

$$-\frac{1}{f_\pi}(\varepsilon\cdot\Delta)\Delta_{\perp\rho}T_2^\pi(x,\xi,\Delta^2)\Big]. \quad \text{Tensorial} \tag{3.34}$$

As the GPDs the TDAs depend on three kinematical variables, the LC momentum fraction x, the skewdness parameter ξ and the longitudinal momentum square Δ^2. The mesonic TDAs have many other features in common with meson GPDs.

General arguments, such as Lorentz invariance, lead to some important properties of GPDs. Taking their first Mellin moment, one can relate GPDs to

[‡]If p and p' are respectively the momenta of the initial and final particles in the TDAs, we have $(p'-p)=\Delta$, $P=1/2(p+p')$ and $2\xi=-\Delta^+/P^+$. We also have $\xi\approx x_B/(2-x_B)$.

the corresponding form factors through the sum rules. Also their higher Mellin moments are polynomials in the skewness variable ξ by Lorentz invariance.

Similarly, as a consequence of Lorentz invariance, TDAs are constrained by sum rules and polynomial expansions. The first Mellin moments of π-γ transition distribution functions are related to the vector and axial-vector transition form factors, F_V and F_A, through the sum rules. The definition of these form factors is given from the vector and axial-vector currents [208]

$$\langle\gamma(p')|\,\bar{\psi}(0)\gamma_\mu\tau^-\psi(0)\,|\pi(p)\rangle = -i\,e\,\varepsilon^\nu\,\epsilon_{\mu\nu\rho\sigma}\,p'^{\rho}\,p^\sigma\,\frac{F_V(\Delta^2)}{m_\pi} \quad , \tag{3.35}$$

$$\begin{aligned}\langle\gamma(p')|\,\bar{\psi}(0)\gamma_\mu\gamma_5\tau^-\psi(0)\,|\pi(p)\rangle &= e\,\varepsilon^\nu\left(p'_\mu\,p_\nu - g_{\mu\nu}\,p'.p\right)\frac{F_A\,(\Delta^2)}{m_\pi} \\ &\quad + e\,\varepsilon^\nu\left((p'-p)_\mu\;p_\nu\frac{2\sqrt{2}f_\pi}{m_\pi^2-\Delta^2} - \sqrt{2}f_\pi\,g_{\mu\nu}\right),\end{aligned} \tag{3.36}$$

with $f_\pi \simeq 133$ MeV the pion decay constant, $\varepsilon^{0123} = 1$ and $\tau^- = (\tau_1 - i\,\tau_2)/2$. All the structure of the decaying pion is included in the form factors F_V and F_A. The vector current only contains a Lorentz structure associated with the F_V form factor. The axial form factor F_A also gives the structure of the pion but contains additional terms required by electromagnetic gauge invariance. The second term on the right-hand side of Eq. (3.36), which corresponds to the axial current for a point-like pion, contains a pion pole coming from the pion inner bremsstrahlung: the incoming pion and outgoing photon couple with the axial current through a virtual pion as required by the Partial Conservation of the Axial Current (PCAC). The third term in Eq. (3.36) is a pion-photon-axial current contact term, proportional to $f_\pi g_{\mu\nu}$. The transition form factors F_A and F_V are well measured [209].

Since the TDAs satisfy similar polynomiality conditions to GPDs they may be constructed from a spectral decomposition, in analogy with the construction of GPDs through double distributions [210]. The x and ξ dependence of the TDAs is then given as

$$\int_{-1}^{1}\mathrm{d}\beta\int_{-1+|\beta|}^{1-|\beta|}d\alpha\;\delta(x-\beta-\xi\alpha)f(\beta,\alpha).$$

Note however that TDAs possess different properties than GPDs with respect to time reversal since initial and final states are different. A consequence of this is the appearance of odd-powers of ξ in their moments in x.

Recently several models calculations for TDAs describing the pion to photon transition appeared in literature. However, so far, only the vectorial and the axial TDAs have been analyzed. We briefly recall here some results about these two mesonic TDAs, specifying their definitions and properties.

To leading twist, the vectorial and axial TDAs are defined as

$$\int \frac{\mathrm{d}z^-}{2\pi} e^{ixP^+z^-} \left\langle \gamma\left(p'\right)\right| \bar{\psi}\left(-\frac{z}{2}\right) \gamma^+\tau^-\psi\left(\frac{z}{2}\right) \left|\pi^+\left(p\right)\right\rangle\Big|_{z^+=z^\perp=0}$$
$$= i\, e\, \varepsilon_\nu\, \epsilon^{+\nu\rho\sigma}\, P_\rho\, \Delta_\sigma\, \frac{V^{\pi^+\to\gamma}\left(x,\xi,\Delta^2\right)}{\sqrt{2}f_\pi} \quad ,$$
$$\int \frac{\mathrm{d}z^-}{2\pi} e^{ixP^+z^-} \left\langle \gamma\left(p'\right)\right| \bar{\psi}\left(-\frac{z}{2}\right) \gamma^+\gamma_5\tau^-\psi\left(\frac{z}{2}\right) \left|\pi^+\left(p\right)\right\rangle\Big|_{z^+=z^\perp=0}$$
$$= e\, \left(\varepsilon^\perp\cdot\mathbf{\Delta}^\perp\right) \frac{A^{\pi^+\to\gamma}\left(x,\xi,t\right)}{\sqrt{2}f_\pi} + e\, \left(\varepsilon\cdot\Delta\right) \frac{2\sqrt{2}f_\pi}{m_\pi^2-\Delta^2}\, \epsilon\left(\xi\right)\, \phi\left(\frac{x+\xi}{2\xi}\right) \quad ,(3.37)$$

with $\epsilon(\xi)$ equal to 1 for $\xi > 0$, and equal to -1 for $\xi < 0$. Here $V(x,\xi,\Delta^2)$ and $A(x,\xi,\Delta^2)$ are respectively the vector and axial TDAs. Hence the axial matrix element contains the axial TDA and the pion pole contribution that has been isolated in a model independent way [211, 212]. The latter term is parametrized by a point-like pion propagator multiplied by the distribution amplitude of an on-shell pion, $\phi(x)$. Notice that the pion DA obeys the normalization condition $\int_0^1 dx\, \phi(x) = 1$; the connection through the sum rules of Eq. (3.37) with Eqs. (3.35) and (3.36) is therefore obvious.

The contribution of a pion pole is not a new feature of large-distance distributions. TDAs like GPDs are low-energy quantities in QCD though their degrees of freedom are quarks and gluons. One thus expects chiral symmetry to manifest itself, what implies a matching between the degrees of freedom of parton distributions and the low-energy degrees of freedom such as pions. Actually, in the region $x \in [-|\xi|, |\xi|]$, the emission of a $q\bar{q}$ pair from the initial state can be assimilated to a meson distribution amplitude.
Recent ongoing analysis [213] seems to show that the contribution of interference between the axial term and the pion pole should be important for the experimental analysis of the mTDAs because it gives rise to an enhancement of the process cross section.

Here we have defined the TDAs in the particular case of a transition from a π^+ to a photon, parametrizing the processes, $H\bar{H} \to \gamma^*\gamma$ and $\gamma^*H \to H\gamma$. Symmetries relate the latter distributions to TDAs involved in other processes. For instance, one could wish to study the γ-π^- TDAs entering the factorized amplitude of the process $\gamma_L^*\gamma \to M^\pm\pi^\mp$, with M being either ρ_L or π.

Analogously it is possible to define the γ-$\pi^{\pm}$ TDAs

$$\begin{aligned}
&\int \frac{\mathrm{d}z^-}{2\pi} e^{ixP^+z^-} \left\langle \pi^{\pm}(p) \right| \bar{\psi}\left(-\frac{z}{2}\right) \gamma^+ \tau^{\pm} \psi\left(\frac{z}{2}\right) \left| \gamma(p'\varepsilon) \right\rangle \Big|_{z^+=z^\perp=0} \\
&= i\, e\, \varepsilon_\nu\, \epsilon^{+\nu\rho\sigma}\, P_\rho\, (p-p')_\sigma\, \frac{V^{\gamma\to\pi^{\pm}}(x,-\xi,\Delta^2)}{\sqrt{2} f_\pi} \quad , \\
&\int \frac{\mathrm{d}z^-}{2\pi} e^{ixP^+z^-} \left\langle \pi^{\pm}(p) \right| \bar{\psi}\left(-\frac{z}{2}\right) \gamma^+ \gamma_5 \tau^{\pm} \psi\left(\frac{z}{2}\right) \left| \gamma(p'\varepsilon) \right\rangle \Big|_{z^+=z^\perp=0} \\
&= -e\, \left(\varepsilon^\perp \cdot (\mathbf{p}^\perp - \mathbf{p'}^\perp)\right) \frac{A^{\gamma\to\pi^{\pm}}(x,-\xi,\Delta^2)}{\sqrt{2} f_\pi} \\
&\pm e\, (\varepsilon \cdot (p-p'))\, \frac{2\sqrt{2} f_\pi}{m_\pi^2 - \Delta^2}\, \epsilon(-\xi)\, \phi\left(\frac{x+\xi}{2\xi}\right). \qquad (3.38)
\end{aligned}$$

Time reversal transformation relates the π^+-γ TDAs to γ-π^+ TDAs in the following way

$$D^{\pi^+\to\gamma}(x,\xi,\Delta^2) \;=\; D^{\gamma\to\pi^+}(x,-\xi,\Delta^2) \quad , \qquad (3.39)$$

where $D = V, A$. Moreover CPT relates the $\pi \to \gamma$ TDAs to their analog for a transition from a photon to a π^-

$$\begin{aligned}
V^{\pi^+\to\gamma}(x,\xi,\Delta^2) &= V^{\gamma\to\pi^-}(-x,-\xi,\Delta^2) \quad , \\
A^{\pi^+\to\gamma}(x,\xi,\Delta^2) &= -A^{\gamma\to\pi^-}(-x,-\xi,\Delta^2) \quad . \qquad (3.40)
\end{aligned}$$

In Refs. [211, 214], the vectorial and axial TDAs were modeled via double-distributions and more recently in the spectral quark model [215]. Other approaches [216] used to construct pion GPDs could provide us with reasonable modelling of the mesonic TDAs. Let us cite for instance the Nambu-Jona Lasinio Model [212]. Finally, we can say that, so far, all the model calculations are in good agreement with each other; and, moreover, lattice QCD, which has been recently applied to extract moments of pion GPDs [217], could also be applied to the TDA case.

From the experimental side the introduction of the $\gamma \to$meson TDAs completes the kinematical domain for the reactions $\gamma\gamma^\star \to M_1 M_2$ in the framework of QCD factorization. Data have already been collected at LEP and CLEO on these reactions, mostly in the GDA domain for $\rho\rho$ final states, with some phenomenological success [218]. More data are obviously needed and are eagerly waited for in the TDA region, and much hope comes from the high luminosity electron colliders. This requires in general the exclusive detection of two mesons, when tagging simultaneously one outgoing electron.

Another way to access the mesonic TDAs is to study DVCS on virtual pion target, which may be studied [219] at Hermes and JLab in the reaction

$\gamma^\star p \to \gamma\pi^+ n$, when the transition $p \to n$ is dominated by the pion pole and the π^+ flies in the direction of the $\gamma^\star$ in the $\gamma\pi^+$ center of mass system.

3.3.2 Baryonic Transition Distribution Amplitudes

We will treat in a great detail the nucleon to pion TDAs in the next section, here we recall some theoretical results recently obtained.

Let us concentrate here on the $p \to \pi$ TDAs, for completeness we mention that the proton to photon TDAs, entering the description of backward DVCS, have been defined in Ref. [220]. The leading twist TDAs for the $p \to \pi^0$ transition are defined from the correlator (see later) :

$$\langle \pi^0(p_\pi)|\, \epsilon^{ijk} u^i_\alpha(z_1\, n) u^j_\beta(z_2\, n) d^k_\gamma(z_3\, n)\, |p(p_1, s_1)\rangle.$$

These TDAs are matrix elements of the same operator that appears in baryonic distribution amplitudes. The known evolution equations of this operator lead to derive evolution equations which have different forms in different regions. Indeed, since the correlator involves the FT of the same operator, this implies that they are governed by the same RGEs, but for the TDAs case the kinematics is different and this leads to definitions of one ERBL and two DGLAP regions much in the same spirit as in the GPD case, so that the evolution equations in momentum space depend on the signs of the quark momentum fractions x_i. We have: ERBL for $x_i \geq 0$, DGLAP1 when $x_1 \geq 0; x_2 \geq 0; x_3 \leq 0$, and DGLAP2 when $x_1 \geq 0; x_2 \leq 0; x_3 \leq 0$.

As for DAs, an asymptotic solution for this evolution equation exists (so far for the ERBL region only), but the phenomenological study of electromagnetic form factors leads us to strongly doubt that it is of any phenomenological relevance. In some sense, this is not a surprise since the corresponding asymptotic solution ($\delta(x)$) for parton distribution functions is far from a realistic description of DIS data. Thus it should not be taken as a realistic input for phenomenology.

On the other hand, there exists an interesting soft limit [207] when the emerging pion momentum is small, which allows to relate proton $\to$ pion TDAs to proton DAs. The well-known "soft pion" theorems [221, 222] indeed allow to write:

$$\langle \pi^a(p_\pi)|\mathcal{O}|P(p_1, s_1)\rangle \to -\frac{i}{f_\pi}\langle 0|[Q^a_5, \mathcal{O}]|P(p, s)\rangle$$

when $\xi \to 1$ ($E_\pi \to 0$, $\Delta_\perp = 0$); the neglected nucleon pole term, which does not contribute at threshold but is likely to be important for ξ significantly different from 1, may also be taken into account. One then gets relations between the nucleon DAs [71] A_1, V_1 and T_1 on the one hand and the $p \to \pi$

TDAs $V_1^{p\pi^0}$, $A_1^{p\pi^0}$ and $T_1^{p\pi^0}$ on the other hand :

$$V_1^{p\pi^0}(x_1,x_2,x_3,\xi,M^2) = \frac{1}{4\xi}V_1\Big(\frac{x_1}{2\xi},\frac{x_2}{2\xi},\frac{x_3}{2\xi}\Big),$$
$$A_1^{p\pi^0}(x_1,x_2,x_3,\xi,M^2) = \frac{1}{4\xi}A_1\Big(\frac{x_1}{2\xi},\frac{x_2}{2\xi},\frac{x_3}{2\xi}\Big),$$
$$T_1^{p\pi^0}(x_1,x_2,x_3,\xi,M^2) = \frac{3}{4\xi}T_1\Big(\frac{x_1}{2\xi},\frac{x_2}{2\xi},\frac{x_3}{2\xi}\Big).$$

As mentioned above, $p \to \pi$ baryonic TDAs appear in the description of backward electro-production of a pion on a proton target. In terms of angle, in the $\gamma^\star p$ center of momentum (CM) frame, the angle between the $\gamma^\star$ and the pion, $\theta_\pi^\star$, is close to 180°. We then have $|u| \ll s$ and $t \simeq -(s+Q^2)$, in contrast to the fixed angle regime $u \simeq t \simeq -(s+Q^2)/2$ ($\theta_\pi^\star \simeq 90°$) and the forward (GPD) one $|t| \ll s$ and $u \simeq -(s+Q^2)$ ($\theta_\pi^\star \simeq 0°$).

The TDAs appear also in similar electro-production processes such as $ep \to e\ (p,\Delta^+)\ (\eta,\rho^0)$, $ep \to e\ (n,\Delta)\ (\pi^+,\rho^+)$, $ep \to e\ \Delta^{++}\ (\pi^-,\rho^-)$. Those processes have already been analyzed, at backward angles, at JLab in the resonance region, i.e. $\sqrt{s_{\gamma^\star p}} = W < 1.8$ GeV, in order to study the baryonic transition form factors in the π channel [223] or in the η channel [224, 225]. Data are being extracted in some channels above the resonance region. The number of events seems large enough to expect to get cross section measurements for $\Delta_\perp^2 < 1$ GeV^2, which is the region described in terms of TDAs. Hermes analysis[226] for forward electroproduction may also be extended to larger values of $-t$. It has to be noted though that present studies are limited to Q^2 of order a few GeV^2, which gives no guarantee to reach the TDA regime yet. Higher-Q^2 data may be obtained at JLab-12 GeV and in muon-production at Compass within the next few years. Besides comparisons with forthcoming experimental data, one may also consider results from global Partial Wave Analysis (e.g. SAID [227]).

Crossed reactions involving TDAs in proton-antiproton annihilation (GSI-FAIR [228]), with time-like photons (i.e. di-leptons) can also be studied with other mesons than a pion, e.g. $\bar{p}p \to \gamma^\star\ (\eta,\rho^0)$, or on a different target than proton $\bar{p}N \to \gamma^\star\pi$. Finally, one may also consider associated J/ψ production with a pion $\bar{p}p \to \psi\ \pi^0$ or another meson $\bar{p}p \to \psi\ (\eta,\rho^0)$, which involve the *same* TDAs as with an off-shell photon or in backward electro-production. They will serve as very strong tests of the universality of the TDAs in different processes.

In the next section we present the LCWFs representation for all the eight TDAs within the MCM, and we also give some numerical predictions for all the TDAs in different kinematical regimes with the momentum part of the WF described by means of the parameterization of Ref. [63].
Some of the results reported here have already been presented in Ref. [229].

3.3.3 The $N \to \pi$ Transition Distribution Amplitudes

Kinematics and Definitions for the subprocess $\gamma^\star p \to p'\pi_0$

Working in the one-photon-exchange approximation in Ref. [207] it has been shown that the five-fold differential cross section for the process $ep \to e'p'\pi^0$ can be reduced to a two-fold one, in the center-of-mass (CM) frame of the outgoing pion-nucleon system, multiplied by a flux factor Γ:

$$\frac{d^5\sigma}{dE_{e'}d^2\Omega_e d^2\Omega_\pi^*} = \Gamma \frac{d^2\sigma}{d^2\Omega_\pi^*}, \tag{3.41}$$

with

$$\Gamma = \frac{\alpha_{em}}{2\pi}\frac{E_{e'}}{E_e}\frac{W^2 - M^2}{2MQ^2}\frac{1}{1-\epsilon}, \tag{3.42}$$

where E_e is the energy of the initial electron in the laboratory (LAB) frame, $E_{e'}$ the energy of the outgoing electron, W the invariant mass of the $p'\pi^0$ pair, ϵ the polarization parameter and, Ω_e and Ω_π^* the solid angles for the scattered electron in the LAB frame and for the pion in the $p'\pi^0$ CM frame, respectively.

The differential solid angle for the pion can be expressed as $d\Omega_\pi^* = d\varphi d\cos\theta_\pi^*$, where φ is the azimuthal angle between the leptonic and hadronic plane, while θ_π^* is defined as the polar angle between the photon and the pion in the CM frame of the proton-pion pair.

In the scaling regime, the amplitude for the subprocess $\gamma^\star p \to p'\pi_0$ in the backward kinematics, i.e. small momentum transfer $u = (p_\pi - p_1)^2$ or $\theta_\pi^* \simeq \pi$ involves the TDAs $T(x_i, \xi, \Delta^2)$, where with $x_i (i = 1, 2, 3)$ we denote the fractions of + momenta, whose supports are within [-1 + ξ, 1 + ξ], and with ξ the skewedness variable that parameterizes the change of longitudinal momentum of the incoming hadron in the proton $\to$ meson transition. The fields with positive momentum fraction, $x_i \geqslant 0$, describe creation of quarks, whereas those with negative momentum fraction, $x_i < 0$, the absorption of antiquarks. Moreover, momentum conservation implies (choosing $\xi > 0$)

$$\sum_i x_i = 2\xi. \tag{3.43}$$

The general matrix element describing the transition from a nucleon to a meson state reads

$$\langle \pi | \epsilon^{ijk} q_\alpha^{i'}(z_1 n)[z_1; z_0]_{i'i} q^{j'} j_\beta(z_2 n)[z_2; z_0]_{j'j} q_\gamma^{k'}(z_3 n)[z_3; z_0]_{k'k} | N \rangle. \tag{3.44}$$

The spinorial and Lorentz decomposition of the matrix element (3.44) follows the same line as in the case of the baryon distribution amplitudes (DAs) [49, 52] (see Cap. 2).

For the definition of the TDAs we parameterize the momenta of the particles involved in the subprocess $\gamma^\star p \to p'\pi_0$ as shown in Fig. (3.1). In such a

way, performing a Sudakov decomposition[§], the momenta read

$$
\begin{aligned}
p_1 &= (1+\xi)p + \frac{M^2}{1+\xi}n, \qquad (3.45)\\
q &\simeq -2\xi\left(1 - \frac{(\Delta_T^2+M^2)}{Q^2}\right)p + \frac{Q^2}{2\xi\left(1-\frac{(\Delta_T^2+M^2)}{Q^2}\right)}n,\\
p_\pi &= (1-\xi)p + \frac{m_\pi^2+\Delta_T^2}{1-\xi}n + \Delta_T,\\
p_2 &\simeq 2\xi\frac{(\Delta_T^2+M^2)}{Q^2}p + \left[\frac{Q^2}{2\xi\left(1-\frac{(\Delta_T^2+M^2)}{Q^2}\right)} - \frac{m_\pi^2+\Delta_T^2}{1-\xi} + \frac{M^2}{1+\xi}\right]n - \Delta_T,\\
\Delta &= p_\pi - p_1 = -2\xi p + \left[\frac{m_\pi^2+\Delta_T^2}{1-\xi} - \frac{M^2}{1+\xi}\right]n + \Delta_T,
\end{aligned}
$$

where we have defined $\xi = -\Delta^+/2P^+$ with $P = \frac{1}{2}(p_1+p_\pi)$ and we have kept the first-order corrections in the masses and Δ_T^2. We also have $u = \Delta^2 = -2\xi\left[\frac{m_\pi^2+\Delta_T^2}{1-\xi} - \frac{M^2}{1+\xi}\right] - \Delta_T^2$ or, equivalently, $\Delta_T^2 = -\frac{1-\xi}{1+\xi}\left[u + 2\xi\left(\frac{m_\pi^2}{1-\xi} - \frac{M^2}{1+\xi}\right)\right]$. As in Ref. [207] we rewrite the general matrix element describing a transition from a nucleon to a pion (3.44) introducing eight TDAs: two vectorial $V_{1,2}^{p\pi^0}(x_i,\xi,\Delta^2)$, two axial $A_{1,2}^{p\pi^0}(x_i,\xi,\Delta^2)$ and four tensorial $T_{1,\dots,4}^{p\pi^0}(x_i,\xi,\Delta^2)$,

$$
\begin{aligned}
&4\mathcal{F}\left(\langle\pi^0(p_\pi)|\epsilon^{ijk}u_\alpha^i(z_1n)u_\beta^j(z_2n)d_\gamma^k(z_3n)|P(p_1,s_1)\rangle\right) =\\
&i\frac{f_N}{f_\pi}\Big[V_1^{p\pi^0}(\not{p}C)_{\alpha\beta}(N^+)_\gamma + A_1^{p\pi^0}(\not{p}\gamma^5C)_{\alpha\beta}(\gamma^5N^+)_\gamma\\
&+T_1^{p\pi^0}(\sigma_{p\mu}C)_{\alpha\beta}(\gamma^\mu N^+)_\gamma + M^{-1}V_2^{p\pi^0}(\not{p}C)_{\alpha\beta}(\not{\Delta}_T N^+)_\gamma\\
&+M^{-1}A_2^{p\pi^0}(\not{p}\gamma^5C)_{\alpha\beta}(\gamma^5\not{\Delta}_T N^+)_\gamma + M^{-1}T_2^{p\pi^0}(\sigma_{p\Delta_T}C)_{\alpha\beta}(N^+)_\gamma\\
&+M^{-1}T_3^{p\pi^0}(\sigma_{p\mu}C)_{\alpha\beta}(\sigma^{\mu\Delta_T}N^+)_\gamma + M^{-2}T_4^{p\pi^0}(\sigma_{p\Delta_T}C)_{\alpha\beta}(\not{\Delta}_T N^+)_\gamma\Big] \qquad (3.46)
\end{aligned}
$$

where f_N is the value of the nucleon wave function at the origin, estimated through QCD sum rules to be of the order 5.3×10^{-3} GeV^2 [53], and we have used the definition of $\sigma^{\mu\nu} = 1/2[\gamma^\mu,\gamma^\nu]$.

In a completely analogous way to the DA case we define with the symbol $D_{\alpha\beta,\gamma}^{\uparrow/\downarrow}$ the left-hand side of Eq. (3.46), where, again, α,β and γ are Dirac indexes and $\uparrow$ / $\downarrow$ indicates the helicity value of the incoming nucleon. In such

[§]We choose the auxiliary null vectors p^μ and n^μ in such a way that $2p\cdot n = 1$. The cartesian components are given by

$$
p = \frac{P^+}{\sqrt{2}}(1,0,0,1), \qquad\qquad n = \frac{1}{2\sqrt{2}P^+}(1,0,0,-1).
$$

a way we can express the eight TDAs in terms of linear combinations of these matrix elements (see Appendix D) as

$$V_1^{p\pi_0} = -i\frac{1}{2^{\frac{1}{4}}\sqrt{1+\xi}(P^+)^{\frac{3}{2}}}\frac{f_\pi}{f_N}\Big(D^{\uparrow}_{12,1}+D^{\uparrow}_{21,1}\Big), \tag{3.47}$$

$$A_1^{p\pi_0} = i\frac{1}{2^{\frac{1}{4}}\sqrt{1+\xi}(P^+)^{\frac{3}{2}}}\frac{f_\pi}{f_N}\Big(D^{\uparrow}_{12,1}-D^{\uparrow}_{21,1}\Big), \tag{3.48}$$

$$T_1^{p\pi_0} = i\frac{1}{2^{\frac{1}{4}}\sqrt{1+\xi}(P^+)^{\frac{3}{2}}}\frac{f_\pi}{f_N}\left[D^{\uparrow}_{11,2}+\frac{(\Delta_{T1}-i\Delta_{T2})}{(\Delta_{T1}+i\Delta_{T2})}D^{\uparrow}_{22,2}\right], \tag{3.49}$$

$$V_2^{p\pi_0} = -i\frac{M}{(\Delta_{T1}+i\Delta_{T2})}\frac{1}{2^{\frac{1}{4}}\sqrt{1+\xi}(P^+)^{\frac{3}{2}}}\frac{f_\pi}{f_N}\Big(D^{\uparrow}_{12,2}+D^{\uparrow}_{21,2}\Big), \tag{3.50}$$

$$A_2^{p\pi_0} = -i\frac{M}{(\Delta_{T1}+i\Delta_{T2})}\frac{1}{2^{\frac{1}{4}}\sqrt{1+\xi}(P^+)^{\frac{3}{2}}}\frac{f_\pi}{f_N}\Big(D^{\uparrow}_{12,2}-D^{\uparrow}_{21,2}\Big), \tag{3.51}$$

$$T_2^{p\pi_0} = i\frac{M}{\Delta_T^2}\frac{1}{2^{\frac{1}{4}}\sqrt{1+\xi}(P^+)^{\frac{3}{2}}}\frac{f_\pi}{f_N}\Big[(\Delta_{T1}-i\Delta_{T2})D^{\uparrow}_{22,1} -(\Delta_{T1}+i\Delta_{T2})D^{\uparrow}_{11,1}\Big], \tag{3.52}$$

$$T_3^{p\pi_0} = i\frac{M}{\Delta_T^2}\frac{1}{2^{\frac{1}{4}}\sqrt{1+\xi}(P^+)^{\frac{3}{2}}}\frac{f_\pi}{f_N}\Big[(\Delta_{T1}-i\Delta_{T2})D^{\uparrow}_{22,1} +(\Delta_{T1}+i\Delta_{T2})D^{\uparrow}_{11,1}\Big], \tag{3.53}$$

$$T_4^{p\pi_0} = i\frac{2M^2}{(\Delta_{T1}+i\Delta_{T2})^2}\frac{1}{2^{\frac{1}{4}}\sqrt{1+\xi}(P^+)^{\frac{3}{2}}}\frac{f_\pi}{f_N}D^{\uparrow}_{22,2}. \tag{3.54}$$

Thus to calculate the leading twist TDAs we must give an expression for all the $D^{\uparrow/\downarrow}_{\alpha\beta,\gamma}$ matrix elements involved in the previous equations.

3.3.4 The Overlap Representation for the Transition Distribution Amplitudes

In this section we give the general overlap representation for the nucleon to pion TDAs. The calculation starts in a similar way to the DAs, namely substituting the expression for the free quark field (1.52) in the definition (3.44),

$$\begin{aligned}
&4\mathcal{F}\Big(\langle\pi^0(p_\pi)|\epsilon^{ijk}u^i_\alpha(z_1n)u^j_\beta(z_2n)d^k_\gamma(z_3n)|P(p_1,s_1)\rangle\Big)\\
&= 4(p\cdot n)^3\int_{-\infty}^{+\infty}\prod_j\frac{\mathrm{d}z_j}{(2\pi)^3}e^{ix_kz_k(p\cdot n)}\langle\pi^0(p_\pi)|\epsilon^{ijk}u^i_\alpha(z_1n)u^j_\beta(z_2n)d^k_\gamma(z_3n)|P(p_1,s_1)\rangle\\
&= \frac{4}{8}\int_{-\infty}^{+\infty}\prod_j\frac{\mathrm{d}z_j}{(2\pi)^3}e^{\frac{i}{2}x_kz_k}\langle\pi^0(p_\pi)|\epsilon^{ijk}u^i_\alpha(z_1n)u^j_\beta(z_2n)d^k_\gamma(z_3n)|P(p_1,s_1)\rangle
\end{aligned}$$

$$
\begin{aligned}
= \;& \langle\pi^0(p_\pi)|\frac{\epsilon^{ijk}}{2}\int_{-\infty}^{+\infty}\frac{\prod_j \mathrm{d}z_j}{(2\pi)^3}e^{\frac{i}{2}x_k z_k}\int\frac{\mathrm{d}k_1^+\mathrm{d}^2\mathbf{k}_{1\perp}}{16\pi^3 k_1^+}\int\frac{\mathrm{d}k_2^+\mathrm{d}^2\mathbf{k}_{2\perp}}{16\pi^3 k_2^+}\int\frac{\mathrm{d}k_3^+\mathrm{d}^2\mathbf{k}_{3\perp}}{16\pi^3 k_3^+}\\
& \times\sum_{\lambda_1,\lambda_2,\lambda_3}\Big\{b_1^i(\tilde{k}_1,\lambda_1)u_{+\alpha}(\tilde{k}_1,\lambda_1)\exp[-ik_1^+z_1n^- + i\mathbf{k}_{1\perp}\cdot\mathbf{n}_\perp]\\
& + d_1^{\dagger i}(\tilde{k}_1,\lambda_1)v_{+\alpha}(\tilde{k}_1,\lambda_1)\exp[ik_1^+z_1n^- - i\mathbf{k}_{1\perp}\cdot\mathbf{n}_\perp]\Big\}\\
& \times\Big\{b_2^j(\tilde{k}_2,\lambda_2)u_{+\beta}(\tilde{k}_2,\lambda_2)\exp[-ik_2^+z_2n^- + i\mathbf{k}_{2\perp}\cdot\mathbf{n}_\perp]\\
& \; + d_2^{\dagger j}(\tilde{k}_2,\lambda_2)v_{+\beta}(\tilde{k}_2,\lambda_2)\exp[ik_2^+z_2n^- - i\mathbf{k}_{2\perp}\cdot\mathbf{n}_\perp]\Big\}\\
& \times\Big\{b_3^k(\tilde{k}_3,\lambda_3)u_{+\gamma}(\tilde{k}_3,\lambda_3)\exp[-ik_3^+z_3n^- + i\mathbf{k}_{3\perp}\cdot\mathbf{n}_\perp]\\
& \; + d_3^{\dagger k}(\tilde{k}_3,\lambda_3)v_{+\gamma}(\tilde{k}_3,\lambda_3)\exp[ik_3^+z_3n^- - i\mathbf{k}_{3\perp}\cdot\mathbf{n}_\perp]\Big\}\\
& \times\Theta(k_1^+)\Theta(k_2^+)\Theta(k_3^+)|P(p_1,s_1)\rangle\\
= \;& \langle\pi^0(p_\pi)|\frac{\epsilon^{ijk}}{2}\int_{-\infty}^{+\infty}\frac{\prod_j \mathrm{d}z_j}{(2\pi)^3}e^{\frac{i}{2}\Sigma_k x_k z_k}\int\frac{\mathrm{d}k_1^+\mathrm{d}^2\mathbf{k}_{1\perp}}{16\pi^3 k_1^+}\int\frac{\mathrm{d}k_2^+\mathrm{d}^2\mathbf{k}_{2\perp}}{16\pi^3 k_2^+}\int\frac{\mathrm{d}k_3^+\mathrm{d}^2\mathbf{k}_{3\perp}}{16\pi^3 k_3^+}\\
& \times\sum_{\lambda_1,\lambda_2,\lambda_3}\Big\{b_1^i(\tilde{k}_1,\lambda_1)b_2^j(\tilde{k}_2,\lambda_2)b_3^k(\tilde{k}_3,\lambda_3)u_{+\alpha}(\tilde{k}_1,\lambda_1)u_{+\beta}(\tilde{k}_2,\lambda_2)u_{+\gamma}(\tilde{k}_3,\lambda_3)\\
& \times\exp[-i(k_1^+z_1n^- + k_2^+z_2n^- + k_3^+z_3n^-)]\\
& \; + b_1^i(\tilde{k}_1,\lambda_1)b_2^j(\tilde{k}_2,\lambda_2)d_3^{\dagger k}(\tilde{k}_3,\lambda_3)u_{+\alpha}(\tilde{k}_1,\lambda_1)u_{+\beta}(\tilde{k}_2,\lambda_2)v_{+\gamma}(\tilde{k}_3,\lambda_3)\\
& \times\exp[-i(k_1^+z_1n^- + k_2^+z_2n^- - k_3^+z_3n^-)]\\
& \; + b_1^i(\tilde{k}_1,\lambda_1)d_2^{\dagger j}(\tilde{k}_2,\lambda_2)b_3^k(\tilde{k}_3,\lambda_3)u_{+\alpha}(\tilde{k}_1,\lambda_1)v_{+\beta}(\tilde{k}_2,\lambda_2)u_{+\gamma}(\tilde{k}_3,\lambda_3)\\
& \times\exp[-i(k_1^+z_1n^- - k_2^+z_2n^- + k_3^+z_3n^-)]\\
& \; + d_1^{\dagger i}(\tilde{k}_1,\lambda_1)b_2^j(\tilde{k}_2,\lambda_2)b_3^k(\tilde{k}_3,\lambda_3)v_{+\alpha}(\tilde{k}_1,\lambda_1)u_{+\beta}(\tilde{k}_2,\lambda_2)u_{+\gamma}(\tilde{k}_3,\lambda_3)\\
& \times\exp[-i(-k_1^+z_1n^- + k_2^+z_2n^- + k_3^+z_3n^-)]\\
& \; + b_1^i(\tilde{k}_1,\lambda_1)d_2^{\dagger j}(\tilde{k}_2,\lambda_2)d_3^{\dagger k}(\tilde{k}_3,\lambda_3)u_{+\alpha}(\tilde{k}_1,\lambda_1)v_{+\beta}(\tilde{k}_2,\lambda_2)v_{+\gamma}(\tilde{k}_3,\lambda_3)\\
& \times\exp[-i(k_1^+z_1n^- - k_2^+z_2n^- - k_3^+z_3n^-)]\\
& \; + d_1^{\dagger i}(\tilde{k}_1,\lambda_1)b_2^j(\tilde{k}_2,\lambda_2)d_3^{\dagger k}(\tilde{k}_3,\lambda_3)v_{+\alpha}(\tilde{k}_1,\lambda_1)u_{+\beta}(\tilde{k}_2,\lambda_2)v_{+\gamma}(\tilde{k}_3,\lambda_3)\\
& \times\exp[-i(-k_1^+z_1n^- + k_2^+z_2n^- - k_3^+z_3n^-)]\\
& \; + d_1^{\dagger i}(\tilde{k}_1,\lambda_1)d_2^{\dagger j}(\tilde{k}_2,\lambda_2)b_3^k(\tilde{k}_3,\lambda_3)v_{+\alpha}(\tilde{k}_1,\lambda_1)v_{+\beta}(\tilde{k}_2,\lambda_2)u_{+\gamma}(\tilde{k}_3,\lambda_3)\\
& \times\exp[-i(-k_1^+z_1n^- - k_2^+z_2n^- + k_3^+z_3n^-)]\\
& \; + d_1^{\dagger i}(\tilde{k}_1,\lambda_1)d_2^{\dagger j}(\tilde{k}_2,\lambda_2)d_3^{\dagger k}(\tilde{k}_3,\lambda_3)v_{+\alpha}(\tilde{k}_1,\lambda_1)v_{+\beta}(\tilde{k}_2,\lambda_2)v_{+\gamma}(\tilde{k}_3,\lambda_3)\\
& \times\exp[i(k_1^+z_1n^- + k_2^+z_2n^- + k_3^+z_3n^-)]\Big\}\\
& \times\Theta(k_1^+)\Theta(k_2^+)\Theta(k_3^+)|P(p_1,s_1)\rangle. \qquad (3.55)
\end{aligned}
$$

Among all the operatorial combinations in braces in the previous formula we keep the one involving three annihilators of the "good" components of the quark fields.

Then, integrating over the z_i variables we get

$$\langle\pi^0(p_\pi)|4(P^+)^3\epsilon^{ijk}\int\frac{\mathrm{d}k_1^+\mathrm{d}^2\mathbf{k}_{1\perp}}{16\pi^3k_1^+}\int\frac{\mathrm{d}k_2^+\mathrm{d}^2\mathbf{k}_{2\perp}}{16\pi^3k_2^+}\int\frac{\mathrm{d}k_3^+\mathrm{d}^2\mathbf{k}_{3\perp}}{16\pi^3k_3^+}\Theta(k_1^+)\Theta(k_2^+)\Theta(k_3^+)$$
$$\times\sum_{\lambda_1,\lambda_2,\lambda_3}b_1^i(\tilde{k}_1,\lambda_1)b_2^j(\tilde{k}_2,\lambda_2)b_3^k(\tilde{k}_3,\lambda_3)u_{+\alpha}(k_1^+,\lambda_1)u_{+\beta}(k_2^+,\lambda_2)u_{+\gamma}(k_3^+,\lambda_3)$$
$$\times\delta\Big(x_1P^+-k_1^+\Big)\delta\Big(x_2P^+-k_2^+\Big)\delta\Big(x_3P^+-k_3^+\Big)|P(p_1,s_1)\rangle. \tag{3.56}$$

Now, we have to insert in Eq. (3.56) the expression of the nucleon state. In the calculation of the TDAs only the pion-nucleon component of the proton wave function contributes because the contribution from the bare nucleon component vanish after the matching with the pion state. Thus, in front-form Hamiltonian dynamics the nucleon state reads (see Eq. (3.25))

$$\begin{aligned}|N\pi(p_1,s_1)\rangle \;=\; &\int\mathrm{d}y\mathrm{d}^2\mathbf{k}_\perp\int_0^y\prod_{i=1'}^{3'}\frac{\mathrm{d}\xi_i}{\sqrt{\xi_i}}\int_0^{(1-y)}\prod_{i=4'}^{5'}\frac{\mathrm{d}\xi_i}{\sqrt{\xi_i}}\int\frac{\prod_{i=1'}^{5'}\mathrm{d}^2\mathbf{k}'_{i\perp}}{[2(2\pi)^3]^4}\\
&\times\delta\Big(y-\sum_{i=1'}^{3'}\xi_i\Big)\delta^{(2)}\Big(\mathbf{k}_\perp-\sum_{i=1'}^{3'}\mathbf{k}'_{i\perp}\Big)\delta\Big(1-\sum_{i=1'}^{5'}\xi_i\Big)\delta^{(2)}\Big(\sum_{i=1'}^{5'}\mathbf{k}'_{i\perp}\Big)\\
&\times\sum_{\lambda_i,\tau_i,c_i}\sum_{\lambda'}\phi^{\lambda(N,N\pi)}_{\lambda'0}(y,\mathbf{k}_\perp)\sqrt{y(1-y)}\\
&\times\tilde{\Psi}^{N,[f]}_{\lambda'}(y,\mathbf{k}_\perp;\{\xi_i,\mathbf{k}'_{i\perp};\lambda_i,\tau_i,c_i\}_{i=1',\cdots,3'})\\
&\times\tilde{\Psi}^{\pi,[f]}_{0}(1-y,-\mathbf{k}_\perp;\{\xi_i,\mathbf{k}'_{i\perp};\lambda_i,\tau_i\}_{i=4',5'})\\
&\times\prod_{i=1'}^{5'}|\xi_ip_1^+,\mathbf{k}'_{i\perp}+\xi_i\mathbf{p}_{1\perp},\lambda_i,\tau_i,c_i;q\rangle,\end{aligned}\tag{3.57}$$

where λ_i,τ_i and c_i are the spin, isospin and colour variables of the quarks, respectively, and the wave functions $\tilde{\Psi}^{N,[f]}_{\lambda'}$ and $\tilde{\Psi}^{\pi,[f]}_{\lambda''}$ incorporate the Jacobian $\mathcal{J}$ of the transformation from the intrinsic variables with respect to the hadron rest-frame ($\{\zeta_i,\kappa_{i\perp}\}$) to the intrinsic variables with respect to the nucleon rest frame ($\{\xi_i,\mathbf{k}'_{i\perp}\}$), i.e.

$$\begin{aligned}\tilde{\Psi}^{N,[f]}_{\lambda'}(\{\xi_i,\mathbf{k}'_{i\perp};\lambda_i,\tau_i\}_{i=1',2',3'}) &= \sqrt{\mathcal{J}(\xi_{1'},\xi_{2'},\xi_{3'})}\tilde{\Psi}^{N,[f]}_{\lambda'}(\{\zeta_i,\kappa_{i\perp};\lambda_i,\tau_i\}_{i=1',2',3'})\\
&= \frac{1}{y^{\frac{3}{2}}}\tilde{\Psi}^{N,[f]}_{\lambda'}(\{\zeta_i,\kappa_{i\perp};\lambda_i,\tau_i\}_{i=1',2',3'}),\end{aligned}\tag{3.58}$$

$$\begin{aligned}\tilde{\Psi}^{\pi,[f]}_{\lambda''}(\{\xi_i,\mathbf{k}'_{i\perp};\lambda_i,\tau_i\}_{i=4',5'}) &= \sqrt{\mathcal{J}(\xi_{4'},\xi_{5'})}\tilde{\Psi}^{\pi,[f]}_{\lambda''}(\{\zeta_i,\kappa_{i\perp};\lambda_i,\tau_i\}_{i=4',5'})\\
&= \frac{1}{(1-y)}\tilde{\Psi}^{\pi,[f]}_{\lambda''}(\{\zeta_i,\kappa_{i\perp};\lambda_i,\tau_i\}_{i=4',5'}).\end{aligned}\tag{3.59}$$

The relations between the variables ($\{\zeta_i,\kappa_{i\perp}\}$) and ($\{\xi_i,\mathbf{k}'_{i\perp}\}$), is given by:

for $i = 1', 2', 3'$:

$$\zeta_i = \frac{\xi_i}{y}, \qquad \mathbf{k}'_{i\perp} = \kappa_{i\perp} + \zeta_i \, \mathbf{k}_\perp; \tag{3.60}$$

for $i = 4', 5'$:

$$\zeta_i = \frac{\xi_i}{(1-y)}, \qquad \mathbf{k}'_{i\perp} = \kappa_{i\perp} - \zeta_i \, \mathbf{k}_\perp. \tag{3.61}$$

Inserting the nucleon state representation Eq. (3.56) becomes

$$\begin{aligned}
&\langle \pi^0(p_\pi)|4(P^+)^3\epsilon^{ijk}\int \mathrm{d}y \mathrm{d}^2\mathbf{k}_\perp \int_0^y \prod_{i=1'}^{3'} \frac{\mathrm{d}\xi_i}{\sqrt{\xi_i}} \int_0^{(1-y)} \prod_{i=4'}^{5'} \frac{\mathrm{d}\xi_i}{\sqrt{\xi_i}} \int \frac{\prod_{i=1'}^{5'} \mathrm{d}^2\mathbf{k}'_{i\perp}}{[2(2\pi)^3]^4} \\
&\times \int \frac{\mathrm{d}k_1^+ \mathrm{d}^2\mathbf{k}_{1\perp}}{16\pi^3 k_1^+} \int \frac{\mathrm{d}k_2^+ \mathrm{d}^2\mathbf{k}_{2\perp}}{16\pi^3 k_2^+} \int \frac{\mathrm{d}k_3^+ \mathrm{d}^2\mathbf{k}_{3\perp}}{16\pi^3 k_3^+} \Theta(k_1^+)\Theta(k_2^+)\Theta(k_3^+) \frac{1}{y\sqrt{(1-y)}} \\
&\times \delta\Big(y - \sum_{i=1'}^{3'} \xi_i\Big) \delta^{(2)}\Big(\mathbf{k}_\perp - \sum_{i=1'}^{3'} \mathbf{k}'_{i\perp}\Big) \delta\Big(1 - \sum_{i=1'}^{5'} \xi_i\Big) \delta^{(2)}\Big(\sum_{i=1'}^{5'} \mathbf{k}'_{i\perp}\Big) \\
&\times \sum_{\lambda_1,\lambda_2,\lambda_3} b_1^i(\tilde{k}_1,\lambda_1) b_2^j(\tilde{k}_2,\lambda_2) b_3^k(\tilde{k}_3,\lambda_3) u_{+\alpha}(k_1^+,\lambda_1) u_{+\beta}(k_2^+,\lambda_2) u_{+\gamma}(k_3^+,\lambda_3) \\
&\times \prod_{j=1}^{3} \delta\Big(x_j P^+ - k_j^+\Big) \sum_{\lambda_i,\tau_i,c_i} \sum_{\lambda'} \phi_{\lambda' 0}^{\lambda(N,N\pi)}(y,\mathbf{k}_\perp) \tilde{\Psi}_{\lambda'}^{N,[f]}(\{\zeta_i,\kappa_{i\perp};\lambda_i,\tau_i,c_i\}) \\
&\times \tilde{\Psi}_0^{\pi,[f]}(\{\zeta_i,\kappa_{i\perp};\lambda_i,\tau_i,c_i\}) \prod_{i=1'}^{5'} |\xi_i p_1^+, \mathbf{k}'_{i\perp}, \lambda_i, \tau_i, c_i; q\rangle,
\end{aligned} \tag{3.62}$$

where recalling Eqs. (3.45) we set $\mathbf{p}_{1\perp} = 0$. To proceed in our calculations, we have to clarify the partonic content of the proton state in terms of single-parton operators acting on the perturbative vacuum $|0\rangle$, i.e.

$$\begin{aligned}
&\prod_{i=1'}^{5'} |\xi_i p_1^+, \mathbf{k}'_{i\perp} + \xi_i \mathbf{p}_{1\perp}, \lambda_i, \tau_i, c_i; q\rangle = \\
&\frac{1}{\sqrt{3!}} \Big[b^{\dagger l}(\xi_{1'} p_1^+, \mathbf{k}'_{1'\perp}, \lambda_{1'}, \tau_{1'}) b^{\dagger m}(\xi_{2'} p_1^+, \mathbf{k}'_{2'\perp}, \lambda_{2'}, \tau_{2'}) b^{\dagger n}(\xi_{3'} p_1^+, \mathbf{k}'_{3'\perp}, \lambda_{3'}, \tau_{3'}) \Big]_N \\
&\times \Big[b^{\dagger r}(\xi_{4'} p_1^+, \mathbf{k}'_{4'\perp}, \lambda_{4'}, \tau_{4'}) d^{\dagger s}(\xi_{5'} p_1^+, \mathbf{k}'_{5'\perp}, \lambda_{5'} = -\lambda_{4'}, \tau_{5'} = -\tau_{4'}) \Big]_{\pi^0} |0\rangle,
\end{aligned} \tag{3.63}$$

with l, m, n, r and s colour indexes. Through this replacement Eq. (3.62) turns

out to be

$$\begin{aligned}
&\langle\pi^0(p_\pi)|4(P^+)^3\frac{\epsilon^{ijk}}{\sqrt{6}}\int \mathrm{d}y\mathrm{d}^2\mathbf{k}_\perp\int_0^y\prod_{i=1'}^{3'}\frac{\mathrm{d}\xi_i}{\sqrt{\xi_i}}\int_0^{(1-y)}\prod_{i=4'}^{5'}\frac{\mathrm{d}\xi_i}{\sqrt{\xi_i}}\int\frac{\prod_{i=1'}^{5'}\mathrm{d}^2\mathbf{k}'_{i\perp}}{[2(2\pi)^3]^4}\\
&\times\int\frac{\mathrm{d}k_1^+\mathrm{d}^2\mathbf{k}_{1\perp}}{16\pi^3k_1^+}\int\frac{\mathrm{d}k_2^+\mathrm{d}^2\mathbf{k}_{2\perp}}{16\pi^3k_2^+}\int\frac{\mathrm{d}k_3^+\mathrm{d}^2\mathbf{k}_{3\perp}}{16\pi^3k_3^+}\Theta(k_1^+)\Theta(k_2^+)\Theta(k_3^+)\frac{1}{y\sqrt{(1-y)}}\\
&\times\delta\Big(y-\sum_{i=1'}^{3'}\xi_i\Big)\delta^{(2)}\Big(\mathbf{k}_\perp-\sum_{i=1'}^{3'}\mathbf{k}'_{i\perp}\Big)\delta\Big(1-\sum_{i=1'}^{5'}\xi_i\Big)\delta^{(2)}\Big(\sum_{i=1'}^{5'}\mathbf{k}'_{i\perp}\Big)\\
&\times\sum_{\lambda_1,\lambda_2,\lambda_3}b_1^i(\tilde{k}_1,\lambda_1)b_2^j(\tilde{k}_2,\lambda_2)b_3^k(\tilde{k}_3,\lambda_3)u_{+\alpha}(k_1^+,\lambda_1)u_{+\beta}(k_2^+,\lambda_2)u_{+\gamma}(k_3^+,\lambda_3)\\
&\times\prod_{j=1}^{3}\delta\Big(x_jP^+-k_j^+\Big)\sum_{rs}\sum_{lmn}\sum_{\lambda_i,\tau_i,\lambda'}\phi_{\lambda'0}^{\lambda(N,N\pi)}(y,\mathbf{k}_\perp)\tilde{\Psi}_{\lambda'}^{N,[f]}(\{\zeta_i,\kappa_{i\perp};\lambda_i,\tau_i\})\frac{\epsilon_{lmn}}{\sqrt{6}}\frac{\delta_{rs}}{\sqrt{3}}\\
&\times\tilde{\Psi}_0^{\pi,[f]}(\{\zeta_i,\kappa_{i\perp};\lambda_i,\tau_i\})\Big[b^{\dagger r}(\xi_{4'}p_1^+,\mathbf{k}'_{4'\perp},\lambda_{4'},\tau_{4'})d^{\dagger s}(\xi_{5'}p_1^+,\mathbf{k}'_{5'\perp},-\lambda_{4'},-\tau_{4'})\Big]_{\pi^0}\\
&\times\Big[b^{\dagger l}(\xi_{1'}p_1^+,\mathbf{k}'_{1'\perp},\lambda_{1'},\tau_{1'})b^{\dagger m}(\xi_{2'}p_1^+,\mathbf{k}'_{2'\perp},\lambda_{2'},\tau_{2'})b^{\dagger n}(\xi_{3'}p_1^+,\mathbf{k}'_{3'\perp},\lambda_{3'},\tau_{3'})\Big]_N|0\rangle,
\end{aligned}\tag{3.64}$$

where we have made explicit the colour component of the baryon and meson WFs. Then, making use of the relations in Eq. (1.53), and introducing an obvious shorthand notation[¶] we can rewrite the previous equation in the following way,

$$\begin{aligned}
&\langle\pi^0(p_\pi)|\frac{4}{\sqrt{3!}}(P^+)^3\epsilon^{ijk}\int \mathrm{d}y\mathrm{d}^2\mathbf{k}_\perp\int_0^y\prod_{i=1'}^{3'}\frac{\mathrm{d}\xi_i}{\sqrt{\xi_i}}\int_0^{(1-y)}\prod_{i=4'}^{5'}\frac{\mathrm{d}\xi_i}{\sqrt{\xi_i}}\int\frac{\prod_{i=1'}^{5'}\mathrm{d}^2\mathbf{k}'_{i\perp}}{[2(2\pi)^3]^4}\\
&\times\int\prod_{j=1}^{3}\frac{\mathrm{d}k_j^+\mathrm{d}^2\mathbf{k}_{j\perp}}{16\pi^3k_j^+}\Theta(k_1^+)\Theta(k_2^+)\Theta(k_3^+)\frac{1}{y\sqrt{(1-y)}}\prod_{j=1}^{3}\delta\Big(x_jP^+-k_j^+\Big)\\
&\times\delta\Big(y-\sum_{i=1'}^{3'}\xi_i\Big)\delta^{(2)}\Big(\mathbf{k}_\perp-\sum_{i=1'}^{3'}\mathbf{k}'_{i\perp}\Big)\delta\Big(1-\sum_{i=1'}^{5'}\xi_i\Big)\delta^{(2)}\Big(\sum_{i=1'}^{5'}\mathbf{k}'_{i\perp}\Big)\\
&\times\sum_{\lambda_{1,2,3}}\sum_{\lambda_i,\tau_i,c_i}u_{+\alpha}(k_1^+,\lambda_1)u_{+\beta}(k_2^+,\lambda_2)u_{+\gamma}(k_3^+,\lambda_3)\sum_{\lambda'}\phi_{\lambda'0}^{\lambda(N,N\pi)}(y,\mathbf{k}_\perp)\\
&\times\frac{\epsilon_{lmn}}{\sqrt{6}}\frac{\delta_{rs}}{\sqrt{3}}\tilde{\Psi}_{\lambda'}^{N,[f]}(\{\zeta_i,\kappa_{i\perp};\lambda_i,\tau_i,c_i\}_{i=1',\cdots,3'})\tilde{\Psi}_0^{\pi,[f]}(\{\zeta_i,\kappa_{i\perp};\lambda_i,\tau_i,c_i\}_{i=4',5'})
\end{aligned}$$

[¶]For instance,

$$\{b_1^i,b_{1'}^{\dagger l}\}=\{b^i(\tilde{k}_1,\lambda_1),b^{\dagger l}(\xi_{1'}p_1^+,\mathbf{k}'_{1'\perp},\lambda_{1'},\tau_{1'})\}.$$

$$
\begin{aligned}
&\times\Big\{\Big[\{b_1^i,b_{3'}^{\dagger n}\}\{b_2^j,b_{2'}^{\dagger m}\}\{b_3^k,b_{1'}^{\dagger l}\}-\{b_1^i,b_{2'}^{\dagger m}\}\{b_2^j,b_{3'}^{\dagger n}\}\{b_3^k,b_{1'}^{\dagger l}\}\\
&\quad-\{b_1^i,b_{3'}^{\dagger n}\}\{b_2^j,b_{1'}^{\dagger l}\}\{b_3^k,b_{2'}^{\dagger m}\}+\{b_1^i,b_{1'}^{\dagger l}\}\{b_2^j,b_{3'}^{\dagger n}\}\{b_3^k,b_{2'}^{\dagger m}\}\\
&\quad+\{b_1^i,b_{2'}^{\dagger m}\}\{b_2^j,b_{1'}^{\dagger l}\}\{b_3^k,b_{3'}^{\dagger n}\}-\{b_1^i,b_{1'}^{\dagger l}\}\{b_2^j,b_{2'}^{\dagger m}\}\{b_3^k,b_{3'}^{\dagger n}\}\Big]b_{4'}^{\dagger r}d_{5'}^{\dagger s}\\
&-\Big[\{b_1^i,b_{4'}^{\dagger r}\}\{b_2^j,b_{2'}^{\dagger m}\}\{b_3^k,b_{1'}^{\dagger l}\}-\{b_1^i,b_{2'}^{\dagger m}\}\{b_2^j,b_{4'}^{\dagger r}\}\{b_3^k,b_{1'}^{\dagger l}\}\\
&\quad-\{b_1^i,b_{4'}^{\dagger r}\}\{b_2^j,b_{1'}^{\dagger l}\}\{b_3^k,b_{2'}^{\dagger m}\}+\{b_1^i,b_{1'}^{\dagger l}\}\{b_2^j,b_{4'}^{\dagger r}\}\{b_3^k,b_{2'}^{\dagger m}\}\\
&\quad+\{b_1^i,b_{2'}^{\dagger m}\}\{b_2^j,b_{1'}^{\dagger l}\}\{b_3^k,b_{4'}^{\dagger r}\}-\{b_1^i,b_{1'}^{\dagger l}\}\{b_2^j,b_{2'}^{\dagger m}\}\{b_3^k,b_{4'}^{\dagger r}\}\Big]b_{3'}^{\dagger n}d_{5'}^{\dagger s}\\
&+\Big[\{b_1^i,b_{4'}^{\dagger r}\}\{b_2^j,b_{3'}^{\dagger n}\}\{b_3^k,b_{1'}^{\dagger l}\}-\{b_3^k,b_{3'}^{\dagger n}\}\{b_2^j,b_{1'}^{\dagger l}\}\{b_1^i,b_{4'}^{\dagger r}\}\\
&\quad-\{b_3^k,b_{1'}^{\dagger l}\}\{b_2^j,b_{4'}^{\dagger r}\}\{b_1^i,b_{3'}^{\dagger n}\}+\{b_1^i,b_{3'}^{\dagger n}\}\{b_2^j,b_{1'}^{\dagger l}\}\{b_3^k,b_{4'}^{\dagger r}\}\\
&\quad+\{b_1^i,b_{1'}^{\dagger l}\}\{b_2^j,b_{4'}^{\dagger r}\}\{b_3^k,b_{3'}^{\dagger n}\}-\{b_1^i,b_{1'}^{\dagger l}\}\{b_2^j,b_{3'}^{\dagger n}\}\{b_3^k,b_{4'}^{\dagger r}\}\Big]b_{2'}^{\dagger m}d_{5'}^{\dagger s}\\
&+\Big[\{b_1^i,b_{3'}^{\dagger n}\}\{b_2^j,b_{4'}^{\dagger r}\}\{b_3^k,b_{2'}^{\dagger m}\}-\{b_3^k,b_{2'}^{\dagger m}\}\{b_2^j,b_{3'}^{\dagger n}\}\{b_1^i,b_{4'}^{\dagger r}\}\\
&\quad+\{b_3^k,b_{3'}^{\dagger n}\}\{b_2^j,b_{2'}^{\dagger m}\}\{b_1^i,b_{4'}^{\dagger r}\}-\{b_1^i,b_{2'}^{\dagger m}\}\{b_2^j,b_{4'}^{\dagger r}\}\{b_3^k,b_{3'}^{\dagger n}\}\\
&\quad-\{b_1^i,b_{3'}^{\dagger n}\}\{b_2^j,b_{2'}^{\dagger m}\}\{b_3^k,b_{4'}^{\dagger r}\}+\{b_1^i,b_{2'}^{\dagger m}\}\{b_2^j,b_{3'}^{\dagger n}\}\{b_3^k,b_{4'}^{\dagger r}\}\Big]b_{1'}^{\dagger l}d_{5'}^{\dagger s}\Big\}|0\rangle.
\end{aligned}
\tag{3.65}
$$

The previous equations between braces contains four terms, but just one of them contributes, i.e. the one involving the operators $b_{4'}^{\dagger r}d_{5'}^{\dagger s}$. This is because the other terms do not respect the requirements of momentum conservation in the scalar product of the initial and final pion states.

Making explicit the commutators which multiply $b_{4'}^{\dagger r}d_{5'}^{\dagger s}$ we get

$$
\begin{aligned}
&\langle\pi^0(p_\pi)|\frac{4}{\sqrt{3!}}(P^+)^3\epsilon^{ijk}\int \mathrm{d}y\mathrm{d}^2\mathbf{k}_\perp\int_0^y\prod_{i=1'}^{3'}\frac{\mathrm{d}\xi_i}{\sqrt{\xi_i}}\int_0^{(1-y)}\prod_{i=4'}^{5'}\frac{\mathrm{d}\xi_i}{\sqrt{\xi_i}}\int\frac{\prod_{i=1'}^{5'}\mathrm{d}^2\mathbf{k}'_{i\perp}}{[2(2\pi)^3]^4}\\
&\times\frac{1}{y\sqrt{(1-y)}}\prod_{j=1}^{3}\int\frac{\mathrm{d}k_j^+\mathrm{d}^2\mathbf{k}_{j\perp}}{k_j^+}\Theta(k_j^+)\delta\Big(x_jP^+-k_j^+\Big)\\
&\times\delta\Big(y-\sum_{i=1'}^{3'}\xi_i\Big)\delta^{(2)}\Big(\mathbf{k}_\perp-\sum_{i=1'}^{3'}\mathbf{k}'_{i\perp}\Big)\delta\Big(1-\sum_{i=1'}^{5'}\xi_i\Big)\delta^{(2)}\Big(\sum_{i=1'}^{5'}\mathbf{k}'_{i\perp}\Big)\\
&\times\sum_{\lambda_1,\lambda_2,\lambda_3}\sum_{\lambda_i,\tau_i,c_i}u_{+\alpha}(k_1^+,\lambda_1)u_{+\beta}(k_2^+,\lambda_2)u_{+\gamma}(k_3^+,\lambda_3)\sum_{\lambda'}\phi_{\lambda'0}^{\lambda(N,N\pi)}(y,\mathbf{k}_\perp)\\
&\times\tilde{\Psi}_{\lambda'}^{N,[f]}(\{\zeta_i,\kappa_{i\perp};\lambda_i,\tau_i,c_i\}_{i=1',\cdots,3'})\tilde{\Psi}_0^{\pi,[f]}(\{\zeta_i,\kappa_{i\perp};\lambda_i,\tau_i,c_i\}_{i=4',5'})
\end{aligned}
$$

$$
\begin{aligned}
&\times\xi_{1'}\xi_{2'}\xi_{3'}(p_1^+)^3\Big\{\delta(\xi_{3'}p_1^+-k_1^+)\delta(\xi_{2'}p_1^+-k_2^+)\delta(\xi_{1'}p_1^+-k_3^+)\delta^{(2)}(\mathbf{k'}_{3'\perp}-\mathbf{k}_{1\perp})\\
&\times\delta^{(2)}(\mathbf{k'}_{2'\perp}-\mathbf{k}_{2\perp})\delta^{(2)}(\mathbf{k'}_{1'\perp}-\mathbf{k}_{3\perp})\delta_{3'u}\delta_{\lambda_{3'}\lambda_1}\delta_{ni}\delta_{2'u}\delta_{\lambda_{2'}\lambda_2}\delta_{mj}\delta_{1'd}\delta_{\lambda_{1'}\lambda_3}\delta_{lk}\\
&-\delta(\xi_{2'}p_1^+-k_1^+)\delta(\xi_{3'}p_1^+-k_2^+)\delta(\xi_{1'}p_1^+-k_3^+)\delta^{(2)}(\mathbf{k'}_{2'\perp}-\mathbf{k}_{1\perp})\\
&\times\delta^{(2)}(\mathbf{k'}_{3'\perp}-\mathbf{k}_{2\perp})\delta^{(2)}(\mathbf{k'}_{1'\perp}-\mathbf{k}_{3\perp})\delta_{2'u}\delta_{\lambda_{2'}\lambda_1}\delta_{mi}\delta_{3'u}\delta_{\lambda_{3'}\lambda_2}\delta_{nj}\delta_{1'd}\delta_{\lambda_{1'}\lambda_3}\delta_{lk}\\
&-\delta(\xi_{3'}p_1^+-k_1^+)\delta(\xi_{1'}p_1^+-k_2^+)\delta(\xi_{2'}p_1^+-k_3^+)\delta^{(2)}(\mathbf{k'}_{3'\perp}-\mathbf{k}_{1\perp})\\
&\times\delta^{(2)}(\mathbf{k'}_{1'\perp}-\mathbf{k}_{2\perp})\delta^{(2)}(\mathbf{k'}_{2'\perp}-\mathbf{k}_{3\perp})\delta_{3'u}\delta_{\lambda_{3'}\lambda_1}\delta_{ni}\delta_{1'u}\delta_{\lambda_{1'}\lambda_2}\delta_{lj}\delta_{2'd}\delta_{\lambda_{2'}\lambda_3}\delta_{mk}\\
&+\delta(\xi_{1'}p_1^+-k_1^+)\delta(\xi_{3'}p_1^+-k_2^+)\delta(\xi_{2'}p_1^+-k_3^+)\delta^{(2)}(\mathbf{k'}_{1'\perp}-\mathbf{k}_{1\perp})\\
&\times\delta^{(2)}(\mathbf{k'}_{3'\perp}-\mathbf{k}_{2\perp})\delta^{(2)}(\mathbf{k'}_{2'\perp}-\mathbf{k}_{3\perp})\delta_{1'u}\delta_{\lambda_{1'}\lambda_1}\delta_{li}\delta_{3'u}\delta_{\lambda_{3'}\lambda_2}\delta_{nj}\delta_{2'd}\delta_{\lambda_{2'}\lambda_3}\delta_{mk}\\
&+\delta(\xi_{2'}p_1^+-k_1^+)\delta(\xi_{1'}p_1^+-k_2^+)\delta(\xi_{3'}p_1^+-k_3^+)\delta^{(2)}(\mathbf{k'}_{2'\perp}-\mathbf{k}_{1\perp})\\
&\times\delta^{(2)}(\mathbf{k'}_{1'\perp}-\mathbf{k}_{2\perp})\delta^{(2)}(\mathbf{k'}_{3'\perp}-\mathbf{k}_{3\perp})\delta_{2'u}\delta_{\lambda_{2'}\lambda_1}\delta_{mi}\delta_{1'u}\delta_{\lambda_{1'}\lambda_2}\delta_{lj}\delta_{3'd}\delta_{\lambda_{3'}\lambda_3}\delta_{nk}\\
&-\delta(\xi_{1'}p_1^+-k_1^+)\delta(\xi_{2'}p_1^+-k_2^+)\delta(\xi_{3'}p_1^+-k_3^+)\delta^{(2)}(\mathbf{k'}_{1'\perp}-\mathbf{k}_{1\perp})\\
&\times\delta^{(2)}(\mathbf{k'}_{2'\perp}-\mathbf{k}_{2\perp})\delta^{(2)}(\mathbf{k'}_{3'\perp}-\mathbf{k}_{3\perp})\delta_{1'u}\delta_{\lambda_{1'}\lambda_1}\delta_{li}\delta_{2'u}\delta_{\lambda_{2'}\lambda_2}\delta_{mj}\delta_{3'd}\delta_{\lambda_{3'}\lambda_3}\delta_{nk}\Big\}\\
&\times\frac{\epsilon_{lmn}}{\sqrt{6}}\frac{\delta_{rs}}{\sqrt{3}}\Big[b^{\dagger r}(\xi_{4'}p_1^+,\mathbf{k'}_{4'\perp},\lambda_{4'},\tau_{4'})d^{\dagger s}(\xi_{5'}p_1^+,\mathbf{k'}_{5'\perp},-\lambda_{4'},-\tau_{4'})\Big]_{\pi^0}|0\rangle. \quad (3.66)
\end{aligned}
$$

Now making use of the relation $\epsilon_{ijk\cdots}\epsilon_{ijk\cdots}=n!$, where $i,j,k,...=1,...,n$, after some calculations it is possible to see that the previous equation becomes

$$
\begin{aligned}
&-\langle\pi^0(p_\pi)|4(P^+)^3\int \mathrm{d}y\mathrm{d}^2\mathbf{k}_\perp\int_0^y\prod_{i=1'}^{3'}\frac{\mathrm{d}\xi_i}{\sqrt{\xi_i}}\int_0^{(1-y)}\prod_{i=4'}^{5'}\frac{\mathrm{d}\xi_i}{\sqrt{\xi_i}}\int\frac{\prod_{i=1'}^{5'}\mathrm{d}^2\mathbf{k'}_{i\perp}}{[2(2\pi)^3]^4}\\
&\times\frac{1}{y\sqrt{(1-y)}}\prod_{j=1}^{3}\int\frac{\mathrm{d}k_j^+\mathrm{d}^2\mathbf{k}_{j\perp}}{k_j^+}\Theta(k_j^+)\delta\Big(x_jP^+-k_j^+\Big)\\
&\times\delta\Big(y-\sum_{i=1'}^{3'}\xi_i\Big)\delta^{(2)}\Big(\mathbf{k}_\perp-\sum_{i=1'}^{3'}\mathbf{k'}_{i\perp}\Big)\delta\Big(1-\sum_{i=1'}^{5'}\xi_i\Big)\delta^{(2)}\Big(\sum_{i=1'}^{5'}\mathbf{k'}_{i\perp}\Big)\\
&\times\sum_{\lambda_1,\lambda_2,\lambda_3}\sum_{\lambda_i,\tau_i}u_{+\alpha}(k_1^+,\lambda_1)u_{+\beta}(k_2^+,\lambda_2)u_{+\gamma}(k_3^+,\lambda_3)\sum_{\lambda'}\phi_{\lambda'0}^{\lambda(N,N\pi)}(y,\mathbf{k}_\perp)\\
&\times\tilde{\Psi}_{\lambda'}^{N,[f]}(\{\zeta_i,\kappa_{i\perp};\lambda_i,\tau_i\}_{i=1',\cdots,3'})\tilde{\Psi}^{\pi,[f]}(\{\zeta_i,\kappa_{i\perp};\lambda_i,\tau_i\}_{i=4',5'})\\
&\times\sum_{r,s}\frac{\delta_{rs}}{\sqrt{3}}\Big[b^{\dagger r}(\xi_{4'}p_1^+,\mathbf{k'}_{4'\perp},\lambda_{4'},\tau_{4'})d^{\dagger s}(\xi_{5'}p_1^+,\mathbf{k'}_{5'\perp},\lambda_{5'}=-\lambda_{4'},\tau_{5'}=-\tau_{4'})\Big]_{\pi^0}
\end{aligned}
$$

$$
\begin{aligned}
&\times\xi_{1'}\xi_{2'}\xi_{3'}(p_1^+)^3\Big\{\delta(\xi_{3'}p_1^+-k_1^+)\delta(\xi_{2'}p_1^+-k_2^+)\delta(\xi_{1'}p_1^+-k_3^+)\delta^{(2)}(\mathbf{k}'_{3'\perp}-\mathbf{k}_{1\perp})\\
&\times\delta^{(2)}(\mathbf{k}'_{2'\perp}-\mathbf{k}_{2\perp})\delta^{(2)}(\mathbf{k}'_{1'\perp}-\mathbf{k}_{3\perp})\delta_{3'u}\delta_{\lambda_{3'}\lambda_1}\delta_{2'u}\delta_{\lambda_{2'}\lambda_2}\delta_{1'd}\delta_{\lambda_{1'}\lambda_3}\\
&+\delta(\xi_{2'}p_1^+-k_1^+)\delta(\xi_{3'}p_1^+-k_2^+)\delta(\xi_{1'}p_1^+-k_3^+)\delta^{(2)}(\mathbf{k}'_{2'\perp}-\mathbf{k}_{1\perp})\\
&\times\delta^{(2)}(\mathbf{k}'_{3'\perp}-\mathbf{k}_{2\perp})\delta^{(2)}(\mathbf{k}'_{1'\perp}-\mathbf{k}_{3\perp})\delta_{2'u}\delta_{\lambda_{2'}\lambda_1}\delta_{3'u}\delta_{\lambda_{3'}\lambda_2}\delta_{1'd}\delta_{\lambda_{1'}\lambda_3}\\
&+\delta(\xi_{3'}p_1^+-k_1^+)\delta(\xi_{1'}p_1^+-k_2^+)\delta(\xi_{2'}p_1^+-k_3^+)\delta^{(2)}(\mathbf{k}'_{3'\perp}-\mathbf{k}_{1\perp})\\
&\times\delta^{(2)}(\mathbf{k}'_{1'\perp}-\mathbf{k}_{2\perp})\delta^{(2)}(\mathbf{k}'_{2'\perp}-\mathbf{k}_{3\perp})\delta_{3'u}\delta_{\lambda_{3'}\lambda_1}\delta_{1'u}\delta_{\lambda_{1'}\lambda_2}\delta_{2'd}\delta_{\lambda_{2'}\lambda_3}\\
&+\delta(\xi_{1'}p_1^+-k_1^+)\delta(\xi_{3'}p_1^+-k_2^+)\delta(\xi_{2'}p_1^+-k_3^+)\delta^{(2)}(\mathbf{k}'_{1'\perp}-\mathbf{k}_{1\perp})\\
&\times\delta^{(2)}(\mathbf{k}'_{3'\perp}-\mathbf{k}_{2\perp})\delta^{(2)}(\mathbf{k}'_{2'\perp}-\mathbf{k}_{3\perp})\delta_{1'u}\delta_{\lambda_{1'}\lambda_1}\delta_{3'u}\delta_{\lambda_{3'}\lambda_2}\delta_{2'd}\delta_{\lambda_{2'}\lambda_3}\\
&+\delta(\xi_{2'}p_1^+-k_1^+)\delta(\xi_{1'}p_1^+-k_2^+)\delta(\xi_{3'}p_1^+-k_3^+)\delta^{(2)}(\mathbf{k}'_{2'\perp}-\mathbf{k}_{1\perp})\\
&\times\delta^{(2)}(\mathbf{k}'_{1'\perp}-\mathbf{k}_{2\perp})\delta^{(2)}(\mathbf{k}'_{3'\perp}-\mathbf{k}_{3\perp})\delta_{2'u}\delta_{\lambda_{2'}\lambda_1}\delta_{1'u}\delta_{\lambda_{1'}\lambda_2}\delta_{3'd}\delta_{\lambda_{3'}\lambda_3}\\
&+\delta(\xi_{1'}p_1^+-k_1^+)\delta(\xi_{2'}p_1^+-k_2^+)\delta(\xi_{3'}p_1^+-k_3^+)\delta^{(2)}(\mathbf{k}'_{1'\perp}-\mathbf{k}_{1\perp})\\
&\times\delta^{(2)}(\mathbf{k}'_{2'\perp}-\mathbf{k}_{2\perp})\delta^{(2)}(\mathbf{k}'_{3'\perp}-\mathbf{k}_{3\perp})\delta_{1'u}\delta_{\lambda_{1'}\lambda_1}\delta_{2'u}\delta_{\lambda_{2'}\lambda_2}\delta_{3'd}\delta_{\lambda_{3'}\lambda_3}\Big\}|0\rangle. \qquad (3.67)
\end{aligned}
$$

Then specifying the dependencies of the nucleon LCWF one obtains

$$
\begin{aligned}
&-\langle\pi^0(p_\pi)|\frac{4}{\sqrt{3}}(P^+)^3\int \mathrm{d}y\mathrm{d}^2\mathbf{k}_\perp\int_0^y\prod_{i=1'}^{3'}\frac{\mathrm{d}\xi_i}{\sqrt{\xi_i}}\int_0^{(1-y)}\prod_{i=4'}^{5'}\frac{\mathrm{d}\xi_i}{\sqrt{\xi_i}}\int\frac{\prod_{i=1'}^{5'}\mathrm{d}^2\mathbf{k}'_{i\perp}}{[2(2\pi)^3]^4}\\
&\times\frac{1}{y\sqrt{(1-y)}}\prod_{j=1}^{3}\int\frac{\mathrm{d}k_j^+\mathrm{d}^2\mathbf{k}_{j\perp}}{k_j^+}\Theta(k_j^+)\delta\Big(x_jP^+-k_j^+\Big)\\
&\times\delta\Big(y-\sum_{i=1'}^{3'}\xi_i\Big)\delta^{(2)}\Big(\mathbf{k}_\perp-\sum_{i=1'}^{3'}\mathbf{k}'_{i\perp}\Big)\delta\Big(1-\sum_{i=1'}^{5'}\xi_i\Big)\delta^{(2)}\Big(\sum_{i=1'}^{5'}\mathbf{k}'_{i\perp}\Big)\\
&\times\sum_{\lambda_1,\lambda_2,\lambda_3}\sum_{\lambda'}\phi_{\lambda'0}^{\lambda(N,N\pi)}(y,\mathbf{k}_\perp)\xi_{1'}\xi_{2'}\xi_{3'}(p_1^+)^3u_{+\alpha}(k_1^+,\lambda_1)u_{+\beta}(k_2^+,\lambda_2)u_{+\gamma}(k_3^+,\lambda_3)\\
&\times\sum_{\substack{\lambda_{4'},\lambda_{5'}\\ \tau_{4'},\tau_{5'}}}\tilde{\Psi}^{\pi,[f]}(\{\zeta_i,\kappa_{i\perp};\lambda_i,\tau_i\}_{i=4',5'})\\
&\times\sum_r\Big[b^{\dagger r}(\xi_{4'}p_1^+,\mathbf{k}'_{4'\perp},\lambda_{4'},\tau_{4'})d^{\dagger r}(\xi_{5'}p_1^+,\mathbf{k}'_{5'\perp},\lambda_{5'}=-\lambda_{4'},\tau_{5'}=-\tau_{4'})\Big]_{\pi^0}\\
&\times\Big\{\tilde{\Psi}_{\lambda'}^{N,[f]}\Big(\{\zeta_{1'},\kappa_{1'\perp};\lambda_{3'},-1/2\}\{\zeta_{2'},\kappa_{2'\perp};\lambda_{2'},1/2\}\{\zeta_{3'},\kappa_{3'\perp};\lambda_{1'},1/2\}\Big)\\
&\times\delta(\xi_{3'}p_1^+-k_1^+)\delta(\xi_{2'}p_1^+-k_2^+)\delta(\xi_{1'}p_1^+-k_3^+)\delta_{\lambda_{3'}\lambda_1}\delta_{\lambda_{2'}\lambda_2}\delta_{\lambda_{1'}\lambda_3}\\
&\times\delta^{(2)}(\mathbf{k}'_{3'\perp}-\mathbf{k}_{1\perp})\delta^{(2)}(\mathbf{k}'_{2'\perp}-\mathbf{k}_{2\perp})\delta^{(2)}(\mathbf{k}'_{1'\perp}-\mathbf{k}_{3\perp})
\end{aligned}
$$

$$
\begin{aligned}
&+\tilde{\Psi}^{N,[f]}_{\lambda'}\Big(\{\zeta_{1'},\kappa_{1'\perp};\lambda_{3'},-1/2\}\{\zeta_{2'},\kappa_{2'\perp};\lambda_{2'},1/2\}\{\zeta_{3'},\kappa_{3'\perp};\lambda_{1'},1/2\}\Big)\\
&\times\delta(\xi_{2'}p_1^+-k_1^+)\delta(\xi_{3'}p_1^+-k_2^+)\delta(\xi_{1'}p_1^+-k_3^+)\delta_{\lambda_{2'}\lambda_1}\delta_{\lambda_{3'}\lambda_2}\delta_{\lambda_{1'}\lambda_3}\\
&\times\delta^{(2)}(\mathbf{k}'_{2'\perp}-\mathbf{k}_{1\perp})\delta^{(2)}(\mathbf{k}'_{3'\perp}-\mathbf{k}_{2\perp})\delta^{(2)}(\mathbf{k}'_{1'\perp}-\mathbf{k}_{3\perp})\\
&+\tilde{\Psi}^{N,[f]}_{\lambda'}\Big(\{\zeta_{1'},\kappa_{1'\perp};\lambda_{2'},1/2\}\{\zeta_{2'},\kappa_{2'\perp};\lambda_{3'},-1/2\}\{\zeta_{3'},\kappa_{3'\perp};\lambda_{1'},1/2\}\Big)\\
&\times\delta(\xi_{3'}p_1^+-k_1^+)\delta(\xi_{1'}p_1^+-k_2^+)\delta(\xi_{2'}p_1^+-k_3^+)\delta_{\lambda_{3'}\lambda_1}\delta_{\lambda_{1'}\lambda_2}\delta_{\lambda_{2'}\lambda_3}\\
&\times\delta^{(2)}(\mathbf{k}'_{3'\perp}-\mathbf{k}_{1\perp})\delta^{(2)}(\mathbf{k}'_{1'\perp}-\mathbf{k}_{2\perp})\delta^{(2)}(\mathbf{k}'_{2'\perp}-\mathbf{k}_{3\perp})\\
&+\tilde{\Psi}^{N,[f]}_{\lambda'}\Big(\{\zeta_{1'},\kappa_{1'\perp};\lambda_{1'},1/2\}\{\zeta_{2'},\kappa_{2'\perp};\lambda_{3'},-1/2\}\{\zeta_{3'},\kappa_{3'\perp};\lambda_{2'},1/2\}\Big)\\
&\times\delta(\xi_{1'}p_1^+-k_1^+)\delta(\xi_{3'}p_1^+-k_2^+)\delta(\xi_{2'}p_1^+-k_3^+)\delta_{\lambda_{1'}\lambda_1}\delta_{\lambda_{3'}\lambda_2}\delta_{\lambda_{2'}\lambda_3}\\
&\times\delta^{(2)}(\mathbf{k}'_{1'\perp}-\mathbf{k}_{1\perp})\delta^{(2)}(\mathbf{k}'_{3'\perp}-\mathbf{k}_{2\perp})\delta^{(2)}(\mathbf{k}'_{2'\perp}-\mathbf{k}_{3\perp})\\
&+\tilde{\Psi}^{N,[f]}_{\lambda'}\Big(\{\zeta_{1'},\kappa_{1'\perp};\lambda_{2'},1/2\}\{\zeta_{2'},\kappa_{2'\perp};\lambda_{1'},1/2\}\{\zeta_{3'},\kappa_{3'\perp};\lambda_{3'},-1/2\}\Big)\\
&\times\delta(\xi_{1'}p_1^+-k_1^+)\delta(\xi_{2'}p_1^+-k_2^+)\delta(\xi_{3'}p_1^+-k_3^+)\delta_{\lambda_{1'}\lambda_1}\delta_{\lambda_{2'}\lambda_2}\delta_{\lambda_{3'}\lambda_3}\\
&\times\delta^{(2)}(\mathbf{k}'_{2'\perp}-\mathbf{k}_{1\perp})\delta^{(2)}(\mathbf{k}'_{1'\perp}-\mathbf{k}_{2\perp})\delta^{(2)}(\mathbf{k}'_{3'\perp}-\mathbf{k}_{3\perp})\\
&+\tilde{\Psi}^{N,[f]}_{\lambda'}\Big(\{\zeta_{1'},\kappa_{1'\perp};\lambda_{1'},1/2\}\{\zeta_{2'},\kappa_{2'\perp};\lambda_{2'},1/2\}\{\zeta_{3'},\kappa_{3'\perp};\lambda_{3'},-1/2\}\Big)\\
&\times\delta(\xi_{1'}p_1^+-k_1^+)\delta(\xi_{2'}p_1^+-k_2^+)\delta(\xi_{3'}p_1^+-k_3^+)\delta_{\lambda_{1'}\lambda_1}\delta_{\lambda_{2'}\lambda_2}\delta_{\lambda_{3'}\lambda_3}\\
&\times\delta^{(2)}(\mathbf{k}'_{1'\perp}-\mathbf{k}_{1\perp})\delta^{(2)}(\mathbf{k}'_{2'\perp}-\mathbf{k}_{2\perp})\delta^{(2)}(\mathbf{k}'_{3'\perp}-\mathbf{k}_{3\perp})\Big\}|0\rangle, \qquad (3.68)
\end{aligned}
$$

and summing over the helicities $\lambda_{1'},...,\lambda_{3'}$,

$$
\begin{aligned}
&-\langle\pi^0(p_\pi)|\frac{8}{\sqrt{3}}(P^+)^3\int \mathrm{d}y\mathrm{d}^2\mathbf{k}_\perp\int_0^y\prod_{i=1'}^{3'}\frac{\mathrm{d}\xi_i}{\sqrt{\xi_i}}\int_0^{(1-y)}\prod_{i=4'}^{5'}\frac{\mathrm{d}\xi_i}{\sqrt{\xi_i}}\int\frac{\prod_{i=1'}^{5'}\mathrm{d}^2\mathbf{k}'_{i\perp}}{[2(2\pi)^3]^4}\\
&\times\frac{1}{y\sqrt{(1-y)}}\prod_{j=1}^{3}\int\frac{\mathrm{d}k_j^+\mathrm{d}^2\mathbf{k}_{j\perp}}{k_j^+}\Theta(k_j^+)\delta\Big(x_jP^+-k_j^+\Big)\\
&\times\delta\Big(y-\sum_{i=1'}^{3'}\xi_i\Big)\delta^{(2)}\Big(\mathbf{k}_\perp-\sum_{i=1'}^{3'}\mathbf{k}'_{i\perp}\Big)\delta\Big(1-\sum_{i=1'}^{5'}\xi_i\Big)\delta^{(2)}\Big(\sum_{i=1'}^{5'}\mathbf{k}'_{i\perp}\Big)\\
&\times\sum_{\lambda_1,\lambda_2,\lambda_3}\sum_{\lambda'}\phi^{\lambda(N,N\pi)}_{\lambda'0}(y,\mathbf{k}_\perp)\xi_{1'}\xi_{2'}\xi_{3'}(p_1^+)^3u_{+\alpha}(k_1^+,\lambda_1)u_{+\beta}(k_2^+,\lambda_2)u_{+\gamma}(k_3^+,\lambda_3)\\
&\times\sum_{\substack{\lambda_{4'},\lambda_{5'}\\ \tau_{4'},\tau_{5'}}}\tilde{\Psi}^{\pi,[f]}(\{\zeta_i,\kappa_{i\perp};\lambda_i,\tau_i\}_{i=4',5'})
\end{aligned}
$$

$$
\begin{aligned}
&\times\sum_{r}\Big[b^{\dagger r}(\xi_{4'}p_1^+,\mathbf{k}'_{4'\perp},\lambda_{4'},\tau_{4'})d^{\dagger r}(\xi_{5'}p_1^+,\mathbf{k}'_{5'\perp},\lambda_{5'}=-\lambda_{4'},\tau_{5'}=-\tau_{4'})\Big]_{\pi^0}\\
&\times\Bigg\{\tilde{\Psi}^{N,[f]}_{\lambda'}\Big(\{\zeta_{1'},\kappa_{1'\perp};\lambda_3,-1/2\}\{\zeta_{2'},\kappa_{2'\perp};\lambda_2,1/2\}\{\zeta_{3'},\kappa_{3'\perp};\lambda_1,1/2\}\Big)\\
&\times\delta(\xi_{3'}p_1^+-k_1^+)\delta(\xi_{2'}p_1^+-k_2^+)\delta(\xi_{1'}p_1^+-k_3^+)\\
&\times\delta^{(2)}(\mathbf{k}'_{3'\perp}-\mathbf{k}_{1\perp})\delta^{(2)}(\mathbf{k}'_{2'\perp}-\mathbf{k}_{2\perp})\delta^{(2)}(\mathbf{k}'_{1'\perp}-\mathbf{k}_{3\perp})\\
&+\tilde{\Psi}^{N,[f]}_{\lambda'}\Big(\{\zeta_{1'},\kappa_{1'\perp};\lambda_2,1/2\}\{\zeta_{2'},\kappa_{2'\perp};\lambda_3,-1/2\}\{\zeta_{3'},\kappa_{3'\perp};\lambda_1,1/2\}\Big)\\
&\times\delta(\xi_{3'}p_1^+-k_1^+)\delta(\xi_{1'}p_1^+-k_2^+)\delta(\xi_{2'}p_1^+-k_3^+)\\
&\times\delta^{(2)}(\mathbf{k}'_{3'\perp}-\mathbf{k}_{1\perp})\delta^{(2)}(\mathbf{k}'_{1'\perp}-\mathbf{k}_{2\perp})\delta^{(2)}(\mathbf{k}'_{2'\perp}-\mathbf{k}_{3\perp})\\
&+\tilde{\Psi}^{N,[f]}_{\lambda'}\Big(\{\zeta_{1'},\kappa_{1'\perp};\lambda_1,1/2\}\{\zeta_{2'},\kappa_{2'\perp};\lambda_2,1/2\}\{\zeta_{3'},\kappa_{3'\perp};\lambda_3,-1/2\}\Big)\\
&\times\delta(\xi_{1'}p_1^+-k_1^+)\delta(\xi_{2'}p_1^+-k_2^+)\delta(\xi_{3'}p_1^+-k_3^+)\\
&\times\delta^{(2)}(\mathbf{k}'_{1'\perp}-\mathbf{k}_{1\perp})\delta^{(2)}(\mathbf{k}'_{2'\perp}-\mathbf{k}_{2\perp})\delta^{(2)}(\mathbf{k}'_{3'\perp}-\mathbf{k}_{3\perp})\Bigg\}|0\rangle.
\end{aligned}
$$

At this point, performing the integrations over k_j^+, $\mathbf{k}_{j\perp}$ and ξ_i with $i=1',...,3'$

$$
\begin{aligned}
&-\langle\pi^0(p_\pi)|\frac{24}{\sqrt{3x_1x_2x_3}}\Big(P^+/p_1^+\Big)^{\frac{3}{2}}\int \mathrm{d}y\mathrm{d}^2\mathbf{k}_\perp\int_0^{(1-y)}\prod_{i=4'}^{5'}\frac{\mathrm{d}\xi_i}{\sqrt{\xi_i}}\int\frac{\prod_{i=1'}^{5'}\mathrm{d}^2\mathbf{k}'_{i\perp}}{[2(2\pi)^3]^4}\\
&\times\frac{1}{y\sqrt{(1-y)}}\delta\Big(y-\sum_{j=1}^{3}x_j\frac{P^+}{p_1^+}\Big)\delta^{(2)}\Big(\mathbf{k}_\perp-\sum_{i=1'}^{3'}\mathbf{k}'_{i\perp}\Big)\delta\Big(1-\sum_{j=1}^{3}x_j\frac{P^+}{p_1^+}-\sum_{i=4'}^{5'}\xi_i\Big)\\
&\times\delta^{(2)}\Big(\sum_{i=1'}^{5'}\mathbf{k}'_{i\perp}\Big)\times\sum_{\lambda_1,\lambda_2,\lambda_3}\sum_{\lambda'}\phi^{\lambda(N,N\pi)}_{\lambda'0}(y,\mathbf{k}_\perp)u_{+\alpha}(x_1P^+,\lambda_1)u_{+\beta}(x_2P^+,\lambda_2)\\
&\times u_{+\gamma}(x_3P^+,\lambda_3)\sum_{\substack{\lambda_{4'},\lambda_{5'}\\ \tau_{4'},\tau_{5'}}}\tilde{\Psi}^{\pi,[f]}(\{\zeta_i,\kappa_{i\perp};\lambda_i,\tau_i\}_{i=4',5'})\\
&\times\tilde{\Psi}^{N,[f]}_{\lambda'}\Big(\Big\{\frac{x_1P^+}{yp_1^+},\kappa_{1'\perp};\lambda_1,1/2\Big\}\Big\{\frac{x_2P^+}{yp_1^+},\kappa_{2'\perp};\lambda_2,1/2\Big\}\Big\{\frac{x_3P^+}{yp_1^+},\kappa_{3'\perp};\lambda_3,-1/2\Big\}\Big)\\
&\times\sum_{r}\Big[b^{\dagger r}(\xi_{4'}p_1^+,\mathbf{k}'_{4'\perp},\lambda_{4'},\tau_{4'})d^{\dagger r}(\xi_{5'}p_1^+,\mathbf{k}'_{5'\perp},\lambda_{5'}=-\lambda_{4'},\tau_{5'}=-\tau_{4'})\Big]|0\rangle. \qquad (3.69)
\end{aligned}
$$

To proceed we have to insert the expression for the pion state $\langle\pi^0(p_\pi)|$ as done before for the nucleon state $|N\pi(p_1,s_1)\rangle$ and make the calculations along

the same line. We can express the pionic bra in the following way[‖],

$$\langle\pi^0(p_\pi)| = \langle 0|\sum_{\lambda_{\pi^0 l},\tau_{\pi^0 l}}\int\frac{\mathrm{d}z_1\mathrm{d}z_2}{\sqrt{z_1 z_2}}\frac{\mathrm{d}^2\mathbf{k}_{\pi^0 1\perp}\mathrm{d}^2\mathbf{k}_{\pi^0 2\perp}}{16\pi^3}\delta(1-z_1-z_2)\delta^{(2)}(\mathbf{k}_{\pi^0 1\perp}+\mathbf{k}_{\pi^0 2\perp})$$
$$\times\sum_{tv}\frac{\delta_{tv}}{\sqrt{3}}\Big[\tilde{\Psi}^{\pi^0,[f]}(\{z_l,\mathbf{k}_{\pi^0 l\perp};\lambda_{\pi^0 l},\tau_{\pi^0 l},c_l\}_{l=1,2})\Big]^*$$
$$\times\Big[b^t(z_1 p_\pi^+,\mathbf{k}_{\pi^0 1\perp}+z_1\mathbf{p}_{\pi\perp},\lambda_{\pi^0 1},\tau_{\pi^0 1})d^v(z_2 p_\pi^+,\mathbf{k}_{\pi^0 2\perp}+z_2\mathbf{p}_{\pi\perp},\lambda_{\pi^0 2},\tau_{\pi^0 2}\Big], \quad (3.70)$$

where t and v are colour indexes. Inserting this state in Eq. (3.69) we get

$$= -\langle 0|\sum_{\lambda_{\pi^0 l},\tau_{\pi^0 l}}\int\frac{\mathrm{d}z_1\mathrm{d}z_2}{\sqrt{z_1 z_2}}\frac{\mathrm{d}^2\mathbf{k}_{\pi^0 1\perp}\mathrm{d}^2\mathbf{k}_{\pi^0 2\perp}}{16\pi^3}\delta(1-z_1-z_2)\delta^{(2)}(\mathbf{k}_{\pi^0 1\perp}+\mathbf{k}_{\pi^0 2\perp})$$
$$\times\frac{1}{\sqrt{3}}\sum_t\Big[\tilde{\Psi}^{\pi^0,[f]}(\{z_l,\mathbf{k}_{\pi^0 l\perp};\lambda_{\pi^0 l},\tau_{\pi^0 l}\}_{l=1,2})\Big]^*$$
$$\times\Big[b^t(z_1 p_\pi^+,\mathbf{k}_{\pi^0 1\perp}+z_1\mathbf{p}_{\pi\perp},\lambda_{\pi^0 1},\tau_{\pi^0 1})d^t(z_2 p_\pi^+,\mathbf{k}_{\pi^0 2\perp}+z_2\mathbf{p}_{\pi\perp},\lambda_{\pi^0 2},\tau_{\pi^0 2}\Big]$$
$$\times\frac{24}{\sqrt{3x_1x_2x_3}}\Big(P^+/p_1^+\Big)^{\frac{3}{2}}\int\mathrm{d}y\mathrm{d}^2\mathbf{k}_\perp\int_0^{(1-y)}\prod_{i=4'}^{5'}\frac{\mathrm{d}\xi_i}{\sqrt{\xi_i}}\int\frac{\prod_{i=1'}^{5'}\mathrm{d}^2\mathbf{k}'_{i\perp}}{[2(2\pi)^3]^4}\frac{1}{y\sqrt{1-y}}$$
$$\times\delta\Big(y-\sum_{j=1}^{3}x_j\frac{P^+}{p_1^+}\Big)\delta^{(2)}\Big(\mathbf{k}_\perp-\sum_{i=1'}^{3'}\mathbf{k'}_{i\perp}\Big)\delta\Big(1-\sum_{j=1}^{3}x_j\frac{P^+}{p_1^+}-\sum_{i=4'}^{5'}\xi_i\Big)\delta^{(2)}\Big(\sum_{i=1'}^{5'}\mathbf{k}'_{i\perp}\Big)$$
$$\times\sum_{\lambda_1,\lambda_2,\lambda_3}\sum_{\lambda'}\phi_{\lambda' 0}^{\lambda(N,N\pi)}\Big(y,\mathbf{k}_\perp\Big)u_{+\alpha}(x_1P^+,\lambda_1)u_{+\beta}(x_2P^+,\lambda_2)$$
$$\times u_{+\gamma}(x_3P^+,\lambda_3)\sum_{\substack{\lambda_{4'},\lambda_{5'}\\ \tau_{4'},\tau_{5'}}}\tilde{\Psi}^{\pi,[f]}(\{\zeta_i,\kappa_{i\perp};\lambda_i,\tau_i\}_{i=4',5'})$$
$$\times\tilde{\Psi}^{N,[f]}_{\lambda'}\Bigg(\Big\{\frac{x_1P^+}{yp_1^+},\kappa_{1'\perp};\lambda_1,1/2\Big\}\Big\{\frac{x_2P^+}{yp_1^+},\kappa_{2'\perp};\lambda_2,1/2\Big\}\Big\{\frac{x_3P^+}{yp_1^+},\kappa_{3'\perp};\lambda_3,-1/2\Big\}\Bigg)$$
$$\times\sum_r\Big[b^{\dagger r}(\xi_{4'}p_1^+,\mathbf{k}'_{4'\perp},\lambda_{4'},\tau_{4'})d^{\dagger r}(\xi_{5'}p_1^+,\mathbf{k}'_{5'\perp},\lambda_{5'}=-\lambda_{4'},\tau_{5'}=-\tau_{4'})\Big]_{\pi^0}|0\rangle,$$

[‖]We put an auxiliar index π^0 wherever the notation could have been source of confusion.

and thanks to the anticommutation relations (1.53)

$$
\begin{aligned}
&-\frac{24}{\sqrt{x_1x_2x_3}}\left(\frac{P^+}{p_1^+}\right)^{\frac{3}{2}}\sum_{\lambda_{\pi^0 l},\tau_{\pi^0 l}}\int \mathrm{d}y\mathrm{d}^2\mathbf{k}_\perp\int\frac{\mathrm{d}z_1\mathrm{d}z_2}{\sqrt{z_1z_2}}\int \mathrm{d}^2\mathbf{k}_{\pi^0 1\perp}\mathrm{d}^2\mathbf{k}_{\pi^0 2\perp}\\
&\times\delta(1-z_1-z_2)\delta^{(2)}(\mathbf{k}_{\pi^0 1\perp}+\mathbf{k}_{\pi^0 2\perp})\left[\tilde{\Psi}^{\pi^0,[f]}(\{z_l,\mathbf{k}_{\pi^0 l\perp};\lambda_{\pi^0 l},\tau_{\pi^0 l}\}_{l=1,2})\right]^*\\
&\times\int_0^{(1-y)}\prod_{i=4'}^{5'}\frac{\mathrm{d}\xi_i}{\sqrt{\xi_i}}\int\frac{\prod_{i=1'}^{5'}\mathrm{d}^2\mathbf{k}'_{i\perp}}{[2(2\pi)^3]^3}\frac{1}{y\sqrt{1-y}}\delta\left(y-\sum_{j=1}^{3}x_j\frac{P^+}{p_1^+}\right)\\
&\times\delta^{(2)}\left(\mathbf{k}_\perp-\sum_{i=1'}^{3'}\mathbf{k}'_{i\perp}\right)\delta\left(1-\sum_{j=1}^{3}x_j\frac{P^+}{p_1^+}-\sum_{i=4'}^{5'}\xi_i\right)\delta^{(2)}\left(\sum_{i=1'}^{5'}\mathbf{k}'_{i\perp}\right)\\
&\times\sum_{\lambda_1,\lambda_2,\lambda_3}\sum_{\lambda'}\phi_{\lambda' 0}^{\lambda(N,N\pi)}\left(y,\mathbf{k}_\perp\right)u_{+\alpha}(x_1P^+,\lambda_1)u_{+\beta}(x_2P^+,\lambda_2)u_{+\gamma}(x_3P^+,\lambda_3)\\
&\times\sum_{\substack{\lambda_{4'},\lambda_{5'}\\ \tau_{4'},\tau_{5'}}}\tilde{\Psi}^{\pi,[f]}(\{\zeta_i,\kappa_{i\perp};\lambda_i,\tau_i\}_{i=4',5'})\\
&\times\tilde{\Psi}^{N,[f]}_{\lambda'}\left(\left\{\frac{x_1P^+}{yp_1^+},\kappa_{1'\perp};\lambda_1,1/2\right\}\left\{\frac{x_2P^+}{yp_1^+},\kappa_{2'\perp};\lambda_2,1/2\right\}\left\{\frac{x_3P^+}{yp_1^+},\kappa_{3'\perp};\lambda_3,-1/2\right\}\right)\\
&\times z_1z_2(p_\pi^+)^2\delta(z_1p_\pi^+-\xi_{4'}p_1^+)\delta(z_2p_\pi^+-\xi_{5'}p_1^+)\delta^{(2)}\left(\mathbf{k}_{\pi^0 1\perp}+z_1\mathbf{p}_{\pi\perp}-\mathbf{k}'_{4'\perp}\right)\\
&\times\delta^{(2)}\left(\mathbf{k}_{\pi^0 2\perp}+z_2\mathbf{p}_{\pi\perp}-\mathbf{k}'_{5'\perp}\right)\delta_{\lambda_{\pi^0 1}\lambda_{4'}}\delta_{\lambda_{\pi^0 2}\lambda_{5'}}\delta_{\tau_{\pi^0 1}\tau_{4'}}\delta_{\tau_{\pi^0 2}\tau_{5'}}.
\end{aligned}
\tag{3.71}
$$

Now we perform the integration over ξ_i and $\mathbf{k}'_{i\perp}$. The condition imposed by momentum conservation are:

$$1-y=\xi_{4'}+\xi_{5'}=(z_1+z_2)\frac{p_\pi^+}{p_1^+}=\frac{p_\pi^+}{p_1^+}. \tag{3.72}$$

Furthermore we note that the intrinsic variables

$$\zeta_{4'} = \frac{\xi_{4'}}{1-y}=\frac{z_1}{1-y}\frac{p_\pi^+}{p_1^+}=z_1, \tag{3.73}$$

$$\zeta_{5'} = \frac{\xi_{5'}}{1-y}=\frac{z_2}{1-y}\frac{p_\pi^+}{p_1^+}=z_2. \tag{3.74}$$

For the transverse components of the momentum we have

$$-\mathbf{k}_\perp=\mathbf{k}'_{4'\perp}+\mathbf{k}'_{5'\perp}=\mathbf{k}_{\pi^0 1\perp}+\mathbf{k}_{\pi^0 2\perp}+(z_1+z_2)\mathbf{p}_{\pi\perp}=\mathbf{p}_{\pi\perp}, \tag{3.75}$$

and the intrinsic variables become

$$\kappa_{4'\perp} = \mathbf{k}'_{4'\perp}+\zeta_{4'\perp}\mathbf{k}_\perp=\mathbf{k}_{\pi^0 1\perp}+z_1\mathbf{p}_{\pi\perp}+z_1\mathbf{k}_\perp \tag{3.76}$$

$$= \mathbf{k}_{\pi^0 1\perp}+z_{1\perp}\mathbf{p}_{\pi\perp}-z_1\mathbf{p}_{\pi\perp}=\mathbf{k}_{\pi^0 1\perp}, \tag{3.77}$$

$$\kappa_{5'\perp} = \mathbf{k}'_{5'\perp}+\zeta_{5'\perp}\mathbf{k}_\perp=\mathbf{k}_{\pi^0 2\perp}+z_2\mathbf{p}_{\pi\perp}+z_2\mathbf{k}_\perp \tag{3.78}$$

$$= \mathbf{k}_{\pi^0 2\perp}+z_2\mathbf{p}_{\pi\perp}-z_2\mathbf{p}_{\pi\perp}=\mathbf{k}_{\pi^0 2\perp}. \tag{3.79}$$

As a result, Eq. (3.71) becomes

$$
\begin{aligned}
&-\frac{24}{\sqrt{x_1x_2x_3}}\left(\frac{P^+}{p_1^+}\right)^{\frac{3}{2}}\int\frac{\mathrm{d}y\mathrm{d}^2\mathbf{k}_\perp}{[2(2\pi)^3]^2}\int\prod_{i=1'}^{3'}\mathrm{d}^2\mathbf{k'}_{i\perp}\frac{1}{y}\sqrt{1-y}\\
&\delta\left(y-2\xi\frac{P^+}{p_1^+}\right)\delta\left(1-2\xi\frac{P^+}{p_1^+}-\frac{p_\pi^+}{p_1^+}\right)\delta^{(2)}\left(\mathbf{k}_\perp-\sum_{i=1'}^{3'}\mathbf{k'}_{i\perp}\right)\\
&\times\delta^{(2)}\left(\mathbf{p}_{\pi\perp}+\sum_{i=1'}^{3'}\mathbf{k'}_{i\perp}\right)\sum_{\lambda_1,\lambda_2,\lambda_3}\sum_{\lambda'}\phi_{\lambda'0}^{\lambda(N,N\pi)}\left(y,\mathbf{k}_\perp\right)\\
&u_{+\alpha}(x_1P^+,\lambda_1)u_{+\beta}(x_2P^+,\lambda_2)u_{+\gamma}(x_3P^+,\lambda_3)\\
&\times\tilde{\Psi}_{\lambda'}^{N,[f]}\left(\left\{\frac{x_1P^+}{yp_1^+},\kappa_{1'\perp};\lambda_1,1/2\right\}\left\{\frac{x_2P^+}{yp_1^+},\kappa_{2'\perp};\lambda_2,1/2\right\}\left\{\frac{x_3P^+}{yp_1^+},\kappa_{3'\perp};\lambda_3,-1/2\right\}\right)\\
=\;&-\frac{24}{\sqrt{x_1x_2x_3}}\left(\frac{1}{2\xi}\right)^{\frac{3}{2}}\int\frac{\mathrm{d}y\mathrm{d}^2\mathbf{k}_\perp}{[2(2\pi)^3]^2}\int\prod_{i=1'}^{3'}\mathrm{d}^2\mathbf{k'}_{i\perp}\sqrt{y(1-y)}\\
&\times\delta\left(y-2\xi\frac{P^+}{p_1^+}\right)\delta\left(1-2\xi\frac{P^+}{p_1^+}-\frac{p_\pi^+}{p_1^+}\right)\delta^{(2)}\left(\mathbf{k}_\perp-\sum_{i=1'}^{3'}\mathbf{k'}_{i\perp}\right)\\
&\times\delta^{(2)}\left(\mathbf{p}_{\pi\perp}+\sum_{i=1'}^{3'}\mathbf{k'}_{i\perp}\right)\sum_{\lambda_1,\lambda_2,\lambda_3}\sum_{\lambda'}\phi_{\lambda'0}^{\lambda(N,N\pi)}\left(y,\mathbf{k}_\perp\right)\\
&\times u_{+\alpha}(x_1P^+,\lambda_1)u_{+\beta}(x_2P^+,\lambda_2)u_{+\gamma}(x_3P^+,\lambda_3)\\
&\times\tilde{\Psi}_{\lambda'}^{N,[f]}\left(\left\{\frac{x_1}{2\xi},\kappa_{1'\perp};\lambda_1,1/2\right\}\left\{\frac{x_2}{2\xi},\kappa_{2'\perp};\lambda_2,1/2\right\}\left\{\frac{x_3}{2\xi},\kappa_{3'\perp};\lambda_3,-1/2\right\}\right),
\end{aligned}
\tag{3.80}
$$

where we have made use of the normalization of the pion WF. Now we change the variable of integration from $\mathbf{k'}_{i\perp}$ to $\kappa_{i\perp}$ with the result**

$$
\begin{aligned}
D_{\alpha\beta,\gamma}^{\lambda}\;=\;&-\frac{24}{\sqrt{x_1x_2x_3}}\left(\frac{1}{2\xi}\right)^{\frac{3}{2}}\sum_{\lambda_1,\lambda_2,\lambda_3}u_{+\alpha}(x_1P^+,\lambda_1)u_{+\beta}(x_2P^+,\lambda_2)u_{+\gamma}(x_3P^+,\lambda_3)\\
&\times\sum_{\lambda'}\int\frac{\mathrm{d}y\mathrm{d}^2\mathbf{k}_\perp}{[2(2\pi)^3]^2}\phi_{\lambda'0}^{\lambda(N,N\pi)}\left(y,\mathbf{k}_\perp\right)\sqrt{y(1-y)}\delta\left(1-y-\frac{p_\pi^+}{p_1^+}\right)\\
&\times\int\prod_{i=1}^{3}\mathrm{d}^2\kappa_{i\perp}\delta^{(2)}\left(\sum_{i=1}^{3}\kappa_{i\perp}\right)\delta^{(2)}\left(\mathbf{p}_{\pi\perp}+\mathbf{k}_\perp\right)\\
&\times\tilde{\Psi}_{\lambda'}^{N,[f]}\left(\left\{\frac{x_1}{2\xi},\kappa_{1\perp};\lambda_1,1/2\right\}\left\{\frac{x_1}{2\xi},\kappa_{2\perp};\lambda_2,1/2\right\}\left\{\frac{x_1}{2\xi},\kappa_{3\perp};\lambda_3,-1/2\right\}\right).
\end{aligned}
\tag{3.81}
$$

**Where for the sake of convenience we have also replaced the dummy primed indexes ($i=1',2',3'$) with the indexes without a prime ($i=1,2,3$).

This last equation is the LCWF representation for the generic matrix element entering the definition of the TDAs. About the result in Eq. (3.81) we point out an interesting feature. The dependence from the light-cone momentum fraction in the LCWF is rescaled by a factor 2ξ with respect to the DAs case, as found in Ref. [207] in the so-called "soft pion limit" [221, 222] ($\Delta_\perp = 0, \xi \to 1$) and for the pion-nucleon GDAs in Ref. [230].

Matrix Elements to be calculated

From the Eqs. (3.47) it is easy to see that the only matrix elements that one has to calculate are: $D^{\uparrow}_{12,1}$, $D^{\uparrow}_{21,1}$, $D^{\uparrow}_{11,2}$, $D^{\uparrow}_{11,1}$, $D^{\uparrow}_{22,1}$, $D^{\uparrow}_{12,2}$, $D^{\uparrow}_{22,2}$ and $D^{\uparrow}_{21,2}$. Then, since the Dirac indexes entering the definitions of the matrix elements that we have to calculate in deriving the overlap representation for the TDAs automatically fix[††] the helicities of the active partons, the conservation of the total angular momentum allows to understand whether the three partons have to carry also orbital angular momentum (OAM). Namely if the partonic LCWFs can have only S-wave components or must have also higher wave contributions. Indeed, the value of the spin of the nucleon, s_1, should be obtained as a combination of the total angular momenta of the three quarks involved in the process. This means that if the helicities of the three partons do not sum up to give the proton spin, a contribution from the OAM is needed. In the following we report a table which summarize and clarify these statements.

[††]This is because of the form of the quark LC spinors

$$u_+(x_i P^+, \uparrow) = \sqrt{\frac{x_i P^+}{\sqrt{2}}} \begin{pmatrix} 1 \\ 0 \\ 1 \\ 0 \end{pmatrix} \quad \text{and} \quad u_+(x_i P^+, \downarrow) = \sqrt{\frac{x_i P^+}{\sqrt{2}}} \begin{pmatrix} 0 \\ 1 \\ 0 \\ -1 \end{pmatrix}, \quad i = 1, ..., 3.$$

Indeed, the choice of α, β or γ directly fixes the quark spin, e.g. $\alpha = 1$ or 3 means spin 1/2, and $\alpha = 2$ or 4 means spin -1/2 .

Table 3.1: Summary of the combinations of helicities and OAM carried by the active partons as results from the total angular momentum conservation law.

	s_1	λ_1	λ_2	λ_3	OAM
$D^{\uparrow}_{12,1}$	1/2	1/2	−1/2	1/2	*No*
$D^{\uparrow}_{21,1}$	1/2	−1/2	1/2	1/2	*No*
$D^{\uparrow}_{11,2}$	1/2	1/2	1/2	−1/2	*No*
$D^{\uparrow}_{11,1}$	1/2	1/2	1/2	1/2	*Yes*
$D^{\uparrow}_{22,2}$	1/2	−1/2	−1/2	−1/2	*Yes*
$D^{\uparrow}_{12,2}$	1/2	1/2	−1/2	−1/2	*Yes*
$D^{\uparrow}_{21,2}$	1/2	−1/2	1/2	−1/2	*Yes*
$D^{\uparrow}_{22,1}$	1/2	−1/2	−1/2	1/2	*Yes*

Hereafter we specify the result (3.81) for the eight matrix elements:

$$
\begin{aligned}
D^{\uparrow}_{12,1} &= -\frac{24}{\sqrt{x_1x_2x_3}}\left(\frac{1}{2\xi}\right)^{\frac{3}{2}} u_{+1}(x_1P^+,1/2)u_{+2}(x_2P^+,-1/2)u_{+1}(x_3P^+,1/2) \\
&\quad\times\sum_{\lambda'}\int\frac{\mathrm{d}y\mathrm{d}^2\mathbf{k}_\perp}{[2(2\pi)^3]^2}\phi^{\lambda(N,N\pi)}_{\lambda'0}\left(y,\mathbf{k}_\perp\right)\sqrt{y(1-y)}\delta\left(1-y-\frac{p^+_\pi}{p^+_1}\right) \\
&\quad\times\int\prod_{i=1}^{3}\mathrm{d}^2\kappa_{i\perp}\delta^{(2)}\left(\sum_{i=1}^{3}\kappa_{i\perp}\right)\delta^{(2)}\left(\mathbf{p}_{\pi\perp}+\mathbf{k}_\perp\right) \\
&\quad\times\tilde{\Psi}^{N,[f]}_{\lambda'}\left(\left\{\frac{x_1}{2\xi},\kappa_{1\perp};\frac{1}{2},\frac{1}{2}\right\}\left\{\frac{x_1}{2\xi},\kappa_{2\perp};-\frac{1}{2},\frac{1}{2}\right\}\left\{\frac{x_1}{2\xi},\kappa_{3\perp};\frac{1}{2},-\frac{1}{2}\right\}\right) \\
&= -\frac{24}{\sqrt{2\sqrt{2}}}\left(\frac{P^+}{2\xi}\right)^{\frac{3}{2}}\sum_{\lambda'}\int\frac{\mathrm{d}y\mathrm{d}^2\mathbf{k}_\perp}{[2(2\pi)^3]^2}\phi^{\lambda(N,N\pi)}_{\lambda'0}\left(y,\mathbf{k}_\perp\right)\sqrt{y(1-y)} \\
&\quad\times\delta\left(1-y-\frac{p^+_\pi}{p^+_1}\right)\int\prod_{i=1}^{3}\mathrm{d}^2\kappa_{i\perp}\delta^{(2)}\delta^{(2)}\left(\mathbf{p}_{\pi\perp}+\mathbf{k}_\perp\right) \\
&\quad\times\tilde{\Psi}^{N,[f]}_{\lambda'}\left(\left\{\frac{x_1}{2\xi},\kappa_{1\perp};\frac{1}{2},\frac{1}{2}\right\}\left\{\frac{x_1}{2\xi},\kappa_{2\perp};-\frac{1}{2},\frac{1}{2}\right\}\left\{\frac{x_1}{2\xi},\kappa_{3\perp};\frac{1}{2},-\frac{1}{2}\right\}\right);
\end{aligned}
\tag{3.82}
$$

$$
\begin{aligned}
D^{\uparrow}_{11,2} &= -\frac{24}{\sqrt{2\sqrt{2}}}\left(\frac{P^+}{2\xi}\right)^{\frac{3}{2}}\sum_{\lambda'}\int\frac{\mathrm{d}y\mathrm{d}^2\mathbf{k}_\perp}{[2(2\pi)^3]^2}\phi^{\lambda(N,N\pi)}_{\lambda' 0}\left(y,\mathbf{k}_\perp\right)\sqrt{y(1-y)} \\
&\times\delta\left(1-y-\frac{p^+_\pi}{p^+_1}\right)\int\prod_{i=1}^{3}\mathrm{d}^2\kappa_{i\perp}\delta^{(2)}\delta^{(2)}\left(\mathbf{p}_{\pi\perp}+\mathbf{k}_\perp\right) \\
&\times\tilde{\Psi}^{N,[f]}_{\lambda'}\left(\left\{\frac{x_1}{2\xi},\kappa_{1\perp};\frac{1}{2},\frac{1}{2}\right\}\left\{\frac{x_1}{2\xi},\kappa_{2\perp};\frac{1}{2},\frac{1}{2}\right\}\left\{\frac{x_1}{2\xi},\kappa_{3\perp};-\frac{1}{2},-\frac{1}{2}\right\}\right);
\end{aligned}
\tag{3.83}
$$

$$
\begin{aligned}
D^{\uparrow}_{21,1} &= -\frac{24}{\sqrt{2\sqrt{2}}}\left(\frac{P^+}{2\xi}\right)^{\frac{3}{2}}\sum_{\lambda'}\int\frac{\mathrm{d}y\mathrm{d}^2\mathbf{k}_\perp}{[2(2\pi)^3]^2}\phi^{\lambda(N,N\pi)}_{\lambda' 0}\left(y,\mathbf{k}_\perp\right)\sqrt{y(1-y)} \\
&\times\delta\left(1-y-\frac{p^+_\pi}{p^+_1}\right)\int\prod_{i=1}^{3}\mathrm{d}^2\kappa_{i\perp}\delta^{(2)}\delta^{(2)}\left(\mathbf{p}_{\pi\perp}+\mathbf{k}_\perp\right) \\
&\times\tilde{\Psi}^{N,[f]}_{\lambda'}\left(\left\{\frac{x_1}{2\xi},\kappa_{1\perp};-\frac{1}{2},\frac{1}{2}\right\}\left\{\frac{x_1}{2\xi},\kappa_{2\perp};\frac{1}{2},\frac{1}{2}\right\}\left\{\frac{x_1}{2\xi},\kappa_{3\perp};\frac{1}{2},-\frac{1}{2}\right\}\right);
\end{aligned}
\tag{3.84}
$$

$$
\begin{aligned}
D^{\uparrow}_{22,2} &= -\frac{24}{\sqrt{2\sqrt{2}}}\left(\frac{P^+}{2\xi}\right)^{\frac{3}{2}}\sum_{\lambda'}\int\frac{\mathrm{d}y\mathrm{d}^2\mathbf{k}_\perp}{[2(2\pi)^3]^2}\phi^{\lambda(N,N\pi)}_{\lambda' 0}\left(y,\mathbf{k}_\perp\right)\sqrt{y(1-y)} \\
&\times\delta\left(1-y-\frac{p^+_\pi}{p^+_1}\right)\int\prod_{i=1}^{3}\mathrm{d}^2\kappa_{i\perp}\delta^{(2)}\delta^{(2)}\left(\mathbf{p}_{\pi\perp}+\mathbf{k}_\perp\right) \\
&\times\tilde{\Psi}^{N,[f]}_{\lambda'}\left(\left\{\frac{x_1}{2\xi},\kappa_{1\perp};-\frac{1}{2},\frac{1}{2}\right\}\left\{\frac{x_1}{2\xi},\kappa_{2\perp};-\frac{1}{2},\frac{1}{2}\right\}\left\{\frac{x_1}{2\xi},\kappa_{3\perp};-\frac{1}{2},-\frac{1}{2}\right\}\right);
\end{aligned}
\tag{3.85}
$$

$$
\begin{aligned}
D^{\uparrow}_{12,2} &= -\frac{24}{\sqrt{2\sqrt{2}}}\left(\frac{P^+}{2\xi}\right)^{\frac{3}{2}}\sum_{\lambda'}\int\frac{\mathrm{d}y\mathrm{d}^2\mathbf{k}_\perp}{[2(2\pi)^3]^2}\phi^{\lambda(N,N\pi)}_{\lambda' 0}\left(y,\mathbf{k}_\perp\right)\sqrt{y(1-y)} \\
&\times\delta\left(1-y-\frac{p^+_\pi}{p^+_1}\right)\int\prod_{i=1}^{3}\mathrm{d}^2\kappa_{i\perp}\delta^{(2)}\delta^{(2)}\left(\mathbf{p}_{\pi\perp}+\mathbf{k}_\perp\right) \\
&\times\tilde{\Psi}^{N,[f]}_{\lambda'}\left(\left\{\frac{x_1}{2\xi},\kappa_{1\perp};\frac{1}{2},\frac{1}{2}\right\}\left\{\frac{x_1}{2\xi},\kappa_{2\perp};-\frac{1}{2},\frac{1}{2}\right\}\left\{\frac{x_1}{2\xi},\kappa_{3\perp};-\frac{1}{2},-\frac{1}{2}\right\}\right);
\end{aligned}
\tag{3.86}
$$

$$
\begin{aligned}
D^{\uparrow}_{11,1} &= -\frac{24}{\sqrt{2\sqrt{2}}}\left(\frac{P^+}{2\xi}\right)^{\frac{3}{2}}\sum_{\lambda'}\int\frac{\mathrm{d}y\mathrm{d}^2\mathbf{k}_\perp}{[2(2\pi)^3]^2}\phi^{\lambda(N,N\pi)}_{\lambda' 0}\left(y,\mathbf{k}_\perp\right)\sqrt{y(1-y)} \\
&\quad\times\delta\left(1-y-\frac{p^+_\pi}{p^+_1}\right)\int\prod_{i=1}^{3}\mathrm{d}^2\kappa_{i\perp}\delta^{(2)}\delta^{(2)}\left(\mathbf{p}_{\pi\perp}+\mathbf{k}_\perp\right) \\
&\quad\times\tilde{\Psi}^{N,[f]}_{\lambda'}\Bigg(\left\{\frac{x_1}{2\xi},\kappa_{1\perp};\frac{1}{2},\frac{1}{2}\right\}\left\{\frac{x_1}{2\xi},\kappa_{2\perp};\frac{1}{2},\frac{1}{2}\right\}\left\{\frac{x_1}{2\xi},\kappa_{3\perp};\frac{1}{2},-\frac{1}{2}\right\}\Bigg);
\end{aligned}
\tag{3.87}
$$

$$
\begin{aligned}
D^{\uparrow}_{22,1} &= -\frac{24}{\sqrt{2\sqrt{2}}}\left(\frac{P^+}{2\xi}\right)^{\frac{3}{2}}\sum_{\lambda'}\int\frac{\mathrm{d}y\mathrm{d}^2\mathbf{k}_\perp}{[2(2\pi)^3]^2}\phi^{\lambda(N,N\pi)}_{\lambda' 0}\left(y,\mathbf{k}_\perp\right)\sqrt{y(1-y)} \\
&\quad\times\delta\left(1-y-\frac{p^+_\pi}{p^+_1}\right)\int\prod_{i=1}^{3}\mathrm{d}^2\kappa_{i\perp}\delta^{(2)}\delta^{(2)}\left(\mathbf{p}_{\pi\perp}+\mathbf{k}_\perp\right) \\
&\quad\times\tilde{\Psi}^{N,[f]}_{\lambda'}\Bigg(\left\{\frac{x_1}{2\xi},\kappa_{1\perp};-\frac{1}{2},\frac{1}{2}\right\}\left\{\frac{x_1}{2\xi},\kappa_{2\perp};-\frac{1}{2},\frac{1}{2}\right\}\left\{\frac{x_1}{2\xi},\kappa_{3\perp};\frac{1}{2},-\frac{1}{2}\right\}\Bigg);
\end{aligned}
\tag{3.88}
$$

$$
\begin{aligned}
D^{\uparrow}_{21,2} &= -\frac{24}{\sqrt{2\sqrt{2}}}\left(\frac{P^+}{2\xi}\right)^{\frac{3}{2}}\sum_{\lambda'}\int\frac{\mathrm{d}y\mathrm{d}^2\mathbf{k}_\perp}{[2(2\pi)^3]^2}\phi^{\lambda(N,N\pi)}_{\lambda' 0}\left(y,\mathbf{k}_\perp\right)\sqrt{y(1-y)} \\
&\quad\times\delta\left(1-y-\frac{p^+_\pi}{p^+_1}\right)\int\prod_{i=1}^{3}\mathrm{d}^2\kappa_{i\perp}\delta^{(2)}\delta^{(2)}\left(\mathbf{p}_{\pi\perp}+\mathbf{k}_\perp\right) \\
&\quad\times\tilde{\Psi}^{N,[f]}_{\lambda'}\Bigg(\left\{\frac{x_1}{2\xi},\kappa_{1\perp};-\frac{1}{2},\frac{1}{2}\right\}\left\{\frac{x_1}{2\xi},\kappa_{2\perp};\frac{1}{2},\frac{1}{2}\right\}\left\{\frac{x_1}{2\xi},\kappa_{3\perp};-\frac{1}{2},-\frac{1}{2}\right\}\Bigg).
\end{aligned}
\tag{3.89}
$$

Now, introducing the expressions (C.10) for the LCWFs and defining $x'_i = x_i/2\xi$ and $a'_i = (m + x'_i M_0)$, we get

- $D^{\uparrow}_{11,2}$:

$$
\begin{aligned}
\lambda'=\frac{1}{2} \quad \Rightarrow \qquad & \tilde{\Psi}^{N,[f]}_{1/2}\left(\left\{\frac{x_1}{2\xi},\kappa_{1\perp};\frac{1}{2},\frac{1}{2}\right\}\left\{\frac{x_1}{2\xi},\kappa_{2\perp};\frac{1}{2},\frac{1}{2}\right\}\left\{\frac{x_1}{2\xi},\kappa_{3\perp};-\frac{1}{2},-\frac{1}{2}\right\}\right)\\
= \; & \frac{2}{\sqrt{3}}(2\pi)^3\left[\frac{1}{M_0}\frac{\omega_1\omega_2\omega_3}{x'_1x'_2x'_3}\right]^{\frac{1}{2}}\psi(\kappa_1,\kappa_2,\kappa_3)\\
& \times\sum_{\mu_1\mu_2\mu_3}\langle\mu_1|\frac{m+x'_1M_0+i\sigma^*\cdot(\hat{\mathbf{z}}\times\kappa_{1\perp})}{\sqrt{(m+x'_1M_0)^2+\kappa^2_{1\perp}}}|1/2\rangle\\
& \times\langle\mu_2|\frac{m+x'_2M_0+i\sigma^*\cdot(\hat{\mathbf{z}}\times\kappa_{2\perp})}{\sqrt{(m+x'_2M_0)^2+\kappa^2_{2\perp}}}|1/2\rangle\\
& \times\langle\mu_3|\frac{m+x'_3M_0+i\sigma^*\cdot(\hat{\mathbf{z}}\times\kappa_{3\perp})}{\sqrt{(m+x'_3M_0)^2+\kappa^2_{3\perp}}}|-1/2\rangle\\
& \times\sum_{M_{S_{12}}}\langle 1/2,\mu_1;1/2,\mu_2|1,M_{S_{12}}\rangle\langle 1,M_{S_{12}};1/2,\mu_3|1/2,1/2\rangle\\
= \; & \frac{2}{\sqrt{3}}(2\pi)^3\left[\frac{(2\xi)^3}{M_0}\frac{\omega_1\omega_2\omega_3}{x_1x_2x_3}\right]^{\frac{1}{2}}\psi(\kappa_1,\kappa_2,\kappa_3)\prod_{i=1}^{3}\frac{1}{\sqrt{N(x'_i,\boldsymbol{\kappa}_{\perp i})}}\\
& \times\left\{(\sqrt{2/3})\left[a'_1a'_2a'_3\right]+(1/\sqrt{6})\left[a'_1\kappa^L_2\kappa^R_3\right]+(1/\sqrt{6})\left[\kappa^L_1a'_2\kappa^R_3\right]\right\},
\end{aligned}
$$

$$
\begin{aligned}
\lambda'=-\frac{1}{2} \quad \Rightarrow \qquad & \tilde{\Psi}^{N,[f]}_{-1/2}\left(\left\{\frac{x_1}{2\xi},\kappa_{1\perp};\frac{1}{2},\frac{1}{2}\right\}\left\{\frac{x_1}{2\xi},\kappa_{2\perp};\frac{1}{2},\frac{1}{2}\right\}\left\{\frac{x_1}{2\xi},\kappa_{3\perp};-\frac{1}{2},-\frac{1}{2}\right\}\right)\\
= \; & \frac{2}{\sqrt{3}}(2\pi)^3\left[\frac{1}{M_0}\frac{\omega_1\omega_2\omega_3}{x'_1x'_2x'_3}\right]^{\frac{1}{2}}\psi(\kappa_1,\kappa_2,\kappa_3)\\
& \times\sum_{\mu_1\mu_2\mu_3}\langle\mu_1|\frac{m+x'_1M_0+i\sigma^*\cdot(\hat{\mathbf{z}}\times\kappa_{1\perp})}{\sqrt{(m+x'_1M_0)^2+\kappa^2_{1\perp}}}|1/2\rangle\\
& \times\langle\mu_2|\frac{m+x'_2M_0+i\sigma^*\cdot(\hat{\mathbf{z}}\times\kappa_{2\perp})}{\sqrt{(m+x'_2M_0)^2+\kappa^2_{2\perp}}}|1/2\rangle\\
& \times\langle\mu_3|\frac{m+x'_3M_0+i\sigma^*\cdot(\hat{\mathbf{z}}\times\kappa_{3\perp})}{\sqrt{(m+x'_3M_0)^2+\kappa^2_{3\perp}}}|-1/2\rangle\\
& \times\sum_{M_{S_{12}}}\langle 1/2,\mu_1;1/2,\mu_2|1,M_{S_{12}}\rangle\langle 1,M_{S_{12}};1/2,\mu_3|1/2,-1/2\rangle\\
= \; & \frac{2}{\sqrt{3}}(2\pi)^3\left[\frac{(2\xi)^3}{M_0}\frac{\omega_1\omega_2\omega_3}{x_1x_2x_3}\right]^{\frac{1}{2}}\psi(\kappa_1,\kappa_2,\kappa_3)\prod_{i=1}^{3}\frac{1}{\sqrt{N(x'_i,\boldsymbol{\kappa}_{\perp i})}}\\
& \times\left\{(1/\sqrt{6})\left[a'_1\kappa^L_2a'_3\right]+(1/\sqrt{6})\left[\kappa^L_1a'_2a'_3\right]+(\sqrt{2/3})\left[\kappa^L_1\kappa^L_2\kappa^R_3\right]\right\}.
\end{aligned}
$$

- $D^{\uparrow}_{12,1}$:

$$
\begin{aligned}
\lambda'=\frac{1}{2} \quad \Rightarrow \qquad & \tilde{\Psi}^{N,[f]}_{1/2}\left(\left\{\frac{x_1}{2\xi},\kappa_{1\perp};\frac{1}{2},\frac{1}{2}\right\}\left\{\frac{x_1}{2\xi},\kappa_{2\perp};-\frac{1}{2},\frac{1}{2}\right\}\left\{\frac{x_1}{2\xi},\kappa_{3\perp};\frac{1}{2},-\frac{1}{2}\right\}\right) \\
= \; & \frac{2}{\sqrt{3}}(2\pi)^3\left[\frac{1}{M_0}\frac{\omega_1\omega_2\omega_3}{x'_1x'_2x'_3}\right]^{\frac{1}{2}}\psi(\kappa_1,\kappa_2,\kappa_3) \\
& \times\sum_{\mu_1\mu_2\mu_3}\langle\mu_1|\frac{m+x'_1M_0+i\sigma^*\cdot(\hat{\mathbf{z}}\times\kappa_{1\perp})}{\sqrt{(m+x'_1M_0)^2+\kappa^2_{1\perp}}}|1/2\rangle \\
& \times\langle\mu_2|\frac{m+x'_2M_0+i\sigma^*\cdot(\hat{\mathbf{z}}\times\kappa_{2\perp})}{\sqrt{(m+x'_2M_0)^2+\kappa^2_{2\perp}}}|-1/2\rangle \\
& \times\langle\mu_3|\frac{m+x'_3M_0+i\sigma^*\cdot(\hat{\mathbf{z}}\times\kappa_{3\perp})}{\sqrt{(m+x'_3M_0)^2+\kappa^2_{3\perp}}}|1/2\rangle \\
& \times\sum_{M_{S_{12}}}\langle 1/2,\mu_1;1/2,\mu_2|1,M_{S_{12}}\rangle\langle 1,M_{S_{12}};1/2,\mu_3|1/2,1/2\rangle \\
= \; & \frac{2}{\sqrt{3}}(2\pi)^3\left[\frac{(2\xi)^3}{M_0}\frac{\omega_1\omega_2\omega_3}{x_1x_2x_3}\right]^{\frac{1}{2}}\psi(\kappa_1,\kappa_2,\kappa_3)\prod_{i=1}^{3}\frac{1}{\sqrt{N(x'_i,\boldsymbol{\kappa}_{\perp i})}} \\
& \times\left\{(-\sqrt{2/3})\left[a'_1\kappa^R_2\kappa^L_3\right]-(1/\sqrt{6})\left[a'_1a'_2a'_3\right]+(1/\sqrt{6})\left[\kappa^L_1\kappa^R_2a'_3\right]\right\},
\end{aligned}
$$

$$
\begin{aligned}
\lambda'=-\frac{1}{2} \quad \Rightarrow \qquad & \tilde{\Psi}^{N,[f]}_{-1/2}\left(\left\{\frac{x_1}{2\xi},\kappa_{1\perp};\frac{1}{2},\frac{1}{2}\right\}\left\{\frac{x_1}{2\xi},\kappa_{2\perp};-\frac{1}{2},\frac{1}{2}\right\}\left\{\frac{x_1}{2\xi},\kappa_{3\perp};\frac{1}{2},-\frac{1}{2}\right\}\right) \\
= \; & \frac{2}{\sqrt{3}}(2\pi)^3\left[\frac{1}{M_0}\frac{\omega_1\omega_2\omega_3}{x'_1x'_2x'_3}\right]^{\frac{1}{2}}\psi(\kappa_1,\kappa_2,\kappa_3) \\
& \times\sum_{\mu_1\mu_2\mu_3}\langle\mu_1|\frac{m+x'_1M_0+i\sigma^*\cdot(\hat{\mathbf{z}}\times\kappa_{1\perp})}{\sqrt{(m+x'_1M_0)^2+\kappa^2_{1\perp}}}|1/2\rangle \\
& \times\langle\mu_2|\frac{m+x'_2M_0+i\sigma^*\cdot(\hat{\mathbf{z}}\times\kappa_{2\perp})}{\sqrt{(m+x'_2M_0)^2+\kappa^2_{2\perp}}}|-1/2\rangle \\
& \times\langle\mu_3|\frac{m+x'_3M_0+i\sigma^*\cdot(\hat{\mathbf{z}}\times\kappa_{3\perp})}{\sqrt{(m+x'_3M_0)^2+\kappa^2_{3\perp}}}|1/2\rangle \\
& \times\sum_{M_{S_{12}}}\langle 1/2,\mu_1;1/2,\mu_2|1,M_{S_{12}}\rangle\langle 1,M_{S_{12}};1/2,\mu_3|1/2,-1/2\rangle \\
= \; & \frac{2}{\sqrt{3}}(2\pi)^3\left[\frac{(2\xi)^3}{M_0}\frac{\omega_1\omega_2\omega_3}{x_1x_2x_3}\right]^{\frac{1}{2}}\psi(\kappa_1,\kappa_2,\kappa_3)\prod_{i=1}^{3}\frac{1}{\sqrt{N(x'_i,\boldsymbol{\kappa}_{\perp i})}} \\
& \times\left\{(-\sqrt{2/3})\left[\kappa^L_1a'_2a'_3\right]+(1/\sqrt{6})\left[a'_1a'_2\kappa^L_3\right]-(1/\sqrt{6})\left[\kappa^L_1\kappa^R_2\kappa^L_3\right]\right\}.
\end{aligned}
$$

- $D^{\uparrow}_{21,1}$:

$$
\begin{aligned}
\lambda'=\frac{1}{2} \quad \Rightarrow \qquad & \tilde{\Psi}^{N,[f]}_{1/2}\Bigg(\left\{\frac{x_1}{2\xi},\kappa_{1\perp};-\frac{1}{2},\frac{1}{2}\right\}\left\{\frac{x_1}{2\xi},\kappa_{2\perp};\frac{1}{2},\frac{1}{2}\right\}\left\{\frac{x_1}{2\xi},\kappa_{3\perp};\frac{1}{2},-\frac{1}{2}\right\}\Bigg)\\
= \;& \frac{2}{\sqrt{3}}(2\pi)^3\left[\frac{1}{M_0}\frac{\omega_1\omega_2\omega_3}{x'_1x'_2x'_3}\right]^{\frac{1}{2}}\psi(\kappa_1,\kappa_2,\kappa_3)\\
& \times\sum_{\mu_1\mu_2\mu_3}\langle\mu_1|\frac{m+x'_1M_0+i\sigma^*\cdot(\hat{\mathbf{z}}\times\kappa_{1\perp})}{\sqrt{(m+x'_1M_0)^2+\kappa^2_{1\perp}}}|-1/2\rangle\\
& \times\langle\mu_2|\frac{m+x'_2M_0+i\sigma^*\cdot(\hat{\mathbf{z}}\times\kappa_{2\perp})}{\sqrt{(m+x'_2M_0)^2+\kappa^2_{2\perp}}}|1/2\rangle\\
& \times\langle\mu_3|\frac{m+x'_3M_0+i\sigma^*\cdot(\hat{\mathbf{z}}\times\kappa_{3\perp})}{\sqrt{(m+x'_3M_0)^2+\kappa^2_{3\perp}}}|1/2\rangle\\
& \times\sum_{M_{S_{12}}}\langle 1/2,\mu_1;1/2,\mu_2|1,M_{S_{12}}\rangle\langle 1,M_{S_{12}};1/2,\mu_3|1/2,1/2\rangle\\
= \;& -\frac{2}{\sqrt{3}}(2\pi)^3\left[\frac{(2\xi)^3}{M_0}\frac{\omega_1\omega_2\omega_3}{x_1x_2x_3}\right]^{\frac{1}{2}}\psi(\kappa_1,\kappa_2,\kappa_3)\prod_{i=1}^{3}\frac{1}{\sqrt{N(x'_i,\boldsymbol{\kappa}_{\perp i})}}\\
& \times\Bigg\{(\sqrt{2/3})\Big[\kappa^R_1a'_2\kappa^L_3\Big]+(1/\sqrt{6})\Big[a'_1a'_2a'_3\Big]-(\sqrt{1/6})\Big[\kappa^R_1\kappa^L_2a'_3\Big]\Bigg\},
\end{aligned}
$$

$$
\begin{aligned}
\lambda'=-\frac{1}{2} \quad \Rightarrow \qquad & \tilde{\Psi}^{N,[f]}_{-1/2}\Bigg(\left\{\frac{x_1}{2\xi},\kappa_{1\perp};-\frac{1}{2},\frac{1}{2}\right\}\left\{\frac{x_1}{2\xi},\kappa_{2\perp};\frac{1}{2},\frac{1}{2}\right\}\left\{\frac{x_1}{2\xi},\kappa_{3\perp};\frac{1}{2},-\frac{1}{2}\right\}\Bigg)\\
= \;& \frac{2}{\sqrt{3}}(2\pi)^3\left[\frac{1}{M_0}\frac{\omega_1\omega_2\omega_3}{x'_1x'_2x'_3}\right]^{\frac{1}{2}}\psi(\kappa_1,\kappa_2,\kappa_3)\\
& \times\sum_{\mu_1\mu_2\mu_3}\langle\mu_1|\frac{m+x'_1M_0+i\sigma^*\cdot(\hat{\mathbf{z}}\times\kappa_{1\perp})}{\sqrt{(m+x'_1M_0)^2+\kappa^2_{1\perp}}}|-1/2\rangle\\
& \times\langle\mu_2|\frac{m+x'_2M_0+i\sigma^*\cdot(\hat{\mathbf{z}}\times\kappa_{2\perp})}{\sqrt{(m+x'_2M_0)^2+\kappa^2_{2\perp}}}|1/2\rangle\\
& \times\langle\mu_3|\frac{m+x'_3M_0+i\sigma^*\cdot(\hat{\mathbf{z}}\times\kappa_{3\perp})}{\sqrt{(m+x'_3M_0)^2+\kappa^2_{3\perp}}}|1/2\rangle\\
& \times\sum_{M_{S_{12}}}\langle 1/2,\mu_1;1/2,\mu_2|1,M_{S_{12}}\rangle\langle 1,M_{S_{12}};1/2,\mu_3|1/2,-1/2\rangle\\
= \;& -\frac{2}{\sqrt{3}}(2\pi)^3\left[\frac{(2\xi)^3}{M_0}\frac{\omega_1\omega_2\omega_3}{x_1x_2x_3}\right]^{\frac{1}{2}}\psi(\kappa_1,\kappa_2,\kappa_3)\prod_{i=1}^{3}\frac{1}{\sqrt{N(x'_i,\boldsymbol{\kappa}_{\perp i})}}\\
& \times\Bigg\{1/\sqrt{6}\Big[a'_1a'_2\kappa^L_3\Big]-\sqrt{1/6}\Big[\kappa^R_1\kappa^L_2\kappa^L_3\Big]-\sqrt{2/3}\Big[a'_1\kappa^L_2a'_3\Big]\Bigg\}.
\end{aligned}
$$

- $D^{\uparrow}_{12,2}$:

$$
\begin{aligned}
\lambda'=\frac{1}{2} \quad \Rightarrow \qquad & \tilde{\Psi}^{N,[f]}_{1/2}\left(\left\{\frac{x_1}{2\xi},\kappa_{1\perp};\frac{1}{2},\frac{1}{2}\right\}\left\{\frac{x_1}{2\xi},\kappa_{2\perp};-\frac{1}{2},\frac{1}{2}\right\}\left\{\frac{x_1}{2\xi},\kappa_{3\perp};-\frac{1}{2},-\frac{1}{2}\right\}\right) \\
= \; & \frac{2}{\sqrt{3}}(2\pi)^3\left[\frac{1}{M_0}\frac{\omega_1\omega_2\omega_3}{x'_1x'_2x'_3}\right]^{\frac{1}{2}}\psi(\kappa_1,\kappa_2,\kappa_3) \\
& \times\sum_{\mu_1\mu_2\mu_3}\langle\mu_1|\frac{m+x'_1M_0+i\sigma^*\cdot(\hat{\mathbf{z}}\times\kappa_{1\perp})}{\sqrt{(m+x'_1M_0)^2+\kappa^2_{1\perp}}}|1/2\rangle \\
& \times\langle\mu_2|\frac{m+x'_2M_0+i\sigma^*\cdot(\hat{\mathbf{z}}\times\kappa_{2\perp})}{\sqrt{(m+x'_2M_0)^2+\kappa^2_{2\perp}}}|-1/2\rangle \\
& \times\langle\mu_3|\frac{m+x'_3M_0+i\sigma^*\cdot(\hat{\mathbf{z}}\times\kappa_{3\perp})}{\sqrt{(m+x'_3M_0)^2+\kappa^2_{3\perp}}}|-1/2\rangle \\
& \times\sum_{M_{S_{12}}}\langle 1/2,\mu_1;1/2,\mu_2|1,M_{S_{12}}\rangle\langle 1,M_{S_{12}};1/2,\mu_3|1/2,1/2\rangle \\
= \; & \frac{2}{\sqrt{3}}(2\pi)^3\left[\frac{(2\xi)^3}{M_0}\frac{\omega_1\omega_2\omega_3}{x_1x_2x_3}\right]^{\frac{1}{2}}\psi(\kappa_1,\kappa_2,\kappa_3)\prod_{i=1}^{3}\frac{1}{\sqrt{N(x'_i,\boldsymbol{\kappa}_{\perp i})}} \\
& \times\left\{(-\sqrt{2/3})\left[a'_1\kappa^R_2a'_3\right]+(1/\sqrt{6})\left[a'_1a'_2\kappa^R_3\right]-(1/\sqrt{6})\left[\kappa^L_1\kappa^R_2\kappa^R_3\right]\right\},
\end{aligned}
$$

$$
\begin{aligned}
\lambda'=-\frac{1}{2} \quad \Rightarrow \qquad & \tilde{\Psi}^{N,[f]}_{-1/2}\left(\left\{\frac{x_1}{2\xi},\kappa_{1\perp};\frac{1}{2},\frac{1}{2}\right\}\left\{\frac{x_1}{2\xi},\kappa_{2\perp};-\frac{1}{2},\frac{1}{2}\right\}\left\{\frac{x_1}{2\xi},\kappa_{3\perp};-\frac{1}{2},-\frac{1}{2}\right\}\right) \\
= \; & \frac{2}{\sqrt{3}}(2\pi)^3\left[\frac{1}{M_0}\frac{\omega_1\omega_2\omega_3}{x'_1x'_2x'_3}\right]^{\frac{1}{2}}\psi(\kappa_1,\kappa_2,\kappa_3) \\
& \times\sum_{\mu_1\mu_2\mu_3}\langle\mu_1|\frac{m+x'_1M_0+i\sigma^*\cdot(\hat{\mathbf{z}}\times\kappa_{1\perp})}{\sqrt{(m+x'_1M_0)^2+\kappa^2_{1\perp}}}|1/2\rangle \\
& \times\langle\mu_2|\frac{m+x'_2M_0+i\sigma^*\cdot(\hat{\mathbf{z}}\times\kappa_{2\perp})}{\sqrt{(m+x'_2M_0)^2+\kappa^2_{2\perp}}}|-1/2\rangle \\
& \times\langle\mu_3|\frac{m+x'_3M_0+i\sigma^*\cdot(\hat{\mathbf{z}}\times\kappa_{3\perp})}{\sqrt{(m+x'_3M_0)^2+\kappa^2_{3\perp}}}|-1/2\rangle \\
& \times\sum_{M_{S_{12}}}\langle 1/2,\mu_1;1/2,\mu_2|1,M_{S_{12}}\rangle\langle 1,M_{S_{12}};1/2,\mu_3|1/2,-1/2\rangle \\
= \; & \frac{2}{\sqrt{3}}(2\pi)^3\left[\frac{1}{M_0}\frac{\omega_1\omega_2\omega_3}{x'_1x'_2x'_3}\right]^{1/2}\psi(\mathbf{k}_1,\mathbf{k}_2,\mathbf{k}_3)\prod_{i=1}^{3}\frac{1}{\sqrt{N(x'_i,\boldsymbol{\kappa}_{\perp i})}} \\
& \times\left\{(1/\sqrt{6})\left[a'_1a'_2a'_3\right]-(1/\sqrt{6})\left[\kappa^L_1\kappa^R_2a'_3\right]+(\sqrt{2/3})\left[\kappa^L_1a'_2\kappa^R_3\right]\right\};
\end{aligned}
$$

- $D^{\uparrow}_{22,1}$:

$$
\begin{aligned}
\lambda' = \frac{1}{2} \quad \Rightarrow \qquad & \tilde{\Psi}^{N,[f]}_{1/2}\left(\left\{ \frac{x_1}{2\xi}, \kappa_{1\perp}; -\frac{1}{2}, \frac{1}{2} \right\} \left\{ \frac{x_1}{2\xi}, \kappa_{2\perp}; -\frac{1}{2}, \frac{1}{2} \right\} \left\{ \frac{x_1}{2\xi}, \kappa_{3\perp}; \frac{1}{2}, -\frac{1}{2} \right\} \right) \\
= \; & \frac{2}{\sqrt{3}}(2\pi)^3 \left[\frac{1}{M_0} \frac{\omega_1\omega_2\omega_3}{x'_1x'_2x'_3} \right]^{\frac{1}{2}} \psi(\kappa_1, \kappa_2, \kappa_3) \\
& \times \sum_{\mu_1\mu_2\mu_3} \langle \mu_1 | \frac{m + x'_1M_0 + i\sigma^* \cdot (\hat{\mathbf{z}} \times \kappa_{1\perp})}{\sqrt{(m + x'_1M_0)^2 + \kappa^2_{1\perp}}} | -1/2 \rangle \\
& \times \langle \mu_2 | \frac{m + x'_2M_0 + i\sigma^* \cdot (\hat{\mathbf{z}} \times \kappa_{2\perp})}{\sqrt{(m + x'_2M_0)^2 + \kappa^2_{2\perp}}} | -1/2 \rangle \\
& \times \langle \mu_3 | \frac{m + x'_3M_0 + i\sigma^* \cdot (\hat{\mathbf{z}} \times \kappa_{3\perp})}{\sqrt{(m + x'_3M_0)^2 + \kappa^2_{3\perp}}} | 1/2 \rangle \\
& \times \sum_{M_{S_{12}}} \langle 1/2, \mu_1; 1/2, \mu_2 | 1, M_{S_{12}} \rangle \langle 1, M_{S_{12}}; 1/2, \mu_3 | 1/2, 1/2 \rangle \\
= \; & \frac{2}{\sqrt{3}}(2\pi)^3 \left[\frac{(2\xi)^3}{M_0} \frac{\omega_1\omega_2\omega_3}{x_1x_2x_3} \right]^{\frac{1}{2}} \psi(\kappa_1, \kappa_2, \kappa_3) \\
& \times \prod_{i=1}^{3} \frac{1}{\sqrt{N(x'_i, \boldsymbol{\kappa}_{\perp i})}} \\
& \times \left\{ (\sqrt{2/3}) \left[\kappa^R_1 \kappa^R_2 \kappa^L_3 \right] + (1/\sqrt{6}) \left[a'_1 \kappa^R_2 a'_3 \right] + (1/\sqrt{6}) \left[\kappa^R_1 a'_2 \kappa^L_3 \right] \right\},
\end{aligned}
$$

$$
\begin{aligned}
\lambda'=-\frac{1}{2} \quad \Rightarrow \qquad & \tilde{\Psi}^{N,[f]}_{-1/2}\left(\left\{\frac{x_1}{2\xi},\kappa_{1\perp};-\frac{1}{2},\frac{1}{2}\right\}\left\{\frac{x_1}{2\xi},\kappa_{2\perp};-\frac{1}{2},\frac{1}{2}\right\}\left\{\frac{x_1}{2\xi},\kappa_{3\perp};\frac{1}{2},-\frac{1}{2}\right\}\right) \\
= \; & \frac{2}{\sqrt{3}}(2\pi)^3\left[\frac{1}{M_0}\frac{\omega_1\omega_2\omega_3}{x_1'x_2'x_3'}\right]^{\frac{1}{2}}\psi(\kappa_1,\kappa_2,\kappa_3) \\
& \times\sum_{\mu_1\mu_2\mu_3}\langle\mu_1|\frac{m+x_1'M_0+i\sigma^*\cdot(\hat{\mathbf{z}}\times\kappa_{1\perp})}{\sqrt{(m+x_1'M_0)^2+\kappa_{1\perp}^2}}|-1/2\rangle \\
& \times\langle\mu_2|\frac{m+x_2'M_0+i\sigma^*\cdot(\hat{\mathbf{z}}\times\kappa_{2\perp})}{\sqrt{(m+x_2'M_0)^2+\kappa_{2\perp}^2}}|-1/2\rangle \\
& \times\langle\mu_3|\frac{m+x_3'M_0+i\sigma^*\cdot(\hat{\mathbf{z}}\times\kappa_{3\perp})}{\sqrt{(m+x_3'M_0)^2+\kappa_{3\perp}^2}}|1/2\rangle \\
& \times\sum_{M_{S_{12}}}\langle 1/2,\mu_1;1/2,\mu_2|1,M_{S_{12}}\rangle\langle 1,M_{S_{12}};1/2,\mu_3|1/2,-1/2\rangle \\
= \; & \frac{2}{\sqrt{3}}(2\pi)^3\left[\frac{(2\xi)^3}{M_0}\frac{\omega_1\omega_2\omega_3}{x_1x_2x_3}\right]^{\frac{1}{2}}\psi(\kappa_1,\kappa_2,\kappa_3)\prod_{i=1}^{3}\frac{1}{\sqrt{N(x_i',\boldsymbol{\kappa}_{\perp i})}} \\
& \times\Big\{-(1/\sqrt{6})\Big[a_1'\kappa_2^R\kappa_3^L\Big]-(1/\sqrt{6})\Big[(\kappa_1^Ra_2'\kappa_3^L\Big]-\sqrt{2/3}\Big[a_1'a_2'a_3'\Big]\Big\}.
\end{aligned}
$$

- $D^{\uparrow}_{11,1}$:

$$
\begin{aligned}
\lambda'=\frac{1}{2} \quad \Rightarrow \qquad & \tilde{\Psi}^{N,[f]}_{1/2}\left(\left\{\frac{x_1}{2\xi},\kappa_{1\perp};\frac{1}{2},\frac{1}{2}\right\}\left\{\frac{x_1}{2\xi},\kappa_{2\perp};\frac{1}{2},\frac{1}{2}\right\}\left\{\frac{x_1}{2\xi},\kappa_{3\perp};\frac{1}{2},-\frac{1}{2}\right\}\right) \\
= \; & \frac{2}{\sqrt{3}}(2\pi)^3\left[\frac{1}{M_0}\frac{\omega_1\omega_2\omega_3}{x_1'x_2'x_3'}\right]^{\frac{1}{2}}\psi(\kappa_1,\kappa_2,\kappa_3) \\
& \times\sum_{\mu_1\mu_2\mu_3}\langle\mu_1|\frac{m+x_1'M_0+i\sigma^*\cdot(\hat{\mathbf{z}}\times\kappa_{1\perp})}{\sqrt{(m+x_1'M_0)^2+\kappa_{1\perp}^2}}|1/2\rangle \\
& \times\langle\mu_2|\frac{m+x_2'M_0+i\sigma^*\cdot(\hat{\mathbf{z}}\times\kappa_{2\perp})}{\sqrt{(m+x_2'M_0)^2+\kappa_{2\perp}^2}}|1/2\rangle \\
& \times\langle\mu_3|\frac{m+x_3'M_0+i\sigma^*\cdot(\hat{\mathbf{z}}\times\kappa_{3\perp})}{\sqrt{(m+x_3'M_0)^2+\kappa_{3\perp}^2}}|1/2\rangle \\
& \times\sum_{M_{S_{12}}}\langle 1/2,\mu_1;1/2,\mu_2|1,M_{S_{12}}\rangle\langle 1,M_{S_{12}};1/2,\mu_3|1/2,1/2\rangle \\
= \; & \frac{2}{\sqrt{3}}(2\pi)^3\left[\frac{(2\xi)^3}{M_0}\frac{\omega_1\omega_2\omega_3}{x_1x_2x_3}\right]^{\frac{1}{2}}\psi(\kappa_1,\kappa_2,\kappa_3)\prod_{i=1}^{3}\frac{1}{\sqrt{N(x_i',\boldsymbol{\kappa}_{\perp i})}} \\
& \times\Big\{(\sqrt{2/3})\Big[a_1'a_2'\kappa_3^L\Big]-(1/\sqrt{6})\Big[a_1'\kappa_2^La_2'\Big]-(1/\sqrt{6})\Big[\kappa_1^La_2'a_3'\Big]\Big\},
\end{aligned}
$$

$$
\begin{aligned}
\lambda'=-\frac{1}{2} \quad \Rightarrow \qquad & \tilde{\Psi}^{N,[f]}_{-1/2}\left(\left\{\frac{x_1}{2\xi},\kappa_{1\perp};\frac{1}{2},\frac{1}{2}\right\}\left\{\frac{x_1}{2\xi},\kappa_{2\perp};\frac{1}{2},\frac{1}{2}\right\}\left\{\frac{x_1}{2\xi},\kappa_{3\perp};\frac{1}{2},-\frac{1}{2}\right\}\right) \\
= \; & \frac{2}{\sqrt{3}}(2\pi)^3\left[\frac{1}{M_0}\frac{\omega_1\omega_2\omega_3}{x_1'x_2'x_3'}\right]^{\frac{1}{2}}\psi(\kappa_1,\kappa_2,\kappa_3) \\
& \times\sum_{\mu_1\mu_2\mu_3}\langle\mu_1|\frac{m+x_1'M_0+i\sigma^*\cdot(\hat{\mathbf{z}}\times\kappa_{1\perp})}{\sqrt{(m+x_1'M_0)^2+\kappa_{1\perp}^2}}|1/2\rangle \\
& \times\langle\mu_2|\frac{m+x_2'M_0+i\sigma^*\cdot(\hat{\mathbf{z}}\times\kappa_{2\perp})}{\sqrt{(m+x_2'M_0)^2+\kappa_{2\perp}^2}}|1/2\rangle \\
& \times\langle\mu_3|\frac{m+x_3'M_0+i\sigma^*\cdot(\hat{\mathbf{z}}\times\kappa_{3\perp})}{\sqrt{(m+x_3'M_0)^2+\kappa_{3\perp}^2}}|1/2\rangle \\
& \times\sum_{M_{S_{12}}}\langle 1/2,\mu_1;1/2,\mu_2|1,M_{S_{12}}\rangle\langle 1,M_{S_{12}};1/2,\mu_3|1/2,1/2\rangle \\
= \; & \frac{2}{\sqrt{3}}(2\pi)^3\left[\frac{(2\xi)^3}{M_0}\frac{\omega_1\omega_2\omega_3}{x_1x_2x_3}\right]^{\frac{1}{2}}\psi(\kappa_1,\kappa_2,\kappa_3)\prod_{i=1}^{3}\frac{1}{\sqrt{N(x_i',\boldsymbol{\kappa}_{\perp i})}} \\
& \times\left\{(1/\sqrt{6})\left[a_1'\kappa_2^L\kappa_3^L\right]+(1/\sqrt{6})\left[\kappa_1^L a_2'\kappa_3^L\right]-(\sqrt{2/3})\left[\kappa_1^L\kappa_2^L a_3'\right]\right\}.
\end{aligned}
$$

- $D^{\uparrow}_{22,2}$:

$$
\begin{aligned}
\lambda'=\frac{1}{2} \quad \Rightarrow \qquad & \tilde{\Psi}^{N,[f]}_{1/2}\left(\left\{\frac{x_1}{2\xi},\kappa_{1\perp};-\frac{1}{2},\frac{1}{2}\right\}\left\{\frac{x_1}{2\xi},\kappa_{2\perp};-\frac{1}{2},\frac{1}{2}\right\}\left\{\frac{x_1}{2\xi},\kappa_{3\perp};-\frac{1}{2},-\frac{1}{2}\right\}\right) \\
= \; & \frac{2}{\sqrt{3}}(2\pi)^3\left[\frac{1}{M_0}\frac{\omega_1\omega_2\omega_3}{x_1'x_2'x_3'}\right]^{\frac{1}{2}}\psi(\kappa_1,\kappa_2,\kappa_3) \\
& \times\sum_{\mu_1\mu_2\mu_3}\langle\mu_1|\frac{m+x_1'M_0+i\sigma^*\cdot(\hat{\mathbf{z}}\times\kappa_{1\perp})}{\sqrt{(m+x_1'M_0)^2+\kappa_{1\perp}^2}}|-1/2\rangle\langle \\
& \times\mu_2|\frac{m+x_2'M_0+i\sigma^*\cdot(\hat{\mathbf{z}}\times\kappa_{2\perp})}{\sqrt{(m+x_2'M_0)^2+\kappa_{2\perp}^2}}|-1/2\rangle \\
& \times\langle\mu_3|\frac{m+x_3'M_0+i\sigma^*\cdot(\hat{\mathbf{z}}\times\kappa_{3\perp})}{\sqrt{(m+x_3'M_0)^2+\kappa_{3\perp}^2}}|-1/2\rangle \\
& \times\sum_{M_{S_{12}}}\langle 1/2,\mu_1;1/2,\mu_2|1,M_{S_{12}}\rangle\langle 1,M_{S_{12}};1/2,\mu_3|1/2,1/2\rangle \\
= \; & \frac{2}{\sqrt{3}}(2\pi)^3\left[\frac{(2\xi)^3}{M_0}\frac{\omega_1\omega_2\omega_3}{x_1x_2x_3}\right]^{\frac{1}{2}}\psi(\kappa_1,\kappa_2,\kappa_3) \\
& \times\prod_{i=1}^{3}\frac{1}{\sqrt{N(x_i',\boldsymbol{\kappa}_{\perp i})}} \\
& \times\left\{(\sqrt{2/3})\left[\kappa_1^R\kappa_2^R a_3'\right]-(1/\sqrt{6})\left[a_1'\kappa_2^R\kappa_3^R)\right]-(1/\sqrt{6})\left[\kappa_1^R a_2'\kappa_3^R\right]\right\},
\end{aligned}
$$

$$
\begin{aligned}
\lambda'=-\frac{1}{2} \quad \Rightarrow \qquad & \tilde{\Psi}^{N,[f]}_{-1/2}\Bigg(\left\{\frac{x_1}{2\xi},\kappa_{1\perp};-\frac{1}{2},\frac{1}{2}\right\}\left\{\frac{x_1}{2\xi},\kappa_{2\perp};-\frac{1}{2},\frac{1}{2}\right\}\left\{\frac{x_1}{2\xi},\kappa_{3\perp};-\frac{1}{2},-\frac{1}{2}\right\}\Bigg) \\
= \; & \frac{2}{\sqrt{3}}(2\pi)^3\left[\frac{1}{M_0}\frac{\omega_1\omega_2\omega_3}{x_1'x_2'x_3'}\right]^{\frac{1}{2}}\psi(\kappa_1,\kappa_2,\kappa_3) \\
& \times\sum_{\mu_1\mu_2\mu_3}\langle\mu_1|\frac{m+x_1'M_0+i\sigma^*\cdot(\hat{\mathbf{z}}\times\kappa_{1\perp})}{\sqrt{(m+x_1'M_0)^2+\kappa_{1\perp}^2}}|-1/2\rangle\langle \\
& \times\mu_2|\frac{m+x_2'M_0+i\sigma^*\cdot(\hat{\mathbf{z}}\times\kappa_{2\perp})}{\sqrt{(m+x_2'M_0)^2+\kappa_{2\perp}^2}}|-1/2\rangle \\
& \times\langle\mu_3|\frac{m+x_3'M_0+i\sigma^*\cdot(\hat{\mathbf{z}}\times\kappa_{3\perp})}{\sqrt{(m+x_3'M_0)^2+\kappa_{3\perp}^2}}|-1/2\rangle \\
& \times\sum_{M_{S_{12}}}\langle 1/2,\mu_1;1/2,\mu_2|1,M_{S_{12}}\rangle\langle 1,M_{S_{12}};1/2,\mu_3|1/2,1/2\rangle \\
= \; & \frac{2}{\sqrt{3}}(2\pi)^3\left[\frac{(2\xi)^3}{M_0}\frac{\omega_1\omega_2\omega_3}{x_1x_2x_3}\right]^{\frac{1}{2}}\psi(\kappa_1,\kappa_2,\kappa_3)\prod_{i=1}^{3}\frac{1}{\sqrt{N(x_i',\boldsymbol{\kappa}_{\perp i})}} \\
& \times\Bigg\{\sqrt{2/3}\Big[a_1'a_2'\kappa_3^R\Big]-(1/\sqrt{6})\Big[\kappa_1^Ra_2'a_3'\Big]-(1/\sqrt{6})\Big[a_1'\kappa_2^Ra_3'\Big]\Bigg\}.
\end{aligned}
$$

- $D^{\uparrow}_{21,2}$:

$$
\begin{aligned}
\lambda'=\frac{1}{2} \quad \Rightarrow \qquad & \tilde{\Psi}^{N,[f]}_{1/2}\Bigg(\left\{\frac{x_1}{2\xi},\kappa_{1\perp};-\frac{1}{2},\frac{1}{2}\right\}\left\{\frac{x_1}{2\xi},\kappa_{2\perp};\frac{1}{2},\frac{1}{2}\right\}\left\{\frac{x_1}{2\xi},\kappa_{3\perp};-\frac{1}{2},-\frac{1}{2}\right\}\Bigg) \\
= \; & \frac{2}{\sqrt{3}}(2\pi)^3\left[\frac{1}{M_0}\frac{\omega_1\omega_2\omega_3}{x_1'x_2'x_3'}\right]^{\frac{1}{2}}\psi(\kappa_1,\kappa_2,\kappa_3) \\
& \times\sum_{\mu_1\mu_2\mu_3}\langle\mu_1|\frac{m+x_1'M_0+i\sigma^*\cdot(\hat{\mathbf{z}}\times\kappa_{1\perp})}{\sqrt{(m+x_1'M_0)^2+\kappa_{1\perp}^2}}|-1/2\rangle \\
& \times\langle\mu_2|\frac{m+x_2'M_0+i\sigma^*\cdot(\hat{\mathbf{z}}\times\kappa_{2\perp})}{\sqrt{(m+x_2'M_0)^2+\kappa_{2\perp}^2}}|1/2\rangle \\
& \times\langle\mu_3|\frac{m+x_3'M_0+i\sigma^*\cdot(\hat{\mathbf{z}}\times\kappa_{3\perp})}{\sqrt{(m+x_3'M_0)^2+\kappa_{3\perp}^2}}|-1/2\rangle \\
& \times\sum_{M_{S_{12}}}\langle 1/2,\mu_1;1/2,\mu_2|1,M_{S_{12}}\rangle\langle 1,M_{S_{12}};1/2,\mu_3|1/2,1/2\rangle \\
= \; & \frac{2}{\sqrt{3}}(2\pi)^3\left[\frac{(2\xi)^3}{M_0}\frac{\omega_1\omega_2\omega_3}{x_1x_2x_3}\right]^{\frac{1}{2}}\psi(\kappa_1,\kappa_2,\kappa_3)\prod_{i=1}^{3}\frac{1}{\sqrt{N(x_i',\boldsymbol{\kappa}_{\perp i})}} \\
& \times\Bigg\{(-\sqrt{2/3})\Big[\kappa_1^Ra_2'a_3'\Big]-(1/\sqrt{6})\Big[\kappa_1^R\kappa_2^L\kappa_3^R\Big]+(1/\sqrt{6})\Big[a_1'a_2'\kappa_3^R\Big]\Bigg\},
\end{aligned}
$$

$$
\begin{aligned}
\lambda'=-\frac{1}{2} \quad \Rightarrow \qquad & \tilde{\Psi}^{N,[f]}_{-1/2}\left(\left\{\frac{x_1}{2\xi},\kappa_{1\perp};-\frac{1}{2},\frac{1}{2}\right\}\left\{\frac{x_1}{2\xi},\kappa_{2\perp};\frac{1}{2},\frac{1}{2}\right\}\left\{\frac{x_1}{2\xi},\kappa_{3\perp};-\frac{1}{2},-\frac{1}{2}\right\}\right) \\
= \; & \frac{2}{\sqrt{3}}(2\pi)^3\left[\frac{1}{M_0}\frac{\omega_1\omega_2\omega_3}{x_1'x_2'x_3'}\right]^{\frac{1}{2}}\psi(\kappa_1,\kappa_2,\kappa_3) \\
& \times\sum_{\mu_1\mu_2\mu_3}\langle\mu_1|\frac{m+x_1'M_0+i\sigma^*\cdot(\hat{\mathbf{z}}\times\kappa_{1\perp})}{\sqrt{(m+x_1'M_0)^2+\kappa_{1\perp}^2}}|-1/2\rangle \\
& \times\langle\mu_2|\frac{m+x_2'M_0+i\sigma^*\cdot(\hat{\mathbf{z}}\times\kappa_{2\perp})}{\sqrt{(m+x_2'M_0)^2+\kappa_{2\perp}^2}}|1/2\rangle \\
& \times\langle\mu_3|\frac{m+x_3'M_0+i\sigma^*\cdot(\hat{\mathbf{z}}\times\kappa_{3\perp})}{\sqrt{(m+x_3'M_0)^2+\kappa_{3\perp}^2}}|-1/2\rangle \\
& \times\sum_{M_{S_{12}}}\langle 1/2,\mu_1;1/2,\mu_2|1,M_{S_{12}}\rangle\langle 1,M_{S_{12}};1/2,\mu_3|1/2,1/2\rangle \\
= \; & \frac{2}{\sqrt{3}}(2\pi)^3\left[\frac{(2\xi)^3}{M_0}\frac{\omega_1\omega_2\omega_3}{x_1x_2x_3}\right]^{\frac{1}{2}}\psi(\kappa_1,\kappa_2,\kappa_3) \\
& \times\prod_{i=1}^{3}\frac{1}{\sqrt{N(x_i',\boldsymbol{\kappa}_{\perp i})}} \\
& \times\left\{\sqrt{2/3}\Big[a_1'\kappa_2^L\kappa_1^R\Big]-(1/\sqrt{6})\Big[\kappa_1^R\kappa_2^La_3'\Big]+(1/\sqrt{6})\Big[a_1'a_2'a_3'\Big]\right\}.
\end{aligned}
$$

Analytical Results

In this section we collect the analytical results obtained for the matrix elements (Eqs. [(3.82)–(3.89)]) entering the definition of the eight Transition Distribution Amplitudes, see Eqs. (3.47); and then we report explicitly the LCWFs representation for three of them.

$$
\begin{aligned}
D^{\uparrow}_{11,2} \; = \; & -\frac{8(P^+)^{\frac{3}{2}}}{\sqrt{2\sqrt{2}}}\left[\frac{1}{M_0}\frac{\omega_1\omega_2\omega_3}{x_1x_2x_3}\right]^{\frac{1}{2}}\int\frac{\mathrm{d}y\mathrm{d}^2\mathbf{k}_\perp}{16\pi^3}\int\prod_{i=1}^{3}\mathrm{d}^2\kappa_{i\perp}\sqrt{y(1-y)} \\
& \times\delta\left(1-y-\frac{p_\pi^+}{p_1^+}\right)\delta^{(2)}\left(\sum_{i=1}^{3}\kappa_{i\perp}\right)\psi(\kappa_1,\kappa_2,\kappa_3)\prod_{i=1}^{3}\frac{1}{\sqrt{N(x_i',\boldsymbol{\kappa}_{\perp i})}} \\
& \times\Bigg\{\phi^{1/2\,(N,N\pi)}_{1/20}(y,\mathbf{k}_\perp)\Big[\sqrt{2}a_1'a_2'a_3' \\
& \quad +(1/\sqrt{2})a_1'\kappa_2^L\kappa_3^R+(1/\sqrt{2})\kappa_1^La_2'\kappa_3^R \\
& \; +\phi^{1/2\,(N,N\pi)}_{-1/20}(y,\mathbf{k}_\perp)\Big[(1/\sqrt{2})a_1'\kappa_2^La_3' \\
& \quad +(1/\sqrt{2})\kappa_1^La_2'a_3'+(\sqrt{2})\kappa_1^L\kappa_2^R\kappa_3^R\Big]\Bigg\}\delta^{(2)}\Big(\mathbf{p}_{\pi\perp}+\mathbf{k}_\perp\Big); \qquad (3.90)
\end{aligned}
$$

$$
\begin{aligned}
\bullet\ D^{\uparrow}_{12,1} \;=\;& \frac{8(P^+)^{\frac{3}{2}}}{\sqrt{2\sqrt{2}}}\left[\frac{1}{M_0}\frac{\omega_1\omega_2\omega_3}{x_1x_2x_3}\right]^{\frac{1}{2}}\int\frac{\mathrm{d}y\mathrm{d}^2\mathbf{k}_\perp}{16\pi^3}\int\prod_{i=1}^{3}\mathrm{d}^2\kappa_{i\perp}\sqrt{y(1-y)}\\
&\times\delta\Big(1-y-\frac{p_\pi^+}{p_1^+}\Big)\delta^{(2)}\Big(\sum_{i=1}^{3}\kappa_{i\perp}\Big)\psi(\kappa_1,\kappa_2,\kappa_3)\prod_{i=1}^{3}\frac{1}{\sqrt{N(x_i',\boldsymbol{\kappa}_{\perp i})}}\\
&\times\Big\{\phi_{1/20}^{1/2\,(N,N\pi)}(y,\mathbf{k}_\perp)\Big[\sqrt{2}a_1'\kappa_2^R\kappa_3^L\\
&\quad+(1/\sqrt{2})a_1'a_2'a_3'-(1/\sqrt{2})\kappa_1^L\kappa_2^Ra_3'\\
&\quad+\phi_{-1/20}^{1/2\,(N,N\pi)}(y,\mathbf{k}_\perp)\Big[(-\sqrt{2})\kappa_1^La_2'a_3'\\
&\quad+(1/\sqrt{2})a_1'a_2'\kappa_3^L-(1/\sqrt{2})\kappa_1^L\kappa_2^R\kappa_3^L\Big]\Big\}\delta^{(2)}\Big(\mathbf{p}_{\pi\perp}+\mathbf{k}_\perp\Big);\quad(3.91)
\end{aligned}
$$

$$
\begin{aligned}
\bullet\ D^{\uparrow}_{12,2} \;=\;& -\frac{8(P^+)^{\frac{3}{2}}}{\sqrt{2\sqrt{2}}}\left[\frac{1}{M_0}\frac{\omega_1\omega_2\omega_3}{x_1x_2x_3}\right]^{\frac{1}{2}}\int\frac{\mathrm{d}y\mathrm{d}^2\mathbf{k}_\perp}{16\pi^3}\int\prod_{i=1}^{3}\mathrm{d}^2\kappa_{i\perp}\sqrt{y(1-y)}\\
&\times\delta\Big(1-y-\frac{p_\pi^+}{p_1^+}\Big)\delta^{(2)}\Big(\sum_{i=1}^{3}\kappa_{i\perp}\Big)\psi(\kappa_1,\kappa_2,\kappa_3)\prod_{i=1}^{3}\frac{1}{\sqrt{N(x_i',\boldsymbol{\kappa}_{\perp i})}}\\
&\times\Big\{\phi_{1/20}^{1/2\,(N,N\pi)}(y,\mathbf{k}_\perp)\Big[\sqrt{2}a_1'\kappa_2^Ra_3'\\
&\quad-(1/\sqrt{2})a_1'a_2'\kappa_3^R+(1/\sqrt{2})\kappa_1^L\kappa_2^R\kappa_3^R\Big]\\
&\quad+\phi_{-1/20}^{1/2\,(N,N\pi)}(y,\mathbf{k}_\perp)\Big[(1/\sqrt{2})a_1'a_2'a_3'\\
&\quad-(1/\sqrt{2})\kappa_1^L\kappa_2^Ra_3'+(\sqrt{2})\kappa_1^La_2'\kappa_3^R\Big]\Big\}\delta^{(2)}\Big(\mathbf{p}_{\pi\perp}+\mathbf{k}_\perp\Big);\quad(3.92)
\end{aligned}
$$

$$
\begin{aligned}
\bullet\ D^{\uparrow}_{11,1} \;=\;& \frac{8(P^+)^{\frac{3}{2}}}{\sqrt{2\sqrt{2}}}\left[\frac{1}{M_0}\frac{\omega_1\omega_2\omega_3}{x_1x_2x_3}\right]^{\frac{1}{2}}\int\frac{\mathrm{d}y\mathrm{d}^2\mathbf{k}_\perp}{16\pi^3}\int\prod_{i=1}^{3}\mathrm{d}^2\kappa_{i\perp}\sqrt{y(1-y)})\\
&\times\delta\Big(1-y-\frac{p_\pi^+}{p_1^+}\Big)\delta^{(2)}\Big(\sum_{i=1}^{3}\kappa_{i\perp}\Big)\psi(\kappa_1,\kappa_2,\kappa_3)\prod_{i=1}^{3}\frac{1}{\sqrt{N(x_i',\boldsymbol{\kappa}_{\perp i})}}\\
&\times\Big\{\phi_{1/20}^{1/2\,(N,N\pi)}(y,\mathbf{k}_\perp)\Big[\sqrt{2}a_1'a_2'\kappa_3^L\\
&\quad-(1/\sqrt{2})a_1'\kappa_2^La_3'-(1/\sqrt{2})\kappa_1^La_2'a_3'\Big]\\
&\quad+\phi_{-1/20}^{1/2\,(N,N\pi)}(y,\mathbf{k}_\perp)\Big[(1/\sqrt{2})a_1'\kappa_2^L\kappa_3^L\\
&\quad+(1/\sqrt{2})\kappa_1^La_2'\kappa_3^L-(\sqrt{2})\kappa_1^L\kappa_2^La_3'\Big]\Big\}\delta^{(2)}\Big(\mathbf{p}_{\pi\perp}+\mathbf{k}_\perp\Big);\quad(3.93)
\end{aligned}
$$

$$
\begin{aligned}
\bullet\ D^{\uparrow}_{21,1} \;=\;& \frac{8(P^+)^{\frac{3}{2}}}{\sqrt{2\sqrt{2}}}\left[\frac{1}{M_0}\frac{\omega_1\omega_2\omega_3}{x_1x_2x_3}\right]^{\frac{1}{2}}\int\frac{\mathrm{d}y\mathrm{d}^2\mathbf{k}_\perp}{16\pi^3}\int\prod_{i=1}^{3}\mathrm{d}^2\kappa_{i\perp}\sqrt{y(1-y)}\\
&\times\delta\Big(1-y-\frac{p_\pi^+}{p_1^+}\Big)\delta^{(2)}\Big(\sum_{i=1}^{3}\kappa_{i\perp}\Big)\psi(\kappa_1,\kappa_2,\kappa_3)\prod_{i=1}^{3}\frac{1}{\sqrt{N(x_i',\boldsymbol{\kappa}_{\perp i})}}\\
&\times\Big\{\phi_{1/20}^{1/2\,(N,N\pi)}(y,\mathbf{k}_\perp)\Big[\sqrt{2}\kappa_1^Ra_2'\kappa_3^L\\
&\quad+(1/\sqrt{2})a_1'a_2'a_3'-(1/\sqrt{2})\kappa_1^R\kappa_2^La_3'\Big]\\
&+\phi_{-1/20}^{1/2\,(N,N\pi)}(y,\mathbf{k}_\perp)\Big[1/\sqrt{2}a_1'a_2'\kappa_3^L\\
&\quad-1/\sqrt{2}\kappa_1^R\kappa_2^L\kappa_3^L-\sqrt{2}a_1'\kappa_2^La_3'\Big]\Big\}\delta^{(2)}\Big(\mathbf{p}_{\pi\perp}+\mathbf{k}_\perp\Big);
\end{aligned}
\tag{3.94}
$$

$$
\begin{aligned}
\bullet\ D^{\uparrow}_{22,1} \;=\;& -\frac{8(P^+)^{\frac{3}{2}}}{\sqrt{2\sqrt{2}}}\left[\frac{1}{M_0}\frac{\omega_1\omega_2\omega_3}{x_1x_2x_3}\right]^{\frac{1}{2}}\int\frac{\mathrm{d}y\mathrm{d}^2\mathbf{k}_\perp}{16\pi^3}\int\prod_{i=1}^{3}\mathrm{d}^2\kappa_{i\perp}\sqrt{y(1-y)}\\
&\times\delta\Big(1-y-\frac{p_\pi^+}{p_1^+}\Big)\delta^{(2)}\Big(\sum_{i=1}^{3}\kappa_{i\perp}\Big)\psi(\kappa_1,\kappa_2,\kappa_3)\prod_{i=1}^{3}\frac{1}{\sqrt{N(x_i',\boldsymbol{\kappa}_{\perp i})}}\\
&\times\Big\{\phi_{1/20}^{1/2\,(N,N\pi)}(y,\mathbf{k}_\perp)\Big[\sqrt{2}\kappa_1^R\kappa_2^R\kappa_3^L\\
&\quad+(1/\sqrt{2})a_1'\kappa_2^Ra_3'+(1/\sqrt{2})\kappa_1^Ra_2'\kappa_3^L\Big]\\
&+\phi_{-1/20}^{1/2\,(N,N\pi)}(y,\mathbf{k}_\perp)\Big[-(1/\sqrt{2})a_1'\kappa_2^R\kappa_3^L\\
&\quad-(1/\sqrt{2})\kappa_1^ra_2'\kappa_3^L-\sqrt{2}a_1'a_2'a_3'\Big]\Big\}\delta^{(2)}\Big(\mathbf{p}_{\pi\perp}+\mathbf{k}_\perp\Big);
\end{aligned}
\tag{3.95}
$$

$$
\begin{aligned}
\bullet\ D^{\uparrow}_{22,2} \;=\;& -\frac{8(P^+)^{\frac{3}{2}}}{\sqrt{2\sqrt{2}}}\left[\frac{1}{M_0}\frac{\omega_1\omega_2\omega_3}{x_1x_2x_3}\right]^{\frac{1}{2}}\int\frac{\mathrm{d}y\mathrm{d}^2\mathbf{k}_\perp}{16\pi^3}\int\prod_{i=1}^{3}\mathrm{d}^2\kappa_{i\perp}\sqrt{y(1-y)}\\
&\times\delta\Big(1-y-\frac{p_\pi^+}{p_1^+}\Big)\delta^{(2)}\Big(\sum_{i=1}^{3}\kappa_{i\perp}\Big)\psi(\kappa_1,\kappa_2,\kappa_3)\prod_{i=1}^{3}\frac{1}{\sqrt{N(x_i',\boldsymbol{\kappa}_{\perp i})}}\\
&\times\Big\{\phi_{1/20}^{1/2\,(N,N\pi)}(y,\mathbf{k}_\perp)\Big[\sqrt{2}\kappa_1^R\kappa_2^Ra_3'\\
&\quad-(1/\sqrt{2})a_1'\kappa_2^R\kappa_3^R-(1/\sqrt{2})\kappa_1^Ra_2'\kappa_3^R\Big]\\
&+\phi_{-1/20}^{1/2\,(N,N\pi)}(y,\mathbf{k}_\perp)\Big[\sqrt{2}a_1'a_2'\kappa_3^R\\
&\quad-(1/\sqrt{2})\kappa_1^Ra_2'a_3'-(1/\sqrt{2})a_1'\kappa_2^Ra_3'\Big]\Big\}\delta^{(2)}\Big(\mathbf{p}_{\pi\perp}+\mathbf{k}_\perp\Big);
\end{aligned}
\tag{3.96}
$$

$$
\begin{aligned}
\bullet\ D^{\uparrow}_{21,2} \;=\; & -\frac{8(P^+)^{\frac{3}{2}}}{\sqrt{2\sqrt{2}}}\left[\frac{1}{M_0}\frac{\omega_1\omega_2\omega_3}{x_1x_2x_3}\right]^{\frac{1}{2}}\int\frac{\mathrm{d}y\mathrm{d}^2\mathbf{k}_\perp}{16\pi^3}\int\prod_{i=1}^{3}\mathrm{d}^2\kappa_{i\perp}\sqrt{y(1-y)} \\
& \times\delta\left(1-y-\frac{p^+_\pi}{p^+_1}\right)\delta^{(2)}\left(\sum_{i=1}^{3}\kappa_{i\perp}\right)\psi(\kappa_1,\kappa_2,\kappa_3)\prod_{i=1}^{3}\frac{1}{\sqrt{N(x'_i,\boldsymbol{\kappa}_{\perp i})}} \\
& \times\Bigg\{\phi^{1/2\,(N,N\pi)}_{1/20}(y,\mathbf{k}_\perp)\Big[\sqrt{2}\kappa^R_1a'_2a'_3 \\
& \quad +(1/\sqrt{2})\kappa^R_1\kappa^L_2\kappa^R_3-(1/\sqrt{2})a'_1a'_2\kappa^R_3\Big] \\
& \quad +\phi^{1/2\,(N,N\pi)}_{-1/20}(y,\mathbf{k}_\perp)\Big[\sqrt{2}a'_1\kappa^L_2\kappa^R_3 \\
& \quad -(1/\sqrt{2})\kappa^R_1\kappa^L_2a'_3+(1/\sqrt{2})a'_1a'_2a'_3\Big]\Bigg\}\delta^{(2)}\Big(\mathbf{p}_{\pi\perp}+\mathbf{k}_\perp\Big). \quad (3.97)
\end{aligned}
$$

Now we are ready to express the TDAs in the LCWFs formalism. We report here as examples the expressions we obtained for the TDAs $V_1^{p\pi_0}, A_1^{p\pi_0}$ and $T_1^{p\pi_0}$, because these three TDAs are the only ones already studied in literature. Indeed, as already mentioned, in a series of articles Pire and collaborators [207] analyzed them in the so-called "soft-pion limit" [221, 222] (see later) making some predictions for JLab and GSI kinematics.

$$
\begin{aligned}
& V_1^{p\pi_0}=-i\frac{1}{\sqrt{2}P^+}\left(\sqrt{\frac{p^+_1}{\sqrt{2}}}\right)^{-1}\frac{f_\pi}{f_N}\Big(D^{\uparrow}_{12,1}+D^{\uparrow}_{21,1}\Big) \\
& =-i4\sqrt{2}\frac{f_\pi}{f_N}\sqrt{\frac{P^+}{p^+_1}}\left[\frac{1}{M_0}\frac{\omega_1\omega_2\omega_3}{x_1x_2x_3}\right]^{\frac{1}{2}}\int\frac{\mathrm{d}y\mathrm{d}^2\mathbf{k}_\perp}{16\pi^3}\int\prod_{i=1}^{3}\mathrm{d}^2\kappa_{i\perp}\sqrt{y(1-y)} \\
& \times\delta^{(2)}\left(\sum_{i=1}^{3}\kappa_{i\perp}\right)\delta\left(1-y-\frac{p^+_\pi}{p^+_1}\right)\delta^{(2)}\Big(\mathbf{p}_{\pi\perp}+\mathbf{k}_\perp\Big)\psi(\kappa_1,\kappa_2,\kappa_3)\prod_{i=1}^{3}\frac{1}{\sqrt{N(x'_i,\boldsymbol{\kappa}_{\perp i})}} \\
& \times\Bigg\{\phi^{1/2\,(N,N\pi)}_{1/20}(y,\mathbf{k}_\perp)\Big[a'_1a'_2a'_3+a'_1\kappa^R_2\kappa^L_3-\frac{1}{2}\kappa^L_1\kappa^R_2a'_3+\kappa^R_1a'_2\kappa^L_3-\frac{1}{2}\kappa^R_1\kappa^L_2a'_3\Big] \\
& \quad +\phi^{1/2\,(N,N\pi)}_{-1/20}(y,\mathbf{k}_\perp)\Big[a'_1a'_2\kappa^L_3-\kappa^L_1a'_2a'_3-\frac{1}{2}\kappa^R_1\kappa^L_2\kappa^L_3-a'_1\kappa^L_2a'_3-\frac{1}{2}\kappa^L_1\kappa^R_2\kappa^L_3\Big]\Bigg\}; \quad (3.98)
\end{aligned}
$$

$$
\begin{aligned}
A_1^{p\pi_0} &= i\frac{1}{\sqrt{2}P^+}\left(\sqrt{\frac{p_1^+}{\sqrt{2}}}\right)^{-1}\frac{f_\pi}{f_N}\Big(D^{\uparrow}_{12,1}-D^{\uparrow}_{21,1}\Big)\\
&= i4\sqrt{2}\frac{f_\pi}{f_N}\sqrt{\frac{P^+}{p_1^+}}\left[\frac{1}{M_0}\frac{\omega_1\omega_2\omega_3}{x_1x_2x_3}\right]^{\frac{1}{2}}\int\frac{\mathrm{d}y\mathrm{d}^2\mathbf{k}_\perp}{16\pi^3}\int\prod_{i=1}^{3}\mathrm{d}^2\kappa_{i\perp}\sqrt{y(1-y)}\\
&\times\delta^{(2)}\Big(\sum_{i=1}^{3}\kappa_{i\perp}\Big)\delta\Big(1-y-\frac{p_\pi^+}{p_1^+}\Big)\delta^{(2)}\Big(\mathbf{p}_{\pi\perp}+\mathbf{k}_\perp\Big)\psi(\kappa_1,\kappa_2,\kappa_3)\prod_{i=1}^{3}\frac{1}{\sqrt{N(x_i',\boldsymbol{\kappa}_{\perp i})}}\\
&\times\Bigg\{\phi^{1/2\,(N,N\pi)}_{1/20}(y,\mathbf{k}_\perp)\Big[a_1'\kappa_2^R\kappa_3^L-\frac{1}{2}\kappa_1^L\kappa_2^R a_3'-\kappa_1 a_2'\kappa_3^L+\frac{1}{2}\kappa_1^R\kappa_2^L a_3'\Big]\\
&\quad+\phi^{1/2\,(N,N\pi)}_{-1/20}(y,\mathbf{k}_\perp)\Big[-\kappa_1^L a_2'a_3'+\frac{1}{2}\kappa_1^R\kappa_2^L\kappa_3^L+a_1'\kappa_2^L a_3'-\frac{1}{2}\kappa_1^L\kappa_2^R\kappa_3^L\Big]\Bigg\};
\end{aligned}
\tag{3.99}
$$

$$
\begin{aligned}
T_1^{p\pi_0} &= i\frac{1}{\sqrt{2}P^+}\left(\sqrt{\frac{p_1^+}{\sqrt{2}}}\right)^{-1}\frac{f_\pi}{f_N}\left[D^{\uparrow}_{11,2}+\frac{(\Delta_{T1}-i\Delta_{T2})}{(\Delta_{T1}+i\Delta_{T2})}D^{\uparrow}_{22,2}\right]\\
&= -i4\sqrt{2}\frac{f_\pi}{f_N}\sqrt{\frac{P^+}{p_1^+}}\left[\frac{1}{M_0}\frac{\omega_1\omega_2\omega_3}{x_1x_2x_3}\right]^{\frac{1}{2}}\int\frac{\mathrm{d}y\mathrm{d}^2\mathbf{k}_\perp}{16\pi^3}\int\prod_{i=1}^{3}\mathrm{d}^2\mathbf{k}_{i\perp}\sqrt{y(1-y)}\\
&\times\delta^{(2)}\Big(\sum_{i=1}^{3}\kappa_{i\perp}\Big)\delta\Big(1-y-\frac{p_\pi^+}{p_1^+}\Big)\delta^{(2)}\Big(\mathbf{p}_{\pi\perp}+\mathbf{k}_\perp\Big)\psi(\kappa_1,\kappa_2,\kappa_3)\prod_{i=1}^{3}\frac{1}{\sqrt{N(x_i',\boldsymbol{\kappa}_{\perp i})}}\\
&\times\Bigg\{\phi^{1/2\,(N,N\pi)}_{1/2,0}(y,\mathbf{k}_\perp)\Bigg\{\Big[a_1'a_2'a_3'\Big]+\frac{1}{2}\Big[a_1'\kappa_2^L\kappa_3^R\Big]+\frac{1}{2}\Big[\kappa_1^L a_2'\kappa_3^R\Big]\\
&\quad+\frac{(\Delta_{T1}-i\Delta_{T2})}{(\Delta_{T1}+i\Delta_{T2})}\Big[\Big[\kappa_1^R\kappa_2^R a_3'\Big]-\frac{1}{2}\Big[a_1'\kappa_2^R\kappa_3^R\Big]-\frac{1}{2}\Big[\kappa_1^R a_2'\kappa_3^R\Big]\Big]\Bigg\}\\
&\quad+\phi^{1/2\,(N,N\pi)}_{1/2,0}(y,\mathbf{k}_\perp)\Bigg\{\Big[\kappa_1^L\kappa_2^L\kappa_3^R\Big]+\frac{1}{2}\Big[a_1'\kappa_2^L a_3'\Big]+\frac{1}{2}\Big[\kappa_1^L a_2'a_3'\Big]\\
&\quad+\frac{(\Delta_{T1}-i\Delta_{T2})}{(\Delta_{T1}+i\Delta_{T2})}\Big[\Big[a_1'a_2'\kappa_3^R\Big]-\frac{1}{2}\Big[\kappa_1^R a_2'a_3'\Big]-\frac{1}{2}\Big[a_1'\kappa_2^R a_3'\Big]\Big]\Bigg\}\Bigg\}.
\end{aligned}
\tag{3.100}
$$

Numerical Result

In this subsection we report the numerical predictions for the TDAs. In Figs. [(3.2)–(3.7)] are shown some examples of our results for the TDAs obtained with the momentum part of the WF described by means of the parameterization of Ref. [63].

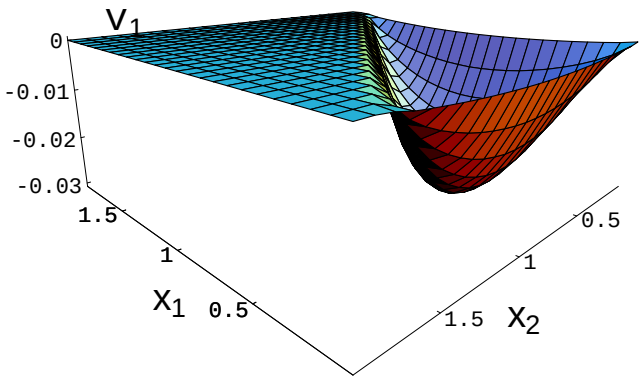

Figure 3.2: Results for the TDA $V_1^{p\pi^0}$ at Δ^2=-0.1GeV^2 and ξ=0.9 obtained with the momentum part of the LCWF taken from [63].

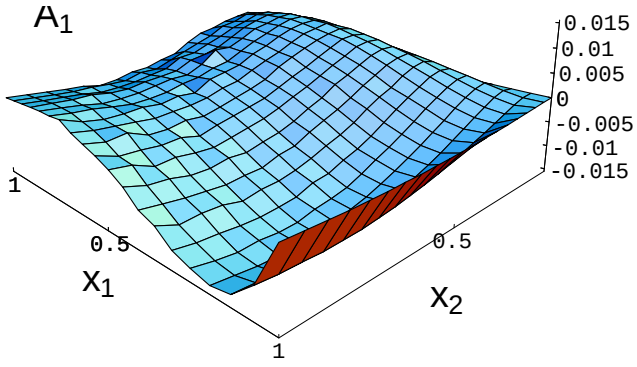

Figure 3.3: Results for the TDA $A_1^{p\pi^0}$ at Δ^2=-0.1GeV^2 and ξ=0.9 obtained with the momentum part of the LCWF taken from [63].

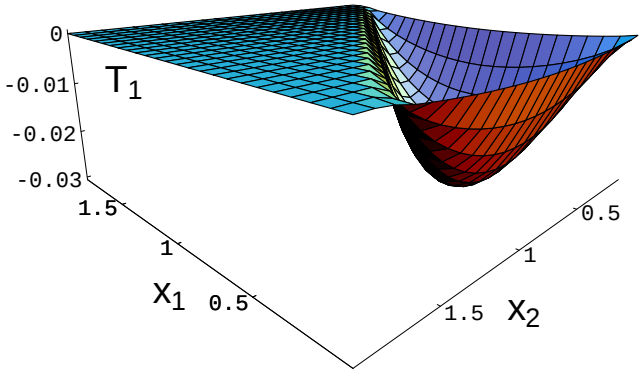

Figure 3.4: Results for the TDA $T_1^{p\pi^0}$ at Δ^2=-0.1GeV^2 and ξ=0.9 obtained with the momentum part of the LCWF taken from [63].

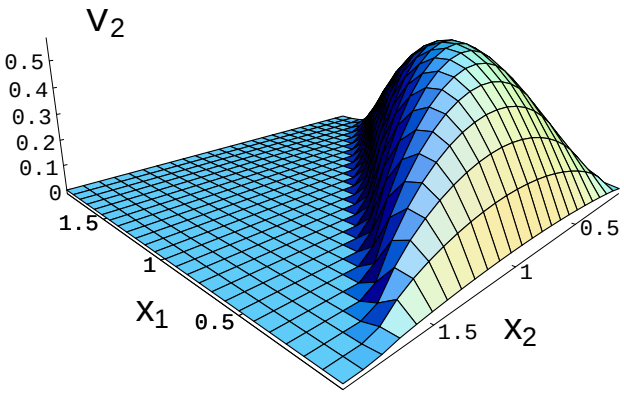

Figure 3.5: Results for the TDA $V_2^{p\pi^0}$ at Δ^2=-0.1GeV^2 and ξ=0.9 obtained with the momentum part of the LCWF taken from [63].

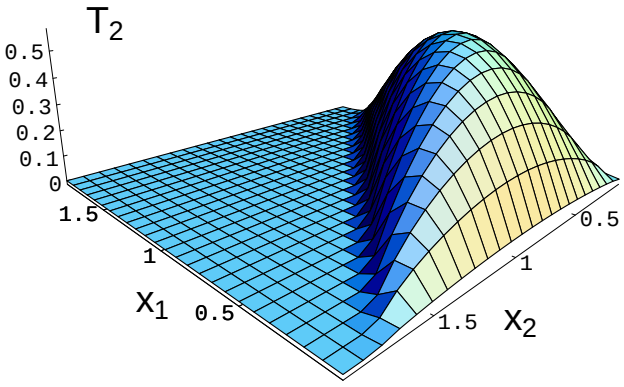

Figure 3.6: Results for the TDA $T_2^{p\pi^0}$ at Δ^2=-0.1GeV^2 and ξ=0.9 obtained with the momentum part of the LCWF taken from [63].

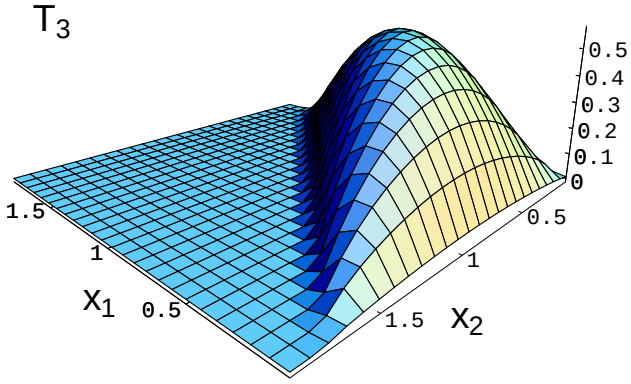

Figure 3.7: Results for the TDA $T_3^{p\pi^0}$ at Δ^2=-0.1GeV^2 and ξ=0.9 obtained with the momentum part of the LCWF taken from [63].

Thanks to the results reported in these figures it is possible to conclude that not only the TDAs that survive the "soft-pion" limit are mesurable and contribute to the cross sections of the processes taken into account, but a significant contribution could come from a not "collinear" kinematics also. The only TDA identically zero in all the kinematics results to be $T_4^{p\pi^0}$.

Chapter 4

Conclusions and future perspectives

The problem of understanding the inner structure of the nucleon is one of the great challenges in present particle and nuclear physics. This issue has been protagonist of an intensive experimental and theoretical investigation over the last decades, in particular by exploring QCD parton model in deep inelastic scattering processes in terms of parton distribution functions, in semi-inclusive deep inelastic scattering in terms of transverse momentum dependent parton distributions, and in exclusive processes by means of the distribution amplitudes, generalized parton distributions and generalized distribution amplitudes.

In this thesis we used the *overlap* representation in term of light-cone wave functions a convenient way to make explicit which kind of information on hadron structure is contained in some of these quantities. Initially, in the first part of the work we confined our analysis to the three-quark sector of the Fock-space expansion of the nucleon state. In other words we truncated the light-cone expansion of the nucleon state to the minimal Fock-space configuration. In the three valence quarks sector we studied the distribution amplitudes and the parton distribution functions, giving a general light-cone wave functions representation and applying the formalism obtained to two different light-cone constituent quark models. The starting point is the three-quark wave function obtained as a solution of the eigenvalue equation in the so-called *instant-form* dynamics. Then, the corresponding solution in light-cone dynamics is derived by means of a unitary transformation represented by the product of Melosh rotations acting on the spin of the individual quarks. In our analysis we constructed the instant form wave function factorizing the momentum part, spherically symmetric and invariant under permutations, from the spin-isospin part. For the spin-isospin part the only assumption we made is the requirement of SU(6) symmetry. The Melosh rotations convert the Pauli spinors of quarks in the rest frame to light-cone spinors and, moreover, introduce spin-flip terms which generate non-zero orbital angular momentum components and

non-trivial correlations among quarks transverse momenta and their spin. Our results for the distribution amplitudes are in much better agreement with data fit and lattice QCD calculations than other model calculations in literature.

As for the parton distribution functions we found, taking into account that we are working within a constituent quark model, a fair description of the unpolarized and polarized distribution function; whereas for the transversity distribution our predictions obtained with the momentum part of the wave function described by the hypercentral constituent quark model are in astonishing agreement with the preliminary extraction from data performed by Anselmino and collaborators. On the other side, the results we got with the Schlumpf parametrization do not compare so well.

In the second part of the thesis we extend our analysis to include the next to leading Fock-state component in the nucleon state expansion, i.e. a five partons configuration composed of a cluster of three quarks and a quark-antiquark pair, in the so-called meson-cloud model. With the term meson-cloud model are indicated all the models that describe the nucleon as a bare nucleon surrounded by a mesonic cloud. Along the years thanks to the meson-cloud model it has been possible to account for some intriguing experimental results which can not be explained within the usual constituent quark model, e.g. breaking of the SU(2) flavour and charge symmetries of the "Dirac sea", the problem of the spin of the proton, etc.
After recalling the description of the nucleon state with the inclusion of the pion-cloud degrees of freedom in terms of light-cone wave functions obtained by Pasquini and Boffi we applied this formalism to the study of a brand-new class of hadronic observables, the transition distribution amplitudes. These new observables enter the description of some peculiar exclusive processes where initial and final states are two different hadronic states.
Working in the framework of the meson-cloud model mentioned above we give the general overlap representation of the eight nucleon to pion TDAs and we give also some numerical estimates of them with the momentum part of the wave function taken from the model of Schlumpf.

Our work shows for the first time in literature that in general not only the three transition distribution amplitudes non vanishing in the limit $\Delta_T \to 0$ are different from zero, but also the other can in principle be measured even if they have no direct connection with the three leading twist distribution amplitudes.

In the future, as a straightforward application of our calculation it would be interesting to give some estimation for the proton decay processes $p \to \pi^0 e^+$ and $p \to \pi^+ \bar{\nu}$ allowed in a Grand Unified Theory (GUT) such as the minimal SU(5). Indeed, the proton decay (partial width) calculation [231],

$$\Gamma(p \to \pi^0 e^+) \propto \alpha_5^2(M_X)|a_1 - A_2|^2 \frac{M}{M_X^4}, \tag{4.1}$$

with α_5 coupling constant of the GUT and M_X unification scale, involves two matrix elements that are equivalent to that entering the transition distribution

amplitudes definition,

$$\langle \pi^0 | \epsilon^{ijk} (u^i C d^j) u^k_\gamma | P \rangle = A_1 N_\gamma, \quad (4.2)$$

$$\langle \pi^+ | \epsilon^{ijk} (u^i C \gamma^5 d^j) (\gamma^5 u^k)_\gamma | P \rangle = A_2 N_\gamma, \quad (4.3)$$

where C is the charge conjugation matrix and N is the nucleon spinor.

Another interesting issue that should be addressed is the possibility to give an impact parameter representation of the transition distribution amplitudes, as done for the generalized parton distributions [232], which would allow the description of the transverse localization of the virtual pion inside the nucleon.

Appendix A

Symmetry properties of the Nucleon Distribution Amplitudes

In this Appendix following Ref. [59] we show why at leading twist-three there is just one independent DA.
Since the operator on the l.h.s. of Eq. (2.15) is symmetric under the exchange of the two u-quarks, this property implies that the V_1- and T_1-functions are symmetric and the A_1-function is antisymmetric under the exchange of the first two arguments, respectively:

$$\begin{aligned} V_1(1,2,3) &= V_1(2,1,3)\,, \\ A_1(1,2,3) &= -A_1(2,1,3)\,, \\ T_1(1,2,3) &= T_1(2,1,3)\,. \end{aligned} \tag{A.1}$$

In addition, the matrix element in Eq. (2.15) has to fulfill the symmetry relation

$$\begin{aligned} &\langle 0|\,\varepsilon^{ijk} u^i_\alpha(1) u^j_\beta(2) d^k_\gamma(3)\,|P\rangle \\ &+ \langle 0|\,\varepsilon^{ijk} u^i_\alpha(1) u^j_\gamma(3) d^k_\beta(2)\,|P\rangle \\ &+ \langle 0|\,\varepsilon^{ijk} u^i_\gamma(3) u^j_\beta(2) d^k_\alpha(1)\,|P\rangle = 0 \end{aligned} \tag{A.2}$$

that follows from the condition that the nucleon state has isospin 1/2:

$$\left(T^2 - \frac{1}{2}\left(\frac{1}{2}+1\right)\right) \langle 0|\,\varepsilon^{ijk} u^i_\alpha(1) u^j_\beta(2) d^k_\gamma(3)\,|P\rangle = 0\,, \tag{A.3}$$

where

$$T^2 = \frac{1}{2}\left(T_+ T_- + T_- T_+\right) + T_3^2 \tag{A.4}$$

and $T_\pm$ are the usual isospin step-up and step-down operators. Defining

$$\begin{aligned}(v_1)_{\alpha\beta,\gamma} &\equiv (\not{p}C)_{\alpha\beta}\left(\gamma_5 N^+\right)_\gamma \\ (a_1)_{\alpha\beta,\gamma} &\equiv (\not{p}\gamma_5 C)_{\alpha\beta}\, N^+_\gamma \\ (t_1)_{\alpha\beta,\gamma} &\equiv (i\sigma_{\perp p}C)_{\alpha\beta}\left(\gamma^\perp\gamma_5 N^+\right)_\gamma \end{aligned} \tag{A.5}$$

and applying the set of Fierz transformations

$$\begin{aligned}(v_1)_{\gamma\beta,\alpha} &= \frac{1}{2}\left(v_1 - a_1 - t_1\right)_{\alpha\beta,\gamma} \\ (a_1)_{\gamma\beta,\alpha} &= \frac{1}{2}\left(-v_1 + a_1 - t_1\right)_{\alpha\beta,\gamma} \\ (t_1)_{\gamma\beta,\alpha} &= -\left(v_1 + a_1\right)_{\alpha\beta,\gamma} \end{aligned} \tag{A.6}$$

one ends up with the condition

$$2T_1(1,2,3) = [V_1 - A_1](1,3,2) + [V_1 - A_1](2,3,1)\,, \tag{A.7}$$

which allows one to express the tensor DA of the leading twist in terms of the vector and axial vector distributions. Since the latter have different symmetry, they can be combined together to define the single independent leading twist-3 proton DA

$$\Phi(x_1,x_2,x_3) = [V_1 - A_1](x_1,x_2,x_3) \tag{A.8}$$

which is well known and received a lot of attention in the literature. The neutron leading twist DA $\Phi_3^n(x_1,x_2,x_3)$ (note the superscript n) can readily be obtained by the interchange of u and d quarks in the defining equation (2.15). For all invariant functions $F = V, A, T$ proton and neutron DAs differ by an overall sign:

$$F^p(1,2,3) = -F^n(1,2,3)\,, \tag{A.9}$$

as follows from the isospin symmetry. This property is retained for all twists.

Appendix B

Matrix elements for the Distribution Amplitudes

Here we report all the matrix elements involved in the definitions of the DAs that it is possible to obtain varying the Dirac indexes α, β and γ, and the nucleon's helicity $\uparrow$ / $\downarrow$ in Eq. (2.15),

- $M^{\uparrow/\downarrow}_{11,\gamma} = -M^{\uparrow/\downarrow}_{13,\gamma} = M^{\uparrow/\downarrow}_{31,\gamma} = -M^{\uparrow/\downarrow}_{33,\gamma}$

$$
\begin{aligned}
M^{\uparrow}_{11,1} &= 0 && \text{(B.1)}\\
M^{\uparrow}_{11,2} &= -\sqrt[4]{2} f_N (p_1^+)^{\frac{3}{2}} T_1 && \text{(B.2)}\\
M^{\uparrow}_{11,3} &= 0 && \text{(B.3)}\\
M^{\uparrow}_{11,4} &= \sqrt[4]{2} f_N (p_1^+)^{\frac{3}{2}} T_1 && \text{(B.4)}\\
M^{\downarrow}_{11,1} &= 0 && \text{(B.5)}\\
M^{\downarrow}_{11,2} &= 0 && \text{(B.6)}\\
M^{\downarrow}_{11,3} &= 0 && \text{(B.7)}\\
M^{\downarrow}_{11,4} &= 0 && \text{(B.8)}
\end{aligned}
$$

- $M^{\uparrow/\downarrow}_{12,\gamma} = -M^{\uparrow/\downarrow}_{14,\gamma} = M^{\uparrow/\downarrow}_{32,\gamma} = -M^{\uparrow/\downarrow}_{34,\gamma}$

$$
\begin{aligned}
M^{\uparrow}_{12,1} &= \frac{1}{\sqrt{2\sqrt{2}}} f_N (p_1^+)^{\frac{3}{2}} \Big(V_1 - A_1 \Big) && \text{(B.9)} \\
M^{\uparrow}_{12,2} &= 0 && \text{(B.10)} \\
M^{\uparrow}_{12,3} &= \frac{1}{\sqrt{2\sqrt{2}}} f_N (p_1^+)^{\frac{3}{2}} \Big(V_1 - A_1 \Big) && \text{(B.11)} \\
M^{\uparrow}_{12,4} &= 0 && \text{(B.12)} \\
M^{\downarrow}_{12,1} &= 0 && \text{(B.13)} \\
M^{\downarrow}_{12,2} &= -\frac{1}{\sqrt{2\sqrt{2}}} f_N (p_1^+)^{\frac{3}{2}} \Big(V_1 + A_1 \Big) && \text{(B.14)} \\
M^{\downarrow}_{12,3} &= 0 && \text{(B.15)} \\
M^{\downarrow}_{12,4} &= \frac{1}{\sqrt{2\sqrt{2}}} f_N (p_1^+)^{\frac{3}{2}} \Big(V_1 + A_1 \Big) && \text{(B.16)}
\end{aligned}
$$

- $M^{\uparrow/\downarrow}_{21,\gamma} = M^{\uparrow/\downarrow}_{23,\gamma} = -M^{\uparrow/\downarrow}_{41,\gamma} = -M^{\uparrow/\downarrow}_{43,\gamma}$

$$
\begin{aligned}
M^{\uparrow}_{21,1} &= \frac{1}{\sqrt{2\sqrt{2}}} f_N (p_1^+)^{\frac{3}{2}} \Big(V_1 + A_1 \Big) && \text{(B.17)} \\
M^{\uparrow}_{21,2} &= 0 && \text{(B.18)} \\
M^{\uparrow}_{21,3} &= \frac{1}{\sqrt{2\sqrt{2}}} f_N (p_1^+)^{\frac{3}{2}} \Big(V_1 + A_1 \Big) && \text{(B.19)} \\
M^{\uparrow}_{21,4} &= 0 && \text{(B.20)} \\
M^{\downarrow}_{21,1} &= 0 && \text{(B.21)} \\
M^{\downarrow}_{21,2} &= \frac{1}{\sqrt{2\sqrt{2}}} f_N (p_1^+)^{\frac{3}{2}} \Big(-V_1 + A_1 \Big) && \text{(B.22)} \\
M^{\downarrow}_{21,3} &= 0 && \text{(B.23)} \\
M^{\downarrow}_{21,4} &= \frac{1}{\sqrt{2\sqrt{2}}} f_N (p_1^+)^{\frac{3}{2}} \Big(V_1 - A_1 \Big) && \text{(B.24)}
\end{aligned}
$$

- $M^{\uparrow/\downarrow}_{22,\gamma} = -M^{\uparrow/\downarrow}_{24,\gamma} = -M^{\uparrow/\downarrow}_{42,\gamma} = M^{\uparrow/\downarrow}_{44,\gamma}$

$$M^{\uparrow}_{22,1} = 0 \tag{B.25}$$
$$M^{\uparrow}_{22,2} = 0 \tag{B.26}$$
$$M^{\uparrow}_{22,3} = 0 \tag{B.27}$$
$$M^{\uparrow}_{22,4} = 0 \tag{B.28}$$
$$M^{\downarrow}_{22,1} = \sqrt[4]{2} f_N (p_1^+)^{\frac{3}{2}} T_1 \tag{B.29}$$
$$M^{\downarrow}_{22,2} = 0 \tag{B.30}$$
$$M^{\downarrow}_{22,3} = \sqrt[4]{2} f_N (p_1^+)^{\frac{3}{2}} T_1 \tag{B.31}$$
$$M^{\downarrow}_{22,4} = 0 \tag{B.32}$$

Appendix C

Light-cone Wave Functions and Melosh Rotations

In this Appendix we derive with a certain detail the spin and isospin part of the LCWFs entering the definition of the DAs and other hadronic observables. The expression for the LCWFs can be obtained, as shown in Ref. [45], thanks to a transformation from the instant-form to the front-form representation of relativistic Hamiltonian dynamics. Following the procedure adopted in [45], we can write a generic nucleon LCWFs as

$$\begin{aligned}\tilde{\Psi}^{N,[f]}_{\lambda}(\{x_i\},\{k_i\},\{\lambda_i\},\{\tau_i\}) &= \tilde{\psi}(\mathbf{k}_1,\mathbf{k}_2,\mathbf{k}_3) \\ &\times \sum_{\mu_1\mu_2\mu_3} D^{1/2*}_{\mu_1\lambda_1}(R_{cf}(\mathbf{k}_1)) D^{1/2*}_{\mu_2\lambda_2}(R_{cf}(\mathbf{k}_2)) \\ &\times D^{1/2*}_{\mu_3\lambda_3}(R_{cf}(\mathbf{k}_3)) \Phi_{\lambda\tau}(\mu_1,\mu_2,\mu_3,\tau_1,\tau_2,\tau_3),\end{aligned} \tag{C.1}$$

where $D^{1/2}_{\lambda\mu}(R_{cf}(\mathbf{k}))$ is a matrix element of the Melosh rotation R_{cf} [46],

$$\begin{aligned}D^{1/2}_{\lambda\mu}(R_{cf}(\mathbf{k})) &= \langle\lambda|R_{cf}(xM_0,\mathbf{k}_\perp)|\mu\rangle \\ &= \langle\lambda|\frac{m+xM_0-i\sigma\cdot(\hat{\mathbf{z}}\times\mathbf{k}_\perp)}{\sqrt{(m+xM_0)^2+\mathbf{k}_\perp^2}}|\mu\rangle.\end{aligned} \tag{C.2}$$

In Eq. (C.2) we have separated the spin-isospin part from the space part of the canonical (in instant form respresentation, note te superscript $[c]$) wave function,

$$\tilde{\Psi}^{[c]}_{\lambda}(\{\mathbf{k}_i\},\{\lambda_i\},\{\tau_i\}) = \tilde{\psi}(\mathbf{k}_1,\mathbf{k}_2,\mathbf{k}_3)\Phi_{\lambda\tau}(\mu_1,\mu_2,\mu_3,\tau_1,\tau_2,\tau_3), \tag{C.3}$$

with

$$\begin{aligned}\Phi_{\lambda\tau}(\mu_1,\mu_2,\mu_3,\tau_1,\tau_2,\tau_3) &= \frac{1}{\sqrt{2}}\Big[\tilde{\Phi}^0_{\lambda}(\mu_1,\mu_2,\mu_3)\tilde{\Phi}^0_{\tau}(\tau_1,\tau_2,\tau_3) \\ &+\tilde{\Phi}^1_{\lambda}(\mu_1,\mu_2,\mu_3)\tilde{\Phi}^1_{\tau}(\tau_1,\tau_2,\tau_3)\Big],\end{aligned} \tag{C.4}$$

and

$$\tilde{\Phi}_{\lambda}^{S_{12}} = \sum_{M_{S_{12}}} \langle 1/2, \mu_1; 1/2, \mu_2 | S_{12}, M_{S_{12}} \rangle \langle S_{12}, M_{S_{12}}; 1/2, \mu_3 | 1/2, \lambda \rangle. \tag{C.5}$$

In the case we are dealing with we can fix the isospin variables of the three quarks involved in the process,

$$\begin{aligned}
\tilde{\Psi}^{N,[f]}(\{x_i\},\{k_i\},\{\lambda_i\},\{uud\}) &= \tilde{\psi}(\mathbf{k}_1,\mathbf{k}_2,\mathbf{k}_3) \sum_{\mu_1\mu_2\mu_3} D^{1/2*}_{\mu_1\lambda_1 2}(R_{cf}(\mathbf{k}_1)) \\
&\quad \times D^{1/2*}_{\mu_2\lambda_2}(R_{cf}(\mathbf{k}_2)) D^{1/2*}_{\mu_3\lambda_3}(R_{cf}(\mathbf{k}_3)) \\
&\quad \times \Phi_{\lambda\tau}\left(\mu_1,\mu_2,\mu_3,\tau_1=\frac{1}{2},\tau_2=\frac{1}{2},\tau_3=-\frac{1}{2}\right) \\
&= \tilde{\psi}(\mathbf{k}_1,\mathbf{k}_2,\mathbf{k}_3)\frac{1}{\sqrt{2}}\tilde{\Phi}^1_{\tau}(1/2,1/2,-1/2) \\
&\quad \times \sum_{\mu_1\mu_2\mu_3} D^{1/2*}_{\mu_1\lambda_1}(R_{cf}(\mathbf{k}_1)) D^{1/2*}_{\mu_2\lambda_2}(R_{cf}(\mathbf{k}_2)) \\
&\quad \times D^{1/2*}_{\mu_3\lambda_3}(R_{cf}(\mathbf{k}_3))\tilde{\Phi}^1_{\lambda}(\mu_1,\mu_2,\mu_3),
\end{aligned} \tag{C.6}$$

where the isospin part of the wave function is

$$\tilde{\Phi}^1_{\tau}(1/2,1/2,-1/2) = \sqrt{\frac{2}{3}}. \tag{C.7}$$

The momentum-dependent wave function in Eq. (C.6) is defined as

$$\tilde{\psi}(\mathbf{k}_1,\mathbf{k}_2,\mathbf{k}_3) = 2(2\pi)^3 \left[\frac{1}{M_0}\frac{\omega_1\omega_2\omega_3}{x_1x_2x_3}\right]^{\frac{1}{2}} \psi(\mathbf{k}_1,\mathbf{k}_2,\mathbf{k}_3), \tag{C.8}$$

where $M_0 = \omega_1 + \omega_2 + \omega_3$ is the mass of the noninteracting three-quark system, with $\omega_i \equiv k_i^0 = (k_i^+ + k_i^-)/\sqrt{2}$.

The spin dependent part in Eq. (C.6) is given by

$$\begin{aligned}
\tilde{\Phi}_{\lambda}(\lambda_1,\lambda_2,\lambda_3) &= \sum_{\mu_1\mu_2\mu_3} D^{1/2*}_{\mu_1\lambda_1 2}(R_{cf}(\mathbf{k}_1)) D^{1/2*}_{\mu_2\lambda_2}(R_{cf}(\mathbf{k}_2)) \\
&\quad \times D^{1/2*}_{\mu_3\lambda_3}(R_{cf}(\mathbf{k}_3))\tilde{\Phi}^1_{\lambda}(\mu_1,\mu_2,\mu_3).
\end{aligned} \tag{C.9}$$

Replacing in Eq. (C.6) the Eqs. (C.7) and (C.8) we get

$$\begin{aligned}
\Psi^{N,[f]}(\{x_i\},\{k_i\},\{\lambda_i\},\{\tau_i\}) &= \frac{2}{\sqrt{3}}(2\pi)^3\left[\frac{1}{M_0}\frac{\omega_1\omega_2\omega_3}{x_1x_2x_3}\right]^{1/2}\psi(\mathbf{k}_1,\mathbf{k}_2,\mathbf{k}_3)\\
&\times\sum_{\mu_1\mu_2\mu_3} D^{1/2*}_{\mu_1\lambda_1}(R_{cf}(\mathbf{k}_1))\; D^{1/2*}_{\mu_2\lambda_2}(R_{cf}(\mathbf{k}_2))\\
&\times D^{1/2*}_{\mu_3\lambda_3}(R_{cf}(\mathbf{k}_3))\tilde{\Phi}^1_\lambda(\mu_1,\mu_2,\mu_3)\\
&= \frac{2}{\sqrt{3}}(2\pi)^3\left[\frac{1}{M_0}\frac{\omega_1\omega_2\omega_3}{x_1x_2x_3}\right]^{1/2}\psi(\mathbf{k}_1,\mathbf{k}_2,\mathbf{k}_3)\\
&\times\sum_{\mu_1\mu_2\mu_3}\langle\mu_1|\frac{m+x_1M_0+i\sigma^*\cdot(\hat{\mathbf{z}}\times\mathbf{k}_{1\perp})}{\sqrt{(m+x_1M_0)^2+\mathbf{k}^2_{1\perp}}}|\lambda_1\rangle\\
&\times\langle\mu_2|\frac{m+x_2M_0+i\sigma^*\cdot(\hat{\mathbf{z}}\times\mathbf{k}_{2\perp})}{\sqrt{(m+x_2M_0)^2+\mathbf{k}^2_{2\perp}}}|\lambda_2\rangle\\
&\times\langle\mu_3|\frac{m+x_3M_0+i\sigma^*\cdot(\hat{\mathbf{z}}\times\mathbf{k}_{3\perp})}{\sqrt{(m+x_3M_0)^2+\mathbf{k}^2_{3\perp}}}|\lambda_3\rangle\\
&\times\sum_{M_{S_{12}}}\langle 1/2,\mu_1;1/2,\mu_2|1,M_{S_{12}}\rangle\\
&\times\langle 1,M_{S_{12}};1/2,\mu_3|1/2,\lambda\rangle.
\end{aligned}$$

In general, we have

$$\begin{aligned}
&\sum_\mu\langle\mu|\frac{m+x_iM_0+i\sigma^*\cdot(\hat{\mathbf{z}}\times\mathbf{k}_\perp)}{\sqrt{(m+x_iM_0)^2+\mathbf{k}^2_\perp}}|\lambda\rangle=\frac{1}{\sqrt{(m+x_iM_0)^2+\mathbf{k}^2_\perp}}\\
&\times\Big[\langle 1/2|m+x_iM_0+i\sigma^*\cdot(\hat{\mathbf{z}}\times\mathbf{k}_\perp)|\lambda\rangle+\langle -1/2|m+x_iM_0+i\sigma^*\cdot(\hat{\mathbf{z}}\times\mathbf{k}_\perp)|\lambda\rangle\Big]\\
=\;&\frac{1}{\sqrt{(m+x_iM_0)^2+\mathbf{k}^2_\perp}}\Bigg[\langle 1/2|m+x_iM_0+i\sigma^*\cdot\begin{Vmatrix}\hat{i}&\hat{j}&\hat{k}\\0&0&1\\k_x&k_y&0\end{Vmatrix}|\lambda\rangle\\
&+\langle -1/2|m+x_iM_0+i\sigma^*\cdot\begin{Vmatrix}\hat{i}&\hat{j}&\hat{k}\\0&0&1\\k_x&k_y&0\end{Vmatrix}|\lambda\rangle\Bigg]\\
=\;&\frac{1}{\sqrt{(m+x_iM_0)^2+\mathbf{k}^2_\perp}}\Big[\langle 1/2|m+x_iM_0+i(\sigma^*_yk_x-\sigma_xk_y)|\lambda\rangle\\
&+\langle -1/2|m+x_iM_0+i(\sigma^*_yk_x-\sigma_xk_y)|\lambda\rangle\Big],
\end{aligned}\tag{C.10}$$

where, as usual

$$\sigma_x=\sigma^*_x=\begin{pmatrix}0&1\\1&0\end{pmatrix}\quad\text{and}\quad\sigma^*_y=-\sigma_y=\begin{pmatrix}0&i\\-i&0\end{pmatrix}.\tag{C.11}$$

Therefore to obtain the final expression for the LCWFs we have to specify the λ_i $(i = 1, ..., 3)$ and λ' dependence. The value of λ' enters only in the Clebsh-Gordan coefficient $\tilde{\Phi}^1_{\lambda'}(\mu_1, \mu_2, \mu_3)$ giving:

$$
\begin{aligned}
&\tilde{\Phi}^1_{1/2}(\mu_1,\mu_2,\mu_3) = \sum_{\mu_1\mu_2\mu_3}\sum_{M_{S_{12}}} \langle 1/2,\mu_1;1/2,\mu_2|1,M_{S_{12}}\rangle \\
&\times\langle 1,M_{S_{12}};1/2,\mu_3|1/2,1/2\rangle \\
=\ &\sum_{\mu_1\mu_2\mu_3}\Big[\langle 1/2,\mu_1;1/2,\mu_2|1,1\rangle\langle 1,1;1/2,\mu_3|1/2,1/2\rangle \\
&+\langle 1/2,\mu_1;1/2,\mu_2|1,0\rangle\langle 1,0;1/2,\mu_3|1/2,1/2\rangle \\
&+\langle 1/2,\mu_1;1/2,\mu_2|1,-1\rangle\langle 1,-1;1/2,\mu_3|1/2,1/2\rangle\Big] \\
=\ &\Big[\langle 1/2,1/2;1/2,1/2|1,1\rangle\langle 1,1;1/2,-1/2|1/2,1/2\rangle\left(\mu_1=\mu_2=\frac{1}{2},\mu_3=-\frac{1}{2}\right) \\
+\ &\langle 1/2,1/2;1/2,-1/2|1,0\rangle\langle 1,0;1/2,1/2|1/2,1/2\rangle\left(\mu_1=\mu_3=\frac{1}{2},\mu_2=-\frac{1}{2}\right) \\
+\ &\langle 1/2,-1/2;1/2,1/2|1,0\rangle\langle 1,0;1/2,1/2|1/2,1/2\rangle\left(\mu_1=-\frac{1}{2},\mu_2=\mu_3=\frac{1}{2}\right)\Big] \\
=\ &\Big[\left(\sqrt{\frac{2}{3}}\right)\ \left(\mu_1=\mu_2=\frac{1}{2},\mu_3=-\frac{1}{2}\right) \\
&-\left(\sqrt{\frac{1}{6}}\right)\ \left(\mu_1=\mu_3=\frac{1}{2},\mu_2=-\frac{1}{2}\right) \\
&-\left(\sqrt{\frac{1}{6}}\right)\ \left(\mu_1=-\frac{1}{2},\mu_2=\mu_3=\frac{1}{2}\right)\Big], \qquad \text{(C.12)}
\end{aligned}
$$

and

$$
\begin{aligned}
&\tilde{\Phi}^1_{-1/2}(\mu_1,\mu_2,\mu_3) = \sum_{\mu_1\mu_2\mu_3}\sum_{M_{S_{12}}} \langle 1/2,\mu_1;1/2,\mu_2|1,M_{S_{12}}\rangle \\
&\times\langle 1,M_{S_{12}};1/2,\mu_3|1/2,-1/2\rangle \\
=\ &\sum_{\mu_1\mu_2\mu_3}\Big[\langle 1/2,\mu_1;1/2,\mu_2|1,1\rangle\langle 1,1;1/2,\mu_3|1/2,-1/2\rangle \\
&+\langle 1/2,\mu_1;1/2,\mu_2|1,0\rangle\langle 1,0;1/2,\mu_3|1/2,-1/2\rangle \\
&+\langle 1/2,\mu_1;1/2,\mu_2|1,-1\rangle\langle 1,-1;1/2,\mu_3|1/2,-1/2\rangle\Big] \\
=\ &\Big[\langle 1/2,1/2;1/2,-1/2|1,0\rangle\langle 1,0;1/2,-1/2|1/2,-1/2\rangle\left(\mu_1=\frac{1}{2},\mu_2=\mu_3=-\frac{1}{2}\right) \\
+\ &\langle 1/2,-1/2;1/2,1/2|1,0\rangle\langle 1,0;1/2,-1/2|1/2,-1/2\rangle\left(\mu_1=\mu_3=-\frac{1}{2},\mu_2=\frac{1}{2}\right) \\
+\ &\langle 1/2,-1/2;1/2,-1/2|1,-1\rangle\langle 1,-1;1/2,1/2|1/2,-1/2\rangle\left(\mu_1=\mu_2=-\frac{1}{2},\mu_3=\frac{1}{2}\right)\Big]
\end{aligned}
$$

$$= \Big[\left(\sqrt{\frac{1}{6}}\right) \ \left(\mu_1 = \frac{1}{2}, \mu_2 = \mu_3 = -\frac{1}{2}\right) + \left(\sqrt{\frac{1}{6}}\right) \ \left(\mu_1 = \mu_3 = -\frac{1}{2}, \mu_2 = \frac{1}{2}\right)$$
$$- \left(\sqrt{\frac{2}{3}}\right) \ \left(\mu_1 = \mu_2 = -\frac{1}{2}, \mu_3 = \frac{1}{2}\right) \Big]. \tag{C.13}$$

Now we are ready to give an expression for the spin and isospin part of the LCWFs appearing in the *overlap* representation (2.24) of the matrix elements $M^{\uparrow/\downarrow}_{\alpha\beta,\gamma}$ in Eqs. (2.16)

- $M^{\uparrow}_{12,1} \Rightarrow \lambda' = \frac{1}{2}$:

$$\tilde{\Psi}^{N,[f]}_{1/2}\Big(\{x_1, \kappa_{1\perp}; 1/2, 1/2\}\{x_2, \kappa_{2\perp}; -1/2, 1/2\}\{x_3, \kappa_{3\perp}; 1/2, -1/2\}\Big)$$
$$= \frac{16\pi^3}{\sqrt{3}}\left[\frac{1}{M_0}\frac{\omega_1\omega_2\omega_3}{x_1x_2x_3}\right]^{\frac{1}{2}} \psi(\kappa_1, \kappa_2, \kappa_3) \sum_{\mu_1\mu_2\mu_3} \langle\mu_1| \frac{m + x_1M_0 + i\sigma^* \cdot (\hat{\mathbf{z}} \times \kappa_{1\perp})}{\sqrt{(m + x_1M_0)^2 + \kappa^2_{1\perp}}} |1/2\rangle$$
$$\times \langle\mu_2| \frac{m + x_2M_0 + i\sigma^* \cdot (\hat{\mathbf{z}} \times \kappa_{2\perp})}{\sqrt{(m + x_2M_0)^2 + \kappa^2_{2\perp}}} |-1/2\rangle \langle\mu_3| \frac{m + x_3M_0 + i\sigma^* \cdot (\hat{\mathbf{z}} \times \kappa_{3\perp})}{\sqrt{(m + x_3M_0)^2 + \kappa^2_{3\perp}}} |1/2\rangle$$
$$\times \sum_{M_{S_{12}}} \langle 1/2, \mu_1; 1/2, \mu_2 | 1, M_{S_{12}}\rangle \langle 1, M_{S_{12}}; 1/2, \mu_3 | 1/2, 1/2\rangle$$
$$= \frac{16\pi^3}{\sqrt{3}}\left[\frac{1}{M_0}\frac{\omega_1\omega_2\omega_3}{x_1x_2x_3}\right]^{\frac{1}{2}} \psi(\kappa_1, \kappa_2, \kappa_3) \prod_i \frac{1}{\sqrt{N(x'_i, \boldsymbol{\kappa}_{\perp i})}} \Big\{ \Big(-\sqrt{2/3}\Big) \Big[a_1 \kappa^R_2 \kappa^L_3\Big]$$
$$- \Big(1/\sqrt{6}\Big) \Big[a_1 a_2 a_3\Big] + \Big(1/\sqrt{6}\Big) \Big[\kappa^L_1 \kappa^R_2 a_3\Big] \Big\};$$

- $M^{\uparrow}_{21,1} \Rightarrow \lambda' = \frac{1}{2}$:

$$\tilde{\Psi}^{N,[f]}_{1/2}\Big(\{x_1, \kappa_{1\perp}; -1/2, 1/2\}\{x_2, \kappa_{2\perp}; 1/2, 1/2\}\{x_3, \kappa_{3\perp}; 1/2, -1/2\}\Big)$$

$$
\begin{aligned}
&= \frac{16\pi^3}{\sqrt{3}}\left[\frac{1}{M_0}\frac{\omega_1\omega_2\omega_3}{x_1x_2x_3}\right]^{\frac{1}{2}}\psi(\kappa_1,\kappa_2,\kappa_3)\sum_{\mu_1\mu_2\mu_3}\langle\mu_1|\frac{m+x_1M_0+i\sigma^*\cdot(\hat{\mathbf{z}}\times\kappa_{1\perp})}{\sqrt{(m+x_1M_0)^2+\kappa_{1\perp}^2}}|-1/2\rangle \\
&\quad \langle\mu_2|\frac{m+x_2M_0+i\sigma^*\cdot(\hat{\mathbf{z}}\times\kappa_{2\perp})}{\sqrt{(m+x_2M_0)^2+\kappa_{2\perp}^2}}|1/2\rangle\langle\mu_3|\frac{m+x_3M_0+i\sigma^*\cdot(\hat{\mathbf{z}}\times\kappa_{3\perp})}{\sqrt{(m+x_3M_0)^2+\kappa_{3\perp}^2}}|1/2\rangle \\
&\quad \times\sum_{M_{S_{12}}}\langle 1/2,\mu_1;1/2,\mu_2|1,M_{S_{12}}\rangle\langle 1,M_{S_{12}};1/2,\mu_3|1/2,1/2\rangle \\
&= -\frac{16\pi^3}{\sqrt{3}}\left[\frac{1}{M_0}\frac{\omega_1\omega_2\omega_3}{x_1x_2x_3}\right]^{\frac{1}{2}}\psi(\kappa_1,\kappa_2,\kappa_3)\prod_i\frac{1}{\sqrt{N(x_i',\boldsymbol{\kappa}_{\perp i})}}\Bigg\{\left(\sqrt{2/3}\right)\left[\kappa_1^R a_2\kappa_3^L\right] \\
&\quad +\left(1/\sqrt{6}\right)\left[a_1a_2a_3\right]-\left(\sqrt{1/6}\right)\left[\kappa_1^R\kappa_2^L a_3\right]\Bigg\};
\end{aligned}
$$

- $M^{\uparrow}_{11,2}\Rightarrow\lambda'=\frac{1}{2}$:

$$
\begin{aligned}
&\tilde{\Psi}^{N,[f]}_{1/2}\Big(\{x_1,\kappa_{1\perp};1/2,1/2\}\{x_2,\kappa_{2\perp};1/2,1/2\}\{x_3,\kappa_{3\perp};-1/2,-1/2\}\Big) \\
&= \frac{16\pi^3}{\sqrt{3}}\left[\frac{1}{M_0}\frac{\omega_1\omega_2\omega_3}{x_1x_2x_3}\right]^{\frac{1}{2}}\psi(\kappa_1,\kappa_2,\kappa_3)\sum_{\mu_1\mu_2\mu_3}\langle\mu_1|\frac{m+x_1M_0+i\sigma^*\cdot(\hat{\mathbf{z}}\times\kappa_{1\perp})}{\sqrt{(m+x_1M_0)^2+\kappa_{1\perp}^2}}|1/2\rangle \\
&\quad \times\langle\mu_2|\frac{m+x_2M_0+i\sigma^*\cdot(\hat{\mathbf{z}}\times\kappa_{2\perp})}{\sqrt{(m+x_2M_0)^2+\kappa_{2\perp}^2}}|1/2\rangle\langle\mu_3|\frac{m+x_3M_0+i\sigma^*\cdot(\hat{\mathbf{z}}\times\kappa_{3\perp})}{\sqrt{(m+x_3M_0)^2+\kappa_{3\perp}^2}}|-1/2\rangle \\
&\quad \times\sum_{M_{S_{12}}}\langle 1/2,\mu_1;1/2,\mu_2|1,M_{S_{12}}\rangle\langle 1,M_{S_{12}};1/2,\mu_3|1/2,1/2\rangle \\
&= \frac{16\pi^3}{\sqrt{3}}\left[\frac{1}{M_0}\frac{\omega_1\omega_2\omega_3}{x_1x_2x_3}\right]^{\frac{1}{2}}\psi(\kappa_1,\kappa_2,\kappa_3)\prod_i\frac{1}{\sqrt{N(x_i,\boldsymbol{k}_{\perp i})}}\Bigg\{\left(\sqrt{2/3}\right)\left[a_1a_2a_3\right] \\
&\quad +\left(1/\sqrt{6}\right)\left[a_1\kappa_2^L\kappa_3^R\right]+\left(1/\sqrt{6}\right)\left[\kappa_1^L a_2\kappa_3^R\right]\Bigg\}.
\end{aligned}
$$

Appendix D

Matrix elements for the TDAs

Here we report all the matrix elements involved in the definitions of the TDAs that it is possible to obtain varying the Dirac indexes α, β and γ, and the nucleon's helicity $\uparrow$ / $\downarrow$ in Eq. (3.46)

- $D^{\uparrow/\downarrow}_{11,\gamma} = D^{\uparrow/\downarrow}_{13,\gamma} = D^{\uparrow/\downarrow}_{31,\gamma} = D^{\uparrow/\downarrow}_{33,\gamma}$

$$D^{\uparrow}_{11,1} = i\frac{P^+}{\sqrt{2}M}\sqrt{\frac{p_1^+}{\sqrt{2}}}\frac{f_N}{f_\pi}\Big(\Delta_{T1} - i\Delta_{T2}\Big)\Big(T_2^{p\pi_0} - T_3^{p\pi_0}\Big) \tag{D.1}$$

$$D^{\uparrow}_{11,2} = i\frac{P^+}{\sqrt{2}}\sqrt{\frac{p_1^+}{\sqrt{2}}}\frac{f_N}{f_\pi}\Big[M^{-2}T_4^{p\pi_0}\Big(\Delta_{T1}^2 + \Delta_{T2}^2\Big) - 2T_1^{p\pi_0}\Big] \tag{D.2}$$

$$D^{\uparrow}_{11,3} = i\frac{P^+}{\sqrt{2}M}\sqrt{\frac{p_1^+}{\sqrt{2}}}\frac{f_N}{f_\pi}\Big(\Delta_{T1} - i\Delta_{T2}\Big)\Big(T_2^{p\pi_0} - T_3^{p\pi_0}\Big) \tag{D.3}$$

$$D^{\uparrow}_{11,4} = i\frac{P^+}{\sqrt{2}}\sqrt{\frac{p_1^+}{\sqrt{2}}}\frac{f_N}{f_\pi}\Big[-M^{-2}T_4^{p\pi_0}\Big(\Delta_{T1}^2 + \Delta_{T2}^2\Big) + 2T_1^{p\pi_0}\Big] \tag{D.4}$$

$$D^{\downarrow}_{11,1} = -i\frac{P^+}{\sqrt{2}M^2}\sqrt{\frac{p_1^+}{\sqrt{2}}}\frac{f_N}{f_\pi}\Big(\Delta_{T1} - i\Delta_{T2}\Big)^2 T_4^{p\pi_0} \tag{D.5}$$

$$D^{\downarrow}_{11,2} = i\frac{P^+}{\sqrt{2}M}\sqrt{\frac{p_1^+}{\sqrt{2}}}\frac{f_N}{f_\pi}\Big(\Delta_{T1} - i\Delta_{T2}\Big)\Big(T_2^{p\pi_0} + T_3^{p\pi_0}\Big) \tag{D.6}$$

$$D^{\downarrow}_{11,3} = -i\frac{P^+}{\sqrt{2}M^2}\sqrt{\frac{p_1^+}{\sqrt{2}}}\frac{f_N}{f_\pi}\Big(\Delta_{T1} - i\Delta_{T2}\Big)^2 T_4^{p\pi_0} \tag{D.7}$$

$$D^{\downarrow}_{11,4} = -i\frac{P^+}{\sqrt{2}M}\sqrt{\frac{p_1^+}{\sqrt{2}}}\frac{f_N}{f_\pi}\Big(\Delta_{T1} - i\Delta_{T2}\Big)\Big(T_2^{p\pi_0} + T_3^{p\pi_0}\Big) \tag{D.8}$$

- $D^{\uparrow/\downarrow}_{12,\gamma} = -D^{\uparrow/\downarrow}_{14,\gamma} = D^{\uparrow/\downarrow}_{32,\gamma} = -D^{\uparrow/\downarrow}_{34,\gamma}$

$$
\begin{aligned}
D^{\uparrow}_{12,1} &= i\frac{P^+}{\sqrt{2}}\sqrt{\frac{p_1^+}{\sqrt{2}}}\frac{f_N}{f_\pi}\Big(V_1^{p\pi_0} - A_1^{p\pi_0}\Big) && \text{(D.9)}\\
D^{\uparrow}_{12,2} &= i\frac{P^+}{\sqrt{2}M}\sqrt{\frac{p_1^+}{\sqrt{2}}}\frac{f_N}{f_\pi}\Big(\Delta_{T1} + i\Delta_{T2}\Big)\Big(V_2^{p\pi_0} + A_2^{p\pi_0}\Big) && \text{(D.10)}\\
D^{\uparrow}_{12,3} &= i\frac{P^+}{\sqrt{2}}\sqrt{\frac{p_1^+}{\sqrt{2}}}\frac{f_N}{f_\pi}\Big(V_1^{p\pi_0} - A_1^{p\pi_0}\Big) && \text{(D.11)}\\
D^{\uparrow}_{12,4} &= -i\frac{P^+}{\sqrt{2}M}\sqrt{\frac{p_1^+}{\sqrt{2}}}\frac{f_N}{f_\pi}\Big(\Delta_{T1} + i\Delta_{T2}\Big)\Big(V_2^{p\pi_0} + A_2^{p\pi_0}\Big) && \text{(D.12)}\\
D^{\downarrow}_{12,1} &= -i\frac{P^+}{\sqrt{2}M}\sqrt{\frac{p_1^+}{\sqrt{2}}}\frac{f_N}{f_\pi}\Big(\Delta_{T1} - i\Delta_{T2}\Big)\Big(V_2^{p\pi_0} - A_2^{p\pi_0}\Big) && \text{(D.13)}\\
D^{\downarrow}_{12,2} &= i\frac{P^+}{\sqrt{2}}\sqrt{\frac{p_1^+}{\sqrt{2}}}\frac{f_N}{f_\pi}\Big(V_1^{p\pi_0} + A_1^{p\pi_0}\Big) && \text{(D.14)}\\
D^{\downarrow}_{12,3} &= -i\frac{P^+}{\sqrt{2}M}\sqrt{\frac{p_1^+}{\sqrt{2}}}\frac{f_N}{f_\pi}\Big(\Delta_{T1} - i\Delta_{T2}\Big)\Big(V_2^{p\pi_0} - A_2^{p\pi_0}\Big) && \text{(D.15)}\\
D^{\downarrow}_{12,4} &= -i\frac{P^+}{\sqrt{2}}\sqrt{\frac{p_1^+}{\sqrt{2}}}\frac{f_N}{f_\pi}\Big(V_1^{p\pi_0} + A_1^{p\pi_0}\Big) && \text{(D.16)}
\end{aligned}
$$

- $D^{\uparrow/\downarrow}_{21,\gamma} = D^{\uparrow/\downarrow}_{23,\gamma} = -D^{\uparrow/\downarrow}_{41,\gamma} = -D^{\uparrow/\downarrow}_{43,\gamma}$

$$
\begin{aligned}
D^{\uparrow}_{21,1} &= i\frac{P^+}{\sqrt{2}}\sqrt{\frac{p_1^+}{\sqrt{2}}}\frac{f_N}{f_\pi}\Big(V_1^{p\pi_0} + A_1^{p\pi_0}\Big) && \text{(D.17)}\\
D^{\uparrow}_{21,2} &= i\frac{P^+}{\sqrt{2}M}\sqrt{\frac{p_1^+}{\sqrt{2}}}\frac{f_N}{f_\pi}\Big(\Delta_{T1} + i\Delta_{T2}\Big)\Big(V_2^{p\pi_0} - A_2^{p\pi_0}\Big) && \text{(D.18)}\\
D^{\uparrow}_{21,3} &= i\frac{P^+}{\sqrt{2}}\sqrt{\frac{p_1^+}{\sqrt{2}}}\frac{f_N}{f_\pi}\Big(V_1^{p\pi_0} + A_1^{p\pi_0}\Big) && \text{(D.19)}\\
D^{\uparrow}_{21,4} &= -i\frac{P^+}{\sqrt{2}M}\sqrt{\frac{p_1^+}{\sqrt{2}}}\frac{f_N}{f_\pi}\Big(\Delta_{T1} + i\Delta_{T2}\Big)\Big(V_2^{p\pi_0} - A_2^{p\pi_0}\Big) && \text{(D.20)}
\end{aligned}
$$

$$D^{\downarrow}_{21,1} = -i\frac{P^+}{\sqrt{2}M}\sqrt{\frac{p_1^+}{\sqrt{2}}}\frac{f_N}{f_\pi}\Big(\Delta_{T1} - i\Delta_{T2}\Big)\Big(V_2^{p\pi_0} + A_2^{p\pi_0}\Big) \quad \text{(D.21)}$$

$$D^{\downarrow}_{21,2} = i\frac{P^+}{\sqrt{2}}\sqrt{\frac{p_1^+}{\sqrt{2}}}\frac{f_N}{f_\pi}\Big(V_1^{p\pi_0} - A_1^{p\pi_0}\Big) \quad \text{(D.22)}$$

$$D^{\downarrow}_{21,3} = -i\frac{P^+}{\sqrt{2}M}\sqrt{\frac{p_1^+}{\sqrt{2}}}\frac{f_N}{f_\pi}\Big(\Delta_{T1} - i\Delta_{T2}\Big)\Big(V_2^{p\pi_0} + A_2^{p\pi_0}\Big) \quad \text{(D.23)}$$

$$D^{\downarrow}_{21,4} = -i\frac{P^+}{\sqrt{2}}\sqrt{\frac{p_1^+}{\sqrt{2}}}\frac{f_N}{f_\pi}\Big(V_1^{p\pi_0} - A_1^{p\pi_0}\Big) \quad \text{(D.24)}$$

- $D^{\uparrow/\downarrow}_{22,\gamma} = -D^{\uparrow/\downarrow}_{24,\gamma} = -D^{\uparrow/\downarrow}_{42,\gamma} = D^{\uparrow/\downarrow}_{44,\gamma}$

$$D^{\uparrow}_{22,1} = -i\frac{P^+}{\sqrt{2}M}\sqrt{\frac{p_1^+}{\sqrt{2}}}\frac{f_N}{f_\pi}\Big(\Delta_{T1} + i\Delta_{T2}\Big)\Big(T_2^{p\pi_0} + T_3^{p\pi_0}\Big) \quad \text{(D.25)}$$

$$D^{\uparrow}_{22,2} = -i\frac{P^+}{\sqrt{2}M^2}\sqrt{\frac{p_1^+}{\sqrt{2}}}\frac{f_N}{f_\pi}\Big(\Delta_{T1} + i\Delta_{T2}\Big)^2 T_4^{p\pi_0} \quad \text{(D.26)}$$

$$D^{\uparrow}_{22,3} = -i\frac{P^+}{\sqrt{2}M}\sqrt{\frac{p_1^+}{\sqrt{2}}}\frac{f_N}{f_\pi}\Big(\Delta_{T1} + i\Delta_{T2}\Big)\Big(T_2^{p\pi_0} + T_3^{p\pi_0}\Big) \quad \text{(D.27)}$$

$$D^{\uparrow}_{22,4} = i\frac{P^+}{\sqrt{2}M^2}\sqrt{\frac{p_1^+}{\sqrt{2}}}\frac{f_N}{f_\pi}\Big(\Delta_{T1} + i\Delta_{T2}\Big)^2 T_4^{p\pi_0} \quad \text{(D.28)}$$

$$D^{\downarrow}_{22,1} = i\frac{P^+}{\sqrt{2}}\sqrt{\frac{p_1^+}{\sqrt{2}}}\frac{f_N}{f_\pi}\Big[M^{-2}T_4^{p\pi_0}\Big(\Delta_{T1}^2 + \Delta_{T2}^2\Big) - 2T_1^{p\pi_0}\Big] \quad \text{(D.29)}$$

$$D^{\downarrow}_{22,2} = -i\frac{P^+}{\sqrt{2}M}\sqrt{\frac{p_1^+}{\sqrt{2}}}\frac{f_N}{f_\pi}\Big(\Delta_{T1} + i\Delta_{T2}\Big)\Big(T_2^{p\pi_0} - T_3^{p\pi_0}\Big) \quad \text{(D.30)}$$

$$D^{\downarrow}_{22,3} = i\frac{P^+}{\sqrt{2}}\sqrt{\frac{p_1^+}{\sqrt{2}}}\frac{f_N}{f_\pi}\Big[M^{-2}T_4^{p\pi_0}\Big(\Delta_{T1}^2 + \Delta_{T2}^2\Big) - 2T_1^{p\pi_0}\Big] \quad \text{(D.31)}$$

$$D^{\downarrow}_{22,4} = i\frac{P^+}{\sqrt{2}M}\sqrt{\frac{p_1^+}{\sqrt{2}}}\frac{f_N}{f_\pi}\Big(\Delta_{T1} + i\Delta_{T2}\Big)\Big(T_2^{p\pi_0} - T_3^{p\pi_0}\Big) \quad \text{(D.32)}$$

Bibliography

[1] H. Yukawa, Prog. Phys. Math. Soc. of Japan **17**, 48 (1935).

[2] M.L. Goldberger, Phys. Rev. **97**, 508 (1995); *ibid.* **99**, 979 (1955); M. Gell-Mann, M.L. Goldberger and W. Thirring, Phys. Rev. **95**, 1612 (1954); *ibid.* **96**, 1428 (1954).

[3] M. Gell-Mann, unpublished (1961); Phys. Rev. **125**, 1067 (1962); Phys. Lett. **8**, 214; Y. Ne'eman, Nucl. Phys. **26**, 222 (1961); M. Gell-Mann and Y. Ne'eman, *The Eightfold Way*, (W.A. Benjamin, New York, 1964); C. Zweig, CERN Rep. 8419/TH412.

[4] S. Sakata, Prog. Theor. Phys. **16**, 686 (1956); M. Ikeda, S. Ogawa and Y. Ohnuki, Prog. Theor. Phys. **22**, 715 (1959).

[5] M.Y. Han and Y. Nambu, Phys. Rev. **139**, B1006 (1965); O.W. Greenberg, Phys. Rev. Lett. **13**, 598 (1964).

[6] H. Fritzsch, M. Gell-Mann, H. Leutwyler, Phys. Lett. B **47**, 365 (1973).

[7] R. Hofstadter, Annu. Rev. Nucl. Sci. **7**, 231 (1957).

[8] J.D. Bjorken, Phys. Rev. **179**, 1547 (1969).

[9] R.P. Feynman, Phys. Rev. Lett. **23**, 1415 (1969).

[10] C.G. Callan and D. Gross, Phys. Rev. Lett. **22**, 156 (1969).

[11] C.N. Yang and R.L. Mills, Phys. Rev. **96**, 191 (1954).

[12] G. 't Hooft, Nucl. Phys. B **33**, 173 (1971); Nucl. Phys. B **35**, 167 (1967).

[13] S. Weinberg, Phys. Rev. Lett. **19**, 1264 (1967).

[14] A. Salam, *Elementary Particle Theory*, ed. N. Svaratholm, Stockholm: Almquist and Forlag (1968).

[15] P.W. Higgs, Phys. Lett. **12**, 132 (1964); Phys. Rev. **145**, 1156 (1966); T.V.B. Kibble, Phys. Rev. **155**, 1554 (1967).

[16] *At the Frontier of Particle Physics*, Edited by M. Shifman (World Scientific, Singapore, 2001).

[17] D.J. Gross and F. Wilczek, Phys. Rev. D **8**, 3497 (1973).

[18] H.D. Politzer, Phys. Rev. Lett. **26**, 1346 (1973).

[19] C.G. Callan, Phys. Rev. D **2**, 1541 (1970).

[20] K. Symanzik, Comm. Math. Phys. **18**, 227 (1970).

[21] Yu.L. Dokshitzer, JETP (Sov. Phys.) **46**, 641 (1977) [Zh. Exsp. Teor. Fiz. **73**, 1216 (1977)];
V.N. Gribov, L.N. Lipatov, Sov. J. Nucl. Phys. **15**, 438 (1972) [Yad. Fiz. **15**, 781, 1218 (1972)];
L.N. Lipatov, Sov. J. Nucl. Phys. **20**, 94 (1975) [Yad. Fiz. **20**, 181 (1974)];
G. Altarelli, G. Parisi, Nucl. Phys. B **126**, 298 (1977).

[22] K.G. Wilson, Phys. Rev. **179**, 1499 (1969).

[23] F. Bloch and A. Nordsieck, Phys. Rev. **52**, 54 (1937).

[24] For a detailed description see: T. Muta, *Foundations of Quantum Chromodynamics* (World Scientific, Singapore, 1987).

[25] T. Kinoshita, J. Math. Phys. **3**, 650 (1962); T.D. Lee and M. Nauenberg, Phys. Rev. **133**, B1549 (1964).

[26] D. Amati, R. Petronzio and G. Veneziano, Nucl. Phys. B **140**, 54 (1978); S. Libby and G. Sterman, Phys. Rev. D **18**, 3252 (1978); A.H. Mueller, Phys. Rev. D **18**, 3705 (1978); R. Ellis *et al.*, Nucl. Phys. B **152**, 285 (1979); A. Efremov and A.V. Radyushkin, Phys. Lett. B **94**, 245 (1980).

[27] P.A.M. Dirac, Rev. Mod. Phys. **21**, 392 (1949).

[28] S. Fubini and G. Furlan, Physics **1**, 229 (1965).

[29] S. Weinberg, Phys. Rev. **150**, 1313 (1966).

[30] L. Susskind, Phys. Rev. **165**, 1535 (1968).

[31] S.J. Brodsky, H.-C. Pauli and S.S. Pinsky, Phys. Rep. **301**, 299 (1998); A. Harindranath, *An Introduction to Light-Front Dynamics for Pedestrians in Light-Front Quantization and Non-Perturbative QCD*, eds. J.P. Vary and F. Wolz (IITAP, Ames, Iowa, USA, 1997), hep-ph/9612244 and references therein.

[32] H. Leutwyler and J. Stern, Ann. Phys. **112**, 94 (1978).

[33] Z. Dziembowski, Phys. Rev D **37**, 2030 (1988).

[34] H.C. Pauli and S.J. Brodsky, Phys. Rev. D 32, 1993 (1985); *idid.*, 2001 (1985).

[35] W.A. Bardeen and R.B. Pearson, Phys. Rev. D **14**, 547 (1976).

[36] R.J. Perry, A. Harindranath and K.G. Wilson, Phys. Rev. Lett. **65**, 2959 (1990).

[37] I. Tamm, J. Physics (Moscow) **9**, 449 (1945); S.M. Dancoff, Phys. Rev. D **78**, 382 (1950).

[38] X. Ji, J.-P. Ma and F. Yuan, Nucl. Phys. B **652**, 383 (2003).

[39] X. Ji, J.-P. Ma and F. Yuan, Eur. Phys. J. C **33**, 75 (2004).

[40] X. Ji, J.-P. Ma and F. Yuan, Phys. Rev. Lett. **90**, 241601 (2003).

[41] I. O. Cherednikov and N. G. Stefanis, Phys. Rev. **D 77**, 094001 (2008); arXiv:0802.2821 [hep-ph].

[42] B. Pasquini, S. Cazzaniga and S. Boffi, Phys. Rev. D **78**, 034025 (2008).

[43] J. Franklin, Phys. Rev. **172**, 1807 (1968).

[44] S. Capstick and N. Isgur, Phys. Rev. D **34**, 2809 (1986).

[45] S. Boffi, B. Pasquini and M. Traini, Nucl. Phys. **B 649**, 243 (2003).

[46] H.J. Melosh, Phys. Rev. D **9**, 1095 (1974).

[47] S.J. Brodsky and G.P. Lepage, in *Perturbative Quantum Chromodynamics*, Edited by A.H. Mueller (World Scientific, Singapore, 1989), p. 93.

[48] G.P. Lepage and S.J. Brodsky, Phys. Lett. B **87**, 359 (1979); Phys. Rev. Lett. **43**, 545 (1979); Phys. Rev. D **22**, 2157 (1980).

[49] V.L. Chernyak and A.R. Zhitnitsky, Phys. Rep. **112**, 173 (1984).

[50] J. Gronberg et al., Phys. Rev. D **57**, 33 (1998).

[51] D. Ashery, For the E791 Collaboration, hep-ex/9910024.

[52] V. Braun, R.J. Fries, N. Mahnke, and E. Stein, Nucl. Phys. B **589**, 381 (2000); *ibidem* **607**, 433 (2001).

[53] V.L. Chernyak, A.A. Ogloblin, and I.R. Zhitnitsky, Z. Phys. C **42**, 569 (1989).

[54] J. B. Kogut and D. E. Soper, Phys. Rev. D **1**, 2901 (1970).

[55] V. Barone, A. Drago, P.G. Ratcliffe, Phys. Rep. 359, 1 (2002);
V. Barone, P.G. Ratcliffe, *Transverse Spin Physics*, World Scientific, Singapore, 2003.

[56] M. Diehl, Th. Feldmann, R. Jakob and P. Kroll, Nucl. Phys. **B596**, 33 (2001); S. Brodsky, M. Diehl and D.S. Hwang, Nucl. Phys. **B596**, 99 (2001).

[57] S.D. Drell and T. Yan, Phys. Rev. Lett. **24**, 181 (1970); G.B. West, Phys. Rev. Lett. **24**, 1206 (1970).

[58] The pioneering papers in this subject are: D. Müller, D. Robaschik, B. Geyer, F.M. Dittes and J. Hořejši, Fortsch. Phys. **42**, 101 (1994); A.V. Radyushkin, Phys. Lett. B **380**, 417 (1996); Phys. Lett. B **385**, 333 (1996); Xiangdong Ji, Phys. Rev. Lett. **78**, 610 (1997); J. Phys. G **24**, 1181 (1998). For recent reviews see: K. Goeke, M.V. Polyakov and M. Vanderhaeghen, Prog. Part. Nucl. Phys. **47**, 401 (2001); A.V. Radyushkin, in *At the Frontier of Particle Physics*, Edited by M. Shifman (World Scientific, Singapore, 2001), Vol. 2, p. 1037; hep-ph/0101225; M. Diehl, Phys. Rep. **388**, 41 (2003); Xiangdong Ji, Ann. Rev. Nucl. Part. Sci. **54**, 413 (2004); A.V. Belitsky and A.V. Radyushkin, Phys. Rep. **418**, 1 (2005); S. Boffi and B. Pasquini, Riv. Nuovo Cim. **30**, 387 (2007), arXiv:0711.2625 [hep-ph].

[59] V.M. Braun, D.Yu. Ivanov, A. Lenz and A. Peters, Phys. Rev. D **75**, 014021 (2007).

[60] P.L. Chung and F. Coester, Phys. Rev. D **44**, 229 (1991).

[61] L.Y. Glozman, W. Plessas, K. Varga and R.F. Wagenbrunn, Phys. Rev. D **58**, 094030 (1998).

[62] P. Faccioli, M. Traini and V. Vento, Nucl. Phys. A **656**, 400 (1999).

[63] F. Schlumpf, J. Phys. G **20**, 237 (1994); PhD Thesis, hep-ph/9211255.

[64] B. Pasquini, M. Pincetti and S. Boffi, Phys. Rev. D **76**, 034020 (2007).

[65] S. Boffi, B. Pasquini and M. Traini, Nucl. Phys. B **649**, 243 (2003); *ibidem* **680**, 147 (2004); *ibidem* A **755**, 545 (2005); Phys. Rev. D **71**, 034022 (2005); B. Pasquini, M. Pincetti and S. Boffi, Phys. Rev. D **72**, 094029 (2005).

[66] B. Pasquini and S. Boffi, Phys. Rev. D **76**, 074011 (2007); R.F. Wagenbrunn *et al.*, Phys. Lett. B **511**, 33 (2001); L.Y. Glozman *et al.*, Phys. Lett. B **516**, 183 (2001); S. Boffi *et al.*, Eur. Phys. J. A **14**, 17 (2002).

[67] B. Pasquini and S. Boffi, Phys. Lett. B **653**, 23 (2007).

[68] B. Pasquini, arXiv:0807.2825 [hep-ph].

[69] M. Ferraris, M.M. Giannini, M. Pizzo, E. Santopinto and L. Tiator, Phys. Lett. B **364**, 231 (1995).

[70] F. Cardarelli, S. Simula, Phys. Rev. C **62**, 065201 (2000).

[71] V.L. Chernyak and A.R. Zhitnitsky, Nucl. Phys. B **201**, 492 (1982); *ibidem* 214, 547(E) (1983).

[72] V.L. Chernyak and I.R. Zhitnitsky, Nucl. Phys. B **246**, 52 (1984).

[73] M. Gari and N.G. Stefanis, Phys. Lett. B **175**, 462 (1986); Phys. Rev. D **35**, 1074 (1987).

[74] R.G. Arnold et al., Phys. Rev. Lett. **57**, 174 (1986).

[75] N.G. Stefanis, Phys. Rev. D **40**, 2305 (1989); *ibidem* D **44**, 1616(E) (1991).

[76] V.L. Chernyak, A.A. Ogloblin, and I.R. Zhitnitsky, Z. Phys. C **42**, 583 (1989).

[77] I.D. King and C.T. Sachrajda, Nucl. Phys. B 279 (1987) 785.

[78] V.L. Chernyak, A.A. Ogloblin, and I.R. Zhitnitsky, Z. Phys. C **42**, 569 (1989).

[79] D.G. Richards, C.T. Sachrajda, and C.J. Scott, Nucl. Phys. B **286**, 683 (1987); G. Martinelli and C.T. Sachrajda, Phys. Lett. B **217**, 319 (1989).

[80] A. Schäfer, Phys. Lett. B **217**, 545 (1989).

[81] Z. Dziembowski and J. Franklin, Phys. Rev D **42**, 905 (1990).

[82] A. De Rújula, H. Georgi and S.L. Glashow, Phys. Rev. D **12**, 147 (1970).

[83] N.G. Stefanis, in: 4th Hellenic School on Elementary Particle Physics, Corfu, Greece, September 2-20, 1992, eds. E. N. Gazis, G. Koutsoumbas, N. D. Tracas, and G. Zoupanos, Physics Department, National Technical University, Athens, Greece, Vol. II, p. 528.

[84] N.G. Stefanis and M. Bergmann, Phys. Rev. D **47**, R3685 (1993).

[85] M. Bergmann and N.G. Stefanis, Phys. Rev. D **48**, R2990 (1993).

[86] M. Bergmann and N.G. Stefanis, Phys. Lett. B **325**, 183 (1994).

[87] N.G. Stefanis and M. Bergmann, Phys. Lett. B **304**, 24 (1993).

[88] G.R. Farrar et al., Nucl. Phys. B **311**, 585 (1988/89).

[89] C.E. Carlson and J.L. Poor, Phys. Rev. D **38**, 2758 (1988).

[90] L. Stuart et al., in: Proc. Workshop on Exclusive Reactions at High Momentum Transfer, Elba, Italy, 24-26 June, 1993, eds. C. E. Carlson, P. Stoler, and M. Taiuti (World Scientific, Singapore, 1994), p. 44.

[91] L. Stuart et al., Phys. Rev. D **58**, 032003 (1998).

[92] P. Stoler, Phys. Rev. Lett. **66**, 1003 (1991); Phys. Rev. D **44**, 73 (1991).

[93] N.G. Stefanis and M. Bergmann, in: Proc. Workshop on Exclusive Reactions at High Momentum Transfer, Elba, Italy, 24-26 June, 1993, eds. C. E. Carlson, P. Stoler, and M. Taiuti (World Scientific, Singapore, 1994) p. 137; *ibidem*, p. 146.

[94] S.V. Mikhailov and A.V. Radyushkin, Yad. Fiz. **52**, 1095 (1990) [Sov. J. Nucl. Phys. 52 (1990) 697].

[95] R. Eckardt, J. Hansper, M.F. Gari, Phys. Lett.B **329**, 345 (1994); Z. Phys. A **350**, 349 (1995); Phys. Rev. D **50**, 26 (1994).

[96] R. Eckardt, J. Hansper, M.F. Gari, hep-ph/9607380; Z. Phys. A **350**, 349 (1995); Phys. Rev. D **51**, 3593 (1995); hep-ph/9503324;

[97] J. Bolz and P. Kroll, Z. Phys A **356**, 327 (1996).

[98] D.E. Soper, Nucl. Phys. B **163**, 93 (1980).

[99] N.G. Stefanis, Eur. Phys. J C **17**, 1 (1999).

[100] A. Erdelyi *et al.*, *Higher Trascendental Functions* (McGraw-Hill, New york, 1953), Vol. II.

[101] QCDSF collaboration, Göckeler *et al.*, arXiv:0710.2489 [hep-lat]; QCDSF/UKQCD collaborations, Göckeler *et al.*, arXiv:0804.1877 [hep-lat].

[102] B. Lampe and E. Reya, Phys. Rep. **332**, 1 (2000);
R.L. Jaffe, hep-ph/9710465;
M. Dittmar *et al.*, hep-ph/0511119.

[103] J.P. Ralston and D. Soper, Nucl. Phys. B **152**, 109 (1979).

[104] J.L. Cortes, B. Pire, and J.P. Ralston, Z. Phys. C **55**, 409 (1992).

[105] Xiangdong Ji, Phys. Lett. B **284**, 137 (1992).

[106] R.L. Jaffe and Xiangdong Ji, Phys. Rev. Lett. **67**, 552 (1991); Nucl. Phys. B **375**, 527 (1992).

[107] G. Bunce, N. Saito, J. Soffer, and W. Vogelsang, Ann. Rev. Nucl. Part. Sci. **50**, 525 (2000).

[108] P. Lenisa, F. Rathmann *et al.* ($\mathcal{PAX}$ Collaboration), *Technical proposal for Antiproton–Proton Scattering Experiments with Polarization*, hep-ex/0505054.

[109] A.V. Efremov, K. Goeke, and P. Schweitzer, Eur. Phys. J. C **35**, 207 (2004).

[110] M. Anselmino, V. Barone, A. Drago, and N.N. Nikolaev, Phys. Lett. B **594**, 97 (2004).

[111] V. Barone, A. Cafarella, C. Corianò, M. Guzzi, and P.G. Ratcliffe, Phys. Lett. B **639**, 483 (2006).

[112] I. Schmidt and J. Soffer, Phys. Lett. B **407**, 331 (1997);
Bo-Qiang Ma, I. Schmidt, and J. Soffer, Phys. Lett. B **441**, 461 (1998).

[113] J. Soffer, Phys. Rev. Lett. **74**, 1292 (1995).

[114] R.L. Jaffe and G.G. Ross, Phys. Lett. B **93**, 313 (1980).

[115] F. Baldracchini, N.S. Craigie, V. Roberto, and M. Socolovsky, Fortschr. Phys. **29**, 505 (1981).

[116] X. Artru and M. Mekhfi, Z. Phys. C **45**, 669 (1990).

[117] M. Anselmino, M. Boglione, U. D'Alesio, A. Kotzinian, F. Murgia, A. Prokudin, and C. Turk, Phys. Rev. D **75**, 054032 (2007).

[118] V.A. Korotkov, W.-D. Nowak and K.A. Oganessyan, Eur. Phys. J. C **18**, 639 (2001).

[119] M. Wakamatsu, Phys. Lett. B **509**, 59 (2001).

[120] P. Schweitzer, D. Urbano, M.V. Polyakov, C. Weiss, P.V. Pobylitsa and K. Goeke, Phys. Rev. D **64**, 034013 (2001).

[121] J. Soffer, M. Stratmann and W. Vogelsang, Phys. Rev. D **65**, 114024 (2002).

[122] M. Anselmino *et al.*, arXiv:0807.0173 [hep-ph].

[123] W. Vogelsang and A. Weber, Phys. Rev. D **48**, 2073 (1993).

[124] A.P. Contogouris, B. Kamal, and J. Merebashvili, Phys. Lett. B **337**, 169 (1994).

[125] B. Kamal, Phys. Rev. D **53**, 1142 (1996).

[126] A. Hayashigaki, Y. Kanazawa, and Y. Koike, Phys. Rev. D **56**, 7350 (1997).

[127] S. Kumano and M. Miyama, Phys. Rev. D **56**, R2504 (1997).

[128] W. Vogelsang, Phys. Rev. D **57**, 1886 (1998).

[129] V. Barone, Phys. Lett. B **409**, 499 (1997).

[130] V. Barone, T. Calarco, and A. Drago, Phys. Lett. B **390**, 287 (1997).

[131] M. Hirai, S. Kumano, and M. Miyama, Comp. Phys. Comm. **111**, 150 (1996).

[132] A. Cafarella and C. Corianò, Comp. Phys. Comm. **160**, 213 (2004).

[133] M. Miyama and S. Kumano, Comp. Phys. Comm. **94**, 185 (1996).

[134] M. Hirai, S. Kumano, and M. Miyama, Comp. Phys. Comm. **108**, 35 (1996).

[135] T. Weigl and W. Melnitchouk, Nucl. Phys. B **465**, 267 (1996);
M. Traini, V. Vento, A. Mair, and A. Zambarda, Nucl. Phys. A **614**, 472 (1997);
B. Pasquini, M. Traini, and S. Boffi, Phys. Rev. D **71**, 034022 (2005).

[136] M. Glück, E. Reya, and A. Vogt, Eur. Phys. J. C **5**, 468 (1998).

[137] M. Glück, E. Reya, M. Stratmann, and W. Vogelsang, Phys. Rev. D **63**, 094005 (2001);
J. Blümlein and H. Böttcher, Nucl. Phys. B **636**, 225 (2002);
Y. Goto *et al.*, Phys. Rev. D **62**, 034017 (2000); Int. J. Mod. Phys. A **18**, 1203 (2003).

[138] O. Martin, A. Schäfer, M. Stratmann, and W. Vogelsang, Phys. Rev. D **57**, 3084 (1998).

[139] O. Martin, A. Schäfer, M. Stratmann, and W. Vogelsang, Phys. Rev. D **60**, 117502 (1999).

[140] C. Bourrely and J. Soffer, Nucl. Phys. B **423**, 329 (1994).

[141] C. Bourrely and J. Soffer, Nucl. Phys. B **445**, 341 (1995).

[142] V. Barone, T. Calarco, and A. Drago, Phys. Rev. D **56**, 527 (1997).

[143] A. Bianconi and M. Radici, Phys. Rev. D **72**, 074013 (2005).

[144] H. Shimizu, G. Sterman, W. Vogelsang, and H. Yokoya, Phys. Rev. D **71**, 114007 (2005).

[145] K. Gottfried, Phys. Rev. Lett. **18**, 1174 (1967).

[146] P. Amaudruz *et al.* Phys. Rev. Lett. **66**, 2712 (1991).

[147] M. Arneodo *et al.* Phys. Rev. D **50**, R1 (1994) .

[148] B. Badełek and J. Kwieciński. Nucl. Phys. B **370**, 278 (1992).

[149] V.R. Zoller. Z. Phys. C **54**, 425 (1992).

[150] H. Khan and P. Hoodhbhoy. Phys. Lett. B **298**, 181 (1993).

[151] W. Melnitchouk and A.W. Thomas. Phys. Rev. D **47**, 3794 (1993).

[152] L.P. Kaptari and A.Yu. Umnikov. Phys. Lett. B **272**, 359 (1991).

[153] A. Baldit *et al.* Phys. Lett. B **332**, 244 (1994).

[154] E.A. Hawker *et al.* (E866 Collaboration), Phys. Rev. Lett. **80**, 3715 (1998).

[155] K. Ackerstaff *et al.* (Hermes Collaboration), Phys. Rev. Lett. **81**, 5519 (1998).

[156] A.W. Thomas, Phys. Lett. B **126**, 97 (1983).

[157] A. Szczurek, J. Speth and G.T. Garvey. Nucl. Phys. A **570**, 765 (1994).

[158] H. Holtmann, N.N. Nikolaev, J. Speth and A. Szczurek, Z. Phys. A **353**, 411 (1994).

[159] S. Forte, Phys. Rev. D **47**, 1842 (1993) .

[160] B.-Q. Ma, A. Schäfer and W. Greiner, Phys. Rev. D **47**, 51 (1993).

[161] D.A. Ross and C.T. Sachrajda, Nucl. Phys. B **149**, 497 (1979).

[162] E.M. Henley and G.A. Miller, Phys. Lett. B **251**, 453 (1990).

[163] A. Signal, A.W. Schreiber and A.W. Thomas, Mod. Phys. Lett. A **6**, 271 (1991).

[164] W. Melnitchouk, A.W. Thomas and A.I. Signal. Z. Phys. A **340**, 85 (1991).

[165] S. Kumano, Phys. Rev. D **43**, 59 (1991).

[166] W-Y.P. Hwang, J. Speth and G.E. Brown. Z. Phys. A **339**, 383 (1991).

[167] V.R. Zoller. Z. Phys. C **53**, 443 (1992).

[168] A. Szczurek and J. Speth. Nucl. Phys. A **555**, 249 (1993).

[169] S.D. Ellis and W.J. Stirling, Phys. Lett. B **256**, 258 (1991).

[170] P.L. McGaughey *et al*, Phys. Rev. Lett. **69**, 1726 (1992).

[171] A.D. Martin, W.J. Stirling and R.G. Roberts. Phys. Rev. D **50**, 6734 (1994).

[172] T.D. Cohen and D.B. Leinweber. Comments Nucl. Part. Phys. **21**, 137 (1993).

[173] J. Ashman *et al*, Nucl. Phys. B 328, 1 (1989).

[174] J. Ellis and R.L. Jaffe. Phys. Rev. D **9**, 1444 (1974).

[175] D. Adams *et al*, Phys. Lett. B **329**, 399 (1994).

[176] P.L. Anthony *et al*, Phys. Rev. Lett. **71**, 959 (1993).

[177] F. Myhrer and A.W. Thomas, Phys. Lett. B **663**, 302 (2008).

[178] J. Friedrich and Th. Walcher, Eur. Phys. J. **A** 17, 607 (2003).

[179] G.A. Miller, Phys. Rev. C 66, 032201 (2002).

[180] Z. Diembowski, Phys. Rev. D **37**, 778 (1988).

[181] J.J. Kelly, Phys. Rev. C **66**, 065203 (2002).

[182] H.-W. Hammer, U.-G. Meißner and D. Drechsel, Phys. Lett. B **586**, 291 (2004); H.-W. Hammer and U.-G. Meißner, Eur. Phys. J. A **20**, 469 (2004).

[183] M.A. Belushkin, H.-W. Hammer and U.-G. Meißner, Phys. Lett. B **586**, 291 (2004);

[184] G.A. Miller, Phys. Rev. Lett. **99**, 112001 (2007).

[185] B. Pasquini and S. Boffi, Phys. Rev. D **73**, 094001 (2006).

[186] S.D. Bass, D. Schütte, Z. Phys. A **357**, 85 (1997).

[187] Z. Dziembowski, H. Holtmann, and A. Szczurek, J. Speth, Ann. of Phys. **258**, 1 (1997).

[188] D.H. Lu, A.W. Thomas, and A.G. Williams, Phys. Rev. C **57**, 2628 (1998).

[189] Y.B. Dong, A. Faessler, and K. Shimizu, Eur. Phys. J. A **6**, 203 (1999).

[190] A. Faessler, Th. Gutsche, V.E. Lyubovitskij, and K. Pumsa-ard, Phys. Rev. D **73**, 114021 (2006).

[191] B. Juliá-Díaz and D.O. Riska, Nucl. Phys. A **780**, 175 (2006).

[192] Q.B. Li and D.O. Riska, Nucl. Phys. A (to be published), nucl-th/0702049.

[193] D.Y. Chen, Y.B. Dong, M.M. Giannini, and E. Santopinto, Nucl. Phys. A **782**, 62c (2007).

[194] J.P.B.C. de Melo, T. Frederico, E. Pace, S. Pisano, and G. Salmè, Nucl. Phys. A **782**, 69c (2007).

[195] S.D. Drell, D.J. Levy, and T.-M. Yan, Phys. Rev. D **1**, 1035 (1970).

[196] V.R. Zoller, Z. Phys. C **53**, 443 (1992).

[197] V.R. Zoller, Z. Phys. C **54**, 425 (1992).

[198] W. Melnitchouk and A.W. Thomas, Phys. Rev. D **47**, 3794 (1993).

[199] W. Koepf, L.L. Frankfurt and M. Strikman, Phys. Rev. D **53**, 2586 (1996).

[200] R.L. Jaffe and G.C. Ross, Phys. Lett. B **93**, 313 (1980).

[201] S.D. Drell, D.J. Levy, and Tung-Mow Yan, Phys. Rev. D **1**, 1035 (1970).

[202] J. C. Collins, L. L. Frankfurt, and M. Strikman, Phys. Rev. D. **56**, 2982 (1997).

[203] M. Diehl *et al.*, Phys. Rev. Lett. **81**, 1782 (1998); Phys. Rev. D **62**, 073014 (2000).

[204] I.V. Anikin, I.O. Cherednikov, N.G. Stefanis and O.V. Teryaev, arXiv:08064551 [hep-ph].

[205] A great wealth of up-to-date informations about the experiments that will be performed at GSI-HESR can be found at this web-page: http://www.gsi.de/zukunftsprojekt/indexe.html.

[206] L.L. Frankfurt, M.V. Polyakov, and M. Strikman, hep-ph/9808449 ; L.L. Frankfurt, P.D. Pobylitsa, M.V. Polyakov, and M. Strikman, Phys. Rev. D **60**, 014010.

[207] B. Pire and L. Szymanowski, Phys. Lett B **622**, 83 (2005); Phys. Rev. D **71**, 111501 (2005); PoS **HEP2005**, 103 (2006). J.P. Lansberg, B. Pire and L. Szymanowski, Phys. Rev. D **75**, 074004 (2007); *ibid.* D **77**, 019902(E) (2008); arXiv:0709.2567 [hep-ph]; Phys. Rev. D **76**, 111502 (2007).

[208] M. Moreno, Phys. Rev. D **16**, 720 (1977); D.A. Bryman, P. Depommier and C. Leroy, Phys. Rept. **88**, 151 (1982).

[209] W. M. Yao *et al.* [Particle Data Group], J. Phys. G **33** (2006) 1.

[210] A. V. Radyushkin, Phys. Rev. D **59** (1999) 014030.

[211] B. C. Tiburzi, Phys. Rev. D **72** (2005) 094001.

[212] A. Courtoy and S. Noguera, Phys. Rev. D **78**, 034002 (2008); Prog. Part. Nucl. Phys. **61**, 170 (2008); arXiv:0804.4337 [hep-ph].

[213] A. Courtoy, *private communication*; A. Courtoy and S. Noguera, *forthcoming*.

[214] J. P. Lansberg, B. Pire and L. Szymanowski, Phys. Rev. D **73** (2006) 074014.

[215] W. Broniowski and E. R. Arriola, Phys. Lett. B **649** (2007) 49.

[216] A. E. Dorokhov and L. Tomio, Phys. Rev. D **62** (2000) 014016 ; F. Bissey *et al.*, Phys. Lett. B **547** (2002) 210; F. Bissey *et al.*, Phys. Lett. B **587** (2004) 189.

[217] D. Brommel *et al.* [QCDSF Collaboration], arXiv:0708.2249 [hep-lat].

[218] I.V. Anikin, B. Pire and O.V. Teryaev, Phys. Rev. D **69**, 014018 (2004) and Phys. Lett. B **626** (2005) 86.

[219] D. Amrath, J.P. Lansberg and M. Diehl, arXiv:0807.4474 [hep-ph].

[220] J. P. Lansberg, B. Pire and L. Szymanowski, Nucl. Phys. A **782** (2007) 16.

[221] S. Adler and R. Dashen, *Currents Algebra* (W.A. Benjamin, New York, 1968).

[222] P.V. Pobylitsa, M.V. Polyakov and M. Strikman, Phys. Rev. Lett. **87**, 022001 (2001); M.V. Polyakov and S. Stratman, hep-ph/0609045.

[223] K.J. Park *et. al.* [CLAS collaboration], Phys. Rev. C **77**, 015208 (2008).

[224] C. S. Armstrong *et al.* [Jefferson Lab E94014 Collaboration], Phys. Rev. D **60**, 052004 (1999).

[225] H. Denizli *et al.* [CLAS Collaboration], Phys. Rev. C **76**, 015204 (2007).

[226] A. Airapetian *et al.* [HERMES Collaboration], arXiv:0707.0222 [hep-ex].

[227] R.A. Arndt, W.J. Briscoe, I.I. Strakovsky and R.L. Workman, AIP Conf. Proc. **904**, 269 (2007); R.A. Arndt *et.al.*, work in progress.

[228] P. Spiller and G. Franchetti, Nucl. Instrum. Meth. A **561**, 305 (2006); see also `http://www.gsi.de/fair`.

[229] M. Pincetti, B. Pasquini and S. Boffi, arXiv:0807.4861 [hep-ph] (2008).

[230] V.M. Braun *et al.*, Phys. Rev. D **75**, 014021 (2007).

[231] M.B. Gavela *et al.*, Nucl. Phys. B **312**, 269 (1989).

[232] M. Burkhardt, Phys. Rev. D **62**, 071503 (2000); *ibidem* **66**, 119903(E) (2002); M. Diehl, Eur. Phys. J. C **25**, 223 (2002), *ibidem* **31**, 277(E) (2003).

List of publications

⋆ B. Pasquini, M. Pincetti and S. Boffi, *Chiral-Odd Generalized Parton Distributions in Constituent Quark Models*, Phys. Rev. D **72**, 094029 (2005), e-Print: hep-ph/0510376.

⋆ M. Pincetti, B. Pasquini and S. Boffi, *Chiral-Odd Generalized Parton Distributions and Transversity in Light-Front Constituent Quark Models*, Czech. J. Phys. **56**, F229 (2006), e-Print: hep-ph/0610051.

⋆ B. Pasquini, M. Pincetti and S. Boffi, *Drell-Yan processes, Transversity and Light-Cone Wavefunctions*, Phys. Rev. D **76**, 034020 (2007), e-Print: hep-ph/0612094.

⋆ M. Pincetti, B. Pasquini and S. Boffi, *Chiral-Odd Generalized Parton Distributions, Transversity and Double Transverse-Spin Asymmetry in Drell-Yan Dilepton Production*, Proceedings of 11^{th} Conference on Problems in Theoretical Nuclear Physics, Cortona, Italy, 11-14 Oct 2006. Edited by A. Covello, L.E. Marcucci, S. Rosati and I. Bombaci (World Scientific, Singapore, 2007), p. 315; e-Print: hep-ph/0612335.

⋆ M. Pincetti, B. Pasquini and S. Boffi, *Nucleon to Pion Transition Distribution Amplitudes in a Light-Cone Quark Model*, to appear in the proceeding of the 2^{nd} International Workshop on Transverse Polarization Phenomena in Hard Processes (Transversity2008), Ferrara, Italy, 28-31 May 2008, e-Print: arXiv:0807.4861 [hep-ph].

ACKNOWLEDGEMENTS

It gives me great pleasure to acknowledge my sincere gratitude to my supervisors Prof. S. Boffi and Dr. B. Pasquini for providing me all the inspiration, encouragement and guidance to carry out my research work and for their prompt and sincere help whenever I needed it most. I have learned many things from them, perhaps Physics has been the less important...I will be forever indebted to them.

It is a mammoth task to individually mention the names of my numerous friends whose friendship I cherish. I would like to thank them all, both in and outside the Departments of Physics in Pavia, for their cooperation and help whenever I approached them, whether it be academic or nonacademic.

Last, but not the least, I would like to thank the members of my family, who stood by me all along my voyage to this point.